Textron Aviation
Raytheon Missile Systems
AIAA Foundation

The 2016 Textron Aviation/Raytheon Missile Systems/AIAA Design/Build/Fly Competition Flyoff was held at Cessna East Field in Wichita, KS on the weekend of April 15-17, 2016. This was the 20th anniversary year since the original competition was held at Ragged Island, MD, in 1997. A total of 145 entries were received, and a new requirement was implemented to write a proposal for review. 137 proposals were submitted and 93 teams were selected for the next phase. 80 teams submitted written reports to be judged, and 69 teams attended the flyoff (25 international). Over 625 students, faculty, and guests were present.

The Missions this year simulated a Distributed Manufacturing system, where the students were required to design two aircraft:

- The Production Aircraft, which carried a payload of a 32oz bottle of Gatorade.
- The Manufacturing Support Aircraft, which is designed to carry the Production Airplane internally.

The Mission Score was the product of the three Flight Scores, and a Bonus mission was added with a timed assembly of the Production Airplane. As in the past, the Final Score is the product of the Mission Score and written Report Score, divided by airplane RAC (airplane and battery weights). More details can be found at the competition website: http://www.aiaadbf.org

The mission requirements this year were very challenging, and furthermore strong winds prevailed for the first two days and it rained much of the third day. Still, there were 217 flight attempts, of which 83 resulted in a valid flight score. 38 teams had successful flight scores and 12 teams completed all three flight missions. The quality of the teams, readiness to compete, and execution of the flights was outstanding.

First place went to San Jose State University with a score of 1300.64, second place to Georgia Tech University at 801.32 and third to University of California Irvine at 610.49. A full listing of the results is shown below. The best paper award, sponsored by the Design Engineering TC for the highest report score, went to Georgia Tech University with a score of 97.00.

We owe our thanks for the success of the DBF competition to the efforts of many volunteers from Textron Aviation, Raytheon Missile Systems, and the AIAA sponsoring technical committees (Applied Aerodynamics, Aircraft Design, Flight Test, and Design Engineering). These volunteers collectively set the rules for the contest, publicize the event, gather entries, judge the written reports, and organize the flyoff. Thanks also go to the Corporate Sponsors: Textron Aviation, Raytheon Missile Systems, and the AIAA Foundation for their financial and logistical support. Special thanks to Textron Aviation for hosting the flyoff this year.

The growth of the DBF since it was initiated has been phenomenal, and the Organizing Committee is committed to make this educational opportunity available to as many students as possible.

Finally, this flyoff marks the final year of my tenure on the DBF Organizing Committee. I am grateful for this opportunity to have served you - the students - and the Aerospace Community at large.

David Levy
For the DBF Organizing Committee

2016 AIAA Design/Build/Fly Competition Final Results

RANK	TEAM		Report	MISSION SCORES					RAC	2016
	Queue #	Name		MF1	MF2	PF1	Bonus	Total		DBF Score
1	30	San Jose State University	86.33	2.00	4.00	2.00	2.00	18.00	1.19	**1300.64**
2	1	Georgia Institute of Technology	97.00	2.00	4.00	1.00	0.00	8.00	0.97	**801.32**
3	14	University of California, Irvine	91.17	2.00	4.00	2.00	2.00	18.00	2.69	**610.49**
4	3	Virginia Tech	95.25	2.00	4.00	2.00	2.00	18.00	5.17	**331.86**
5	21	University of Oklahoma	89.00	2.00	4.00	2.00	0.00	16.00	4.60	**309.51**
6	34	Oregon State University	85.67	2.00	4.00	2.00	2.00	18.00	5.73	**269.13**
7	15	FH JOANNEUM	91.00	2.00	4.00	2.00	2.00	18.00	8.39	**195.16**
8	19	Cornell University	89.00	2.00	4.00	2.00	0.00	16.00	8.55	**166.50**
9	58	Hebei U. of Science & Technology	72.33	2.00	4.00	0.10	0.00	0.80	0.49	**118.77**
10	12	Università di Roma "La Sapienza"	92.33	2.00	4.00	0.10	0.00	0.80	0.65	**113.15**
11	40	Embry-Riddle Aeronautical University - Daytona Beach	84.50	2.00	4.00	2.00	2.00	18.00	14.33	**106.17**
12	44	Embry-Riddle Aeronautical University-Prescott	83.83	2.00	4.00	2.00	2.00	18.00	15.56	**97.01**
13	10	The University of Texas at Austin	92.33	2.00	4.00	2.00	2.00	18.00	18.46	**90.05**
14	26	Arizona State University	88.33	2.00	4.00	2.00	2.00	18.00	23.20	**68.52**
15	7	California Polytechnic State University, San Luis Obispo	94.00	2.00	4.00	0.10	0.00	0.80	1.34	**55.95**
16	4	University of Southern California	94.75	2.00	4.00	0.10	0.00	0.80	1.49	**50.94**
17	18	TEL AVIV UNIVERSITY	89.33	2.00	4.00	0.10	0.00	0.80	2.13	**33.53**
18	9	University of Strathclyde	93.43	2.00	4.00	2.00	0.00	16.00	51.66	**28.94**
19	17	Colorado School of Mines	89.67	2.00	4.00	1.00	0.00	8.00	27.70	**25.89**
20	29	Massachusetts Institute of Tech	86.97	2.00	4.00	0.10	0.00	0.80	5.11	**13.61**
21	23	University of Glasgow	88.67	2.00	4.00	0.10	0.00	0.80	5.46	**12.98**
22	65	University of Central Florida	67.25	2.00	4.00	0.10	0.00	0.80	6.05	**8.89**
23	67	University of California, Los Angeles	65.00	2.00	4.00	0.10	0.00	0.80	8.06	**6.45**
24	22	The Hong Kong University of Science and Technology	88.83	2.00	4.00	0.10	0.00	0.80	11.19	**6.35**
25	35	University of Washington	85.33	2.00	4.00	0.10	0.00	0.80	13.17	**5.18**
26	37	Istanbul Technical University	85.30	2.00	4.00	0.10	0.00	0.80	13.61	**5.01**
27	13	University of California San Diego	92.00	2.00	4.00	0.10	0.00	0.80	14.96	**4.92**
28	24	University of Tennessee, Knoxville	88.67	2.00	4.00	0.10	0.00	0.80	19.96	**3.55**
29	33	University of Notre Dame	86.00	2.00	4.00	0.10	0.00	0.80	30.69	**2.24**
30	43	University of Ljubljana, Faculty of Mechanical Engineering	84.33	2.00	0.10	0.10	0.00	0.02	0.94	**1.79**
31	8	Wichita State University	93.67	2.00	0.10	0.10	0.00	0.02	1.15	**1.63**
32	39	National University of Singapore	84.67	2.00	1.00	0.10	0.00	0.20	21.28	**0.80**
33	5	Universtiy of Colorado Boulder	94.50	2.00	0.10	0.10	0.00	0.02	11.89	**0.16**
34	62	The Pennsylvania State University	67.33	2.00	0.10	0.10	0.00	0.02	8.52	**0.16**
35	27	Saint Louis University	87.00	2.00	0.10	0.10	0.00	0.02	25.46	**0.07**
36	28	UNIVERSIDAD DE SAN BUENAVENTURA BOGOTA	87.00	2.00	0.10	0.10	0.00	0.02	26.77	**0.06**
37	16	University of Maryland, College Park	90.67	2.00	0.10	0.10	0.00	0.02	36.84	**0.05**
38	46	Ghulam Ishaq Khan Institute of Engineering Sciences and Technology	82.93	2.00	0.10	0.10	0.00	0.02	36.30	**0.05**

2016 AIAA Design/Build/Fly Competition Final Results (Continued)

RANK	TEAM		Report	MISSION SCORES					RAC	2016 DBF Score
	Queue #	Name		MF1	MF2	PF1	Bonus	Total		
39	2	Veermata Jijabai Tech Institute	95.50	0.10	0.10	0.10	0.00	0.00	0.00	Passed Tech Inspection
40	6	Rashtreeeya Vidyalaya College Of Engineering	94.33	0.10	0.10	0.10	0.00	0.00	0.00	
41	11	The State University of New York at Buffalo	92.33	0.10	0.10	0.10	0.00	0.00	0.00	
42	20	Universidad Pontificia Bolivariana	89.00	0.10	0.10	0.10	0.00	0.00	0.00	
43	32	Khalifa University	86.00	0.10	0.10	0.10	0.00	0.00	0.00	
44	36	Rice University	85.33	0.10	0.10	0.10	0.00	0.00	0.00	
45	41	University of Mass Lowell	84.33	0.10	0.10	0.10	0.00	0.00	0.00	
46	42	Columbia University in the City of New York	84.33	0.10	0.10	0.10	0.00	0.00	0.00	
47	45	Concordia University	82.93	0.10	0.10	0.10	0.00	0.00	0.00	
48	49	University of South Carolina	82.33	0.10	0.10	0.10	0.00	0.00	0.00	
49	50	Uludag University	80.00	0.10	0.10	0.10	0.00	0.00	0.00	
50	52	University of Arkansas	78.33	0.10	0.10	0.10	0.00	0.00	0.00	
51	55	University of South Alabama	76.00	0.10	0.10	0.10	0.00	0.00	0.00	
52	59	PES University	70.33	0.10	0.10	0.10	0.00	0.00	0.00	
53	63	Cairo University	67.33	0.10	0.10	0.10	0.00	0.00	0.00	
54	66	Colorado State University	66.33	0.10	0.10	0.10	0.00	0.00	0.00	
55	72	University of California, Merced	60.40	0.10	0.10	0.10	0.00	0.00	0.00	
56	73	Sakarya University	59.00	0.10	0.10	0.10	0.00	0.00	0.00	
57	76	Brno University of Technology	57.83	0.10	0.10	0.10	0.00	0.00	0.00	
58	77	ATATÜRK UNIVERSITY	57.00	0.10	0.10	0.10	0.00	0.00	0.00	
59	38	Florida Institute of Technology	85.00	0.10	0.10	0.10	0.00	0.00	0.00	At Flyoff
60	47	North Dakota State University	82.63	0.10	0.10	0.10	0.00	0.00	0.00	
61	48	Worcester Polytechnic Institute	82.33	0.10	0.10	0.10	0.00	0.00	0.00	
62	56	Marmara University	74.67	0.10	0.10	0.10	0.00	0.00	0.00	
63	64	DHA SUFFA UNIVERSITY	67.33	0.10	0.10	0.10	0.00	0.00	0.00	
64	69	Rensselaer Polytechnic Institute	62.00	0.10	0.10	0.10	0.00	0.00	0.00	
65	75	California State University, Long Beach	58.00	0.10	0.10	0.10	0.00	0.00	0.00	
66	78	University of Wisconsin-Madison	55.00	0.10	0.10	0.10	0.00	0.00	0.00	
67	25	University of Florida	88.67	0.10	0.10	0.10	0.00	0.00	0.00	Submitted Report
68	31	University of California, Berkeley	86.33	0.10	0.10	0.10	0.00	0.00	0.00	
69	51	Karabuk University	78.67	0.10	0.10	0.10	0.00	0.00	0.00	
70	53	Rose-Hulman Inst. of Technology	78.17	0.10	0.10	0.10	0.00	0.00	0.00	
71	54	Purdue University	78.00	0.10	0.10	0.10	0.00	0.00	0.00	
72	57	Trine University	74.33	0.10	0.10	0.10	0.00	0.00	0.00	
73	60	College of Aeronautical Engineering, NUST	69.67	0.10	0.10	0.10	0.00	0.00	0.00	
74	61	University Of Alaska Fairbanks	69.00	0.10	0.10	0.10	0.00	0.00	0.00	
75	68	Stanford University	63.33	0.10	0.10	0.10	0.00	0.00	0.00	
76	70	Johns Hopkins University	61.60	0.10	0.10	0.10	0.00	0.00	0.00	
77	71	Wentworth Inst. of Technology	61.25	0.10	0.10	0.10	0.00	0.00	0.00	
78	74	SRM UNIVERSITY	58.75	0.10	0.10	0.10	0.00	0.00	0.00	
79	79	American University of Sharjah	53.67	0.10	0.10	0.10	0.00	0.00	0.00	
80	80	The Hong Kong Polytechnic University	32.50	0.10	0.10	0.10	0.00	0.00	0.00	

First Place Winner: San Jose State University.

Second Place Winner: Georgia Tech University.

Third Place Winner: University of California at Irvine.

2015-2016 DBF Competition
San José State University
Team Cronus

Table of Contents

1.0 Executive Summary

Team Cronus from San Jose State University is currently designing a set of aircraft for the purpose of winning the 2015/2016 AIAA DBF competition. The design process has yielded concepts focused on minimal rated aircraft cost (RAC) and marginally acceptable, though mission capable, flight performance for the expected conditions.

This year's DBF competition requires two aircraft to satisfy the mission guidelines. The first aircraft is the Manufacturing Support (MS) Aircraft that will be used in Missions 1 and 2. The second aircraft is the Production (PR) Aircraft, which will be used in Missions 2 and 3. For the first mission, the MS Aircraft will be flying three laps within five minutes with no payload. For the second mission, the MS Aircraft must fly with the components of the PR Aircraft as its payload. An equal number of laps to the number of components of the PR Aircraft must be flown. Components of the PR Aircraft are defined as the number of moveable pieces to make the PR Aircraft "flight ready" from its transportation configuration. After the first two missions are completed, the PR Aircraft will fly three laps within five minutes with a 32 oz Gatorade bottle as the payload and then complete a bonus mission where it must be assembled from its transportation configuration to its flight configuration in under two minutes.

The general competition mission requirements for both aircraft specify a maximum takeoff distance of 100 ft and the ability to complete 3 laps, with appropriate mission loads, in 5 minutes. Each lap takes the airplane around a 1,000 ft racetrack course with a 360 degree opposite turn downwind. These requirements, along with expected environmental conditions result in a target cruise speed of 70 ft/sec and a stall speeds not to exceed 35 ft/sec for both airplanes. Our Team has estimated that a ground speed of approximately 30 feet per second is required to complete the three laps in five minutes. This allows the aircraft to fly with a 40 feet per second headwind (common at the competition location) and still complete the mission within the time required. The last performance target our team aims to achieve is a take-off distance of 80 feet,which includes a factor of safety of 20%.

The Rated Aircraft Cost (RAC) is a function built from the product of airplane weight, battery weight, and number of subassemblies for the PR Aircraft plus empty weight times battery weight for the MS Aircraft. Studies involving potential tradeoffs of MS Aircraft mass for PR Aircraft subassemblies favored a carrier airplane that could fit the production airplane in a one piece, flight ready condition. The configuration selected for the aircraft is shown in the loading sketches included in Figure 1.0.1.

Figure 1.0.1: Loading of PR Aircraft in MS Aircraft

Due to the the battery weight being in the score's denominator, minimizing the battery weight is necessary in order to maximize the team's score. However, this is a big risk due to the possibility of under powering the aircraft.

To verify our design, each aircraft was tested using the 2015 - 2016 DBF mission standards. Table 1.0.1 tabulates the flight tested performance characteristics for each designated mission. Table 1.0.2 tabulates our current calculated RAC value.

Table 1.0.1: Tested Performance Characteristics

Mission Performance Characteristics			
Parameter	Mission 1	Mission 2	Mission 3
Takeoff Distance (ft)	24	37	72
Cruise Speed (ft/s)	70.1	68.9	85.1
Time to Complete Course (s)	195 (3 Laps)	85 (1 Lap)	165 (3 Laps)
Empty Weight (lb)	1.813	1.813	0.988

Table 1.0.2: RAC Breakdown

Components	EW_1 (lbs)	Et_{Bat1} (lbs)	$N_{Components}$	EW_2 (lbs)	Wt_{Bat2} (lbs)	RAC
Value	0.988	0.375	1	1.813	0.375	1.05

2.0 Management Summary

The team was founded by 6 seniors, working in conjunction with their aircraft design class to optimize the design. In order to comply with DBF regulations and to involve the younger student body, underclassmen were recruited to satisfy the 1/3 minimum rule. This resulted in the total membership increasing to 10 members.

2.1 Team Structure

Team Cronus is composed of 9 active members, including 6 seniors and 3 underclassmen. The general structure of the Team involves a Faculty Advisor, Team Lead, Manager, Computer Aided Design (CAD) Lead, Recorder, Spokesperson and Treasurer. The Team Lead is responsible for consulting with the advisor as well as working with the Team Manager to delegate tasks and ensure timely completion. The Team Manager was also responsible for delegating tasks to the underclassman and coordinating the other

senior members to mentor them during given tasks. Refer to Figure 2.1.1 for a diagram of the Team organization.

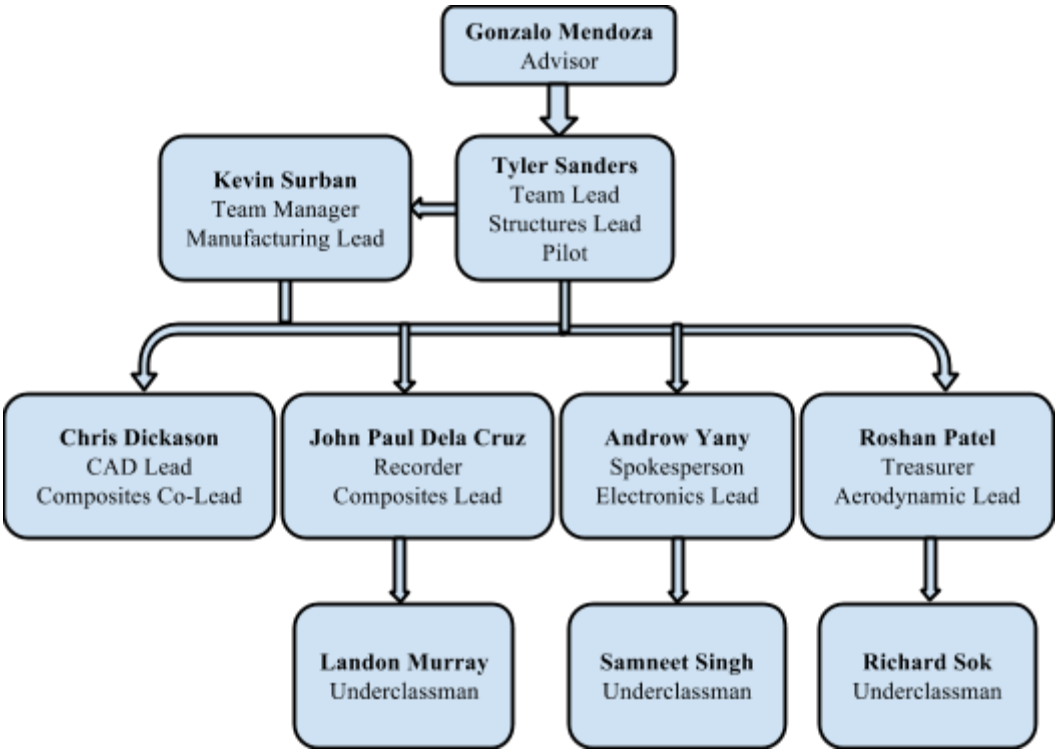

Figure 2.1.1: Group Organization Chart

2.2 Milestone Chart

The Team's goal is to design and manufacture two aircraft to compete in the 2015/2016 DBF competition in approximately seven months. In order to accomplish this goal, the following milestone chart was created and followed closely.

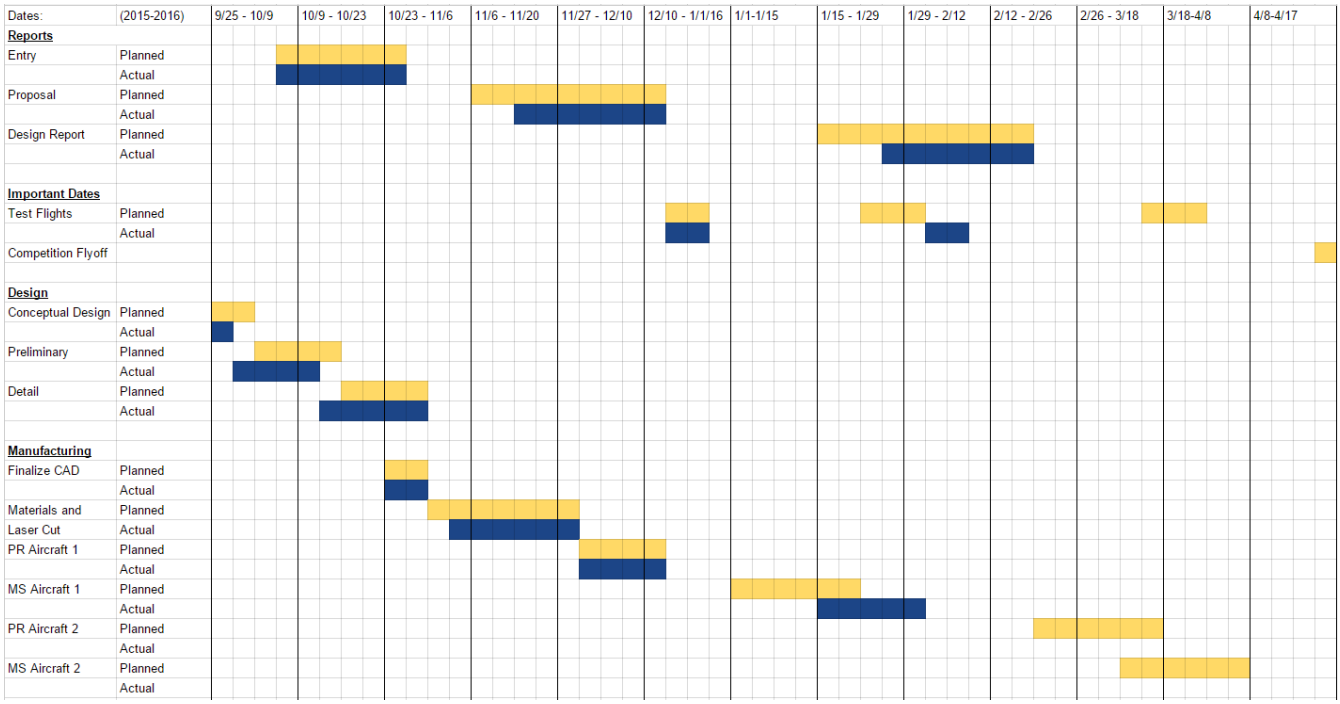

Figure 2.2.1:Milestone Chart

3.0 Conceptual Design

A comprehensive scoring analysis was completed, evaluating the rules and realistically weighing each scoring factor in order to maximize the total score.

3.1 Mission Summary and Scoring Analysis

The overall score of this year's DBF competition is calculated by the following equation:

$$\text{Score} = (\text{Written Report Score} * \text{Total Mission Score}) \div \text{RAC} \quad (3.1)$$

where the Written Report Score is the score received from the submitted report for the contest. The Total Mission Score (eq. 3.2) is the total score received from completing the mission requirements, and RAC is the Rated Aircraft Cost (eq. 3.3).

$$\text{Total Mission Score} = (MF1 * MF2 * PF) + \text{Bonus} \quad (3.2)$$

where MF1 and MF2 are the scores for the Manufacturing Support (MS) Aircraft flights, PF is the score for the Production (PR) Aircraft flight, and Bonus is the score for the bonus mission.

$$\text{RAC} = (EW1 * Et_{Bat1} * N_{Components}) + (EW2 * Wt_{Bat2}) \quad (3.3)$$

The RAC is determined by the aircraft's weight, battery weights (Wt_{Bat}) of both PR and MS, and the number of sub-assemblies that the PR aircraft is broken into for the delivery flight $(N_{Components})$. The 1

subscript following each variable represents the PR Aircraft, whereas the 2 subscript represents the MS Aircraft.

Mission 1– Manufacturing Support Aircraft Arrival Flight

The MS Aircraft will be used for the first mission. The aircraft must takeoff within the prescribed field length, which is 100 feet, and fly three laps in less than five minutes without a payload. The aircraft must land safely in order to receive a score for the first mission. The mission score is given by the following: (MF1 = Score for Mission 1)

- MF1 = 2.0 (Aircraft completes mission)
- MF1 = 0.1 (Aircraft does not complete mission)

Mission 2 – Manufacturing Support Aircraft Delivery Flight

The second mission has a 10 minute time limit. The mission starts with the PR Aircraft's first sub-assembly installed inside the MS Aircraft. The MS must fly one lap for every sub-assembly of the PR Aircraft, land successfully, and unload the sub-assembly. The ground crew will remove the installed sub-assembly then install and secure the next sub-assembly. After the next sub-assembly is installed, the aircraft will taxi to the location behind the start line and take-off for next lap. The time ends when the MS Aircraft delivers all of the PR Aircraft's parts and passes the start line at the end of the final flight. The mission score is given by the following: (MF2 = Score for Mission 2)

- MF2 = 4.0 (Aircraft completes all flight successfully within time window)
- MF2 = 1.0 (Aircraft successfully completes 1 group transportation within time window)
- MF2 = 0.1 (Aircraft does not complete a successful flight)

Mission 3 – Production Aircraft flight

For this mission, the PR Aircraft will fly three laps within five minutes with a 32 oz. factory sealed Gatorade bottle as the payload. The aircraft must complete a safe landing in order to receive a score for this mission. The mission score is given by the following: (PF = Score for Mission 3)

- PF = 2.0 (Aircraft completes flight with full payload within time period)
- PF = 1.0 (Aircraft does not meet minimum requirement for laps or exceeds time limit)
- PF = 0.1 (Aircraft does not complete successful flight)

Mission 4: Bonus Mission (Ground Mission)

Missions 1-3 have to be completed successfully in order to attempt the bonus mission. This mission will be completed in a separate area from the flight area. After the final flight, the team will bring all the PR Aircraft sub-assemblies to the mission area, assemble the PR Aircraft, and re-install the payload within two minutes. The completed aircraft must pass the wing tip lift test and a controls system check in order to

receive a score. Points are only earned in this mission if task can be completed in under two minutes. The mission score is given by the following: (Bonus = Score for Mission 4)

- Bonus = 2.0 (Aircraft successfully passes all requirements)
- Bonus = 0 (Any other result)

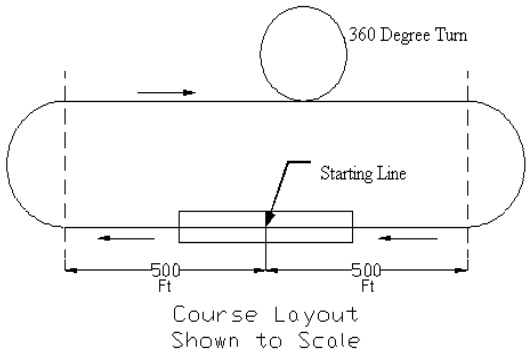

Figure 3.1.1: Flight Mission Profile From DBF Website

Effect of Number of Subassemblies on RAC

A scoring analysis was completed to evaluate the effect of a reduced number of components on MS Aircraft weight. Table 3.1.1 contains a summary of analysis results for 2 and 1 subassembly configurations. The selected single subassembly design leads to a more complex structural configuration, including side hinged doors and a removable wing for the MS airplane. In addition, this configuration results in a challenging performance picture for the MS airplane, with a large area fuselage, very low wing loading, and suboptimal wing aspect ratio. The PR airplane is minimally compromised to minimize MS airplane fuselage area through installation of a box tail. However, this comes at a cost by having a suboptimal aspect ratio (AR) and large wing area, resulting in a low wing loading. The low AR and increased weight will cause a detrimental impact in drag which may cause performance issues for the MS Aircraft.

Table 3.1.1: Scoring analysis of varying MS EW and $N_{components}$.

	2 Components and Lightest MS	Estimated Max MS EW Increase	Estimated Min MS EW Increase
MS EW Increase	0	0.5	0.125
EW1	0.949	1.049	1.049
EW2	1.149	1.149	1.149
Wt_{Bat1}	0.448	0.448	0.448
Wt_{Bat2}	0.448	0.448	0.448
$N_{Components}$	2	1	1
RAC	1.365	1.209	1.041

3.2 Design

This year's DBF competition involves the significant challenge of designing two distinct airplanes which must be lightweight, speedy, controllable, and stable. These requirements, later quantified, will be taken into consideration during every step of the design process to ensure both aircraft meet the specifications and fly well. After analysis of the competition scoring, it is noted that the total score is divided by the aircraft's empty weights. Minimizing the aircraft weight will certainly be a significant factor in the design of the aircraft, but this must be done carefully to maintain structural integrity.

Two missions will be flown with the MS Aircraft: one with and one without the PR Aircraft as the payload. When the PR Aircraft is loaded, it will heavily influence the center of gravity of the MS Aircraft. Also, the MS Aircraft must be strong enough to carry the additional weight. Great emphasis will be placed in designing a single piece PR Aircraft that fits within a reasonable volume, as opposed to carrying multiple subassemblies.

The PR Aircraft's primary mission is to carry a 32 oz Gatorade and fly three laps in a specified time. The team must design the lightest aircraft possible that is strong enough to carry the payload. Referring back to the scoring analysis, the Team can score higher by having the least amount of sub-assembly parts. Not only will a lighter PR Aircraft generate a higher in the competition, but it will also allow more flexibility of storage in the MS Aircraft due to the reduced influence it would have on the center of gravity. Therefore, the team will design the PR Aircraft with the intention of loading it into the MS Aircraft as one component.

3.3 Configuration Selection

Several design configurations were evaluated to determine which one would yield the highest competition score, ensure a good flying aircraft, and meet the performance requirements. Aircraft, wing, fuselage, empennage, and propulsion configurations were evaluated. A preliminary study helped narrow the options for each design to the most viable options. A design matrix was created to determine which configurations would result in the highest score and best flying aircraft. Each configuration was set into a design matrix where it was rated by different Figures of Merit. The Figures of Merit (FoM) were based on the performance requirements designated by the DBF competition mission specifications. Each FoM is weighted differently to ensure that the most important FoM is weighted higher than the least important. The scoring is done as follows: -1 is detrimental, 0 is neutral, and 1 is positive. The configuration yielding the highest total score is the design chosen for that aircraft.

Aircraft Configuration

Table 3.3.1: Figure of Merit Table for MS Aircraft Configuration

Figure of Merit	FOM Value	 Monoplane	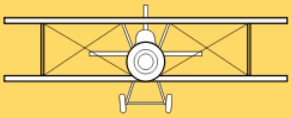 Biplane	 Flying Wing
Weight	0.5	0	1	0
Manufacturability	0.4	1	1	-1
$C_{D,0}$	0.1	0	-1	1
Total	1	0.40	0.3	-0.3

For the MS Aircraft, the Team decided to look at three specific FoMs: weight, manufacturability, and zero-lift drag. Priority was given to weight and manufacturability over the zero-lift drag (Cd_0). The weight was slightly favored due to the heavy influence that weight has on our scoring for the competition. Manufacturability is rated almost as important as weight due to the difficulty of building complex designs, such as a flying wing.

Table 3.3.2: Figure of Merit Table for PR Aircraft Configuration

Figure of Merit	FOM Value	 Monoplane	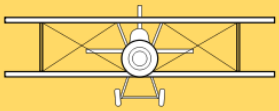 Biplane	 Flying Wing
Weight	0.4	0	1	0
Manufacturability	0.2	1	1	-1
$C_{D,0}$	0.1	0	-1	1
Number of Components	0.3	1	-1	1
Total	1	0.5	-0.4	0.2

For the PR Aircraft, the Team decided to rate the zero-lift drag coefficient the same as the MS Aircraft. It was decided that manufacturability would be weighted less in favor of weight and number of components.

The biplane configuration was given the advantage when it comes to weight because of its reduced wing structure when braced with wires. The relative weight for both monoplane and flying wing configurations

were considered to be neither beneficial nor detrimental. As a result, a score of 1 was given to biplane, and 0 to monoplane and flying wing. For manufacturability, biplane and monoplane configurations are easier to build compared to a flying wing configuration. Therefore, a 1 was given to the biplane and monoplane configurations, while a -1 was given to the flying wing. For zero lift drag coefficient, the flying wing excels because of its low frontal profile. Biplanes have multiple lifting surfaces close to each other, resulting in a drag increase. The monoplane configuration was found to be fairly neutral in this category, and received a 0. A value of 1 and -1 was given to the flying wing and biplane configurations respectively. The monoplane was found to be the best design for both aircraft. The team acknowledges the significance of $C_{D,o}$ and its influence on power requirements; however, the mission requirements do not give extra points for exceptionally fast aircraft.

Wing Configuration

The major FoM's for the wing configuration of the PR Aircraft are weight and stability of the aircraft. The weight of the wing is absolutely crucial for Team Cronus' aircraft because the PR wing will be inserted into the MS wing. The wing must also be removable for insertion of the payload. Hence the weight is heavily weighted for the FoM value.

Table 3.3.3: Figure of Merit Table for PR Aircraft Wing Configuration

Figure of Merit	FOM Value	 Low Wing	 Mid Wing	 High Wing
Weight	0.4	1	0	1
Manufacturability	0.2	1	-1	1
Stability	0.2	-1	0	1
Volume Req. for Transport	0.2	1	1	1
Total	1	0.6	0	1

The following configurations were analyzed for the PR Aircraft: low wing, mid wing and high wing. The FoM's for the wing configuration were weight, manufacturability, stability, and volume required for transport. Low wing configurations have the worst stability compared to the other wing configurations. Given the need to fully enclose the landing gear of the PR aircraft within the MS fuselage, the goal of a single piece PR aircraft, and the desire to minimize the MS volume, the low wing configuration is dismissed as impractical. It offers no significant performance advantage to offset integration complexity. The mid wing configuration

makes the aircraft too heavy due to the reinforcing of wing root at the intersection of the fuselage. The PR Aircraft needs to be as light as possible to maximize the score, making a mid wing configuration an unfavorable choice. The best configuration for this aircraft is the high wing configuration to ensure good lateral stability. A high wing configuration is the best choice because it increases the dihedral effect, which increases lateral stability. The dihedral on the PR aircraft could be used to simplify flight controls, further simplifying packaging and reducing weight.

Table 3.3.4: Figure of Merit Table for MS Aircraft Wing Configuration

Figure of Merit	FOM Value	 Low Wing	 Mid Wing	 High Wing
Weight	0.5	1	0	1
Manufacturability	0.2	1	-1	1
Stability	0.3	-1	0	1
Total	1	0.4	-0.2	1

For the MS Aircraft, similar wing configurations were analyzed as the PR Aircraft. The MS Aircraft wing configuration will be more difficult to construct since the PR aircraft wing will be inserted in the MS wing. This makes weight a crucial design component. The best configuration for this aircraft will be similar to the PR Aircraft, which is a high wing configuration. The high wing configuration is easy to build, weighs the least, and has the best stability out of the three configurations.

Fuselage Configuration

Table 3.3.5: Figure of Merit Table for PR Aircraft Fuselage Configuration

Figure of Merit	FOM Value	 Airfoil	 Conventional	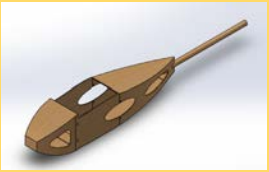 Pod & Boom
Weight	0.4	0	0	-1
Manufacturability	0.2	-1	0	1
$C_{D,0}$	0.2	0	1	-1
Volume Req. for Transport	0.2	0	1	1
Total	1	-0.2	0.4	-0.2

Three different configurations were analyzed for the PR Aircraft fuselage configuration: airfoil, conventional, and pod and boom. The weight was concluded to have the biggest factor in mission and scoring analysis. The pod and boom configuration is a heavier configuration because of additional components required for manufacturing. The conventional fuselage was the best choice because the dimensions of the fuselage will help size for the 32 ounce Gatorade payload.

Table 3.3.6: Figure of Merit Table for MS Aircraft Fuselage Configuration

Figure of Merit	FOM Value	 Airfoil	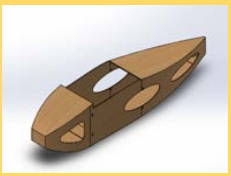 Conventional	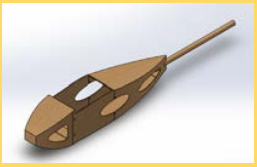 Pod & Boom
Weight	0.5	0	0	-1
Manufacturability	0.3	-1	0	1
$C_{D,0}$	0.2	0	1	-1
Total	1	-0.3	0.2	-0.4

For the MS Aircraft, similar configurations were analyzed: airfoil, conventional, and pod and boom. The most important parameter for the MS Aircraft was weight. The team decided to use the same configuration

as the PR Aircraft since its fuselage was going to be sized around the PR aircraft, hence simplifying the parameters involved.

Empennage Configuration

Table 3.3.7: Figure of Merit Table for PR Aircraft Empennage Configuration

Figure of Merit	FOM Value	 Conventional	 V-Tail	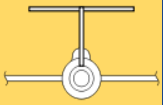 T-Tail	 Box
Weight	0.2	1	0	-1	0
Manufacturability	0.1	1	-1	0	-1
Stability & Control	0.2	1	-1	0	0
Volume Req. for Transport	0.5	-1	0	1	1
Total	1	0	-0.3	0.3	0.4

The following empennage configurations were analyzed for the PR Aircraft: conventional, v-tail, t-tail, and box tail. The most crucial design component for the empennage was the volume that the tail takes up for transport. Since the PR Aircraft will be placed inside of the MS Aircraft, the span of the empennage needs to be minimized so that it can fit inside. In order to achieve this, the PR Aircraft needs to have a box tail empennage configuration, inspired by the 'Vickers Vimmy', a World War I aircraft. This is an unorthodox approach to designing an empennage, because traditional radio controlled aircraft use a conventional tail. A conventional tail is typically easy to manufacture, provides superior stability, and provides large control surfaces. On the other hand, a box tail configuration sacrifices a single control surface into multiple smaller surfaces which increases weight. Nonetheless, the advantage of having a smaller tail is believed to benefit the MS Aircraft aft fuselage volume sufficiently to justify the slight increase in mass, drag and complexity of the PR Aircraft.

Table 3.3.8: Figures of Merit Table for MS Aircraft Empennage Configuration

Figure of Merit	FOM Value	 Conventional	 V-Tail	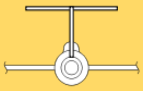 T-Tail	 Box
Weight	0.5	1	0	-1	0
Manufacturability	0.2	1	-1	0	-1
Stability & Control	0.3	1	-1	0	0
Total	1	1	-0.5	-0.5	-0.2

As with previous DBF aircraft, the conventional tail is the one most often chosen because it weighs the least compared to other configurations. It is also one of the easiest designs to construct. A conventional tail also gives the aircraft great stability and control because of a single large control surface for both the elevator and rudder. Hence, conventional tail is the configuration the team will use for the MS Aircraft.

Landing Gear

For both PR and MS Aircraft, there were two different landing gear configurations that were analyzed: tail-dragger and tricycle. The constraints considered for the landing gear configurations were weight, manufacturability, and ground handling. The tricycle landing gear is heavier and larger in size compared to tail-dragger. It would add more weight and drag to the aircraft due to its large front wheel. On the other hand, the tail-dragger weighs less and produces less drag. The tail-drager also has better packaging and sets the aircraft at a favorable incidence for takeoff. After considering all these constraints, the team chose to go with a tail-dragger configuration for both the PR and MS Aircraft.

Table 3.3.9: Figure of Merit Table for PR and MS Aircraft Landing Gear Configuration

Figure of Merit	FOM Value	Tricycle	Tail-Dragger
Weight	0.50	-1	1
Manufacturability	0.20	0	0
Ground Handling	0.30	1	-1
Total	1.00	-0.2	0.20

Propulsion

Table 3.3.10: Figure of Merit Table for PR and MS Aircraft Propeller Configuration

Figure of Merit	FOM Value	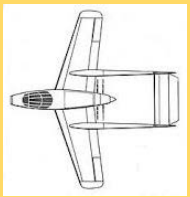 Single Pusher	 Single Tractor	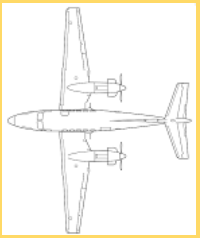 Multi Pusher	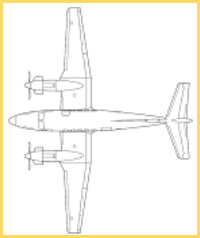 Multi Tractor
Weight	0.4	0	1	-1	-1
Manufacturability	0.1	-1	1	-1	-1
Efficiency	0.5	-1	1	-1	1
Total	1.00	-0.6	1	-1	0.5

The single tractor motor is most often chosen for small aircraft due to its efficiency and ease of manufacturability. When the propeller is placed behind the aircraft, the propeller efficiency drops dramatically and requires cooling ducts to the motor. Whereas on a tractor configuration, a few vents can be placed on the front of the aircraft to provide cooling. It is also easier to manufacture this configuration which can translate into a lighter weight structure. The single tractor motor was chosen for the MS and PR Aircraft because of the low power requirements and the need for packaging simplicity.

4.0 Preliminary Design

After completion of the conceptual design of both aircraft, the preliminary design phase commenced to determine the size of the major components of the aircraft. Preliminary design was accomplished using an iterative process, utilizing multiple trade and parametric studies. A matching graph, static and dynamic stability analysis, and aerodynamic analysis was completed to help determine the preliminary design of both aircraft.

4.1 Design and Analysis Methodology

Fuselage

The fuselage of the PR Aircraft was designed around the 32 oz. Gatorade to minimize the size and structural weight of the fuselage. The CG of the Gatorade will be placed near the desired CG of the aircraft so that the payload does not affect the CG of the aircraft. This is desirable to allow for initial test flights of the PR Aircraft to be conducted without the payload.

The fuselage of the MS Aircraft was designed around the PR fuselage to minimize the weight and size of the MS fuselage. Since the MS will be flying empty in the first mission, most of the electronics, including

the batteries and speed controller, are located in the nose of the fuselage to keep the CG at the desired location.

Wing

There are four important characteristics for the wings that need to be determined in the preliminary design.

Aspect Ratio: The aspect ratio of the MS's wing was chosen to fit the PR's wing inside of it. The aspect ratio for the PR Aircraft was chosen to match the required performance from the matching graph.

Wing Area: A matching graph was constructed for each aircraft to provide the maximum power and wing loading required to meet the performance targets for each mission.

Airfoil: The airfoil for the airplanes was carefully chosen so that flaps could be eliminated and the performance specifications met.

Dihedral: The dihedral of both airplanes had to be equivalent because the PR wing goes inside of the MS wing. The dihedral angle was chosen to improve the roll response using rudder and lateral static stability of both aircraft, allowing the elimination of ailerons.

Empennage

An X-plot was made to determine the size of the horizontal stabilizer for each aircraft. A stability margin between 10-15% was desired to ensure longitudinal stability and performance for both aircraft.

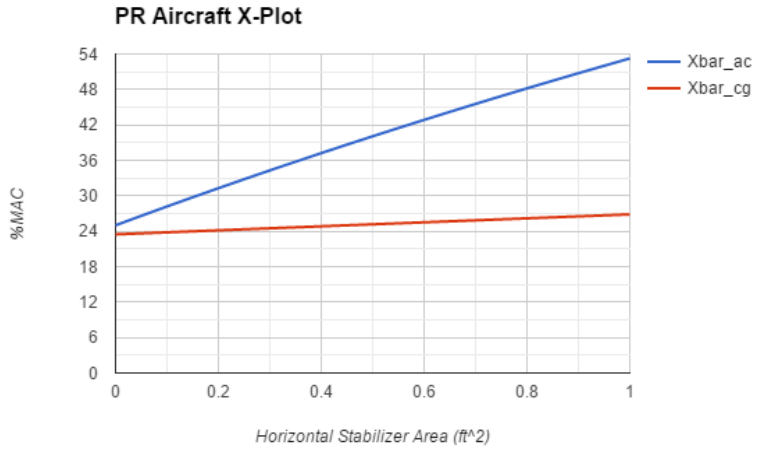

Figure 4.1.1: PR Aircraft X-Plot

It can be determined from Figure 4.1.1 that the PR Aircraft will need a horizontal stabilizer area of 0.35 ft^2 to get a stability margin of 11.1%. Due to the effect of the biplane horizontal stabilizer, the surface area will increase by 10% to account for the decrease in efficiency caused by the interference between the upper and lower stabilizers. The area that will be used for the stability analysis and to build the aircraft will be 0.385 ft^2.

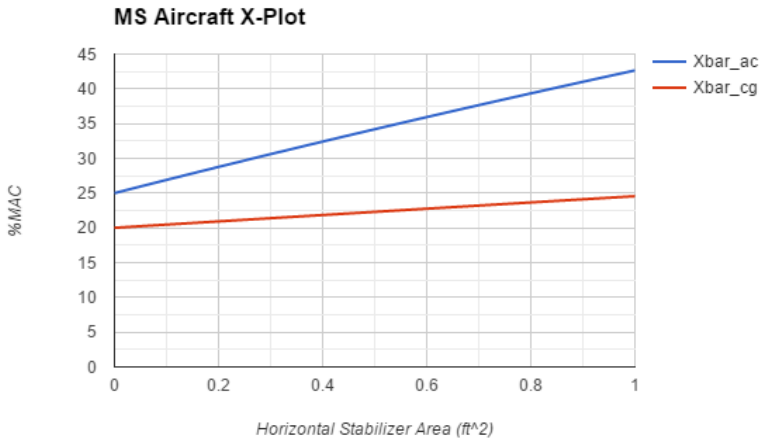

Figure 4.1.2: MS Aircraft X-Plot

The MS Aircraft will need a horizontal stabilizer area of 0.4 ft^2 to get a stability margin of 10.565% according to Figure 4.1.2. This area will be used for the stability analysis of the aircraft. However, approximately 1/3 of the MS Aircraft's horizontal stabilizer is contained within its fuselage. This wide fuselage negatively affects the effectiveness of the stabilizer and can cause instability in the longitudinal axis. This was not represented in the stability derivatives, so it will need to be approximated to ensure that the actual aircraft is stable. The stabilizer will be increased by 1/3 to account for the loss of effectiveness due to the fuselage interference. It will be built with a surface area of 0.532 ft^2.

Propulsion

The three major components of the propulsion system are the battery, propeller, and motor. Each component was selected to create the best combination of a light, efficient, and powerful system.

Battery selection: The battery is one of the most important components because it is a large factor of the RAC. The battery was selected after determining the power required to takeoff and complete each mission within the designated time. Minimizing the number of high performance battery cells is crucial to minimize weight and maintain good performance.

Propeller selection: The propeller was selected to minimize the takeoff distance and maximize the cruise speed.

Motor Selection: The motor had to satisfy the sizing determined by the matching graph in order to provide enough power to meet the performance goals. The motor was selected after determining the power loading of each aircraft.

4.2 Design Trades

The main goal of the design is to minimize weight while meeting mission requirements. A matching graph was used to determine the wing loading and power loading required to meet the performance goals, minimize weight, and minimize the size of each major component.

Matching Graph Analysis

The matching graph analysis was needed to determine the preliminary sizing of both aircraft. The performance equations for climb rate, take-off distance, stall speed, and max airspeed were varied based on the wing loading (W/S) and the power loading (W/P) of each aircraft. These were then plotted on a graph. The design point of both aircraft is the point where all the performance equation lines intersect on the matching graph. The necessary assumptions that were made in order to generate the matching graph are shown in table 4.2.1.

Table 4.2.1: PR and MS list of Assumptions

Assumptions	PR Values	MS Values
Oswald's Efficiency	0.80	0.85
$C_{L,max}$	1.4	1.4
$C_{D,0}$	0.0359	0.0791
Runway Friction Coefficient	0.02	0.02
V_{stall}	35 ft/s	35 ft/s
Density	0.002013 slugs/ft^3	0.002013 slugs/ft^3
Sigma	0.94	0.94
Takeoff Thrust	2 lbf	2 lbf
Gross Weight	3.647 lb	2.596 lb
AR	7	3
V_{max}	80 ft/s	80 ft/s

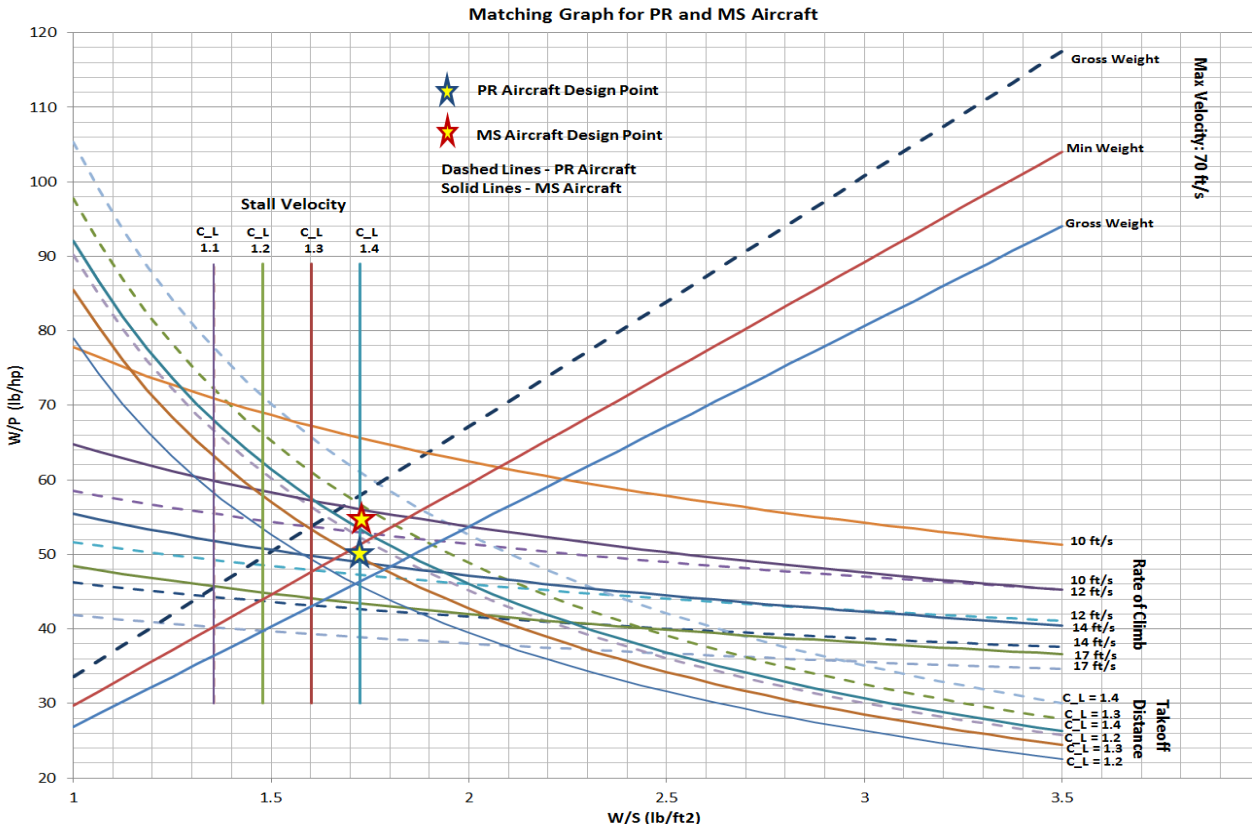

Figure 4.2.1: Matching Graph for PR and MS Aircraft

From the matching graph above, the wing loading, power loading, wing area, power required, and $C_{L,max}$ values were determined for the PR and the MS Aircraft. The following tables (Tables 4.2.2 and 4.2.3) summarize these values for each aircraft.

Table 4.2.2: Sizing of PR Aircraft Based on Matching Graph

PR Aircraft	
Wing Loading	1.73 lb/ft^2
Power Loading	55.0 lb/hp
Wing Area	2.11 ft^2
Power	0.065 hp
$C_{L,max}$	1.4

Table 4.2.3: Sizing of MS Aircraft Based on Matching Graph

MS Aircraft	
Wing Loading	1.73 lb/ft^2
Power Loading	49.0 lb/hp
Wing Area	1.5 ft^2
Power	0.053 hp
$C_{L,max}$	1.4

Figure 4.2.2 and Figure 4.2.3 show the studies that were done to evaluate the chosen aspect ratios for each aircraft, the PR (Figure 4.2.2) and the MS (Figure 4.2.3), by assuming values for the parasitic drag. The figures show that the acceptable aspect ratio (AR) for the PR and MS Aircraft are 7 and 3 respectively. The MS had a design concept such that the PR wing would fit inside it, hence a considerably lower AR.

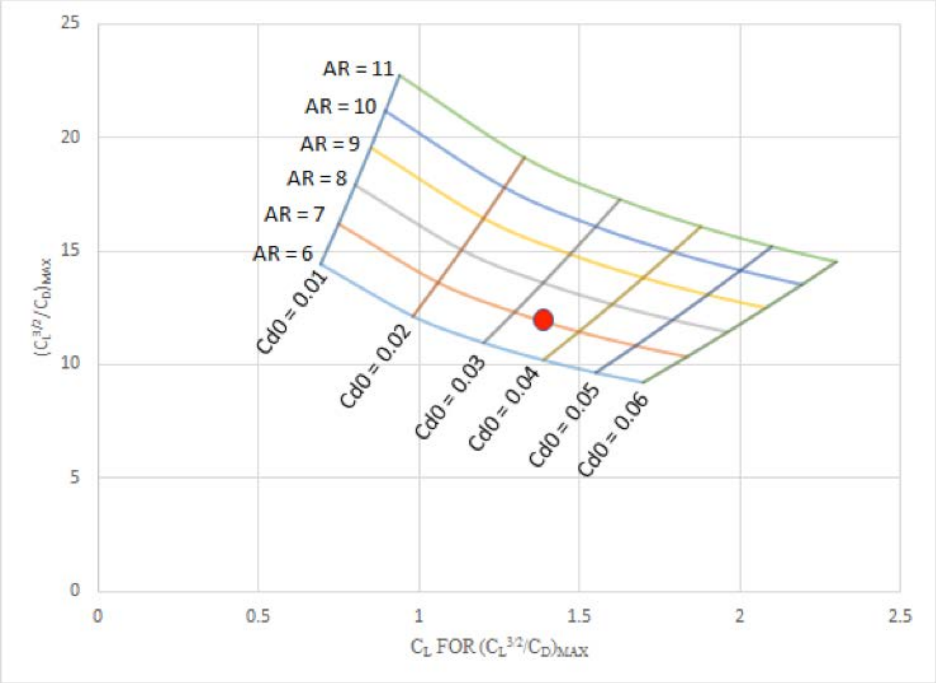

Figure 4.2.2: Effect of Aspect Ratio and Zero Lift Drag on $(C_L^{3/2}/C_D)$ and the Lift Coefficient (Production Aircraft)

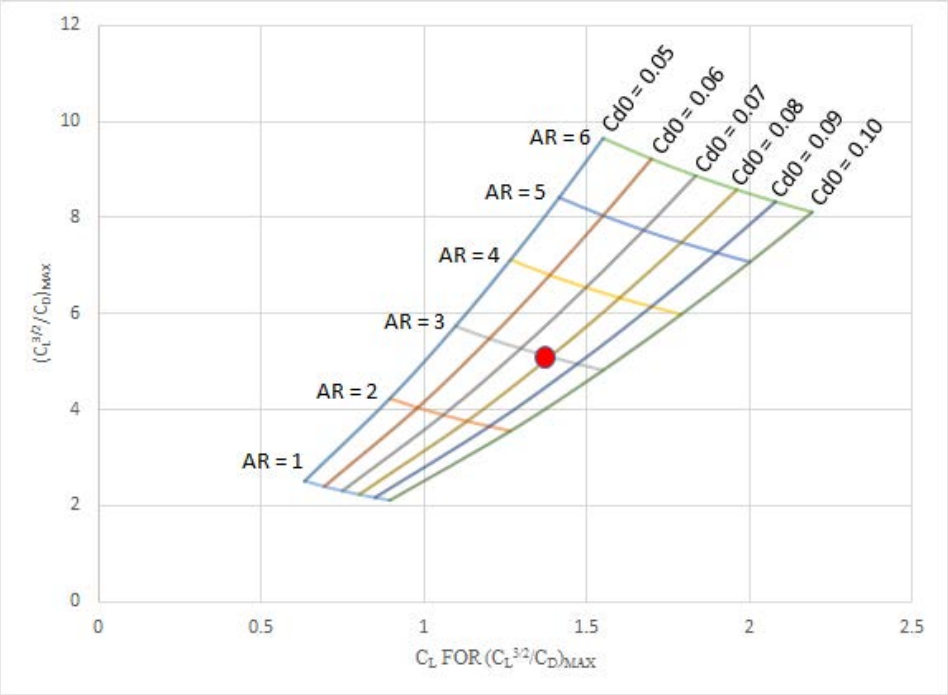

Figure 4.2.3: Effect of Aspect Ratio and Zero Lift Drag on ($C_L^{3/2}/C_D$) and the Lift Coefficient (Manufacturing Aircraft)

Zero Lift Drag Estimation

Zero-lift drag, also known as parasitic drag, is drag caused by the size and shape of the aircraft. To better understand the effects of parasitic drag on both aircraft, the Team used a computational fluid dynamics program (ANSYS Fluent) to perform flow analysis, shown in Figure 4.2.4.

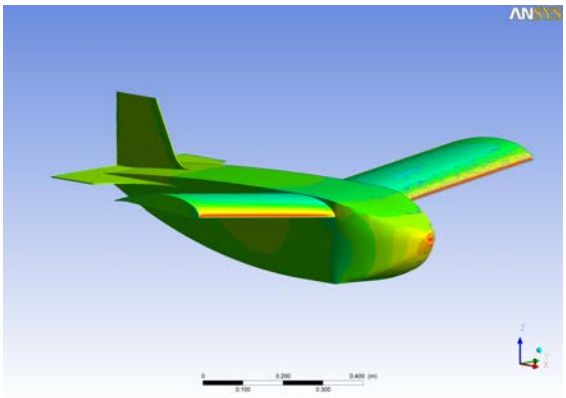

Figure 4.2.4: CFD simulation (pressure distribution of aircraft)

The data from the CFD analysis was tabulated in Table 4.2.3. As expected, the PR Aircraft produced a lower parasitic drag due to its reduced surface area and better aerodynamic shape.

Table 4.2.3: CFD results for PR and MS Aircraft

	PR Aircraft	MS Aircraft
Zero-lift drag ($C_{D,0}$)	0.0359	0.0791

Induced Drag Calculation

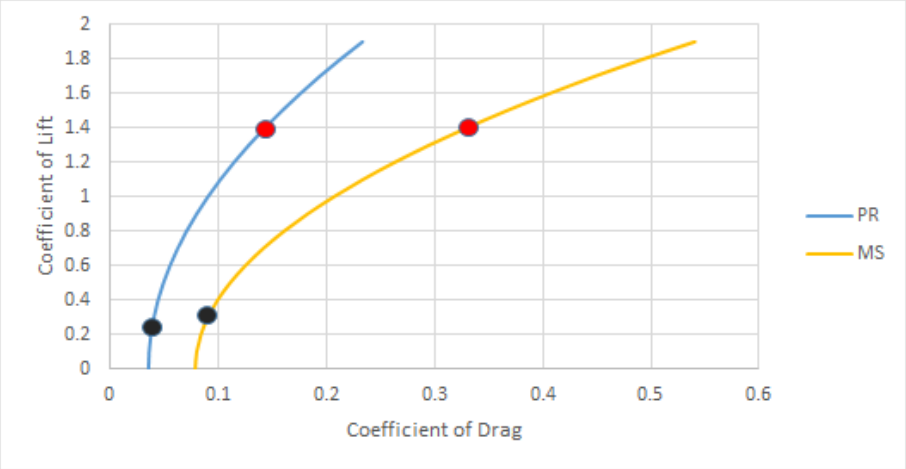

Figure 4.2.5: Drag polar of the PR and MS Aircraft

Induced drag is generated by both aircraft during flight. Induced drag is caused by the production of lift, so as an aircraft produces more lift, its drag increases exponentially as a function of the lift coefficient. The aspect ratio and shape of the wing weighs heavily in the drag generated when the wing produces lift.

$$C_D = C_{D,0} + \frac{C_L^2}{\pi e AR}$$

It was necessary to consider the relationship of C_D at various C_L for the PR and MS Aircraft in order to approximate their performance. In Figure 4.2.5, a red dot and black dot was applied to the respective aircraft in order to illustrate the effect of drag at $C_{L,max}$ (red) of 1.4 and cruise (black), as prescribed on the matching graph. The plot clearly shows that both aircraft are vulnerable to high drag at landing and takeoff, but on the other hand, drag is reduced to smaller value at cruise.

4.3 Mission Model

The missions can be categorized into four maneuvers:

- Takeoff - Without flaps, both aircraft will need to produce maximum power. The motor will be at its maximum allowable power output at this phase of the flight.
- Climb - At this phase, the airplane remains at full throttle with a climb angle of 10 degrees. The missions require the aircraft to be flown at a safe altitude, which is determined by the pilot and judges at the event. This will theoretically be a minimum of 20 feet above ground level.

- Cruise - During all missions, both aircraft are expected to remain at full throttle to complete the laps in the allocated time.
- Turns - There are two types of turns: 180 and 360 degrees. Neither aircraft have ailerons, which limits their ability to roll. It is expected that both aircraft will pull at least 2 g's during the turns.

The four maneuvers are subjected to uncertainties due to the simplification of the mission model. However, it outlines the major phases of the missions. The completion of each maneuver at an optimal level will ensure a good score.

There are three different uncertainties that were looked at while estimating the performance during each mission:

- Power Output: A constant maximum current draw was assumed for the analysis of the power output, even though the voltage and current of the battery varies throughout the flight.
- Winds: The weather conditions and the wind speed in Wichita, Kansas are very different than the weather conditions in California. The lightweight design of both aircraft puts them in danger of strong winds while flying. Both aircraft designs can survive up to 50 mph wind gusts, but the ability to complete the laps in the allotted time with wind that strong remains uncertain.
- Interference Drag: The drag of each component can be calculated easily, but the interference drag between components is very difficult to calculate, especially between the wing and the fuselage. The interference drag was estimated to be around 10% of the total drag.

4.4 Airfoil Selection

The airfoil study involved evaluating $C_{l,max}$, C_d and $(\frac{L}{D})_{max}$ for six different airfoils. The preliminary design of the airplanes eliminated flaps, so it was important to consider the maximum lift and lift-to-drag ratios. Additionally, the study was evaluated at low Reynold's numbers due to the scale of the aircraft.

The airfoils were examined at estimated cruise and takeoff velocities. Various Reynold's numbers were used based on the flight phase, which can be seen in Table 4.4.1. Additionally, the same value for both the PR and MS Aircraft is used as they will be close in size and speed.

Table 4.4.1. Flight Condition Reynold's numbers for both aircraft

Flight Condition	Reynolds Number
Cruise	270,000
Takeoff	140,000

Table 4.4.2: Airfoil Data Comparison

Airfoil	Airfoil Shapes	α @ $C_{l\,max}$ (°)	$C_{l\,max}$	C_d @ $C_{l\,max}$	Max $\frac{L}{D}$
Fx 60-126	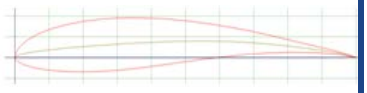	16	1.5	0.05	82.9
GOE 466	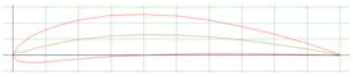	11	1.6	0.030	53.3
MH 114		12	1.9	0.024	82.2
NACA 2414	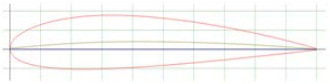	15	1.3	0.06	65.1
NACA 63015	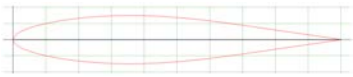	15	1.2	0.05	24
USA98	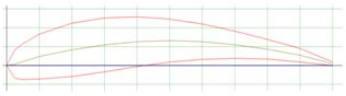	12	1.7	0. 03	84.1

Airfoil Tools and Airfoil Database were used to compile the table above at the takeoff and cruising Reynold's numbers. For the best performing airfoil, a high maximum lift and lift-to-drag ratio is necessary. According to the table above, the optimal airfoil for the competition is the MH 114. The MH 114 produces a $C_{l,max}$ of 1.9, C_d of 0.024 at the $C_{l,max}$, and a $(\frac{L}{D})_{max}$ of 82.2. Overall, the airfoil matched the criteria set by the mission specifications. Due to the nature of the design, both aircraft will need to use the same airfoil in order for the PR wing to fit inside of the MS wing.

4.5 Stability and Control

Stability is an aircraft's ability to resist disturbances and return to its equilibrium. Stability can be defined in two ways: static stability and dynamic stability. Static stability is the natural tendency of the airplane to produce forces opposing a disturbance, while dynamic stability is the tendency of the airplane to damp out oscillations and return to, or close to, steady state.

The Team's main concern dealt with longitudinal stability, as the wing, fuselage, and stabilizer placement of both aircraft is tightly coupled and thus difficult to modify during testing. Lateral stability was also important, particularly since the high dihedral chosen could negatively affect dutch roll stability. However, experience has shown that a properly designed straight wing airplane, with slightly generous vertical fin volume, would typically be sufficiently stable in dutch roll. Thus, the investigation focused on longitudinal stability. A state space computer model of the airplane was developed and its response to elevator inputs evaluated. Hence, our main concern was to establish longitudinal stability. As such, MATLAB was utilized to evaluate the time domain and frequency domain response of both aircraft using a 1 degree elevator input. The objective of these analyses was to investigate the dynamics of the aircraft and to assess the aircraft geometry based on its response.

In longitudinal stability, there exists two modes: short period and phugoid. Short period is typically a highly damped, relatively fast oscillatory mode involving angle of attack (α) and pitch angle (θ), while the phugoid mode manifests as lower damping, slow oscillation in horizontal velocity (u) and pitch angle (θ). In the time domain response, the PR and MS Aircraft generated the graphs seen in Figure 4.5.1.

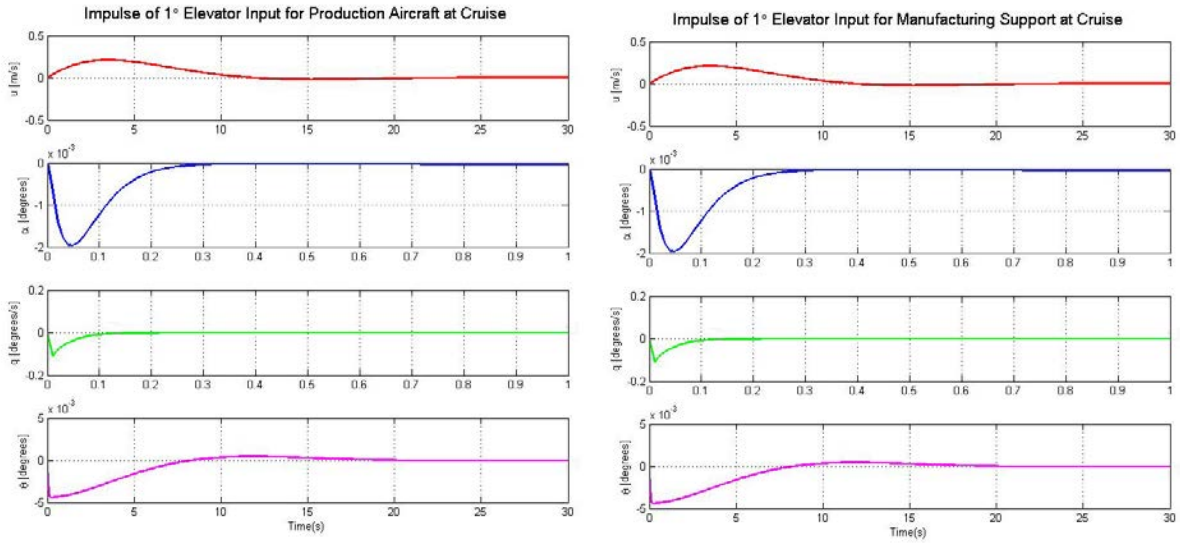

Figure 4.5.1: Time domain response of PR and MS Aircraft using a 1 degree elevator input

The short period and phugoid modes for both aircraft can be isolated for further investigation. As shown in Figure 4.5.2, the short period mode for the PR Aircraft had a settling time of 0.3 - 0.4 seconds while the phugoid mode had a settling time of 70 - 80 seconds.

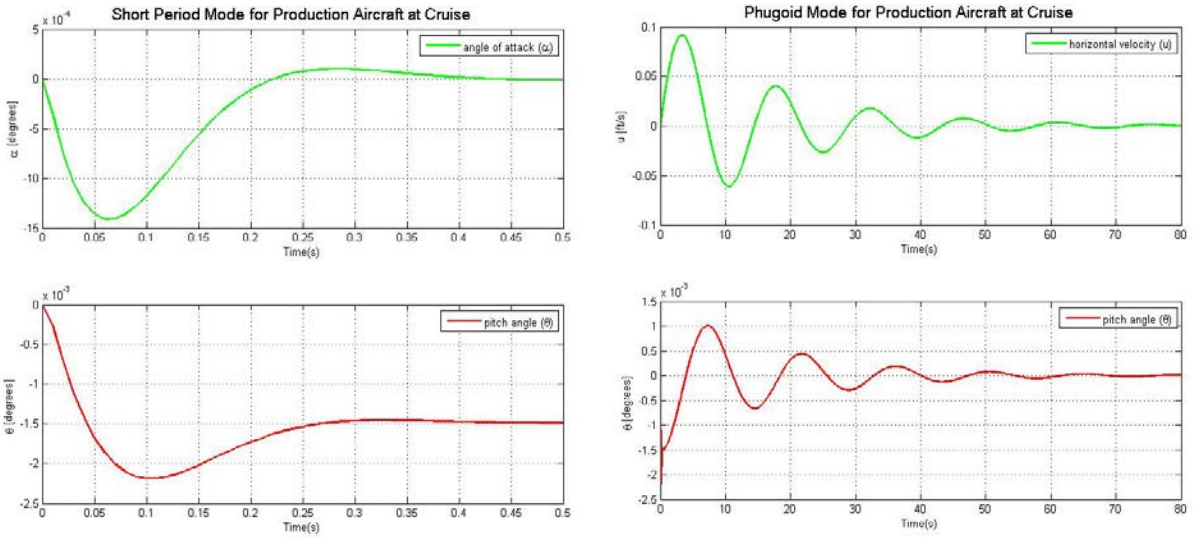

Figure 4.5.2: Isolation view of short period and phugoid mode for the PR Aircraft

The MS Aircraft had a settling time of 0.2 - 0.3 seconds for the short period mode, and the phugoid mode had a settling time of 20 - 30 seconds, as seen in Figure 4.5.3.

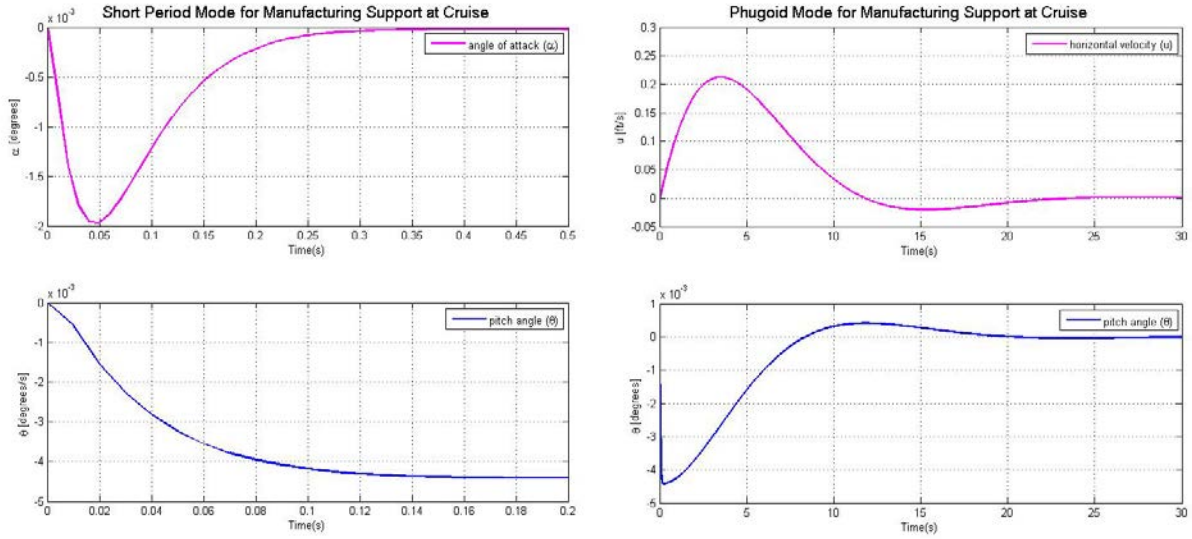

Figure 4.5.3: Isolation view of short period and phugoid mode for the MS Aircraft

The time domain response to a disturbance shows both aircraft to be longitudinally stable. The PR Aircraft response shows low, but still adequate damping for both longitudinal modes. The relatively short coupled design of the plane, combined with its stubby tail surfaces, is believed to be a significant contributor to this behavior. Table 4.5.1 summarizes the frequencies and damping ratios for the PR and MS aircraft.

Table 4.5.1: Damping and natural frequency characteristics of PR and MS Aircraft

	PR Aircraft	MS Aircraft
$\omega_{\text{short period}}$ (rad/s)	18.73	24.25
ω_{phugoid} (rad/s)	0.4393	0.3338
$\zeta_{\text{short period}}$	0.6415	0.9861
ζ_{phugoid}	0.1299	0.6009

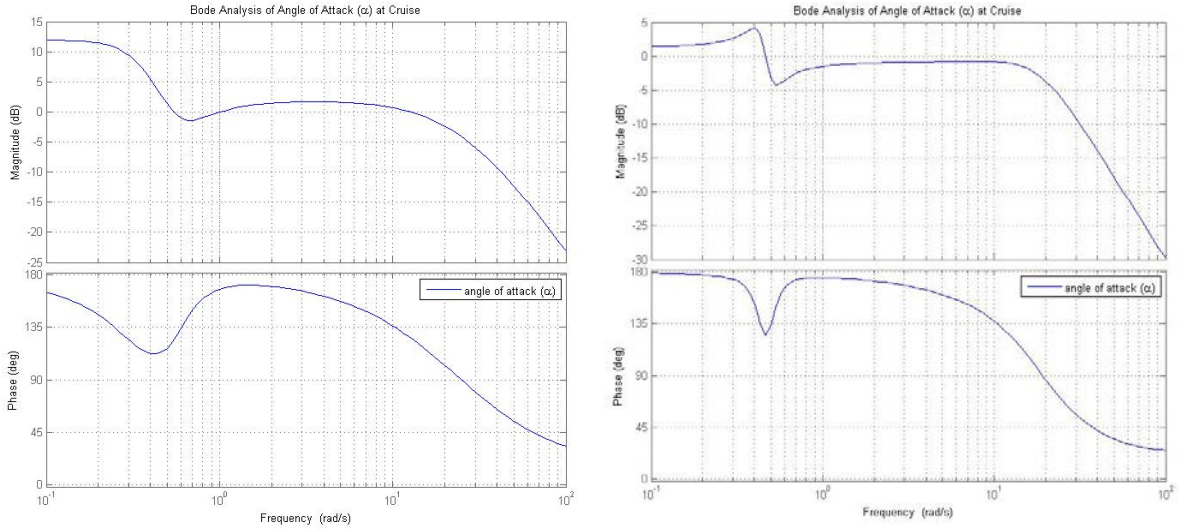

Figure 4.5.4: Frequency response of angle of attack for MS Aircraft (left) and PR Aircraft (right)

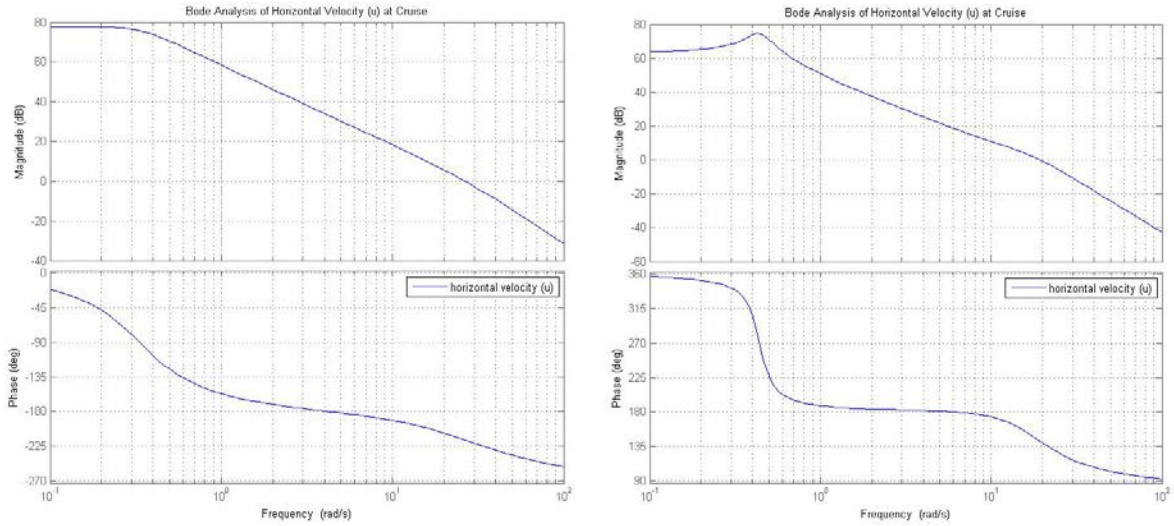

Figure 4.5.5: Frequency response of horizontal velocity for MS Aircraft (left) and PR Aircraft (right)

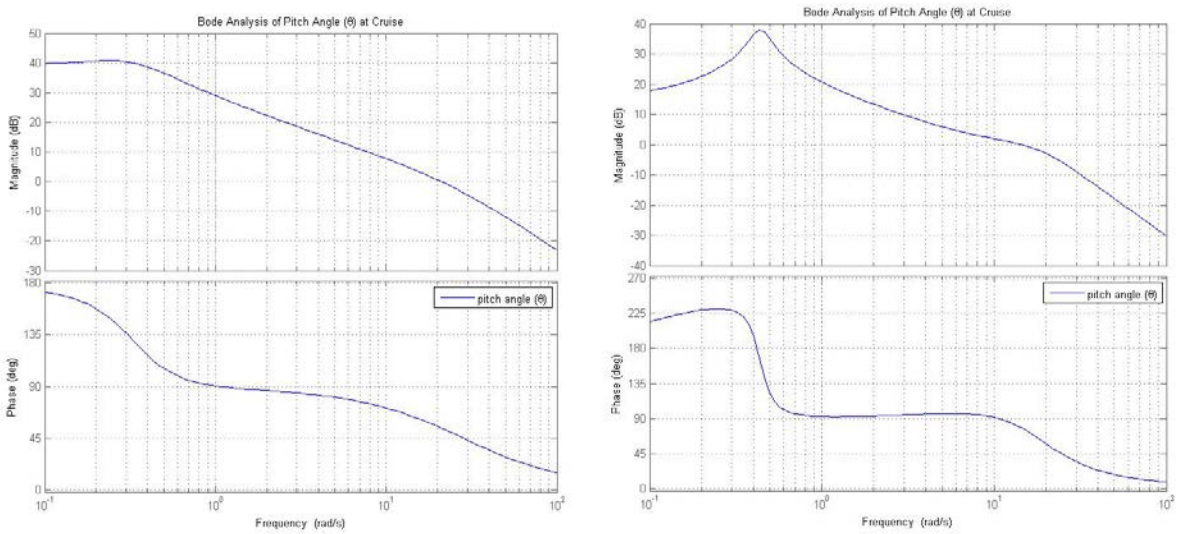

Figure 4.5.6: Frequency response of pitch angle for MS Aircraft (left) and PR Aircraft (right)

The bode analysis in Figure 4.5.4 - Figure 4.5.6 clearly shows the different modes in longitudinal stability for the MS and PR Aircraft. In Figure 4.5.4 and Figure 4.5.6, the sudden drop in the slope at high frequencies is a manifestation of short period mode. Phase graphs for angle of attack and pitch angle show a 180 degree offset due to definition of positive elevator input as trailing edge down, thus commanding negative attitude angles with a positive elevator input. Additionally, phugoid mode is very noticeable in Figure 4.5.5 and Figure 4.5.6, which is in the apparent lower frequency range.

Elevator Effectiveness

The effectiveness of the elevators needed to be assessed to ensure they were large enough to control the aircraft. One criterion was that elevator power should be sufficient to command an aerodynamic stall. This was desirable to ensure the maximum lift capability of the airplane could be exploited on takeoff and landing. The elevator deflection to balance the airplanes at a variety of angles of attack is presented in Figure 4.6.1. The wing has a theoretical stall angle of attack of 13°, so the elevator deflection needs to be sufficient to counter the moment of the wing at this angle of attack to maintain level flight. The elevator deflection was calculated by summing the moment coefficients of the aircraft and ensuring that the elevator produced enough of a moment to counter the total moment of the aircraft. This was calculated for angles of attack from -5 to 14 degrees and the results are plotted in Figure 4.6.1. The elevator effectiveness was also evaluated with the aircraft at their maximum speed and generating 3g's of force. The red dots on the plot show the deflection necessary to generate 3g's at max speed for each aircraft.

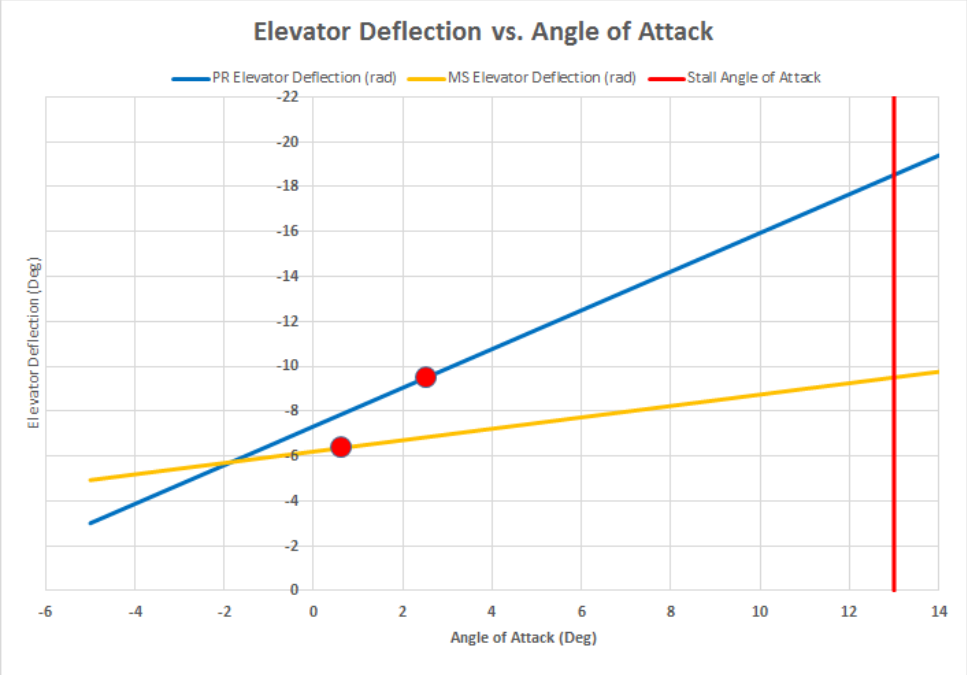

Figure 4.6.1: Elevator deflection versus angle of attack for both aircraft

The PR Aircraft will need an elevator deflection of -19 degrees in order to counter the moment produced by the wing at its stall angle of attack. The MS Aircraft requires an elevator deflection of -9.5 degrees to counter its moment at the same condition. These are both reasonable deflections for the control surface to move, which leads to the determination that the elevators are properly sized for each aircraft. Additionally, the elevator is sufficiently sized to produce more than 3g's at their maximum speed.

4.6 Estimated Mission Performance

Based on preliminary design criterias, the following data can be assessed in Table 4.6.1. To study the effects of the wind condition in Wichita, Kansas, different cases were studied to evaluate the performance during all missions. An assumption was made such that the cruise speeds were constant during the entire flight.

In Mission 1, the MS Aircraft shall fly empty and is anticipated to have a flight time of 88, 135, and 266 seconds at various wind speeds: 0, 15, and 30 knots. As per requirement, the flight time is substantially passing. With a lighter weight, the takeoff distance is smaller than when it's loaded with the PR Aircraft. However, the turn radius will be much larger in Mission 1 in comparison to Mission 2 due to the cruise velocity difference. As shown in Table 4.6.1, Mission 2 will require more runway but it's well below the limit of 100 feet. The plane only flies one lap for this mission and has anticipated 30, 47, and 97 second flight time at the respective wind speeds. In Mission 3, the PR Aircraft is required to have a higher maximum

speed to counteract the wind speed and the weight of the Gatorade. It will also require more runway than the MS Aircraft, about 70 feet.

Table 4.6.1: Estimated Mission Performance

Mission 1		Mission 2		Mission 3	
Manufacturing Support (Unloaded)	1.597 lb	Manufacturing Support (Loaded)	2.596 lb	Production Aircraft (Loaded)	3.647 lb
Takeoff Distance	20.0 ft	Takeoff Distance	27.4 ft	Takeoff Distance	69.9 ft
Cruise Speed (0 Knot Wind)	74.9 ft/s	Cruise Speed (0 Knot Wind)	73.0 ft/s	Cruise Speed (0 Knot Wind)	79.9 ft/s
Ground Speed (15 Knot Wind)	49.6 ft/s	Ground Speed (15 Knot Wind)	47.7 ft/s	Ground Speed (15 Knot Wind)	57.6 ft/s
Ground Speed (30 Knot Wind)	24.9 ft/s	Ground Speed (30 Knot Wind)	23 ft/s	Ground Speed (30 Knot Wind)	29.9 ft/s
Turn bank angle	60°	Turn bank angle	60°	Turn bank angle	60°
Turn radius	101 ft	Turn radius	96 ft	Turn radius	115 ft
Takeoff Time	1 sec	Takeoff Time	1 sec	Takeoff Time	2 sec
Lap Time (0 Knot Wind)	30 sec	Lap Time (0 Knot Wind)	30 sec	Lap Time (0 Knot Wind)	30 sec
Lap Time (15 Knot Wind)	44 sec	Lap Time (15 Knot Wind)	46 sec	Lap Time (15 Knot Wind)	40 sec
Lap Time (30 Knot Wind)	88 sec	Lap Time (30 Knot Wind)	95 sec	Lap Time (30 Knot Wind)	74 sec
Laps	3	Laps	1	Laps	3
Flight Time (0 Knot Wind)	88 sec	Flight Time (0 Knot Wind)	30 sec	Flight Time (0 Knot Wind)	84 sec
Flight Time (15 Knot Wind)	135 sec	Flight Time (15 Knot Wind)	47 sec	Flight Time (15 Knot Wind)	122 sec
Flight Time (30 Knot Wind)	266 sec	Flight Time (30 Knot Wind)	97 sec	Flight Time (30 Knot Wind)	222 sec

5.0 Detail Design

The detailed design of the aircraft is the next step in the refinement of the aircraft. The conceptual and preliminary design sections established generally how the aircraft will look, function, and perform; this section's purpose is to refine those down to aircraft that will meet those specifications.

5.1 Dimensions

Tables 5.1.1 and 5.1.2 detail the specifications for the wing and empennage for the aircraft. Table 5.1.3 details the overall dimensions of the aircraft and specifies the propulsion system that each aircraft will use.

Table 5.1.1: PR Aircraft Surface Dimensions and Specifications

Wing		Vertical Stabilizer		Horizontal Stabilizer	
Airfoil	MH 114	Airfoil	Flat Plate	Airfoil	Flat Plate
Span	45.6 in	Span	4.13 in	Span	8.0 in
Area	301.0 in^2	Area	48.0 in^2	Area	58.7 in^2
Incidence	+2°	Incidence	0°	Incidence	-2°

Table 5.1.2: MS Aircraft Surface Dimensions and Specifications

Wing		Vertical Stabilizer		Horizontal Stabilizer	
Airfoil	MH 114	Airfoil	Flat Plate	Airfoil	Flat Plate
Span	46.1 in	Span	9.7 in	Span	18.2 in
Area	553.5 in^2	Area	78.7 in^2	Area	194.8 in^2
Incidence	+2°	Incidence	0°	Incidence	-2°

Table 5.1.3: Aircraft Dimensions and Propulsion system

PR Aircraft Dimensions		MS Aircraft Dimensions		Propulsion System (Both Aircraft)	
Overall Length	25.3 in	Overall Length	25.3 in	Motor	Model Motors AXI 2820/12
Fuselage Width	4.38 in	Fuselage Width	4.38 in	Speedcontrol	Castle Creations Thunderbird 18
Overall Height	9.5 in	Overall Height	9.5 in	Battery	7 cell Elite 1500 mA
Takeoff Weight (w/o Payload)	1.40 lb	Takeoff Weight (w/o Payload)	1.40 lb	Power (Max)	126 W

5.2 Structural Characteristics

Each of the aircraft structures needed to be designed to handle normal flights load, about +2.8 g's. The PR Aircraft will need the following: a door in the front for access to electrical components, a removeable wing to allow access into the payload bay in the fuselage, and a hole in the aft section of the fuselage to allow access for to the servos. The MS Aircraft will need the following: a door in the front for access to electrical components, a removeable wing and upper-aft fuselage for access to the payload bay, doors in the underside of the wing to allow for the insertion of the PR Aircraft's wing, and a door in the aft section of the fuselage for access to servos. All of these doors pose a challenge to the structural integrity of the aircraft. Most challenging of all are the hinged lower wing covers of the MS Aircraft. Structural concepts and flight loads were investigated to optimally design a structure that can overcome these challenges.

Fuselage

The fuselages consist of three plywood bulkheads: one at the front to mount the motor, one at the leading edge of the wing, and one at the trailing edge of the wing. The bulkheads at the leading and trailing edges of the wing will carry the loads exerted on the fuselage by the wing. The fuselage sides will contain large lightening holes near the centerline of the fuselage, as this is the area with the lowest shear flow. The corners of the square fuselage will contain balsa wood stringers that will help stiffen the structure in these high stress areas. The PR fuselage will have a large circular hole in the center bulkhead to provide support for the payload. A balsa wood cradle will be glued into place on the fuselage floor to hold the aft end of the gatorade bottle from moving side to side and aft in the aircraft. A small balsa string will then be placed on the top of the Gatorade that will press on the lower side of the wing; this will prevent the gatorade from moving vertically. The MS fuselage is configured rather differently, as the PR Aircraft, when carried as payload, is suspended by the wing.

Figure 5.2.1: PR fuselage under construction

Wing

The wings are comprised of a traditional spar and rib wing construction. The spar box is composed of a spruce hardwood upper and lower spar that are connected together by thin balsa wood, called shear webs, at their leading and trailing edges. The shear webs are 1/16” thick balsa wood with its grain running vertically. This will prevent the upper and lower spars from moving in relation to one another during bending loads on the wing. Leading and trailing edge balsa wood sheets give the wing torsional rigidity and allow for large open bays to exist between these sheets. The open bays between the trailing edge sheets and the leading edge sheets will be covered in Monokote; this allows for a very lightweight structure and the Monokote helps carry some of the tension on the lower side of the wing produced during flight. The MS Aircraft will have a large door on the bottom of the wing that is secured to the bottom leading edge sheet using Monokote. The Monokote then acts as a hinge for the door to open. the door is then secured to the lower trailing edge sheet using screws. Screws are used to provide a strong point of contact to keep the wing torsionally strong. Small holes with threads tapped into the wing tip ribs exist on both the PR Aircraft and MS Aircraft. Once the PR wing is placed inside of the MS wing, a 8-32 screw passes through the MS wing tip and into the PR wing tip on both the left and right wing tips. This ensures a strong point that holds the PR Aircraft into the MS Aircraft. Under bending loads, these screws will ensure that the PR Aircraft wing bends along with the MS Aircraft wing.

Figure 5.2.2: MS wing under construction alongside completed PR wing

Empennage

The horizontal and vertical stabilizers are constructed of thin sheets of balsa wood for each aircraft: 3/32” thick for the PR Aircraft and 1/8" thick for the MS Aircraft. The grain of the balsa wood was placed such that it gave each surface the maximum strength in bending. Lightening holes were not implemented on the stabilizers in order to allow for necessary torsional rigidity to prevent aeroelastic effects causing flutter. The elevator and rudder were constructed in a similar fashion; however, lightening holes were placed in these

control surfaces to make them lighter. Due to their chord being small, the holes did not reduce the structure enough to make the surfaces prone to flutter. Attachment stiffness and freeplay in control surfaces are kept to a minimum to minimize the probability of encountering flutter during the normal flight envelope.

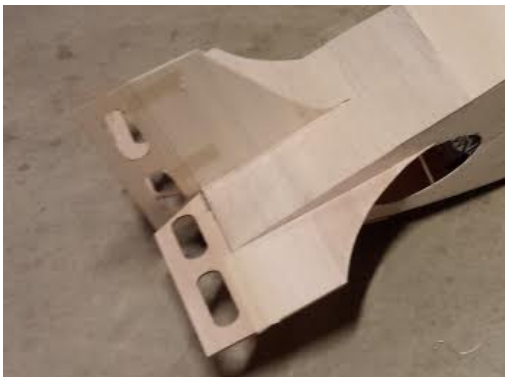

Figure 5.2.3: Empennage design for the MS Aircraft

Landing Gear

The landing gear was constructed with 0.032" thick, 2024-T3 aluminum. The thin aluminum provides enough strength to withstand normal takeoff and landing loads; however, under extreme conditions, the aluminum has the capability to plastically deform a significant amount before failing. Aluminum was chosen over carbon fiber for this reason. The landing gear could have been built with carbon fiber at equivalent weight, but it would not withstand extreme loads as well as the aluminum because it fails at a load very close to its plastic deformation stress. The axles were machined out of 2024-T3 because of the materials light weight compared to steel and ease of manufacturing compared to carbon fiber. One end of the axle was flanged and threaded so that it could be threaded onto the bent aluminum landing gear. The landing gear was then attached to the fuselage using two 4-40 screws.

5.3 System and Subsystem Design

Propulsion

Two different types of motors were considered, brushed and brushless. Brushless motors provide about twice the power to weight ratio compared to brushed motors so they were the obvious choice. The different types of brushless motors need to be considered as well. Inrunner brushless motors provide very high RPM with low torque whereas outrunner brushless motors provide a lot of torque with low RPM. Since both the PR and MS Aircraft will be required to lift heavy payloads and takeoff within a 100 ft takeoff run, the outrunner brushless motor is desired with its high torque output. This motor will have the ability to turn a large diameter propeller and achieve the quick acceleration necessary to make the prescribed takeoff distance. The aircraft needs to cruise at a speed around 70 ft/s to provide a robust design against possible high winds at the competition. By tailoring the pitch of the propeller to the desired cruise speed, the desired

speed can be achieved by the outrunner brushless motors, even with their lower RPM. This type of motor will allow both of the critical design points of takeoff distance and cruise speed to be achieved.

Table 5.3.1: Outrunner brushless motor selection

Motor	Weight (lb)	Input Voltage (V)	Maximum Amperage (A)	Efficiency	Power (Watts)	Power (hp)	RPM
AXI 2212/12	0.126	7.2	28	0.82	165.31	0.222	14040
AXI 2212/20	0.126	7.2	16	0.82	94.46	0.127	8280
AXI 2212/26	0.126	7.2	12	0.80	69.12	0.093	6624

The power requirement for the PR Aircraft is 0.065 hp and the MS Aircraft is 0.053 hp, which was established by the matching graph in Figure 4.2.1. The power of each one of the motors need to be approximated by multiplying the shaft power of the motor by the propeller efficiency. The efficiency of propellers changes based on the velocity of the aircraft. Therefore, the propeller efficiency needed to be better approximated as a function of velocity in order to derive the power delivered by the propeller at each of the critical flight phases which are takeoff and cruise. Several equations were set up for various pitch to diameter ratios to determine the efficiency.

Table 5.3.2: Propeller efficiency and propeller power for selection of motors

Motor	Recommended Propeller	Propeller Efficiency at Takeoff	Propeller Efficiency at Cruise	Propeller Power at Takeoff (hp)	Propeller Power at Cruise (hp)
AXI 2212/12	8x4	0.54	0.81	0.120	0.179
AXI 2212/20	9x5	0.52	0.76	0.066	0.096
AXI 2212/26	11x5.5	0.54	0.72	0.050	0.067

The Model Motors AXI 2212/20 provides sufficient power for both the takeoff and cruise flight conditions, so this is the motor that will be implemented on both aircraft.

The contest rules state that the aircraft need to be powered by either Nickel Metal Hydride (NiMH) or Nickel Cadmium (NiCad) batteries. The NiMH cell was chosen because it is the significantly lighter cell and will deliver all of the power needed. Six Elite 1500 mAh NiMH cells will be used in series. This will give

the required voltage of 7.2 V and the required capacity of greater than 1300 mAh for the minimal amount of weight.

A Castle Creations Thunderbird 18 speed control was chosen to deliver the power from the batteries to the electric motor. This was chosen because of its small lightweight design and its maximum amperage.

Controls

Hitec HS-53 servos were chosen to control the elevator and rudder on each aircraft. These servos deliver the same amount of torque as a traditional nine gram servo but weigh in at only eight grams. They have the capability to deliver the appropriate amount of maximum torque to handle the control loads at each of the aircraft's maximum speed.

Radio Control

A Spektrum DX7 will be used as the transmitter for both aircraft and a Spektrum AR7200 will be used as the receiver. These were chosen because of their broad spectrum technology that operates on 2.4 GHz and eliminates the possibility of another aircraft operating on the same channel. The receiver was also chosen because of its double redundant antenna design and fail safe programming option that automatically inputs full elevator and rudder in the event of a signal loss. A 4 cell, 4.8 V, 2/3 AAA battery pack will power the receiver and servos.

5.4 Weight and Balance

The weight and balance of an aircraft is a very important aspect that ensures the aircraft will have both enough performance, stability, and control for flight.The weight and balance characteristics of each of the two aircraft were evaluated. Both wing planform area and power requirements were estimated based on target weights for each aircraft using the matching graph presented in Section 4. The balance of the aircraft varies based on the placement of the components within the aircraft. If the distribution of mass is too far aft then the aircraft will not have a large enough stability margin and will be unstable in pitch. If the mass is distributed too far forward, then the elevator will not have enough control power to control the aircraft in pitch. The X-Plots in Figures 4.1.1 and 4.1.2 established the size of the horizontal stabilizer necessary to achieve a 10% stability margin with the aircraft's CG at the quarter chord. The aircraft's balance point will need to be on or very near to the quarter chord to achieve desired stability. Figures 5.4.1 and 5.4.2 show the CG of the aircraft's components with yellow markers and the overall CG of the aircraft with the red marker. A coordinate system was established ahead of and below the aircraft to serve as a datum from which the CG of all components could be measured for CG calculations.

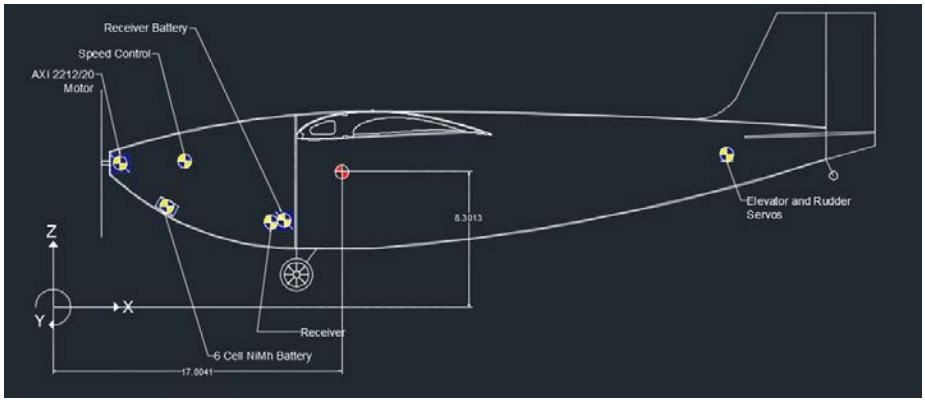

Figure 5.4.1: MS Aircraft CG location

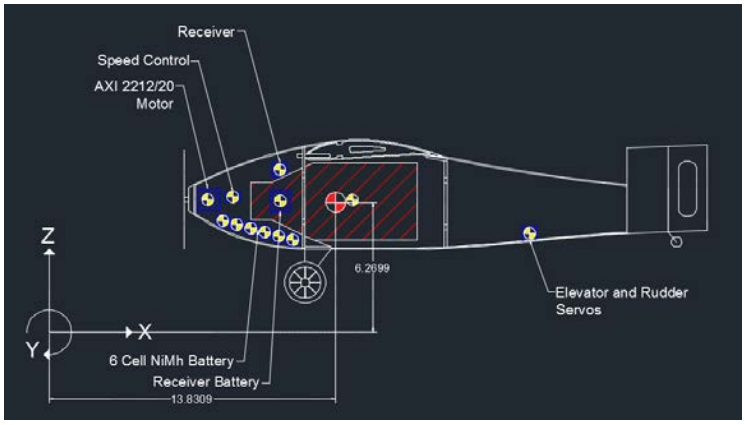

Figure 5.4.2: PR Aircraft CG Location

The mass and CG of the aircraft structures was estimated using Solidworks. A three dimensional model was created that took into account the density of all the materials used. This allows for a more refined approximation of the structural weight, center of gravity, and moment of inertia. The moment of inertia of each component was added to that of the structure to generate an approximation for the final aircraft's inertia. This information was critical to the derivation of dimensional stability derivatives used for the stability and control analysis in section 4.5. The approximate inertia values can be seen in Table 5.4.1. The center of gravity was calculated by summing the mass of all components and their distances from the datum (arm). The arm and mass were then multiplied together for each component to generate their moment. The sum of all of the moments was divided by the total weight of all components to derive the cg of the aircraft. This was done for each aircraft in their configuration for each mission. Table 5.4.2 shows the weight, arm, and moment of each component and the resulting cg for the aircraft as a distance from the datum and in terms of percent chord. The cg of each aircraft falls within 2% of the quarter chord. With the tail sized using the X-Plot in the previous section, the aircraft should be statically stable in pitch with their cg location.

Table 5.4.1: Moments of inertia for the aircraft

	Mission 1 (MS)	Mission 2 (MS with Payload)	Mission 3 (PR with Payload)
Ixx (lb*in^2)	42.432	48.370	47.218
Iyy (lb*in^2)	26.140	110.207	94.212
Izz (lb*in^2)	42.697	132.702	111.042

Table 5.4.2: CG calculation for the aircraft for each mission

	Mission 1 (MS)			Mission 2 (MS with Payload)			Mission 3 (PR)		
Component	Weight (lb)	Arm (in)	Moment (in-lb)	Weight (lb)	Arm (in)	Moment (in-lb)	Weight (lb)	Arm (in)	Moment (in-lb)
Overall Structure	1.090	22.700	24.743	1.090	22.700	24.743	0.400	15.830	6.332
Propulsion Battery	0.324	7.000	2.268	0.324	7.000	2.268	0.324	10.071	3.263
Motor	0.126	6.633	0.836	0.126	6.633	0.836	0.126	7.656	0.965
Speed Control	0.038	8.915	0.339	0.038	8.915	0.339	0.038	8.861	0.337
Elevator Servo	0.018	41.505	0.747	0.018	41.505	0.747	0.018	23.195	0.418
Rudder Servo	0.018	41.505	0.747	0.018	41.505	0.747	0.018	23.195	0.418
Receiver	0.031	13.370	0.414	0.031	13.370	0.414	0.031	11.133	0.345
Receiver Battery	0.120	14.230	1.708	0.120	14.230	1.708	0.120	11.160	1.339
Mission 2 Payload	-	-	-	0.751	18.917	14.206	-	-	-
Mission 3 Payload	-	-	-	-	-	-	2.238	14.480	32.402
Total	1.765	-	31.802	2.516	-	46.008	3.313	-	45.817
Aircraft CG	18.018			18.286			13.831		
Cg in % Chord	24.32%			26.55%			25.47%		

5.5 Mission Performance

The mission performance was first estimated by approximating the radius of the turn for the aircraft. Based on the wing loading, structural integrity of the wing, and cruise speed, it can be approximated that the MS Aircraft will turn with a radius of 101 feet for Mission 1 and 96 feet for Mission 2. The PR Aircraft will have a turn radius of approximately 115 feet. The MS Aircraft has an estimated cruise speed of 74.9 ft/s for Mission 1 and 73.0 ft/s for Mission 2. The PR Aircraft has an estimated cruise speed of 79.9 ft/s. Taking into account the aircraft's turning radii and the course layout, a single lap should be about 2200 ft. The MS Aircraft should complete a single lap in 50 seconds for Mission 1 and 60 seconds for Mission 2. The aircraft will need to fly three laps in under five minutes for Mission 1, and the total flight time comes out to 2.5 minutes. This leaves a factor of safety of 200% to allow for high winds at the contest. Mission 2 only requires one lap for our particular design, so the aircraft will only fly for 60 seconds. The PR Aircraft should complete a single lap in 40 seconds. The aircraft will need to fly three laps in under five minutes, and the

total flight time comes out to two minutes. This also leaves a significant factor of safety to account for high winds. The PR Aircraft does not disassemble in order to fit inside of the MS Aircraft, so the single component design will guarantee full points for the bonus mission. Full points should be received for each mission. Factoring in the RAC (seen in Table 5.5.1), the team should receive a score of 17.14 before the report score is accounted for.

Table 5.5.1: Current aircraft RAC

Components	EW_1 (lbs)	Et_{Bat1} (lbs)	$N_{Components}$	EW_2 (lbs)	Wt_{Bat2} (lbs)	RAC
Value	0.988	0.375	1	1.813	0.375	1.05

5.6 Drawing Package

This section contains a comprehensive CAD package that details the design of the aircraft. Drawings for aircraft dimensioning, structural arrangements, systems layouts, and payload accommodations can be seen for each aircraft.

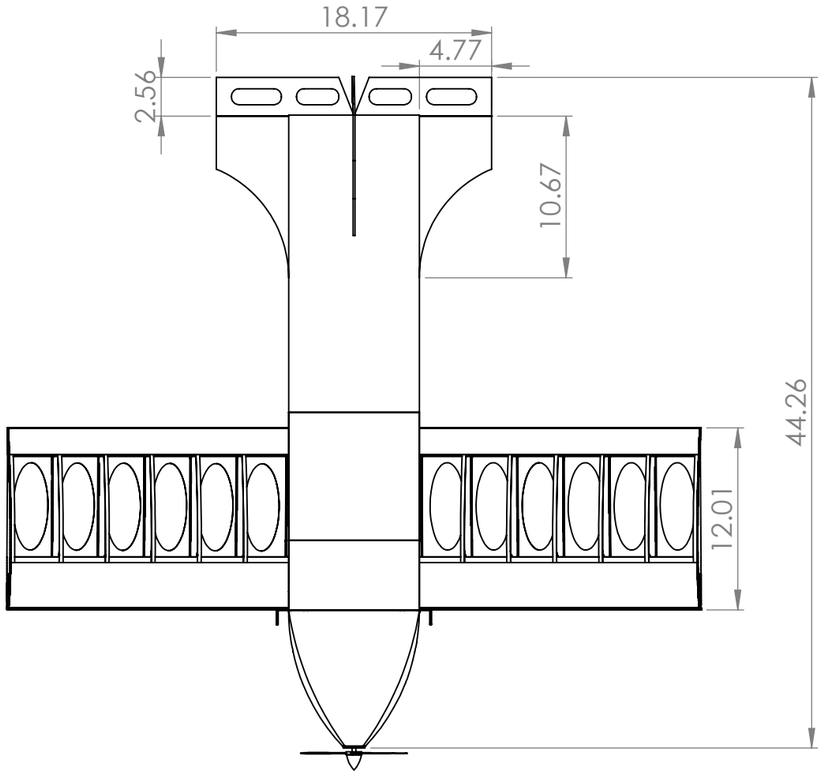

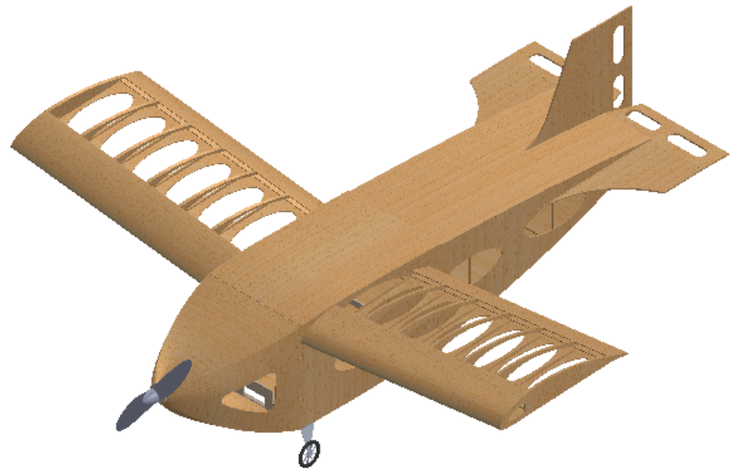

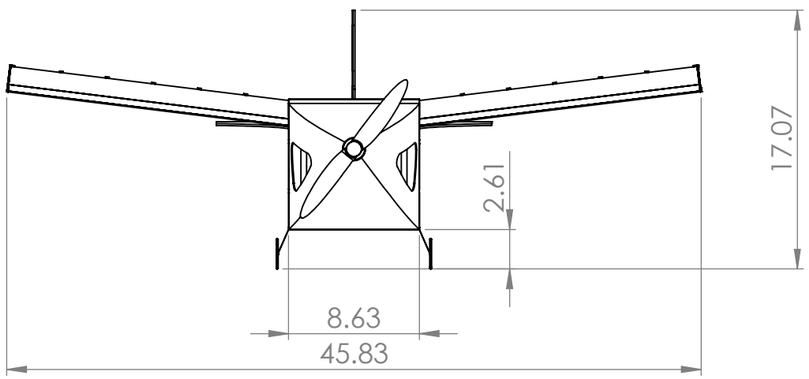

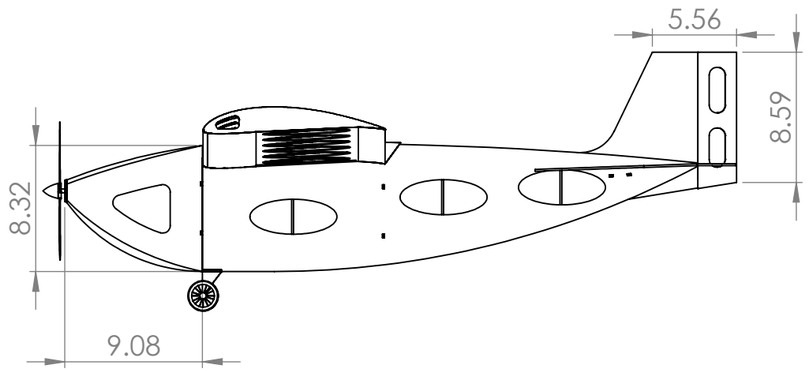

SOLIDWORKS Student Edition.
For Academic Use Only.

AIAA - Design Build Fly 2016

TITLE:
MANUFACTURING SUPPORT
AIRCRAFT
3 - VIEW

UNLESS OTHERWISE SPECIFIED:
DIMENSIONS ARE IN INCHES

SIZE	DWG. NO.	REV
B	5	
SCALE: 1:10	WEIGHT:	SHEET 1 OF 1

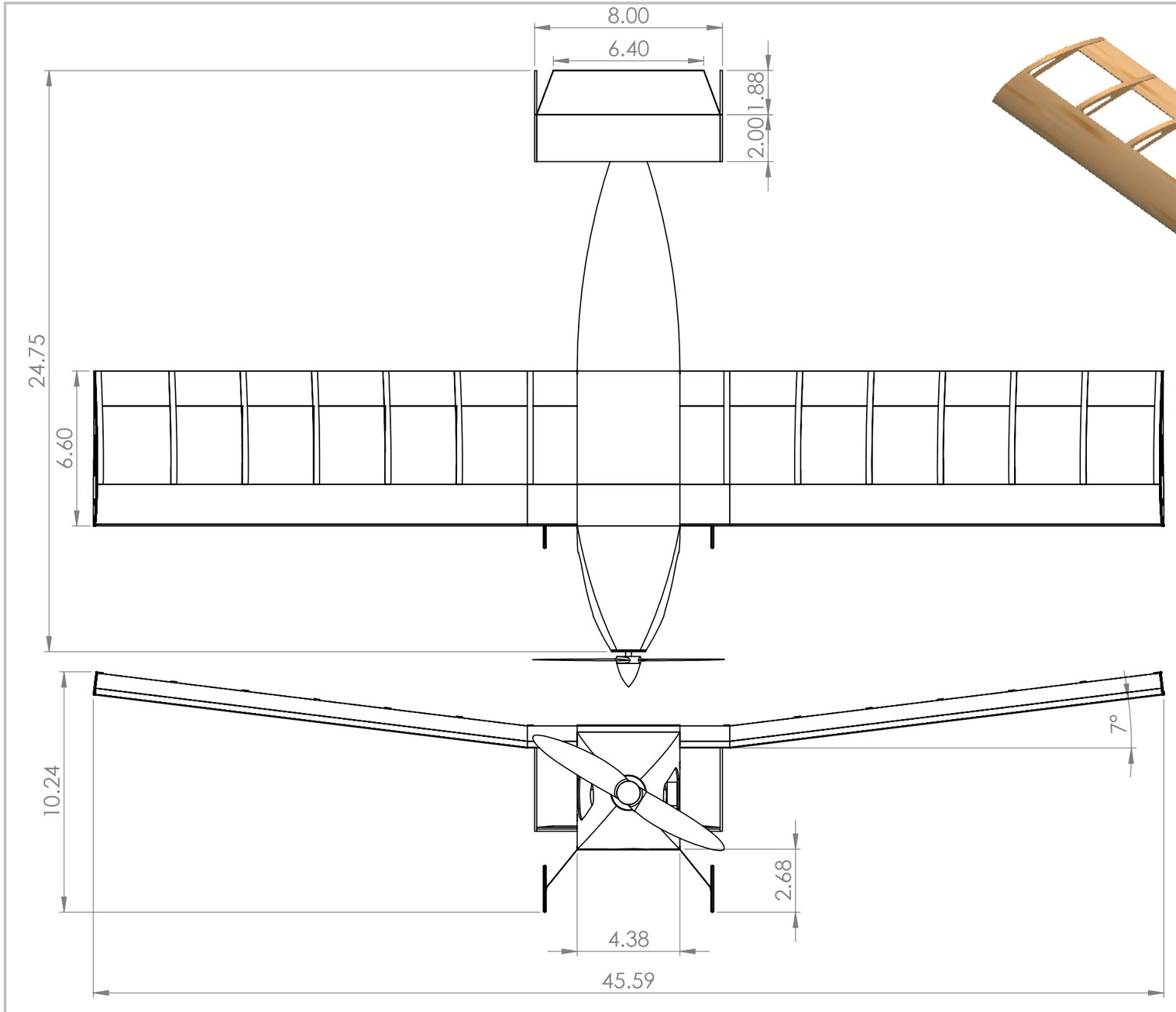

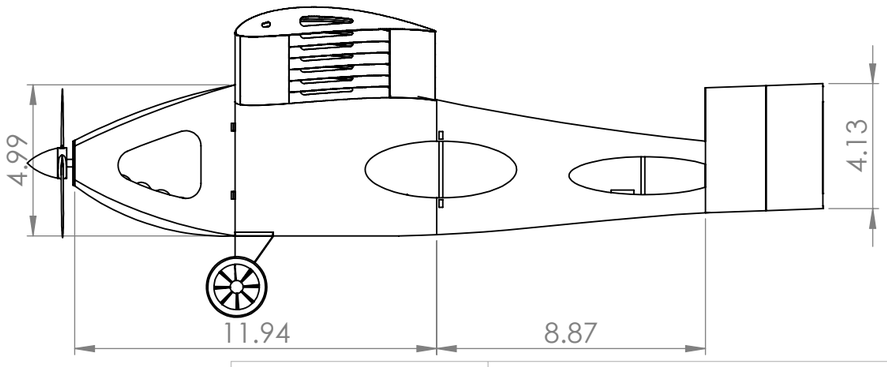

SOLIDWORKS Student Edition.
For Academic Use Only.

AIAA - Design Build Fly 2016

TITLE:
PRODUCTION AIRCRAFT
3 - View

UNLESS OTHERWISE SPECIFIED:
DIMENSIONS ARE IN INCHES

SIZE	DWG. NO.	REV
B	1	
SCALE: 1:5	WEIGHT:	SHEET 1 OF 1

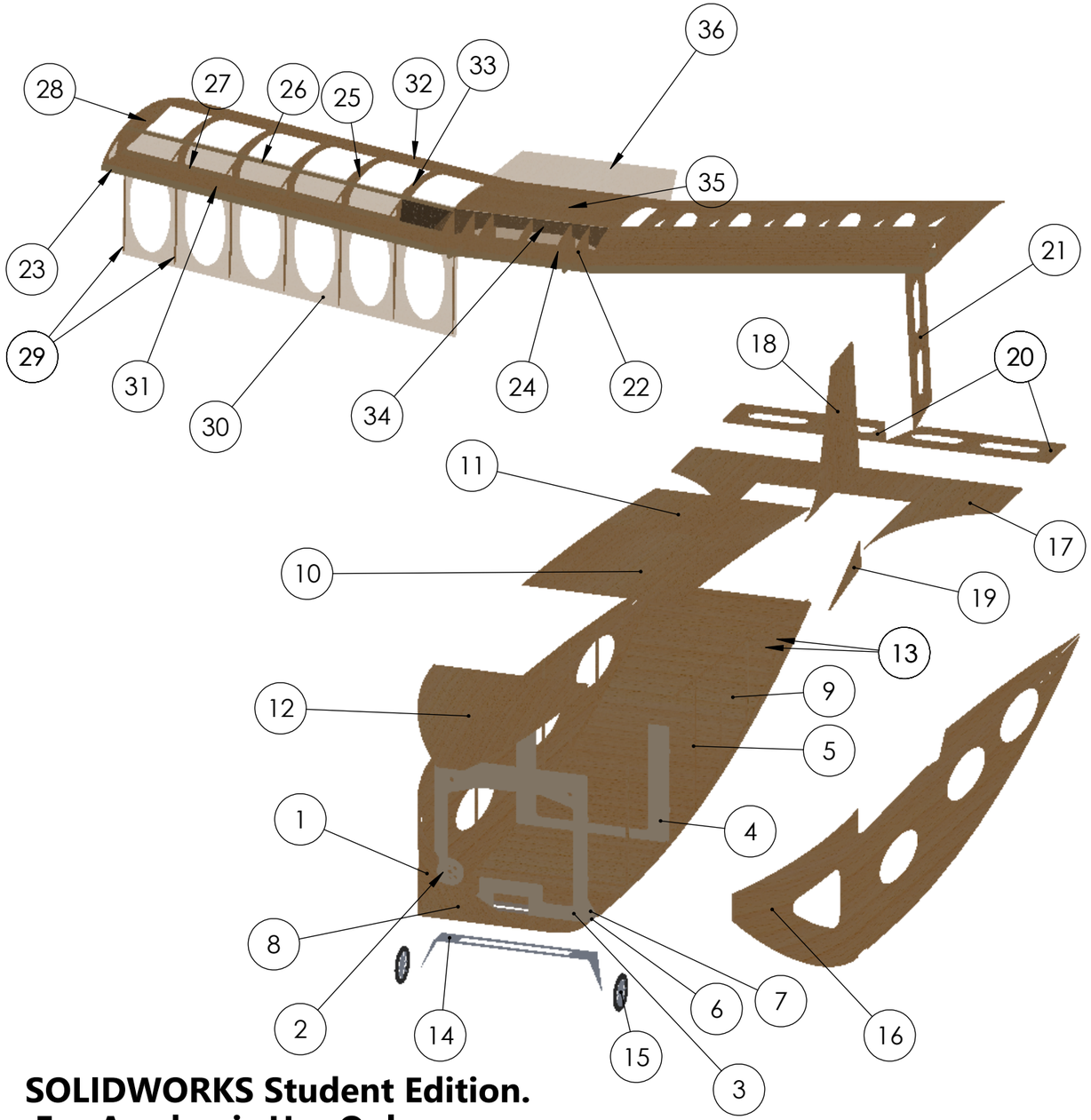

SOLIDWORKS Student Edition.
For Academic Use Only.

	PART	MATERIAL	QTY.
1	LEFT SIDE FUSELAGE	BALSA	1
2	FIREWALL	BIRCH PLYWOOD	1
3	FORWARD BULKHEAD	POPLAR PLYWOOD	1
4	AFT BULKHEAD	POPLAR PLYWOOD	1
5	REAR AIRFRAME	BALSA	1
6	BOTTOM BULKHEAD	POPLAR PLYWOOD	1
7	BULK HEAD SUPORT	POPLAR PLYWOOD	1
8	LOWER FRONT FUSELAGE	BALSA	1
9	LOWER REAR FUSELAGE	BALSA	1
10	FUSELAGE DOOR	BALSA	1
11	UPPER REAR FUSELAGE	BALSA	1
12	UPPER FRONT FUSELAGE	BALSA	1
13	SERVO BARS	BALSA	1
14	LANDING GEAR FRAME	ALUMINUM	1
15	WHEELS	PLASTIC/RUBBER	2
16	RIGHT SIDE FUSELAGE	BALSA	1
17	HORIZONTAL STABILIZER	BALSA	1
18	VERTICAL STABILIZER	BALSA	1
19	LOWER VERT. STABILIZER	BALSA	1
20	ELEVATOR	BALSA	1
21	RUDDER	BALSA	1
22	CONNECTION RIB	BALSA	4
23	FRONT SPAR	SPRUCE	1
24	FUSELAGE RIB	BALSA	4
25	WING RIB	BALSA	16
26	UPPER WING SPAR	SPRUCE	1
27	LOWER WING SPAR	SPRUCE	1
28	END CAP RIB	BALSA	2
29	DOOR RIB	BALSA	16
30	WING DOOR	BALSA	2
31	FRONT WING SHEET	BALSA	1
32	REAR WING SHEET	BALSA	1
33	RIB CAP STRIP	BALSA	12
34	DIHEDERAL BRACE	ALUMINUM/BALSA	1
35	REAR FUSELAGE COVER	BALSA	1
36	WING FAIING	BALSA	1

AIAA - Design Build Fly 2016

TITLE:
MANUFACTURING SUPPORT AIRCRAFT STRUCTURAL ARRANGEMENT

UNLESS OTHERWISE SPECIFIED:
DIMENSIONS ARE IN INCHES

SIZE	DWG. NO.	REV
B	6	

SCALE: 1:7 | WEIGHT: | SHEET 1 OF 1

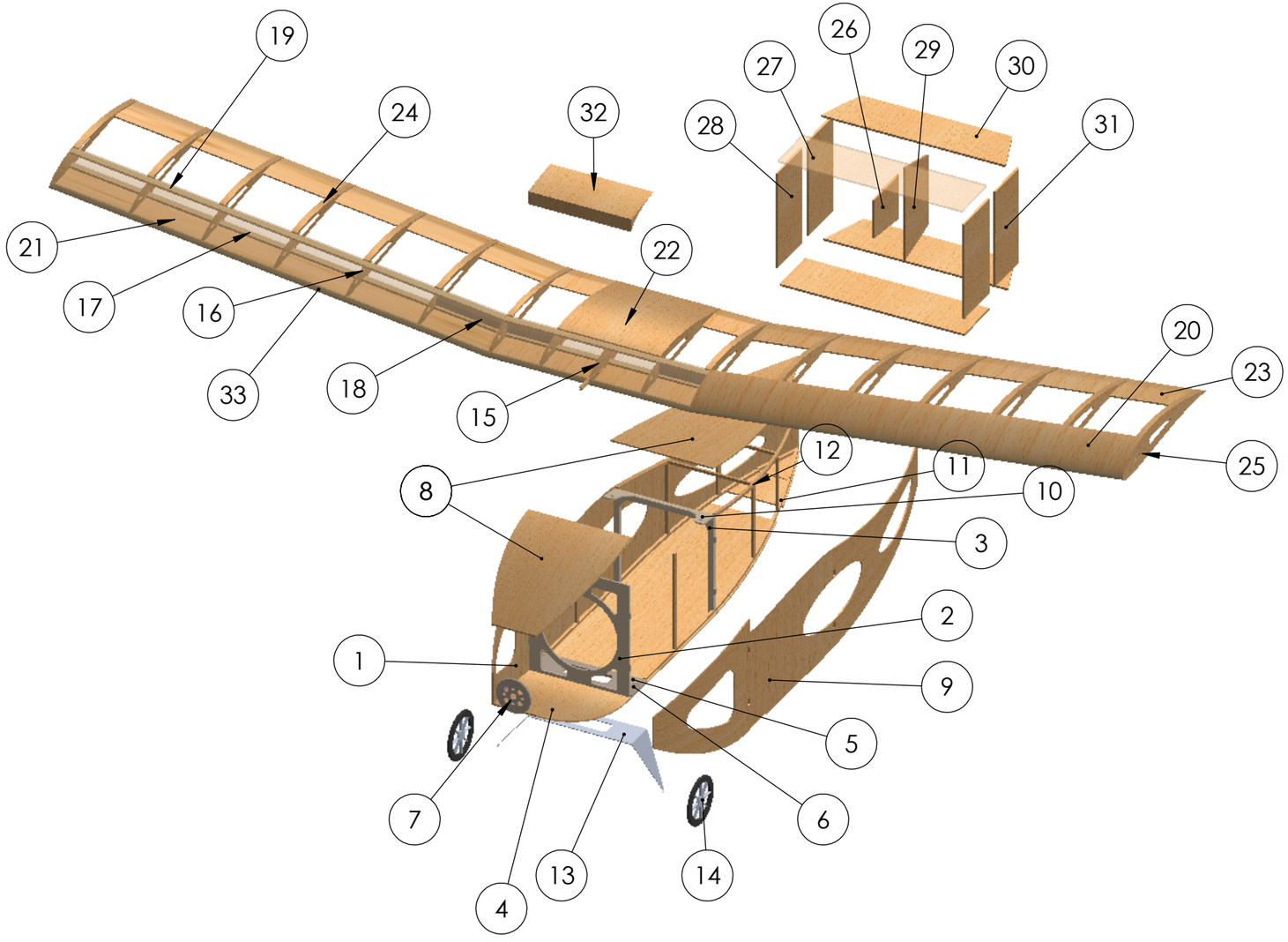

	PART	MATERIAL	QTY.
1	RIGHT FUSELAGE PANEL	BALSA	1
2	FRONT BULKHEAD	POPLAR PLYWOOD	1
3	AFT BULKHEAD	POPLAR PLYWOOD	1
4	BOTTOM FUSELAGE PANEL	BALSA	1
5	LANDING GEAR BULKHEAD	POPLAR PLYWOOD	1
6	BULKHEAD REINFORCEMENT	POPLAR PLYWOOD	1
7	FIREWALL	BIRCH PLYWOOD	1
8	TOP FUSELAGE PANEL	BALSA	1
9	LEFT FUSELAGE PANEL	BALSA	1
10	WING CONNECTION POINT	POPLAR PLYWOOD	1
11	LOWER INTERNAL FRAME	BALSA	1
12	UPPER INTERNAL FRAME	BALSA	1
13	FRONT LANDING GEAR - FRAME	ALUMINUM	1
14	FRONT LANDING GEAR - WHEEL	PLASTIC/RUBBER	2
15	CONNECTION RIBS	BALSA	2
16	WING RIBS	BALSA	16
17	LOWER WING SPAR	SPRUCE	3
18	DIHERDRAL BRACE	POPLAR PLYWOOD	2
19	UPPER WING SPAR	SPRUCE	3
20	UPPER WING PANEL	BALSA	3
21	LOWER WING PANEL	BALSA	3
22	FUSELAGE WING PANEL	BALSA	1
23	REAR LOWER WING PANEL	BALSA	3
24	RIB CAP STRIPS	BALSA	14
25	END RIBS	POPLAR PLYWOOD	2
26	MID VERTICAL STABILIZER - FIXED	BALSA	1
27	HORIZONTAL STABILIZER - FIXED	BALSA	2
28	SIDE VERITCAL STABILIZER - FIXED	BALSA	2
29	MIDDLE RUDDER	BALSA	1
30	ELEVATOR	BALSA	2
31	SIDE RUDDER	BALSA	2
32	WING FAIRING	BALSA	1
33	FRONT SPAR	SPRUCE	1

SOLIDWORKS Student Edition.
For Academic Use Only.

AIAA - Design Build Fly 2016

TITLE:

PRODUCTION AIRCRAFT STRUCTURAL ARRANGEMENT

UNLESS OTHERWISE SPECIFIED:
DIMENSIONS ARE IN INCHES

SIZE	DWG. NO.	REV
B	2	

SCALE: 1:5 | WEIGHT: | SHEET 1 OF 1

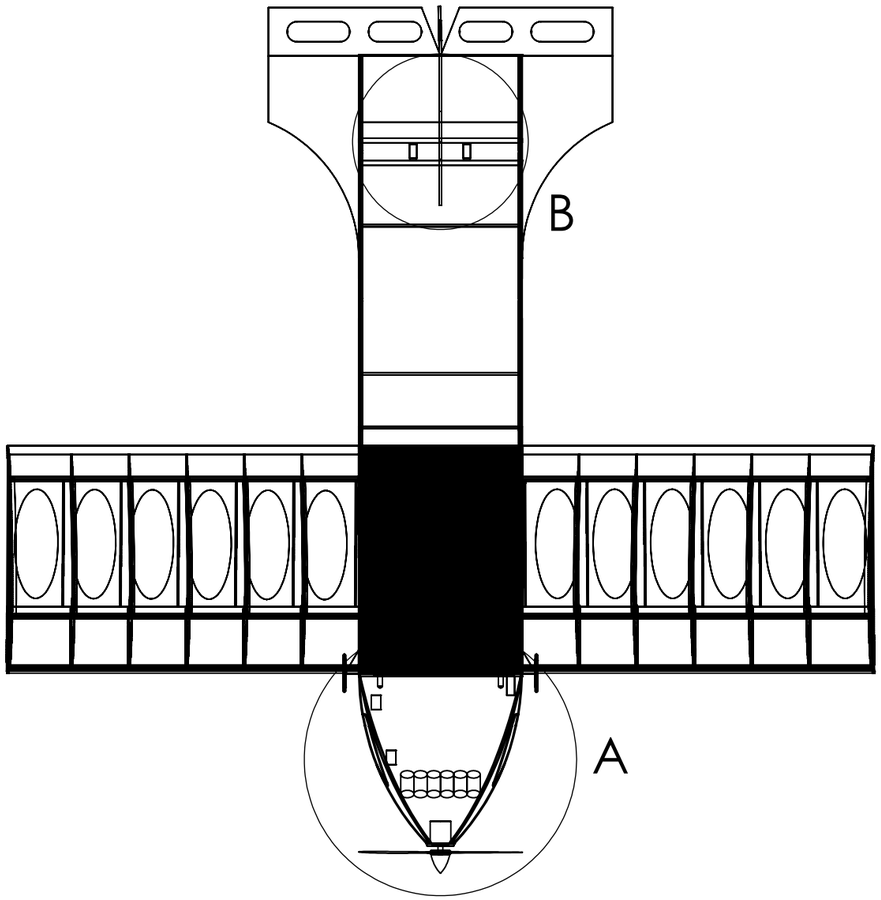

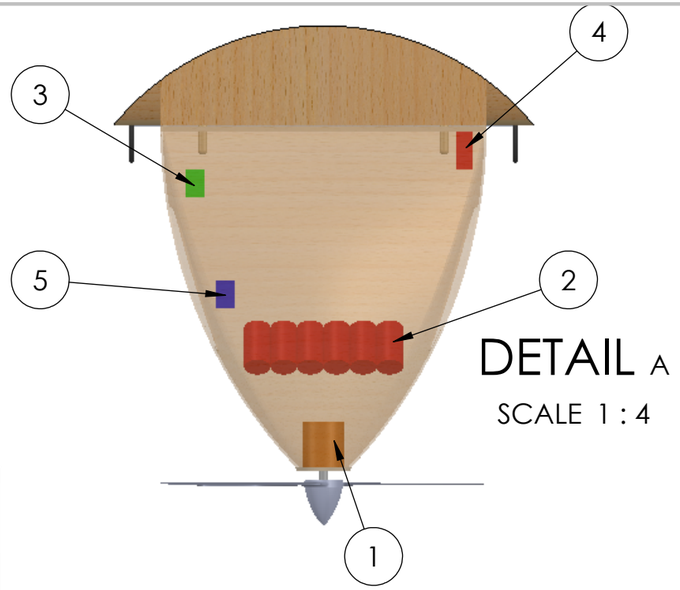

DETAIL A

SCALE 1 : 4

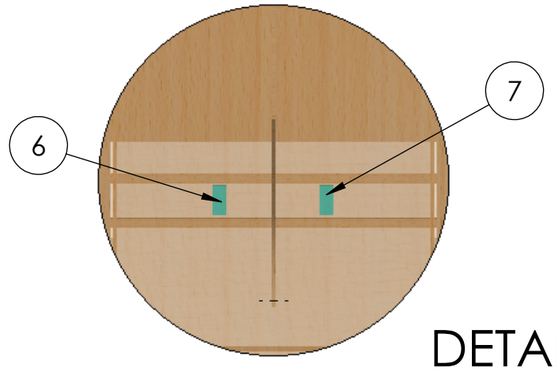

DETAIL B

SCALE 1 : 4

	PART	DESCRIPTION	QTY.
1	MOTOR	AXI2210/20	1
2	MOTOR BATTERY	CUSTOM PACK	1
3	RECIEVER	SPEKTRUM AR400	1
4	RECIEVER BATTER	CUSTOM PACK	1
5	SPEED CONTROL	THUNDERBIRD 18	1
6	RUDDER SERVO	HS-53	1
7	ELEVATOR SERVO	HS-53	1

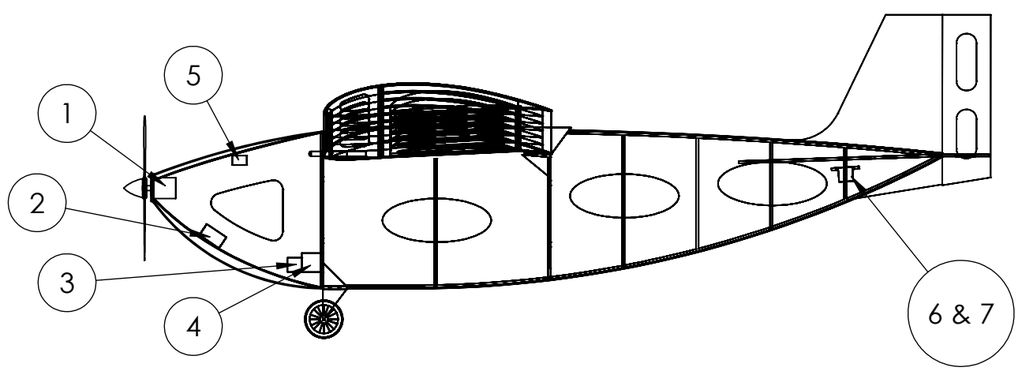

SOLIDWORKS Student Edition.
For Academic Use Only.

AIAA - Design Build Fly 2016

TITLE:

MANUFACTURING SUPPORT
AIRCRAFT SYSTEMS
LAYOUT/LOCATIONS

UNLESS OTHERWISE SPECIFIED:
DIMENSIONS ARE IN INCHES

SIZE	DWG. NO.	REV
B	7	
SCALE: 1:8	WEIGHT:	SHEET 1 OF 1

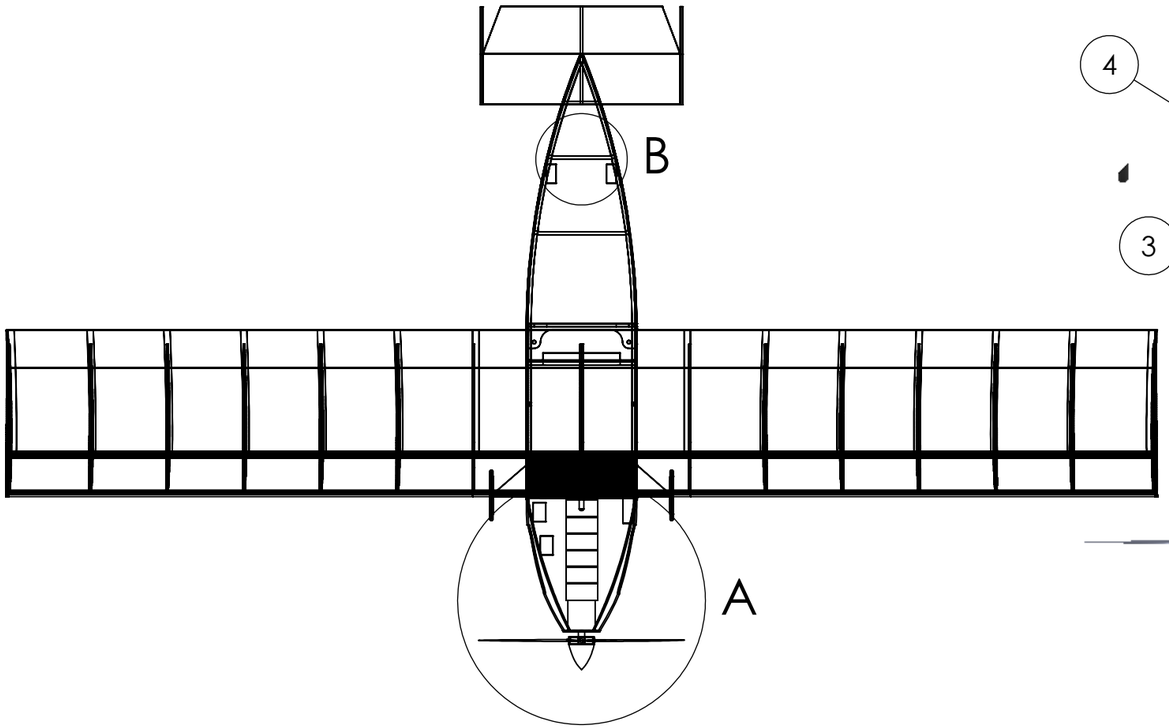

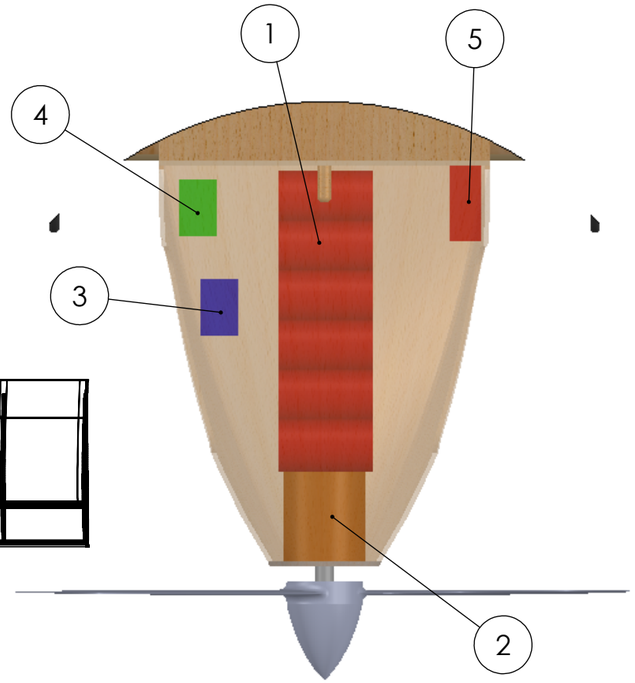

	PART	DESCRIPTION	QTY.
1	MOTOR BATTERY	CUSTOM PACK	1
2	MOTOR	AXI2120/20	1
3	SPEED CONTROL	THUNDERBIRD 18	1
4	RECIEVER	SPEKTRUM AR400	1
5	RECIEVER BATTERY	CUSTOM PACK	1
6	RUDDER SERVO	HS-53	1
7	ELEVATOR SERVO	HS-53	1

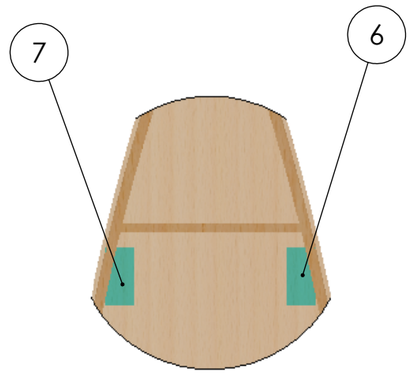

DETAIL A

SCALE 1 : 2

DETAIL B

SCALE 1 : 2

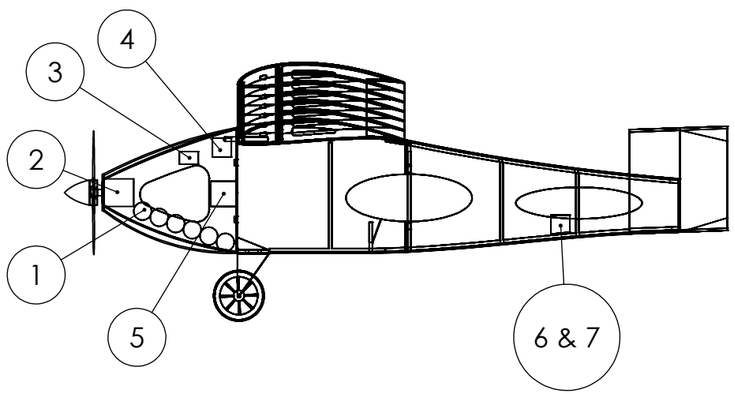

SOLIDWORKS Student Edition.
For Academic Use Only.

AIAA - Design Build Fly 2016

TITLE:

PRODUCTION AIRCRAFT
SYSTEMS LAYOUT/LOCATIONS

UNLESS OTHERWISE SPECIFIED:
DIMENSIONS ARE IN INCHES

SIZE	DWG. NO.	REV
B	3	
SCALE: 1:6	WEIGHT:	SHEET 1 OF 1

PAYLOAD CONFIGURATION

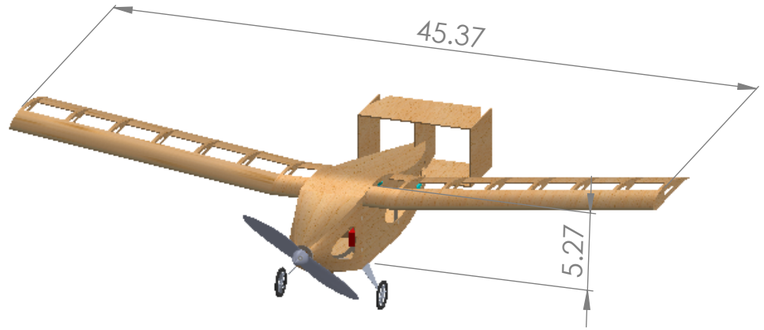

PAYLOAD WEIGHT	~1LBS

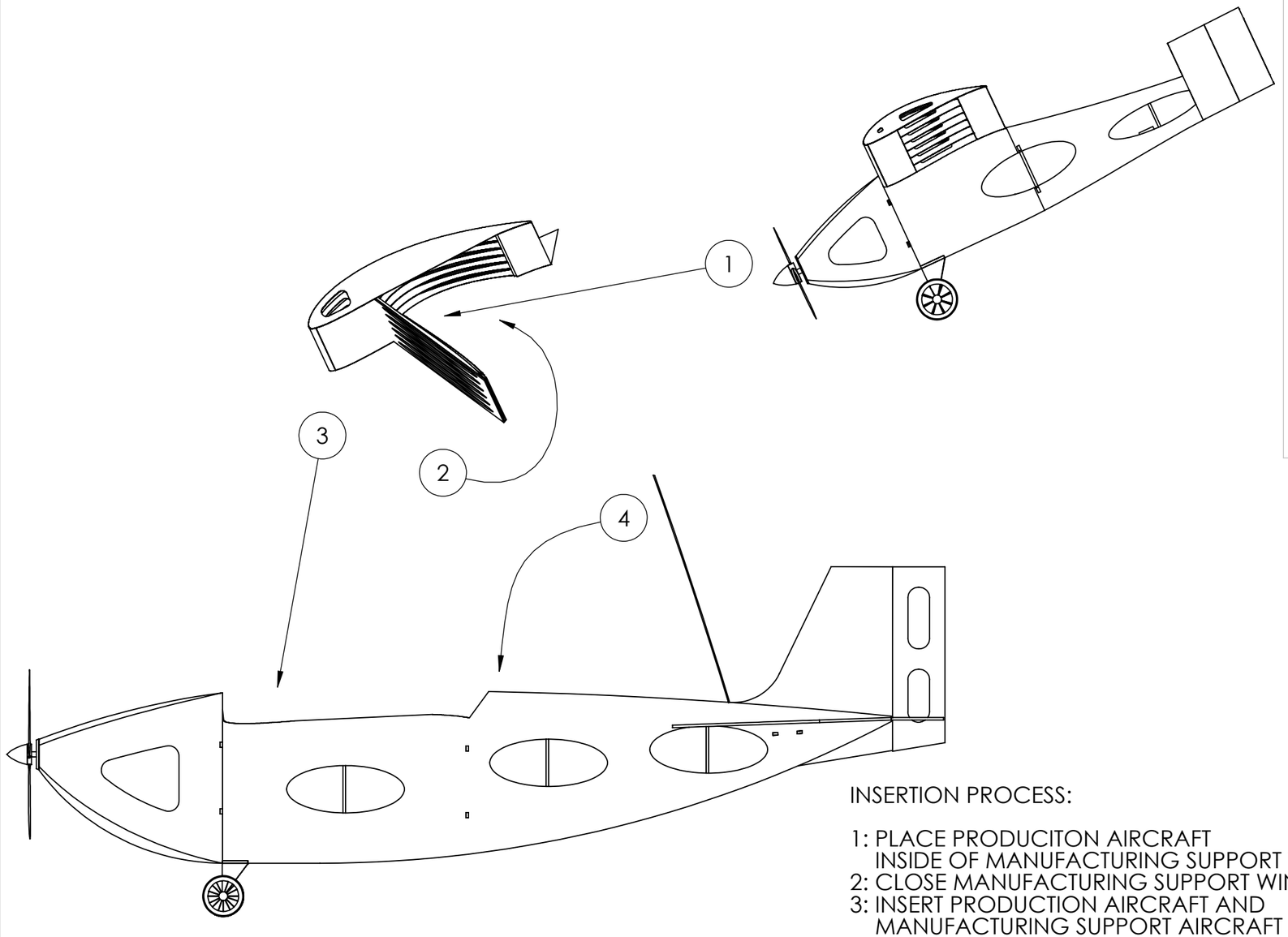

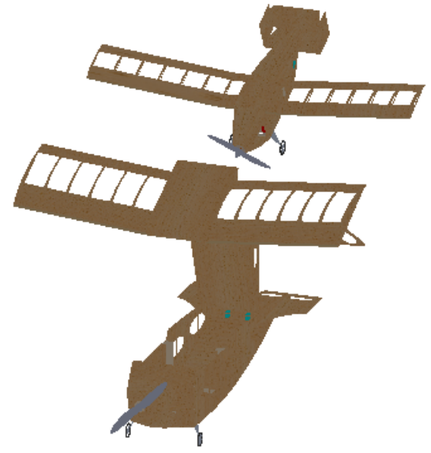

INSERTION PROCESS:

1: PLACE PRODUCITON AIRCRAFT
INSIDE OF MANUFACTURING SUPPORT WING
2: CLOSE MANUFACTURING SUPPORT WING
3: INSERT PRODUCTION AIRCRAFT AND
MANUFACTURING SUPPORT AIRCRAFT WING
INTO MANUFACTURING SUPPORT FUSELAGE
4: CLOSE REAR FUSELAGE DOOR AND LOCK DOWN

SOLIDWORKS Student Edition.
For Academic Use Only.

AIAA - Design Build Fly 2016

TITLE:
MANUFACTURING SUPPORT AIRCRAFT PAYLOAD CONFIGURATION

UNLESS OTHERWISE SPECIFIED: DIMENSIONS ARE IN INCHES	SIZE	DWG. NO.	REV
	B	8	
	SCALE: 1:6	WEIGHT:	SHEET 1 OF 1

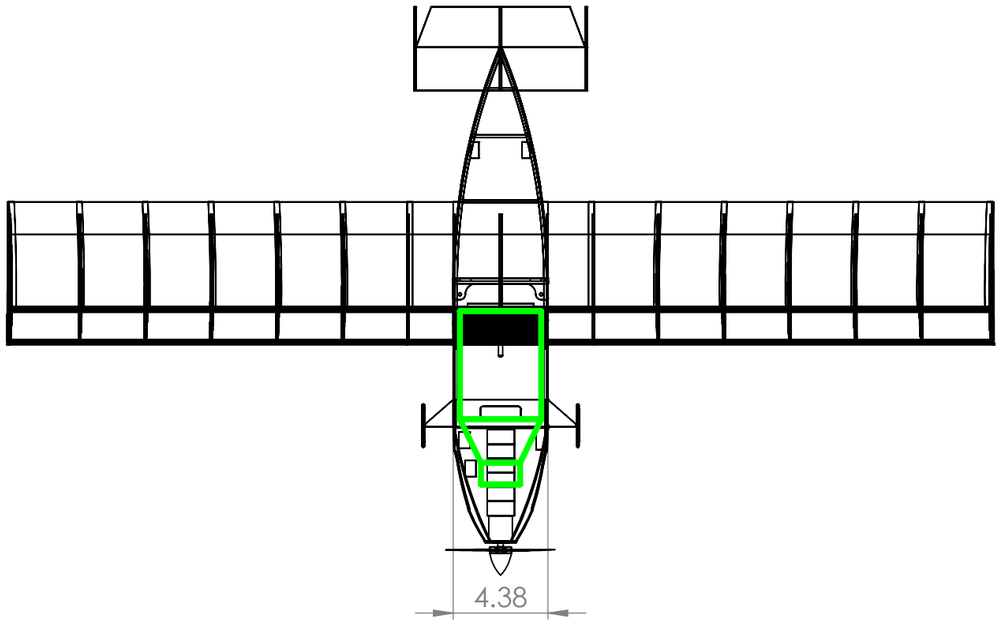

PAYLOAD CONFIGURATION

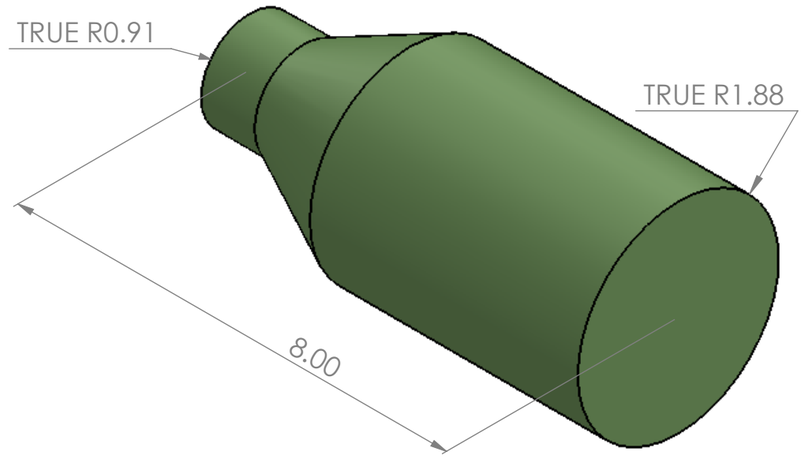

PAYLOAD WEIGHT	2 LBS

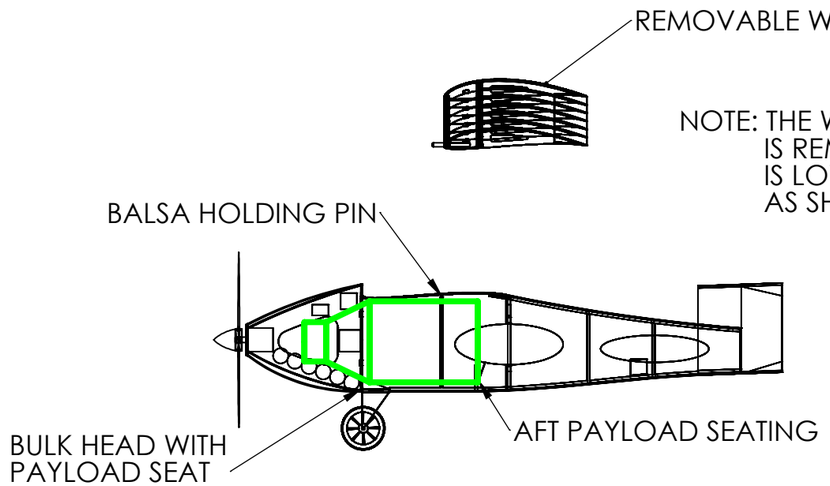

NOTE: THE WING OF THE AIRCRAFT
IS REMOVED AND THE PAYLOAD
IS LOWERED INTO THE PAYLOAD SEATING
AS SHOWN THEN THE WING IS REATTACHED

SOLIDWORKS Student Edition.
For Academic Use Only.

	AIAA - Design Build Fly 2016		
SAN JOSE STATE UNIVERSITY	TITLE: PRODUCTION AIRCRAFT PAYLOAD CONFIGURATION		
UNLESS OTHERWISE SPECIFIED: DIMENSIONS ARE IN INCHES	SIZE B	DWG. NO. 4	REV
	SCALE: 1:7	WEIGHT:	SHEET 1 OF 1

6.0 Manufacturing Plan

The goal in manufacturing was to construct the lightest weight aircraft while still maintaining structural integrity to withstand the flight loads with the various payloads for each aircraft. Different manufacturing techniques were explored for each of the aircraft components to determine which would yield the desired result. The wing, fuselage, empennage, and landing gear underwent a rigorous investigative process to determine the best construction. The schedule for manufacturing can be seen in Figure 6.0.1.

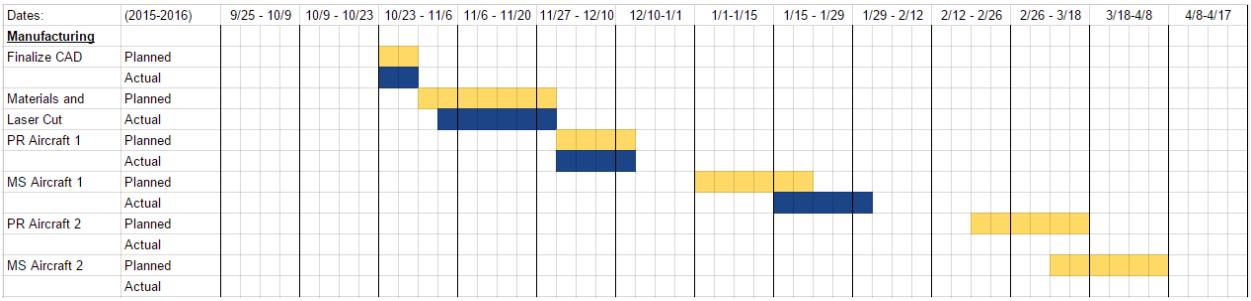

Figure 6.0.1: Manufacturing Milestone Chart

6.1 Materials Selection Process

A variety of materials were investigated to optimize the strength and weight of the aircraft. Carbon fiber, balsa wood, birch and poplar plywood, spruce hardwood, and monokote. The investigation into the use of carbon fiber led to the determination that its complexity to manufacture and necessary specialized tools would prove too difficult for our aircraft. Specialized tools such as vacuum bags and an autoclave were not available to the team. Without these tools, the carbon fiber could potentially contain many flaws and excess epoxy, resulting in overweight and under strength aircraft. Balsa wood was chosen as the principal material for its ease of construction and low weight. Since balsa wood is a relatively weak material, other materials would be necessary to strategically strengthen the structure in high stress areas. Spruce hardwood was chosen as the spar material, poplar plywood for bulkheads and stiffeners in high stress areas, birch plywood for the motor mounts, and monokote for aerodynamic smoothing and torsional stiffening of the wings. Cyanoacrylate would be used to glue the balsa wood together and epoxy for the glueing of hardwoods.

Table 6.1.1: Materials used to build aircraft

Manufacturing Component	Material
Principal Material	Balsa Wood
Structural Material	Birch Plywood
Aerodynamic Surfacing	Monokote
Adhesive	Cyanoacrylate & Epoxy

6.2 Manufacturing

The aircraft were manufactured in several different components then fully assembled: wing, fuselage, empennage, and landing gear. Each component underwent an investigative process to determine the lightest weight structure.

Wing

The wing was built as a traditional aircraft wing structure by incorporating a spar, ribs, and sheeting to achieve the strength necessary for normal flight loads. Construction was done on a pin board so that all pieces could be precisely aligned and pinned in place to avoid wing warp. The wing was constructed in 3 different pieces: left, right, and center section. It was constructed in this manner to allow for seven degrees of dihedral in the outboard wing sections. The center section was constructed first as it would serve as the base for each outer wing section to adhere to. Each wing section was constructed by first gluing a piece of spruce hardwood (lower section of the spar) to the trailing edge of the lower leading edge balsa sheet. This was then pinned to the board and the laser cut ribs were glued to the balsa sheet and spruce hardwood. The upper spruce spar was glued into place in the laser cut slot at the top of each rib. Shear webs were then precisely cut and glued to the upper and lower spars between each rib. These shear webs prevent the upper and lower spars from moving spanwise away from each other when the wing is stressed in flight. The trailing edge balsa sheets were then cut to size and glued to the trailing edge of the ribs using cyanoacrylate. The leading edge balsa block was then glued into place and the upper wing sheeting was adhered to the leading edge, ribs, and upper spar. The outer wing sections were then glued to the center section using epoxy. The joint between the center section and the outer sections yields a very high stress region because of the discontinuity in the spars. A poplar plywood doubler was glued between the sections to increase the strength in this high stress area. The doubler was precisely laser cut to the exact dihedral of the wing so that the outer sections would be set at positive seven degrees with respect to the flat center section. The wing was then covered in Monokote to provide an aerodynamic surface across the open bays in between the ribs and to increase the torsional rigidity of the wing. The wings were built flat on the pin board to eliminate any twist in the wing; however, washout is a desired twist in a wing to prevent the wing tip from stalling before the root. The now complete wing was twisted slightly and the Monokote heated to implement the desired washout of about two degrees. The PR and MS wings were constructed in very similar fashion, the main difference being that the MS wing has a door on the bottom to allow for the PR wing to be inserted. The MS wing also used an aluminum capped poplar plywood spar in the center section because of the spars low moment of inertia, as seen in Figure 6.2.2.

Figure 6.2.1: MS wing section under construction

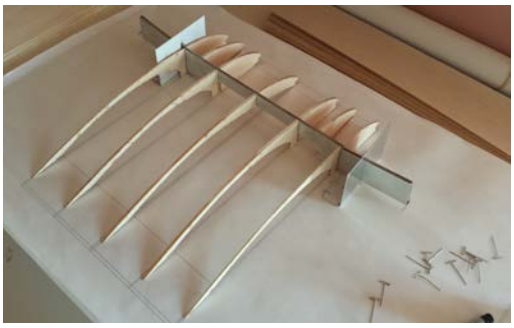

Figure 6.2.2: MS center section under construction

Fuselage

The construction of each fuselage is composed of laser cut bulkheads and fuselage sides. Bulkhead 1 is the motor mount and is composed of birch plywood. Bulkheads 2 and 3 are poplar plywood. The nose is shaped by sanding away excess balsa wood to loft from the round Bulkhead 1 to the rectangular Bulkhead 2. This was done to give each aircraft a more aerodynamic shape. Bulkheads 2 and 3 provide the primary structure to hold the wing to the fuselage. The wings mount to Bulkhead 2 using a wooden dowel protruding from the leading edge of the wings and secure to Bulkhead 3 using 6-32 machine screws.This allows for the wing to be fully removable for loading payloads into their fuselages. The top and bottom of the fuselages are sheeted in thin balsa to give them appropriate strength in the yaw axis. Once this is complete, doors were constructed to cover over areas that necessitate easy access for aircraft operation.

Figure 6.2.3: Basic fuselage structure

Figure 6.2.4: Fuselage nearing completion

Empennage

The pieces of the empennages were laser cut to shape and the various pieces glued together. The complete stabilizers were then glued to their respective fuselages. Once the stabilizers and control

surfaces were covered in Monokote to increase their strength in both torsion and bending, they were connected to each other using Monokote as a hinge.

Landing Gear

The 2024-T6 aluminum was cut out of a large sheet in the necessary shape then precisely bent using a press brake. Lightening holes were machined out using a mill to reduce the amount of material in low stress areas. The axles were machined out of 2024-T6 aluminum billet using a lathe. The threads that hold the landing gear and the axles to one another was cut on the lathe using a tapping die.

7.0 Testing Plan

Testing key components of the team's design is crucial in order to ensure success at the competition. Testing was performed throughout the design and manufacturing process in order to refine and validate structural and electrical choices. Figure 7.0.1 shows the team's schedule for testing various structural and electrical components. The testing concludes with flight testing that helps improve the flying qualities and performance of the aircraft.

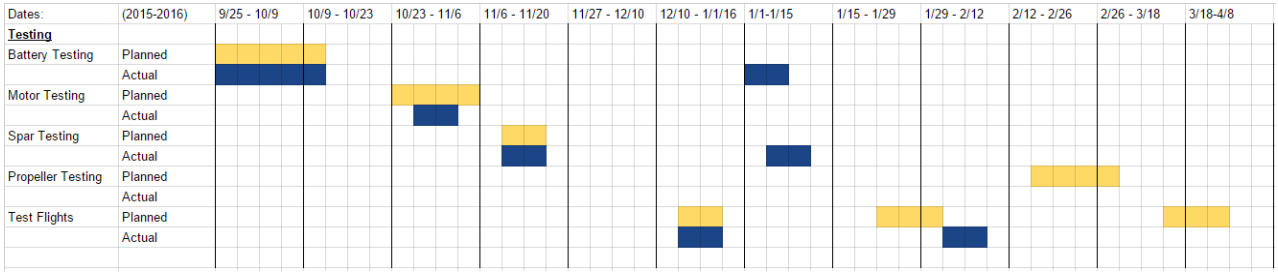

Figure 7.0.1: Development Testing Schedule

7.1 Tests Conducted

Wing Structure Testing

In order to minimize weight, the team decided to eliminate ailerons and only use the rudder for roll control. This simplifies the wing structure and expands the possible structure options.

The team decided to test 3 different spar material options, a foam wing with a carbon spar, balsa wood and hardwood structure, and an aluminum and plywood spar. The team decided to build a mock up wing of each design to determine which wing was optimal based on its weight and strength. The foam wing with a carbon spar failed the wing tip test before the other two options, so this option was quickly discarded. The balsa wood and hardwood structure was the next to fail, followed by the composite spar made of 0.040" thick aluminum and plywood. Although the composite spar was stronger, the balsa wood structure was strong enough for the aircraft designed, failing when 13 pounds of force was applied to the wing tip. The test conducted can be seen in Figure 7.1.1. The wing was held to the table at its center section and a scale

was hung on the wing tip. The weight at the wing tip as gradually increased until it failed at 13 pounds. The test concluded that the balsa and hardwood spar was appropriately sized for the PR Aircraft and was the chosen design for its wing. The team was concerned with the small moment of inertia at the center of the wing spar on the MS wing design. Therefore, the aluminum and plywood spar was utilized to create a strong center section to the wing. The outboard sections of the MS wing were built with the same spar construction as the PR wing. The final test of wing structure was conducted by lifting the aircraft by their wing tips at their gross weights. Figure 7.1.2 shows the PR Aircraft undergoing this test which simulates +2g's of force on the wing. Both aircraft survived the test and have performed great in flight test with no structural issues observed. The PR wing weighs in at 0.244 pounds and the MS wing weighs 0.569 pounds.

Figure 7.1.1: Stress testing first complete wing structure.

Figure 7.1.2: Wing tip test of PR Aircraft w/ payload (Simulating +2g acceleration)

Battery Testing

Battery testing was done to evaluate the best brand of cell as well as quantify the amount of amperage being used by the electric motor. These quantities would prove useful in choosing the correct propeller during flight testing. The current, voltage, and resulting power were all recorded for each battery and propeller. This data can be seen in Table 7.1.1. Six and seven cell 2/3A-cell Venom battery packs were

tested along with six and seven cell 2/3A-cell Elite battery packs. The Elite cell proved to have the least internal resistance, as it produced the most amperage and maintained its voltage the best. The Elite cell was chosen to supply the power for the propulsion system.

Table 7.1.1: Battery testing results

Venom 7.2V 1600 MaH 2/3A-Cell NiMH (4.9 oz.)			
Propeller	Current (A)	Voltage (V)	Power (W)
9x7.5	13.79	6.11	84.26
10x6	13.15	6.29	82.71
11x7	15.46	6.01	92.91
Elite 7.2V 1500 MaH 2/3A-Cell NiMH (5.0 oz.)			
Propeller	Current (A)	Voltage (V)	Power (W)
9x7.5	13.82	6.13	84.72
10x6	13.13	6.34	83.24
11x7	15.55	6.02	93.61
Venom 8.4V 1600 MaH 2/3A-Cell NiMH (5.3 oz.)			
Propeller	Current (A)	Voltage (V)	Power (W)
9x7.5	14.85	7.22	107.00
10x6	13.89	7.53	104.59
11x7	17.51	6.91	120.99
Elite 8.4V 1500 MaH 2/3A-Cell NiMH (6 oz.)			
Propeller	Current (A)	Voltage (V)	Power (W)
9x7.5	15.13	7.30	110.45
10x6	13.92	7.61	105.93
11x7	17.97	7.07	127.05

Flight Testing

In order to ensure a safe and operable aircraft, thorough flight testing and evaluations were done. Flight cards were employed for each flight, which ensured that all the electrical components were working correctly, and that the aircraft was structurally stable and assembled correctly. This included confirmation that the voltages were checked across all batteries used, aircraft remains in tact under full take-off weight

during wing tip testing, and that the flight control surface deflection matched the controller input. This general flight card was followed before the first flight and envelope expansion procedures.

The first flight procedure followed the flight card checklist, and including additional ground testing to check for control surface “freeplay”, as well as a series of propulsion tests; a 30 second linear sweep from zero to full throttle and a sudden acceleration test. These tests ensured that the propulsion system on the aircraft was properly installed, and verified structural stability due to high torque loads from the motor. After the aircraft passed these steps, the aircraft was cleared for the in-flight tests of the checklist.

During the in-flight test, the throttle setting was set to no more than 2/3 of full throttle and a standard take-off into a steady climb is required before proceeding further. After the aircraft has successfully taken off, the aircraft will then be tested for its stability and control characteristics by performing steady turns in both directions, and shallow climbs and dives. If the aircraft lands after successfully performing the in-flight checklist, and sustains minimal to no damage, the aircraft has passed the first flight procedure and can move onto flight envelope expansion. The flight envelope expansion will allow the team to slowly push the limits of the aircraft in a safe manner.

Each flight envelope expansion follows the same pre-flight procedure as the general flight card, but during the in-flight test, numerous stability and control tests are done. This included doublets on each primary control axis, control frequency sweeps on each primary control axis, abrupt power variations, stalling the aircraft and shallow dives at increasing throttle settings. The CG location for each expansion envelope procedure was varied but no more than 10% of static margin.

After the team was comfortable with the aircraft, any additional testing required was documented using the general flight sheet, shown in Figure 7.1.3.

Flight Sheet

General Info:

Date: ____/____/_____

Pilot: _____

Aircraft: MS / PR

Flight #: _____

Flight Purpose:_____

_____

Flight Conditions:

Weather: _____

Temperature: _____

Location: _____

Wind Speed:

Safety Checklist:

( ) Inspect for visual damage

( ) Verify adequate voltage for

- ( ) Transmitter battery
- ( ) Receiver battery
- ( ) Main Battery

( ) Verify range check

Checklist Comments and any additions:

Pre-Flight Checklist:

( ) Verify aircraft is fully assembled and correctly

( ) Verify CG is within designed limits

( ) Power on transmitter

( ) Power on receiver

( ) Test for correct control surface movement with transmitter input

( ) Check propulsion

Post Flight checklist:

( ) Inspect aircraft for any damage

( ) Power off propulsion

( ) Power off receiver

( ) Power off transmitter

Additional Comments:

Figure 7.1.3: General Flight Sheet for Flight Testing

Propeller Testing

Various propellers were tested to better understand the aircraft systems, varying both pitch and diameter. It was found that by increasing the pitch too much without increasing diameter, the propeller became inefficient and would not accelerate to its maximum speed. A balance of pitch and diameter was necessary to accelerate the aircraft and achieve its optimal performance. Takeoff distance, climb rate, and cruise speed were evaluated for each of the propellers. The cruise speed was determined through the use of an Eagle Tree Airspeed Sensor, which uses a pitot-static system to determine the aircraft's airspeed. The aircraft would takeoff, climb to 50 feet, and remain level at full throttle for a lap. This allowed for the airspeed to be measured for the aircraft at level flight.

Table 7.1.2: Propeller testing results

MS Aircraft (w/ Payload)			
Propeller	Takeoff Distance (ft)	Climb Rate Acceptable (Yes/No)	Cruise Speed (ft/s)
9x7.5	60	No	51.3
10x6	51	No	63.1
11x7	37	Yes	68.9
PR Aircraft (w/ Payload)			
Propeller	Takeoff Distance (ft)	Climb Rate Acceptable (Yes/No)	Cruise Speed (ft/s)
9x6	85	Yes	73.3
9x7.5	72	Yes	85.1
10x6	60	Yes	89.5

Landing Gear Testing

The landing gear was tested by performing a drop test. The aircraft was dropped from a height of 12 inches. A high frame rate camera filmed the test. Frameshots from the video were captured and analyzed to look at the max compression of the landing gear. Figure 7.1.4 shows the aircraft before the test began; this serves as a baseline from which to compare the compression image. Figure 7.1.5 shows the landing gear at its maximum deflection. The aluminum landing gear proved to have enough strength to withstand the loads experienced without significant deformation. If the aircraft experiences an even higher load during a landing, the aluminum may plastically deform but can easily be bent back.

Figure 7.1.4: Aircraft before drop test

Figure 7.1.5: Aircraft at max compression during test

8.0 Performance Results

Flight tests were conducted to maximize their performance. Each flight test was carefully documented in order to determine what changes should be made to the aircraft, as seen in Table 8.0.1. Once the aircraft achieved their peak performance, a mock competition was conducted. The aircraft flew the exact course and missions that will be performed at the contest. The aircraft met all of the contest requirements to achieve the maximum score for each mission. A significant factor of safety exists for lap times to ensure that the aircraft will complete the missions in the allotted time with a strong wind. Tables 8.0.2 and 8.0.3 quantify the results of the practice competition and compares those results to the predictions completed during the design phase of the project.

Table 8.0.1: Flight tests conducted

MS Aircraft		
Flight Number	Description	Comments
1	First Flight	Aircraft stability, control, and handling qualities are excellent
2	Envelope Expansion	Expanded envelope following procedure for expansion, recommend different propeller for higher speed
3	Propeller Test	The speed was increased to ~47ft/s using a new 11x7 propeller
4	Flight with Payload	Aircraft handled and performed well with increased weight, CG location good for static stability
5	Mission 1 Test	Aircraft completed 3 laps in 3:15, good robust design in event of high winds
6	Mission 2 Test	Aircraft completed 1 lap in under 10 minutes and took off in 37 feet, aircraft ready for DBF Competition
PR Aircraft		
Flight Number	Description	Comments
1	First Flight	Aircraft statically unstable, move CG forward to 20% chord location
2	CG Analysis	Repeat of first flight procedure with CG at 20% chord location. Aircraft stability, control, and handling qualities are excellent
3	Envelope Expansion	Aircraft flown with payload. Took off in under 100 ft. Speed appropriate to complete laps in allocated time (58 ft/s)
4	Propeller testing	9x7.5 propeller proves most effective, aircraft took off in 100ft Consider modifying battery to improve takeoff distance
5	Takeoff Distance	Adding an extra cell to the battery improved the takeoff distance to 80ft
6	Mission 3 Test	Aircraft completed 3 laps in 3:15, good robust design in event of high winds. Aircraft ready for DBF Competition.

Table 8.0.2: Expected versus actual data collected during flight testing for MS Aircraft

MS Aircraft			
Mission 1			
Parameter	Expected	Actual	Difference
Takeoff Distance (ft)	20.0	24	20%
Cruise Speed (ft/s)	74.85	70.1	6%
Time to Complete 3 Laps (s)	150	195	30%
Empty Weight (lb)	1.441	1.813	26%
Mission 2			
Parameter	Expected	Actual	Difference
Takeoff Distance (ft)	27.4	37	35%
Cruise Speed (ft/s)	73	68.9	6%
Time to Complete 1 Lap (s)	60	85	42%
Empty Weight (lb)	1.441	1.813	26%

Table 8.0.3: Expected versus actual data collected during flight testing for PR Aircraft

PR Aircraft			
Mission 3			
Parameter	Expected	Actual	Difference
Takeoff Distance	69.9	72	3%
Cruise Speed	79.9	85.1	7%
Time to Complete 3 Laps	120	165	38%
Empty Weight	0.751	1.019	36%

Tables 8.0.2 and 8.0.3 show that aircraft have met their performance requirements with a good margin of safety. Each subsystem (motor, battery, radio, and servos) performed perfectly throughout the test. The motor delivers the appropriate amount of thrust for our desired cruise speed and takeoff distance. It delivered results very close to the initial projects for the aircraft. The battery ended up a little heavier than desired because of the addition of another cell to increase performance. Further investigation into batteries may yield something lighter. Refinement of the aircraft structure may reduce weight and eliminate the need for another cell, future flight testing of the next aircraft will determine this. The radio system performed well throughout the flights, with no signal issues presenting. The servos delivered plenty of torque for the control surfaces. The next size down of servo does not have enough torque to control the aircraft, so the current HS-53 servos will remain.

The current prototypes are capable of completing all mission requirements, though RAC remains a challenge owing to weight challenges. The configuration of the aircraft is believed to be optimal for the competition, with good demonstrated flight performance and handling qualities, as well as potential for competitive RAC.Current projections show a reduction of structural weight up to 20% for the MS and PR Aircraft. The final aircraft should perform better due to their reduced weight and will be even more competitive for the 2015-2016 AIAA DBF contest.

References

1. Anderson, John. Fundamentals of Aerodynamics. New York: McGraw-Hill. Print. 2010.
2. Roskam, Jan. Airplane Design. Lawrence, Kan: DARcorporation, 1986. Print

MANUFACTURING SUPPORT AIRCRAFT

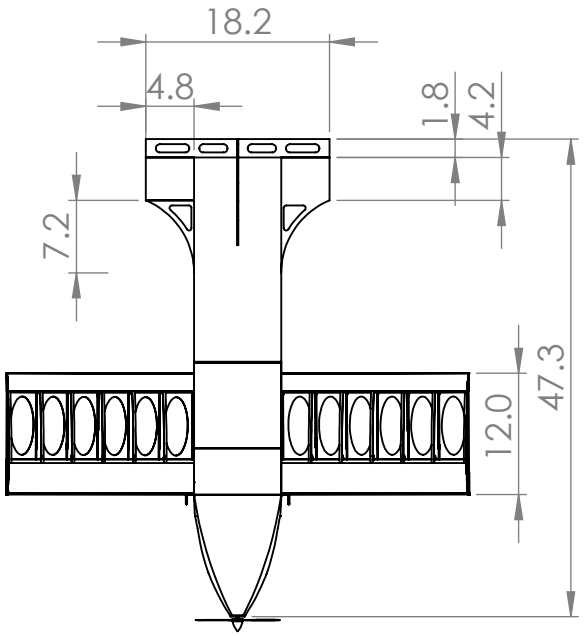

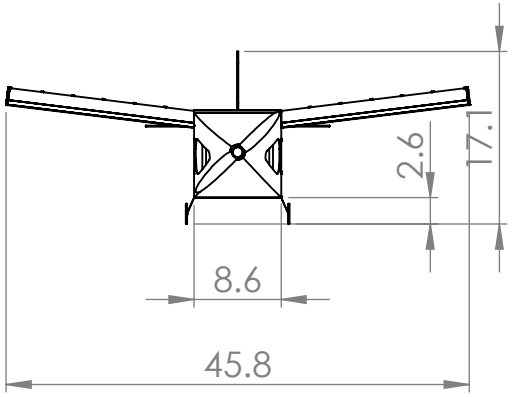

PRODUCTION AIRCRAFT

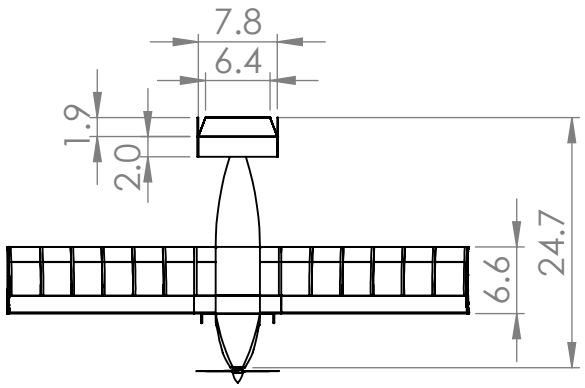

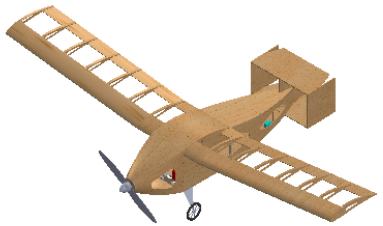

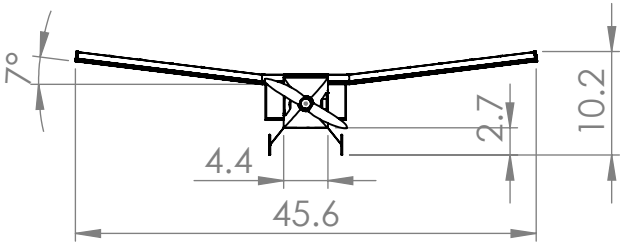

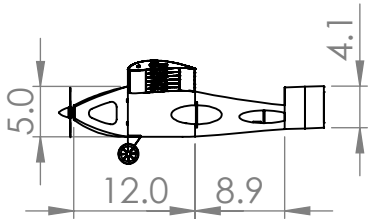

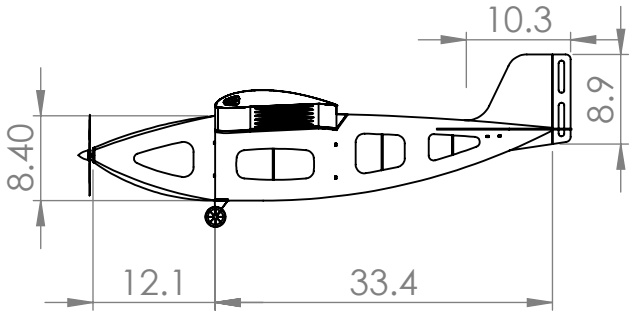

SOLIDWORKS Student Edition.
For Academic Use Only.

AIAA - Design Build Fly 2016

TITLE:

TEAM CRONUS 3-VIEW DRAWINGS

UNLESS OTHERWISE SPECIFIED:
DIMENSIONS ARE IN INCHES

SIZE	DWG. NO.	REV
A	1	

SCALE: 1:19 | WEIGHT: | SHEET 1 OF 1

BUZZBROOSHKA

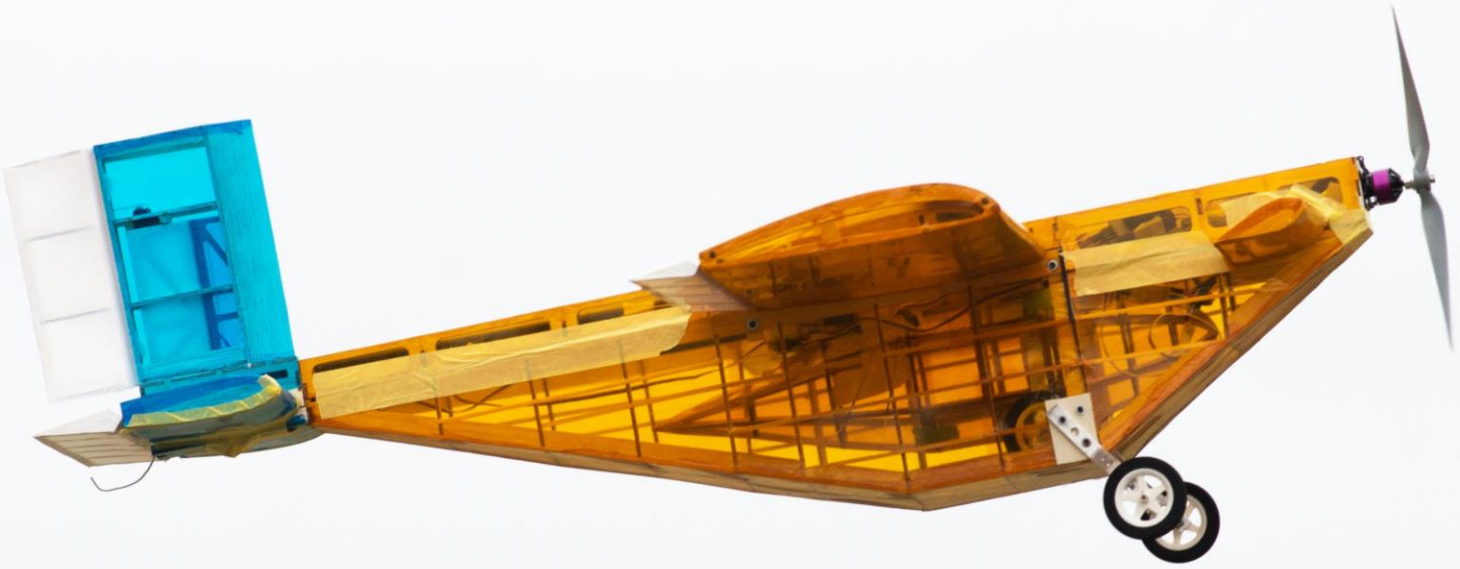

AIAA
DESIGN/BUILD/FLY
2015-2016
DESIGN REPORT

Georgia Institute of Technology

TABLE OF CONTENTS

ACRONYMS AND NOMENCLATURE

C.G.	–	Center of Gravity	e	–	Oswald Efficiency
RAC	–	Rated Aircraft Cost	P	–	Power
TFS	–	Total Flight Score	S	–	Area
GS	–	Ground Score	Kv	–	Motor Voltage Constant (V)
EW	–	Empty Weight	K_D	–	Wing Loading Dissipative Constant
TMS	–	Total Mission Score	K_T	–	Thrust Loading Dissipative Constant
M1	–	Mission One	K_A	–	Regressive Constant
M2	–	Mission Two	$\dot{x}$	–	Position Derivative with respect to time
M3	–	Mission Three	V	–	Velocity
FOM	–	Figures of Merit	$\dot{V}$	–	Velocity Derivative with respect to time
FS	–	Flight Score	m	–	Mass
TOFL	–	Takeoff Field Length	T	–	Thrust
s_g	–	Takeoff Roll Distance	D	–	Drag
NiCad	–	Nickel-Cadmium	$\bar{p}$	–	Dimensionless Rolling Rate
NiMH	–	Nickel-Metal Hydride	$\bar{q}$	–	Dimensionless Pitching Rate
AVL	–	Athena Vortex-Lattice	$\bar{r}$	–	Dimensionless Yawing Rate
$\widetilde{C}_L$	–	Airfoil Section Lift Coefficient	AR	–	Aspect Ratio
$\widetilde{C}_D$	–	Airfoil Section Drag Coefficient	R_e	–	Reynolds Number
$\widetilde{C}_m$	–	Airfoil Section Moment Coefficient	R_T	–	Taper Ratio
C_L	–	Aircraft Lift Coefficient	S_w	–	Wing Area (ft^2)
C_D	–	Aircraft Drag Coefficient	T_S	–	Settling Time (s)
C_f	–	Skin Friction Coefficient	ρ	–	Density
C_Y	–	Aircraft Side Force Coefficient	T_d	–	Doubling Time (s)
C_n	–	Aircraft Yawing Moment Coefficient	W	–	Weight (lbs)
C_m	–	Aircraft Pitching Moment Coefficient	α	–	Angle of Attack (degrees)
C_l	–	Aircraft Rolling Moment Coefficient	β	–	Sideslip Angle (degrees)
$C_{D,i}$	–	Aircraft Induced Drag Coefficient	μ_r	–	Rolling Coefficient of Friction
$C_{D,0}$	–	Aircraft Zero-Lift Drag Coefficient	R_{ls}	–	Wing Sweep
L’	–	Wing Thickness Location Parameter	R_{wf}	–	Wing Fuselage Interference
PA	–	Production Aircraft	MSA	–	Manufacturing Support Aircraft
MTOW	–	Maximum Takeoff Weight	V_{wind}	–	Wind Speed
Θ_{wind}	–	Wind Direciton	$W_{battery}$	–	Batteyr Weight

1. EXECUTIVE SUMMARY

This report details the design, testing, and manufacturing of the Georgia Institute of Technology *Buzzedryoshka* entry in the 2015-2016 AIAA Design/Build/Fly (DBF) competition. The system is made of two aircraft, a Manufacturing Support Aircraft (MSA) and a Production Aircraft (PA) designed to successfully complete the following four tasks:

1. Empty Flight of Manufacturing Support Aircraft
2. Delivery of the Production Aircraft Subassemblies
3. Timely Assembly of Production Aircraft
4. Loaded Flight of Production Aircraft

At the time of this writing, *Buzzedryoshka* has flown 31 times.

1.1 Design Process

Buzzedryoshka is designed for victory. This is achieved through the development of a robust system capable of flying all missions reliably with minimum Rated Aircraft Cost (RAC). The conceptual design of a winning system involved converting the mission requirements and scoring criteria into a list of design metrics that were used to decide the preliminary configuration of the aircraft. Trade studies on wing loading and power were performed using historical data and computer tools to estimate drag and lift. Battery and motor combinations were evaluated to achieve the required propulsion. Stability analysis was performed using a vortex lattice model to determine the size and placement of lifting surfaces. A detailed design with dimensions was created, then prototyped and flight tested to validate assumptions made during the design.

1.2 Key Mission Requirements and Design Features

A successful system design and score arise from the successful balance of key mission requirements. Specific design metrics were developed for each mission requirement and scoring element to maximize system performance and the overall competition score.

Empty Weight: The aircraft's empty weight is a significant driver of total score. Empty weight is the weight of the airframe and propulsion system. The entire aircraft was designed to be as minimalistic as possible without compromising the ability to complete all three flight missions. This was accomplished by judicious use of composite materials combined with a highly efficient built up structure, while simultaneously using the lightest possible motor and battery.

Battery Weight: The final flight score is inversely proportional to the battery weight squared. *Buzzedryoshka* was designed to require as little power as possible to complete all three flight missions. This was accomplished by minimizing drag and structural weight wherever possible.

Takeoff Requirement: The MSA and PA are required to takeoff in 100 feet on all missions. Fulfilling takeoff requirements requires a balance between wing area and propulsive power. This was accomplished with an aerodynamically efficient structure with minimal power required to fulfill the mission requirements.

Subassembly Requirement: The PA is required to fit within the MSA by breaking into multiple subassemblies. It is necessary to design the PA to have as few subassemblies as possible in order to maximize final score. The required number of subassemblies to maximize the final score is one. As a result, the PA was designed as one piece and the MSA was designed in multiple sections to fit around the PA.

1.3 Performance Capabilities of the System

All of the specific design features created to maximize the performance of the system can be summarized by the following performance capabilities:

- PA Max Takeoff Weight 3.39 lbs
- MSA Max Takeoff Weight 2.10 lbs
- Reliable takeoff within 100 feet
- Top speed of 35+ mph
- Single subassembly PA
- Multi-section design of MSA
- Secure storage of payloads in M2 and M3
- Proven capability through two iterations per aircraft and 31 test flights, as shown in Figure 1.1
- Estimated RAC of 0.96 and flight score of 18.73

Figure 1.1: Aircraft in flight.

The final design of the PA is a conventional high wing monoplane configuration with a single motor and tail-dragger gear. The aircraft is designed to simultaneously minimize weight and subassembly count, while maximizing speed. The canards, wings, fuselage and tail of the MSA are designed to assemble around the propeller, wings, fuselage and tail of the PA. The designs build on the teams' previous experience while continuing to push the envelope of practical, minimalistic design processes. The team is confident that this design solution has been optimized to accomplish all performance requirements and maximize total score.

2. MANAGEMENT SUMMARY

The *Buzzedryoshka* team consisted of twenty-six students: one graduate student, eight seniors, six juniors, three sophomores, and eight freshmen. Seventeen of the twenty-six students were returning members from the 2014-2015 Georgia Tech DBF entry. This team composition allows new team members to be mentored by a core of experienced members to build the team knowledge base and lay the foundation for later years.

2.1 Team Organization

Buzzedryoshka used a hierarchical structure to establish leadership amongst its senior members, with responsibilities flowing down to the team's newer members. This hierarchy served as an outline only, as all team members collaborated extensively to reach deadlines, share ideas, learn various disciplines, and produce a more successful aircraft. The work was divided during the design phase into CAD and Structures, Aerodynamics, Electrical and Propulsion, Payload, and Manufacturing. During construction, testing, and report writing, all team members participated fully. Figure 2.1 shows the different positions and the roles of each member of the team.

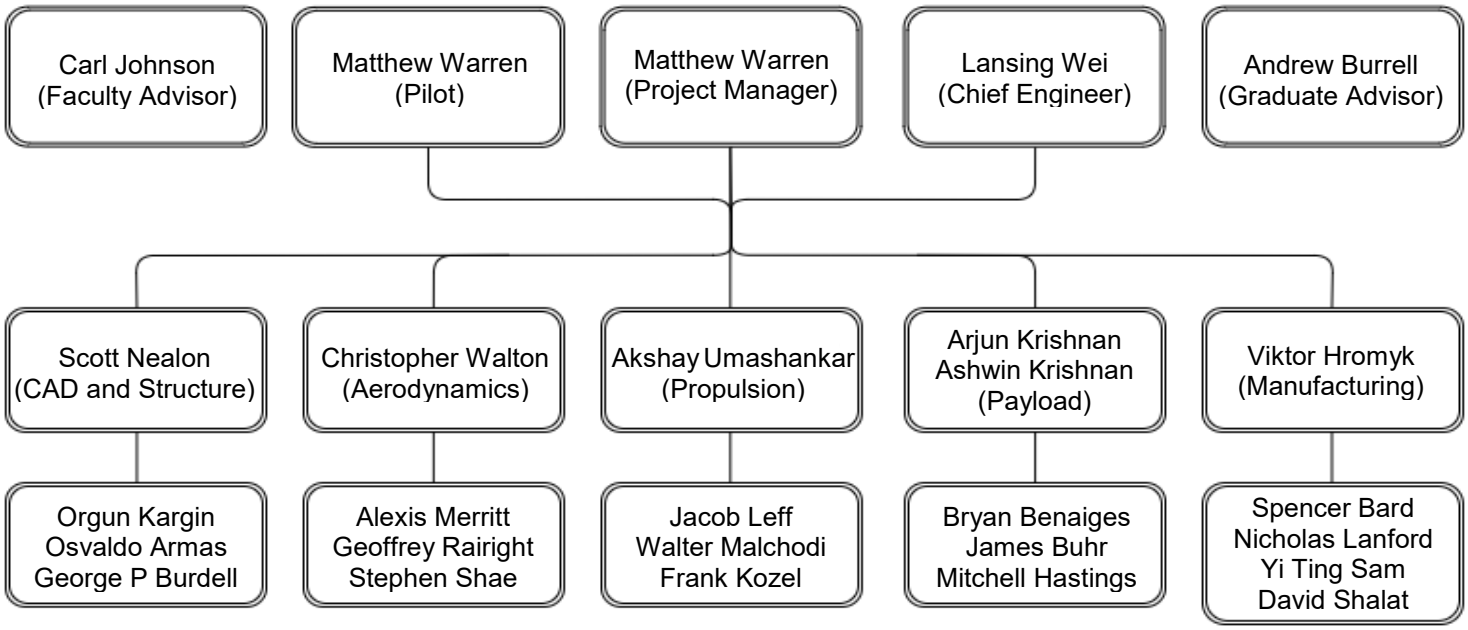

Figure 2.1: Team organization chart.

2.2 Milestone Chart

A milestone chart was established at the beginning of the design process to capture major deadlines and design and manufacturing goals. Progress was monitored by the team leaders to ensure all major milestones were met. The team worked throughout the entire academic year and established stringent deadlines early to ensure testing and flight experience before the competition in April. The team met frequently with the faculty advisors to discuss progress. The milestone chart is shown below in Figure 2.2, capturing planned and actual timing of major events.

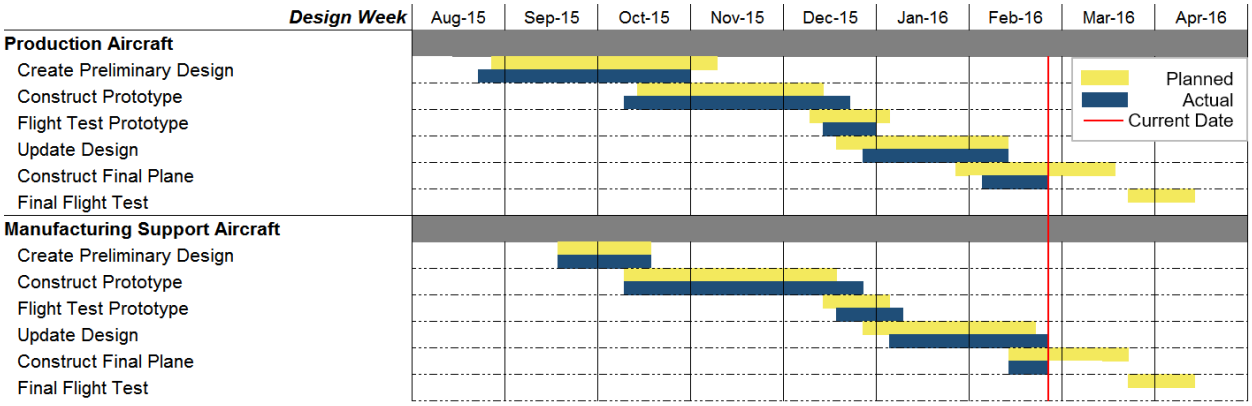

Figure 2.2: Aircraft design milestone chart showing planned and actual objectives.

3. CONCEPTUAL DESIGN

In this early phase of the design, the team analyzed the competition rules to produce a feasible design to maximize score. The rules were distilled into design requirements and scoring factors. Quantitative analysis was performed to pinpoint key scoring drivers and identify the design space. The scoring factors were translated into Figures of Merit (FOM) and used to weigh design choices. The FOM were applied to a design space of three possible system configurations to arrive at an optimized system. The PA is a high wing, conventional tail and single motor configuration that fits as a single piece into the MSA, which has similar configuration and assembles around the PA.

3.1 Mission Requirements

3.1.1 Mission and Score Summary

The AIAA Design/Build/Fly 2015/2016 competition consists of three flight missions, an optional ground mission, and a design report. The total score for each team is calculated as shown in Equation 3.1:

$$Score = Written\ Report\ Score \times (TMS/RAC) \tag{3.1}$$

Where *TMS* stands for the Total Mission Score made up of the two MSA missions (MF1, MF2), the PA mission (PF) and the optional bonus mission as shown in Equation 3.2:

$$TMS = MF1 \times MF2 \times PF + Bonus \quad (3.2)$$

Rated Aircraft Cost (RAC), is calculated from empty weight (EW) and battery weights ($W_{battery}$) of the two aircraft and the number of components ($N_{Components}$) used to construct the PA and is seen in Equation 3.3:

$$RAC = EW_1 \times W_{Battery,1} \times N_{Components} + EW_2 \times W_{Battery,2} \quad (3.3)$$

Equations 3.1 through 3.3 show that battery weights and number of components are the main score drivers, whereas various performance points of the design affect only the flight scores.

All flight missions are flown along the same distance and pattern per lap. For flight missions, the individual portions of the flight pattern seen in Figure 3.1 are as follows:

1. Successful Takeoff within 100 ft.
2. Climb to Safe Altitude
3. 180º U-turn, 500 ft. Upwind from the Start/Finish Line
4. 1000 ft. Downwind
5. 360º Turn Along the Backstretch
6. 180º U-turn
7. 500 ft. Final with a Successful Landing

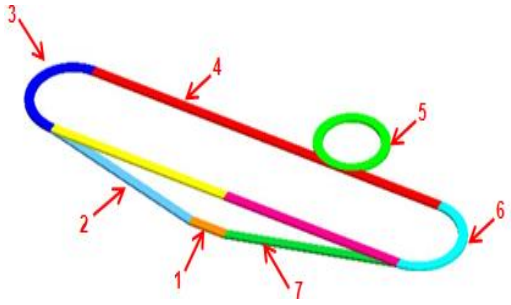

Figure 3.1: Competition flight course.

Each lap is roughly 2500 ft. when accounting for the three turns involved. A complete lap is defined as crossing the start/finish line, completing the defined pattern, then crossing the start/finish line while still in the air. The required number of laps is defined by the mission. The bonus mission will take place after the third flying mission and is driven by the assembly time. The full score is awarded as long as the PA is assembled within two minutes.

Mission 1 MSA Ferry Flight: The aircraft must take off within the designated field length and fly three laps within 5 minutes. Time starts when the aircraft is throttled up and a lap is complete when the aircraft passes the start/finish line. The score is awarded if the aircraft successfully completes the mission. The scoring for MF1 is shown in Table 3.1:

Table 3.1: Scoring Breakdown for Mission 1.

Mission	Description	Score
MF1	Aircraft completes the mission	2.0
MF1	Aircraft does not attempt or complete a successful flight	0.1

Mission 2 MSA delivery flight: This mission simulates the delivery of the PA and must be completed within a 10-minute window. The aircraft must take off in the designated field length, complete one lap carrying a sub assembly internally, return, and land successfully. A new subassembly is loaded and the plane is made ready to fly. The mission ends once every sub assembly has been successfully delivered. The scoring of MF2 is shown in Table 3.2:

Table 3.2: Scoring Breakdown for Mission 2.

Mission	Description	Score
MF2	Aircraft completes all sub-assembly group transport flights successfully within the time window	4.0
MF2	Aircraft completes less than all the sub-assembly flights within the designated time allowance but at least 1 group is successfully transported	1.0
MF2	Aircraft does not attempt or complete a successful flight	0.1

Mission 3: Production Aircraft Flight: The aircraft must take off in the designated field length. The payload for mission three, a factory sealed 32 oz. Gatorade bottle, must be carried internally. The aircraft must fly three laps within the five-minute time limit. Time starts when the aircraft is throttled up and a lap is complete when the aircraft passes the start/finish line. Landing is not included in the five min time limit. Listed in Table 3.3 below are the possible scores for mission three.

Table 3.3: Scoring Breakdown for Mission 3.

Mission	Description	Score
PF3	Aircraft completes the required flight within the time period carrying the full payload	2.0
PF3	Aircraft completes less than the required laps or exceeds the time period	1.0
PF3	Aircraft does not attempt or complete a successful flight	0.1

3.1.2 Aircraft Constraints

The competition rules stipulate specific constraints on the aircraft's takeoff distance, propulsion system, and payload:

Takeoff Distance: The aircraft must have the ability to start and take off completely within a 100 foot runway for all three flight missions.

Propulsion System: The aircraft must be propeller driven and electrically powered, with all components of the propulsion system commercially available. These include the motor, propeller, speed controllers, receivers, and batteries. The battery selection is limited to NiCad or NiMH, but may be of any cell count, voltage, or capacity. There is no limit of the weight of the battery packs. The entire propulsion system must be armed by an external safety plug or fuse. The arming device must be mounted on the exterior of the aircraft and be accessible from behind in a tractor propeller configuration.

Payload: The payload for the PA is a full, factory sealed 32 oz. Gatorade bottle. The MSA payload is the PA broken down into subassemblies. All payloads must be secured within the aircraft's structure so that they do not shift or come loose during flight.

3.1.3 Flight Score Sensitivity Analysis

A sensitivity analysis on the flight scoring drivers was performed to understand the design trades and mission objectives that maximize the total mission score (TMS) as divided by the rated aircraft cost (RAC). It is assumed that the system can complete the missions if the respective flight speeds exceeds the minimum speed and meets the takeoff requirement with payload. The scoring then becomes a function of RAC alone, which is driven by the number of components of the PA, battery weights, and structural weights.

Component count: The flight score is inversely proportional to the number of components of the PA. The effect of Number of components was studied by applying constraints to the scoring equation. The battery weight was estimated at 40% of the system empty weight for both aircraft, and payload fraction for the PA was estimated at 0.65 from historical data. This allowed the RAC to be expressed as a function of MSA empty weight and number of PA components. Final Score was then plotted against empty weight, with both axes being expressed as percentages of baseline values. This is shown in below in Figure 3.2.

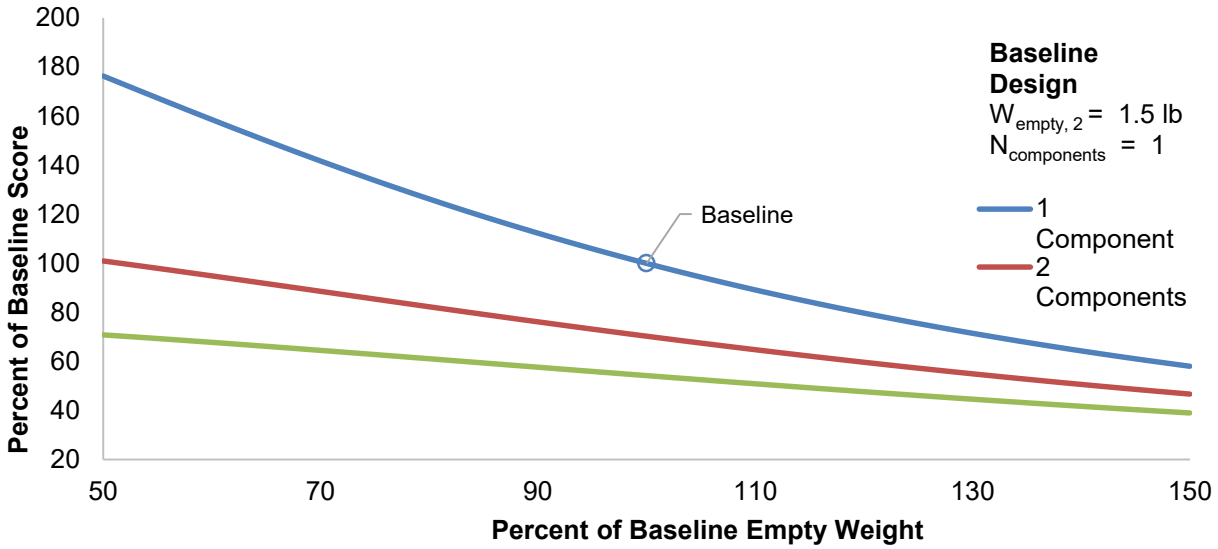

Figure 3.2: Change of score with respect to empty weight and number of components.

As seen in the figure, empty weight of the MSA would need to be reduced by 50% to justify the increase from 1 to 2 components. Achieving a competitive Final Score demands a single-component PA design.

Empty Weight: Aircraft empty weight was divided into propulsion and structural components. The propulsion system weight is proportional to the number of battery cells used. Based on previous team experience, 1,500 mAh NiMH cells were selected as representative batteries, weighing 0.05 lbs each. Based on testing of battery discharge rate, the maximum current draw is 20 amps. The electric motor weight was estimated at 0.5 lbs / kW from past experience, and speed controllers that met the pack voltage were cataloged. The propulsion weight assessment is summarized by Equation 3.4 and Equation 3.5:

$$P_{electric}=n_{cells}\left(1.2\frac{V}{cell}\times 20amps\right) \tag{3.4}$$

$$W_{propulsion}=n_{cells}\left(0.05\frac{lbs}{cell}\right)+P_{electric}\left(0.5\frac{lbs}{kW}\right)+W_{ESC} \tag{3.5}$$

Structural weight was estimated using the team's experience, with a baseline minimum weight which increases with wing area. The coefficients K_A and K_B in Equation 3.6 were adjusted to match past years' Design/Build/Fly planes, and Equation 3.7 summarizes the empty weight assessment:

$$W_{struct}=W_{baseline}+K_A\left(S_{wing}-S_{baseline}\right)^{K_B} \tag{3.6}$$

$$EW=W_{struct}+W_{propulsion} \tag{3.7}$$

Maximum Speed: The MSA and PA need to be able to fly above 35 mph to complete three 2,500 ft. lap lengths within five minutes with the assumed wind conditions. The maximum speed was calculated using simple power-required calculations that stem from the drag polar, and the power available from the propulsion system, as seen in Equation 3.8. Lap numbers were truncated down, since only integer numbers of laps are counted.

$$P_{req}-P_{av}=\left(\frac{1}{2}\rho V_{max}^3 SC_{D,0}+\frac{2W}{\rho V_{max} S\pi ARe}\right)-P_{electric}\eta_{prop}=0 \tag{3.8}$$

Takeoff: Both aircraft must be able to take off within 100 ft. on all missions. This requirement constrains the wing area and power requirement. The governing relation for takeoff is shown in Equation 3.9. The K_D term is a function of dissipative forces and wing loading (W/S), while K_T is a function of propulsive forces and thrust loading (T/W).

$$s_g=\frac{1}{2gK_D}+ln\left(1+\frac{K_D}{K_T}V_{LO}^2\right)\leq 100\ feet \tag{3.9}$$

Since the sizing and payload is driven by the PA, analysis of the MSA follows the PA analysis. As a result, the scoring sensitivity in Figure 3.3 below only shows the RAC for the PA. The plot represents a physics-based tradeoff between speed and aircraft weight, as governed by wing area and battery count. The white area represents configurations that cannot meet the takeoff and speed requirements.

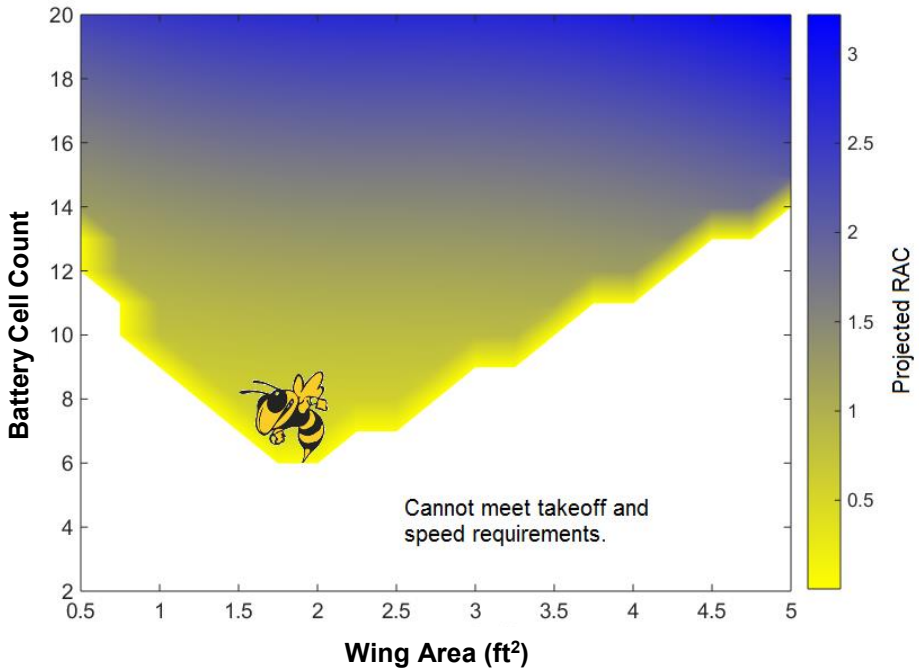

Figure 3.3: A physics-based scoring analysis of the design space for the PA. The team's chosen conceptual design point is noted by Buzz.

The figure demonstrates that the design with the highest scoring-potential which can successfully complete the mission, must have the lowest possible cell count. This corresponds to a 7 cell battery and a wing area of about 1.8 sq. ft. This was the conceptual design point for the PA.

A similar analysis was completed for the MSA. The wing area for the MSA is constrained to be about 50% larger than the PA to internally accommodate the wings of the PA. The estimated payload of the MSA is found from the preliminary analysis of the PA. With wing area fixed at a minimum and payload known, it was only necessary to compute the smallest battery that could meet the mission requirements.

3.1.4 Ground Score Sensitivity Analysis

The bonus mission does not present any aerodynamic trade-offs and must be analyzed separately from the flight missions. Since the PA must be one piece, the assembly time should be short. Due to the pass-fail nature of the bonus mission, it is only necessary to design the PA in a way that allows it to be assembled with payload in just under the required time of 2 minutes.

3.2 Translation into Design Requirements

The scoring analysis revealed four main components that drive the overall flight score:

Component Count: Any component on the PA that is disconnected or moved from its position required for takeoff and flight will be counted as a sub-assembly. Additionally, landing gear that is retracted or removed to fit inside the MSA or a propeller that folds or is removed will count as a sub-assembly. For the maximum achievable score, the component count needs to be the absolute minimum. This suggests a single piece PA with no components removed to fit inside the MSA.

Empty Weight: Any configuration that fails to be as light as possible will not be competitive. Effort must be made to reduce the aircraft empty weight. However, the structure must be able to withstand the expected loads. Such considerations must be carefully balanced to secure the payload and decrease empty weight.

Battery Weights: Larger batteries provide more power and will enable faster flight. However, larger batteries also incur a larger weight penalty. Based on analysis of the scoring, the battery weights will have the largest individual impact and must therefore be optimized to provide the power required without adding unnecessary weight.

Flight Speed: The aircraft must be able to fly the required number of laps in Wichita, Kansas. Figure 3.4 shows a distribution of mean wind speeds in Wichita, Kansas over the past 10 years in April. It is unreasonable to design for the maximum recorded speed so a 97% confidence interval was chosen. The mean wind speed on the day of the competition will be less than about 25 mph with 97% certainty.

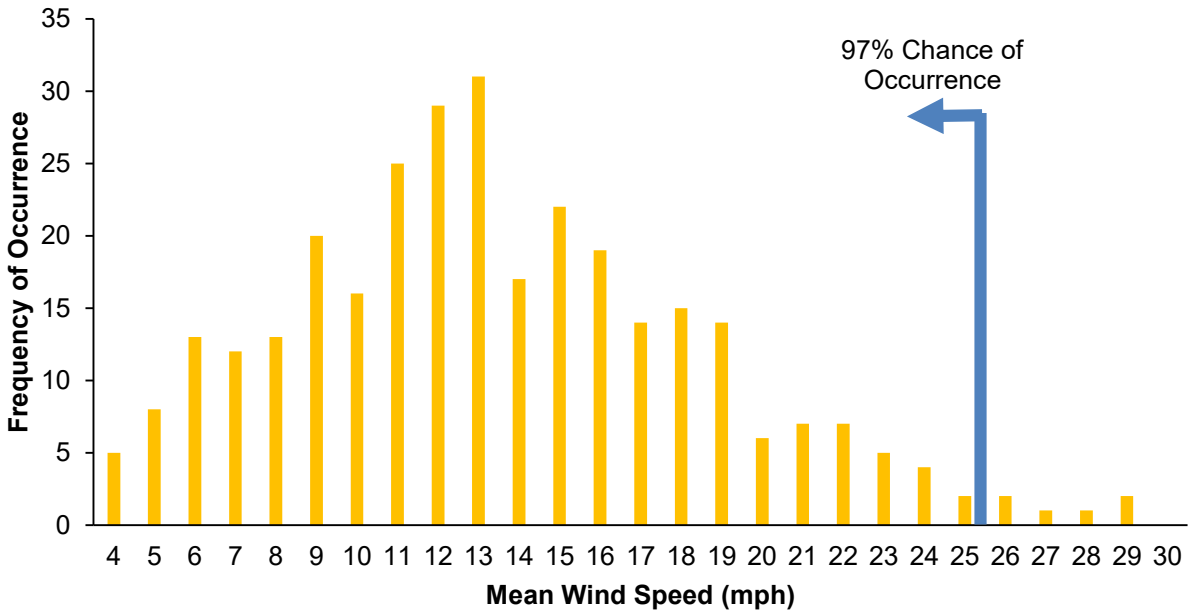

Figure 3.4: Distribution of mean wind speeds in Wichita, Kansas in April.

Any given wind speed corresponds to a required flight speed to finish the missions. This required speed is assumes the plane must travel 1000 ft upwind per lap and 1500 ft downwind per lap. It can be seen in Figure 3.5 that a wind speed of 25 mph translates to an aircraft flight speed of under 35 mph. A minimum flight speed of 35 mph was chosen as a minimum speed for both the PA and the MSA.

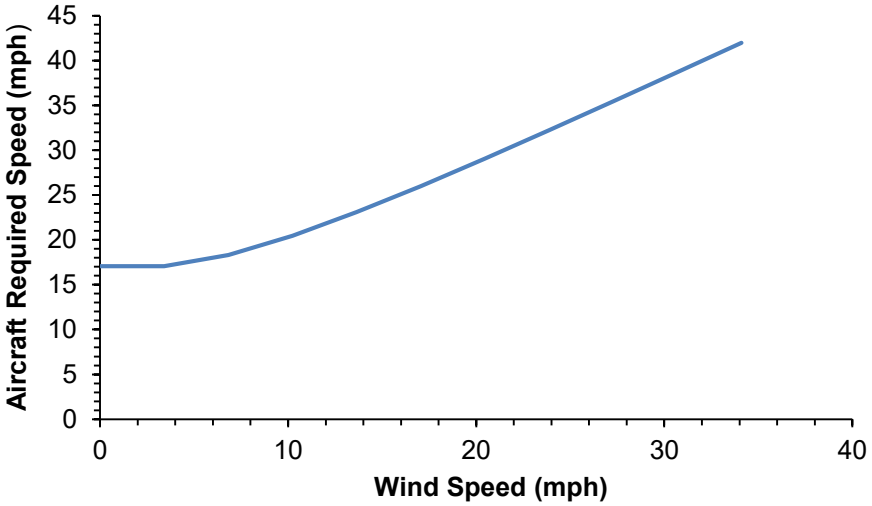

Figure 3.5: Required top speed to complete Mission 3 versus wind speed.

The analysis conducted in Sections 3.1 and 3.2 were translated into qualitative design metrics that were used to evaluate and select an aircraft configuration, summarized for the PA and MSA in Table 3.4 below.

Table 3.4: Rules and requirements translated into design requirements.

Mission/Scoring Requirement	Design Requirement
Minimal Component Count	Simple, Robust Design
Low Empty Weight	Efficient Structure
Minimal Battery Weight	Optimized Propulsion
Enclose Production Aircraft	Unique geometry
	Robust, multi-part Design

These requirements show that minimizing the number of components for the PA is the most critical design consideration, followed closely by battery weights. If a design is as light as possible, it will also likely require less power and have the lowest battery weight. The MSA must fit tightly around the PA to be efficient, indicating that it must have the same configuration.

3.3 Configurations Considered

3.3.1 Aircraft Configuration

Due to the nature of the competition rules, both aircraft had to be developed simultaneously as a system. Since the planes need to nest together, the selection criteria hinged on the complexity of wrapping the MSA around the PA. As a result, several design possibilities are eliminated, but three choices emerged as possible configurations. Each of these configurations were thoroughly analyzed, as detailed below.

In Figure 3.6 through Figure 3.8, the wire frame represents the MSA while the shaded figure represents the PA. Figure 3.6 shows a basic biplane configuration for both the PA and MSA. With a biplane, the MSA would require two removable wings and a two-part, bulbous fuselage to allow the PA to fit inside as a single piece with landing gear. This complexity would present a significant structural challenge and likely increase the weight of the plane. These drawbacks would make this configuration a difficult choice.

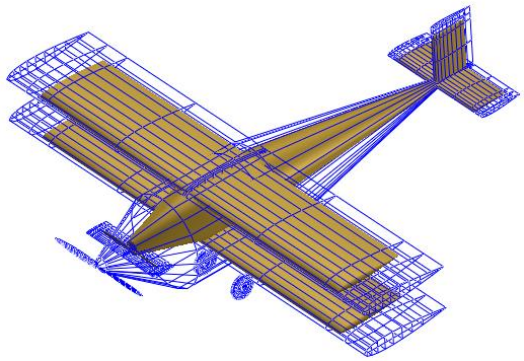

Figure 3.6: Sketch of biplane configuration.

A flying wing configuration was examined, shown in Figure 3.7. In this case, the MSA would need to have a large opening or be built in two halves to allow the PA to be loaded. The MSA would also require a fuselage bottle faring, and landing gear of the PA leading to structural complexity. In addition, a flying wing is sensitive to C.G. and has a high power requirement due to a low $C_{L,max.}$

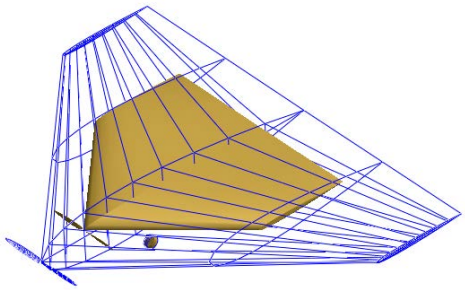

Figure 3.7: Sketch of Flying Wing configuration.

Finally, the team explored a conventional monoplane configuration, illustrated in Figure 3.8. This configuration would still require the wings of the MSA to be detachable and have some method to enclose the PA propeller. However, the fuselage would only require a hatch to accept the PA. Moreover, this configuration would allow for minimization of interference from the PA landing gear and payload bay. As a result, the conventional configuration should be lighter than the biplane and more stable than the flying wing, making it qualitatively superior.

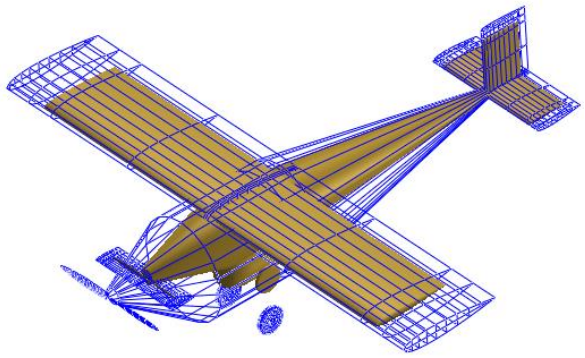

Figure 3.8: Sketches of Conventional configuration.

3.4 Component Weighting and Selection Process

In order to asses each configuration from a quantitative standpoint, Figures of Merit (FOM) were created based on the most important configuration factors. The FOM are shown in Table 3.5. Each FOM was assigned an importance of 0 through 5, with 5 being the most important factor and 0 being a non-factor in design.

Table 3.5: Figures of Merit.

Figure of Merit	0	1	2	3	4	5
Simplicity						5
Weight					4	
Power				3		
Speed				3		
Stability			2			
Drag			2			

All of the configurations could be made with a minimal number of components. As such, the simplicity of enclosing the PA inside of the MSA was the critical design factor. Due to the wind conditions anticipated at the location for this year's competition, Wichita KS, speed was another consideration. Minimizing both weight and the power requirement maximizes flight score and makes them important score drivers.

For final selection, each configuration was given a scoring value for each figure of merit, and that rating was then multiplied by the FOM value. The range of scoring values are shown in Table 3.6. The configuration with the highest total quality was then selected for further analysis in the design process.

Table 3.6: Configuration Scoring Values.

Score	Value
1	Inferior
3	Average
5	Superior

The three configurations discussed previously are shown in Table 3.7 with their respective scores for each of the relevant FOM. These results, combined with those from the qualitative analysis, lead to the team's choice of configuration for the *Buzzedryoshka* aircraft system.

Table 3.7: Aircraft configuration Figure of Merit.

		Aircraft Configurations		
		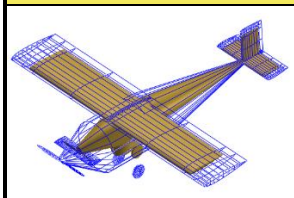	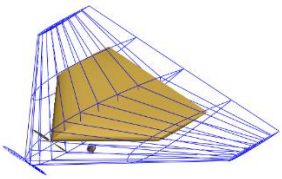	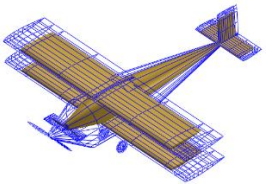
FOM	**Value**	**Conventional**	**Flying Wing**	**Biplane**
Simplicity	**5**	3	2	1
Weight	**4**	4	1	2
Power	**3**	4	2	4
Speed	**3**	4	5	3
Stability	**2**	4	2	4
Drag	**2**	4	2	2
Value	**19**	71	43	46

The complexity of the biplane and power requirement of the flying wing made these designs ill-suited for the PA. The conventional monoplane configuration had the highest total score, and was therefore chosen as the configuration for both aircraft in the combined system.

3.5 Final Conceptual Design Configuration

The final configuration for both the PA and MSA is a high wing, conventional tail aircraft with a single-engine tractor propulsion system as shown in Figure 3.9. Here the MSA is shown exploded into several pieces to show how it the PA will fit within. This configuration offers minimal complexity for nesting, while allowing for greater speed by reducing drag. The empty weight of the aircraft is more heavily influenced by structural design, and is discussed later in this report.

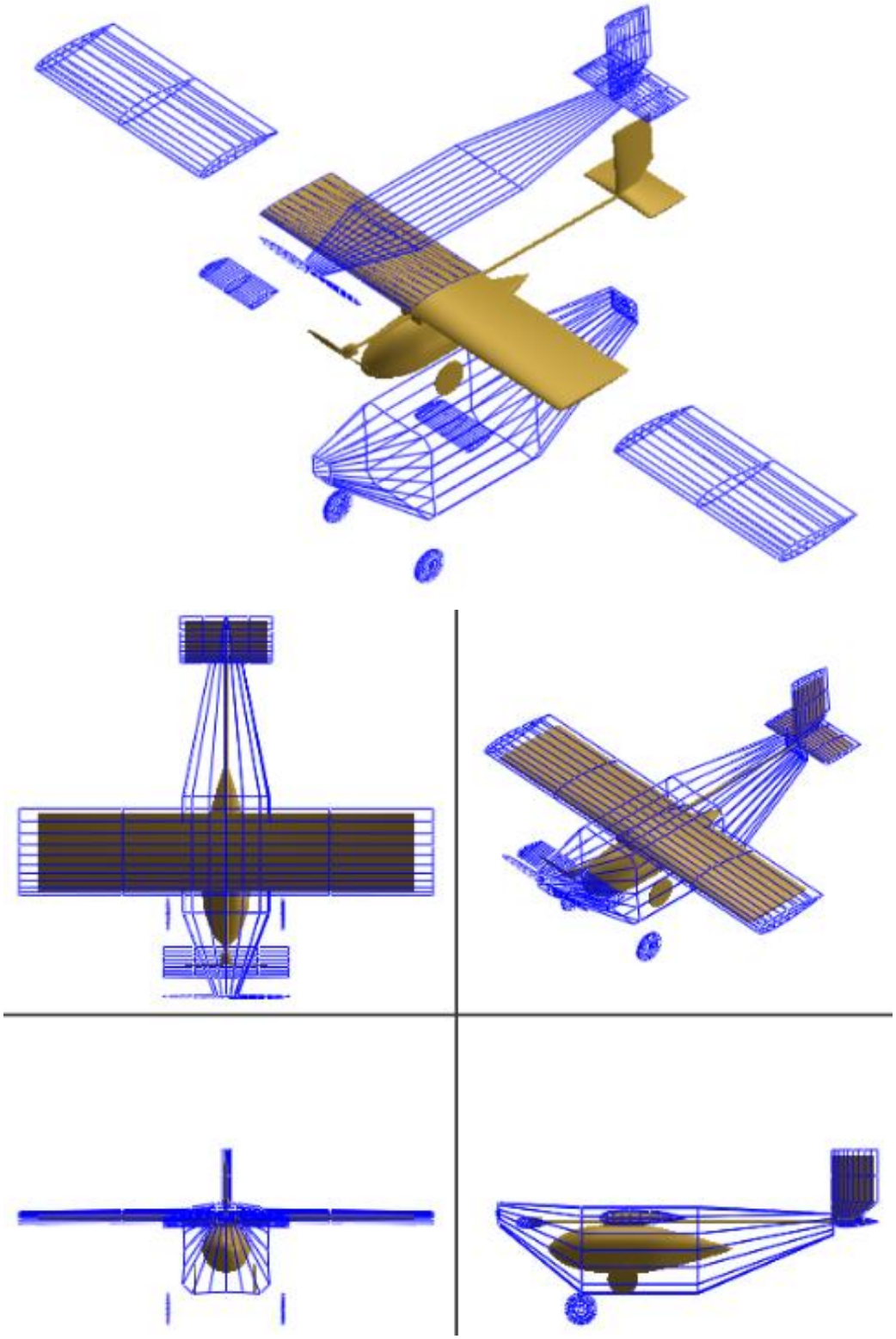

Figure 3.9: Final Configuration.

4. PRELIMINARY DESIGN

The objective of the preliminary design phase was to further narrow the design space. To do this, design/sizing trades for the system were evaluated by examining propulsion system options and wing area sizing for takeoff distance. The weight, drag, motor, propeller data, battery data, and aerodynamic coefficients were calculated and combined to estimate mission performance for all three flight missions.

4.1 Design Methodology

The *Buzzedryoshka* team designed the two aircraft configurations in parallel using an iterative performance-focused multidisciplinary analysis. The team used constraint sizing to select a weight-normalized design point for each plane that could satisfy objectives for all three missions. From these design points, the team analyzed possible propulsion systems, aerodynamic characteristics, built mission models, and compared them to estimates generated as part of the sizing process. After this analysis, the mission performance and stability of the sized aircraft configurations were computed. The design process detailed in sections below is written as sequential, but iterations occurred throughout, as seen in Figure 4.1. An example of iteration would be updating wing area at a constant wing-loading if propulsion weight is found to be lower, re-evaluating stability and mission performance, and re-adjusting the wing or propulsion system if needed. All iterations were performed with the ultimate goal of maximizing overall score. Therefore, the design shown in this report is the final product of a more complex, iterative procedure.

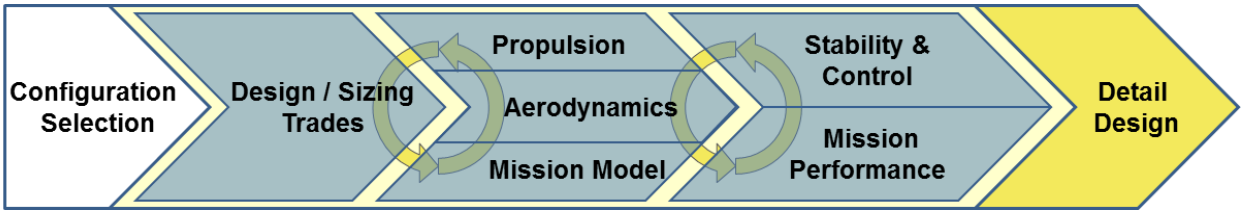

Figure 4.1: The team's preliminary design methodology highlighting multidisciplinary iterations.

4.2 Design Trades

4.2.1 Constraint Sizing

A constraint sizing analysis was conducted to examine the effect of wing loading and power to weight ratio on the performance and scoring potential of each aircraft. The MSA must be designed after the PA to ensure the MSA can carry the PA. As specified in Section 3.1.3, the scoring requires the planes to finish the missions while having a minimal battery weight. Figure 4.2 shows the relationship between wing loading (W/S) and power to weight (P/W) for the PA.

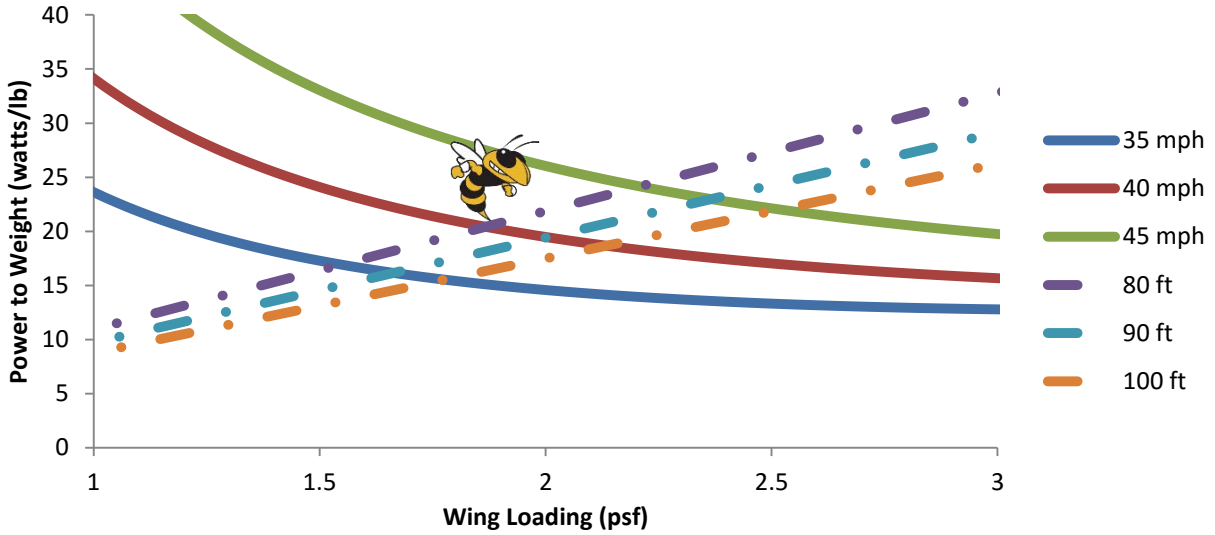

Figure 4.2: Design point of the PA from the constraint plot, marked by Buzz's stinger.

Battery weight is roughly proportional to power available, and the lowest P/W possible will lead to the highest score. Higher W/S allows for lower P/W required at cruise, but higher P/W to meet takeoff requirements. The inverse is also true. The optimal design is at the intersection of the required takeoff distance and minimum speed required. Based on these considerations, a design point just above the 80 ft. takeoff distance and with a top speed just above 40 mph was chosen.

The wing area of the MSA was constrained by its need to closely fit the PA and carry it in Mission 2, creating a fixed minimum W/S of 0.7. Since minimum wing area corresponds to minimum weight, this W/S was used and the propulsion system sized to match, as shown in Figure 4.3 below.

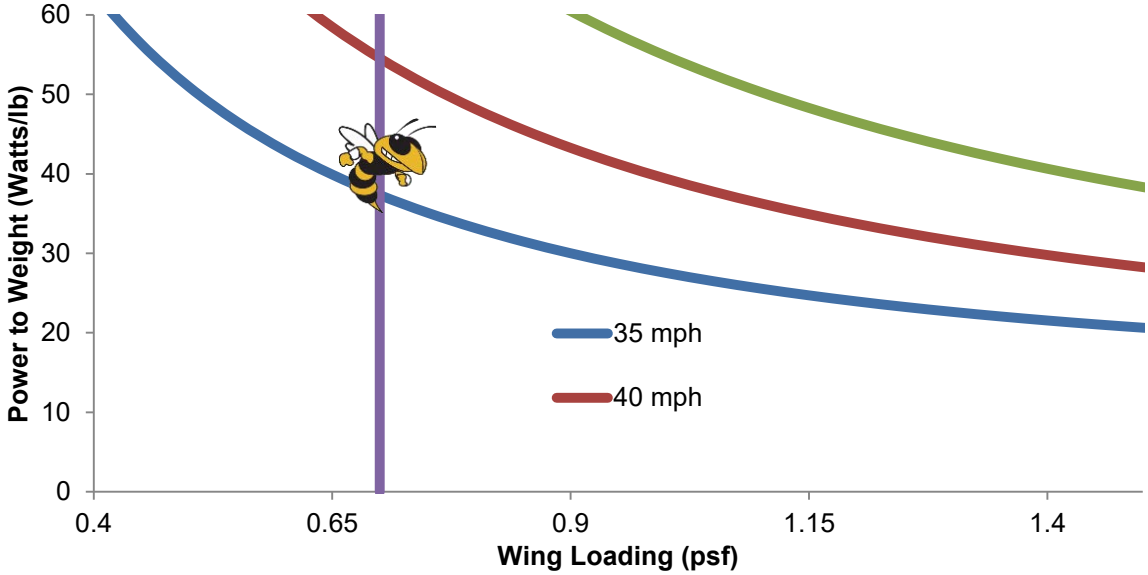

Figure 4.3: Design point of the MSA from the constraint plot, marked by Buzz's stinger.

Note that takeoff curves are not shown in the figure. This is because analysis showed that the P/W required for takeoff was much smaller than that for cruise at higher the speeds shown in the figure. This meant P/W for cruise speed dominated the constraint sizing analysis for the MSA. The final design point for the MSA achieves a cruise speed of just over 35 mph.

The constraint sizing process along with an empirical weight estimate allow a preliminary determination of power and wing area summarized in Table 4.1 for the PA and MSA.

Table 4.1: Preliminary Power and Wing Area.

	Wing loading (psf)	Power Loading (Watts/lb)	Est. Weight (lb)	Surface Area (Sq. ft)	Power Req. (Watt)
Production	1.81	21	3.4	1.875	71.4
Manufacturing	0.71	37	2.1	2.87	77.7

4.2.2 Propulsion System Selection

As seen in Table 4.1, the power requirement for each aircraft is similar. As a consequence, the same propulsion system will be used for both aircraft. The team decided to use a fixed pitch propeller because of reduced complexity and weight. A system efficiency of 50% is empirically assumed leading to a power of around 160 watts for the propulsion system. From the analysis performed in section 3.1.3, a 7-cell 1500mAh battery maximizes RAC. The team wanted a direct-drive brushless out-runner motor with a high motor constant, Kv, to draw more power out of a 7-Cell battery. The team researched motors that fit these criteria and created a database containing over 50 motors from various companies, including Hacker, Tiger, Scorpion, Cobra and AXI.

A propeller database was also generated based on the size of the airplane and speed. The propellers tested were APC 9x9, 10x7, 11x8, 12x8, and 12x10 propellers. MotoCalc, a commercially available motor analysis tool, was then used to estimate the motor efficiency, static thrust, and thrust at 30 mph for each motor and propeller combinations, feasible combinations were selected for further analysis and sorted by weight.

The top motor-battery-propeller combinations were analyzed and their variation with speed was graphed. Allowing the team to evaluate the most effective combination to meet the takeoff and max speed requirement. Two motor combinations were chosen to purchase and test, as shown in Table 4.2. Section 7.2 will go into further detail regarding these tests.

Table 4.2: Final propulsion alternatives.

Motor	Kv	Battery (Cells)	Current (Amps)	Best Propeller	Static Thrust (lb.)	Propulsion System Weight (lb.)
Cobra 2814/12	1390	7 (1,500 mAh)	19.0	12x8	1.89	0.15
Hacker A30-22S	1440	7 (1,500 mAh)	17.0	11x8	1.37	0.24

4.3 Mission Model

4.3.1 Description and Capabilities

The three missions were simulated via a set of first order differential equations (Equations 4.1-4.3) defining the position and orientation of the vehicle throughout the flight. By integrating these equations over time using a 4th Order Runge-Kutta approach in MATLAB and simple logic defining each of the required mission segments, it is possible to define the position, velocity, and orientation of the vehicle over time. The thrust (T) was defined as a function of velocity, with the relationship defined by MotoCalc, the analysis tool used in the propulsion system selection. The drag (D) was represented via a parabolic drag relationship. The load factor was explicitly defined for each turn segment, but if it exceeded the estimated maximum lift coefficient, it was limited to that value.

$$\dot{x} = V \tag{4.1}$$

$$\dot{V} = \frac{T-D}{m} \tag{4.2}$$

$$\dot{\psi} = \frac{g\sqrt{n^2-1}}{V} \tag{4.3}$$

4.3.2 Uncertainties

The approach described above has specific limitations and uncertainties. The lack of a vertical dimension means that it cannot capture any aerodynamic effect due to altitude changes, or for the energy required or saved due to climbing or diving. The lack of any wind model discounts any additional drag due to sideslip in flight, or changes in velocity depending on traveling with or against the wind. The flight path defined for each lap assumes an idealized flight path, with the pilot turning perfectly after each 1000 ft. leg and the turns being optimal turns. Finally, there are additional uncertainties in the mission predictions due to any errors or inaccuracies in the thrust and drag predictions.

4.4 Aerodynamic Characteristics

4.4.1 Airfoil Selection

Using the correct airfoil for the aircraft is key to achieve the aerodynamic characteristics required to compete in this competition. Hundreds of airfoils were analyzed through a MATLAB script at an estimated Reynolds number of 200,000 to choose an airfoil that could provide the requisite lift and moment coefficients. These airfoils were also filtered based on their thickness and manufacturability.

Manufacturability: Complex airfoil geometry, as shown in Figure 4.4, can result in manufacturing error. These imperfections can negatively impact the aerodynamics of the vehicle and therefore its performance. The airfoil must not have a highly cambered or sharp trailing edge while maintaining sufficient thickness to reduce these manufacturing difficulties and obtain the desired performance from an airfoil.

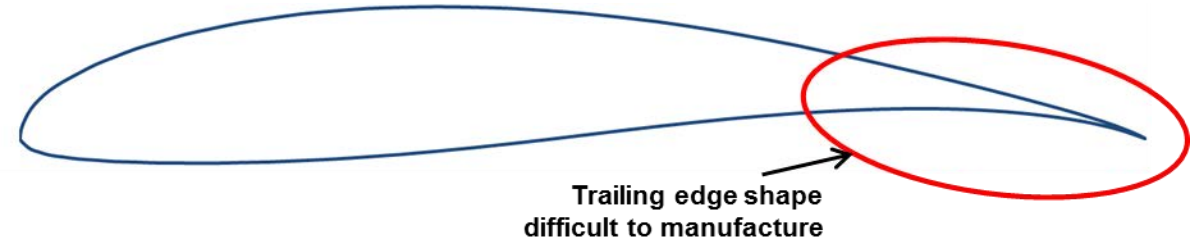

Figure 4.4: Wortmann FX 63-137 showing poor manufacturability.

Thickness: Low thickness airfoils typically have a small leading edge radius that results in abrupt stall at lower angles of attack. Increasing airfoil thickness increases the space for internal structural members that increase the structural rigidity of the airfoil while reducing structural weight. However, this trades with this year's requirement for nesting wings. After testing multiple airfoil types, a thickness greater than 12% was preferred for the MSA to achieve required structural rigidity and allow for nesting wings.

The filtered airfoils were further analyzed based on maximum section lift coefficient and lift to drag ratio. Drag and lift curves for the final four airfoils were constructed using airfoil data obtained from wind tunnel test results from UIUC as shown in Figure 4.5.

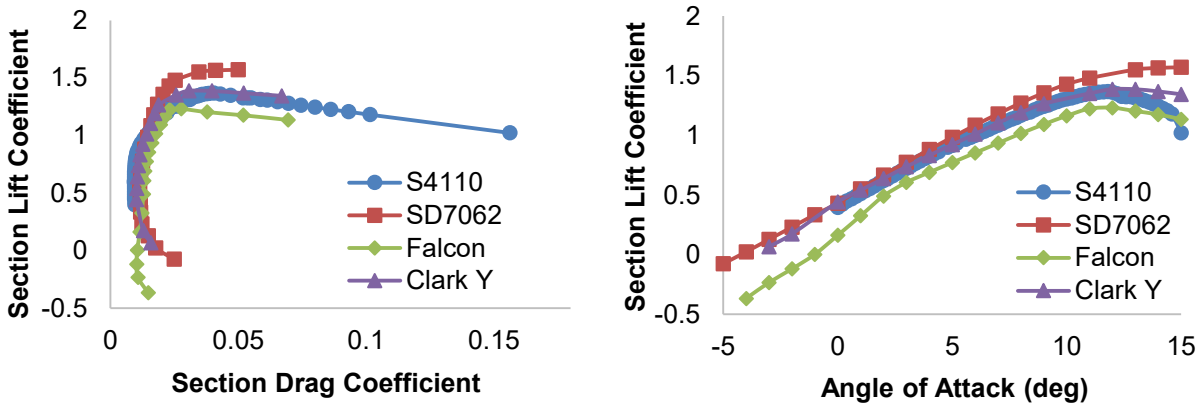

Figure 4.5: Experimental lift and drag characteristics for selected airfoils from UIUC data.

Examination of the drag polar shows that the SD7062 and S4110 airfoils have a more stable sectional drag coefficient ($\tilde{C}_D$) over longer ranges of $\tilde{C}_L$ than the other airfoils. This indicates that for a given range of $\tilde{C}_L$ values, namely those around a $\tilde{C}_L$ of 0.5, the $\tilde{C}_D$ remains relatively low and constant. This is important due to the variance of $\tilde{C}_L$ over the wings caused by downwash due to wingtip vortices and environmental variables such as local wind. A high maximum $\tilde{C}_L$ is a desirable airfoil characteristic as it enables good STOL performance, which is critical due to the 100-foot takeoff requirement.

The SD7062 has a thickness to chord ratio of 14% which aids in both the manufacturing process and increases the geometric stiffness of the wing. The SD7062 also had a higher maximum $\tilde{C}_L$ and lift-to-drag ratio than the other airfoils considered, enabling the team to select the best combination of takeoff performance and speed. In summary, the SD7062 airfoil was selected for its combination of high maximum $\tilde{C}_L$, manufacturability, thickness to chord ratio, and favorable lift to drag ratio.

The S4110 is a thinner airfoil chosen for the PA based on its high maximum C_L, and relatively high lift to drag ratio. While the Clark Y airfoil has comparable performance, the lower thickness presents an advantage at the system level. Although the slender profile will impact the stiffness of the wing, this airfoil will not present any unreasonable manufacturing challenges. The integration of the S4110 airfoil into the SD7062 airfoil is shown in Figure 4.6 below.

Figure 4.6: S4110 inside of SD7062 airfoil.

4.4.2 Lifting Surface Analysis

Athena Vortex Lattice (AVL), an aerodynamic tool developed by Dr. Mark Drela at MIT, was used to model the lifting surfaces of the aircraft to compute the aerodynamic characteristics of the entire aircraft. AVL models lifting surfaces as an infinitely thin sheet of discrete vortices, and models their interactions. The aircraft's tail and control surfaces were sized in AVL to provide desired static stability and trim characteristics. The aircraft configuration and paneling in AVL is seen in Figure 4.7. The lift distribution shown in Figure 4.8 was generated in AVL using elevator trim to maintain flight at a moderate angle of attack on approach and landing. Due to the distribution shape, stall is expected to occur at the wing root, allowing the pilot to maintain roll control using the ailerons that are mounted outboard.

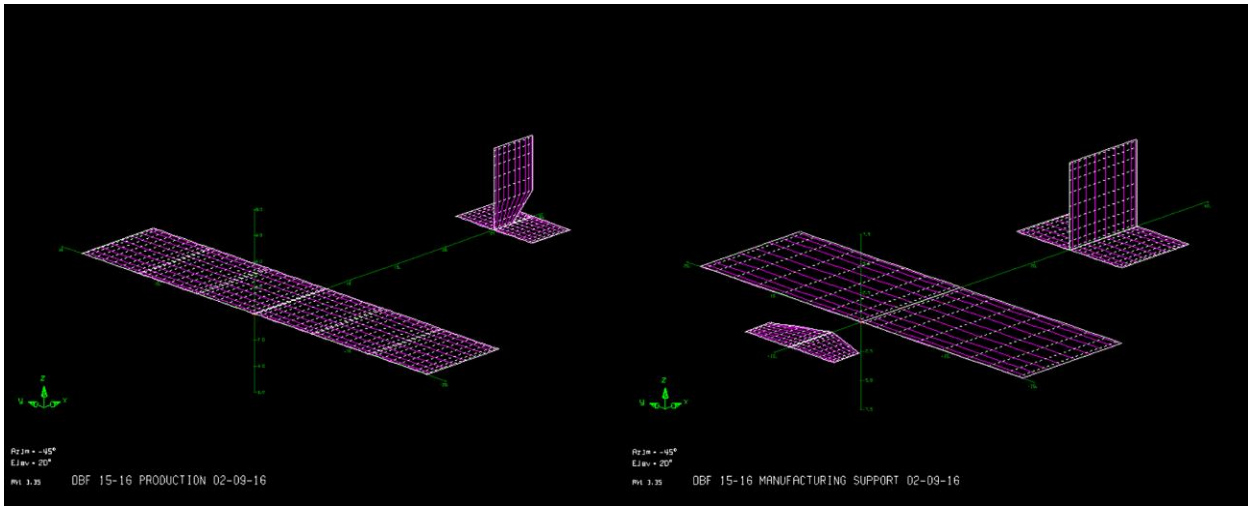

Figure 4.7: AVL model of both aircraft.

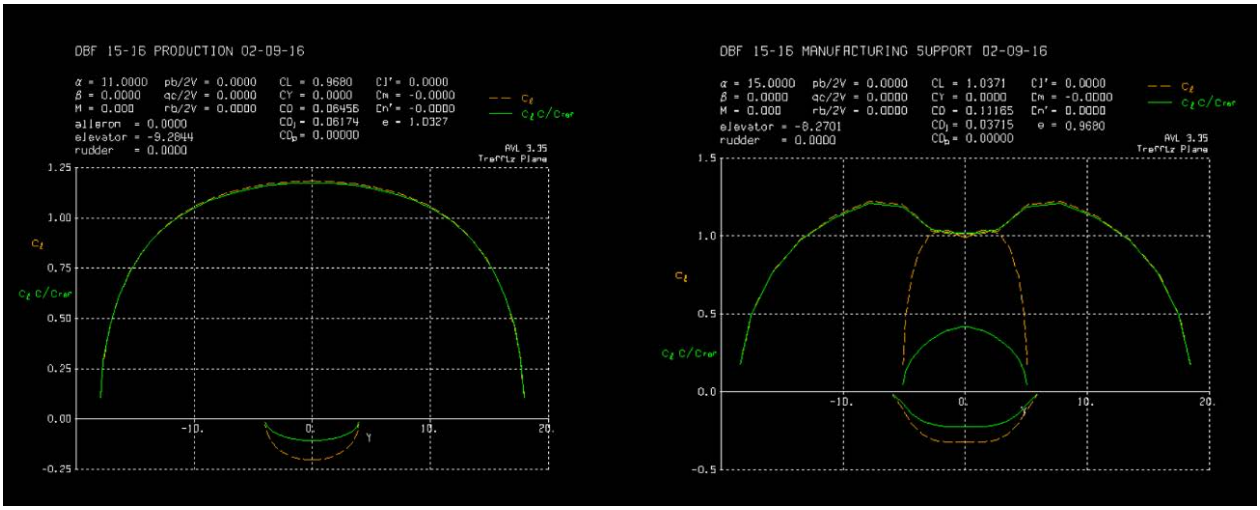

Figure 4.8: AVL predicted lift distribution of both aircraft.

4.4.3 Drag Analysis

A preliminary parasitic drag estimate was obtained by summing each component's drag contributions, computed using the semi-empirical methods from Hoerner's *Fluid Dynamic Drag*, and then normalizing each component according to the wing reference area. Table 4.3 shows the contributions of the major aircraft components, with displaying Figure 4.9 the same data as a percentage breakdown.

Table 4.3: Aircraft zero lift drag estimates.

Production Aircraft

Component	$C_{D,0}$
Landing Gear	0.0258
Fuselage	0.0284
Wing	0.0294
Tail	0.0063
Total	0.0899

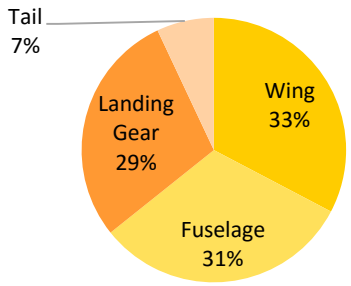

Manufacturing Support Aircraft

Component	$C_{D,0}$
Fuselage	0.0573
Wing	0.0242
Landing Gear	0.0203
Tail	0.0120
Canard	0.0007
Total	0.1138

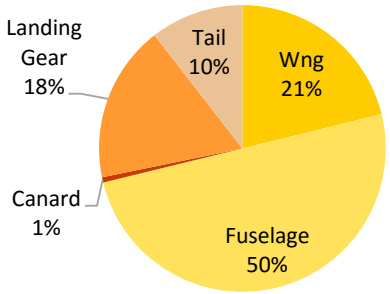

Figure 4.9: Graphical representation of drag estimates.

The main components of the parasitic drag are detailed below:

Wing: The drag coefficient for the wing was calculated using Equation 4.4 from Hoerner:

$$C_{D,0}=R_{wf}R_{LS}C_{f_w}\left(1+L'\left(t/c\right)+100\left(t/c\right)^4\right)\ x\ \frac{S_{wet_w}}{S} \tag{4.4}$$

Equation 4.4 contains terms correcting for wing thickness location, sweep, and wing-fuselage interference (L', R_{LS}, and R_{wf}, respectively). The flat-plate skin friction coefficient (C_f) is a function of Reynolds number approximated for fully turbulent flow. The wing was found to be the largest contributor to zero-lift drag for the PA, with a total $C_{D,0}$ contribution of 0.0258, which is about 33% of the total drag. For the MSA, the wing was found to be the second largest contributor to zero-lift drag, with a total $C_{D,0}$ contribution of 0.0242, which is about 21% of the total drag

Landing Gear: The landing gear components are significant contributors to the overall drag of the aircraft. The main gear and tail gear drag contributions were calculated separately, but both were modeled as a wheel and a flat plate added for the strut. The overall contribution of the landing gear to the drag was about 29% for the PA and 18% for the MSA.

Fuselage: The drag coefficient for the fuselage was determined using Hoerner's method, which computes drag as a function of the body fineness ratio, the Reynold-adjusted skin friction coefficient, and lifting-surface/fuselage interference. The total $C_{D,0}$ contribution fuselage of the MSA was calculated to be 0.0573 and contributes 50% of the total zero-lift drag. The total $C_{D,0}$ contribution fuselage of the PA was calculated to be 0.0284 and contributes 31% of the total zero-lift drag.

Tail: The tail surfaces were modeled as wings and the drag contributions were calculated using the same method as the wing calculation. Overall, the contribution of the tail to the drag were 7% and 11% for the PA and the MSA, respectively, due to their small size.

Canard: The drag coefficient for the MSA canard was calculated using Equation 4.4 from Hoerner. The flat-plate skin friction coefficient (C_f) is a function of Reynolds number approximated for fully turbulent flow. Due to its small size, the canard was found to be one of the smallest contributors to zero-lift drag, with a total $C_{D,0}$ contribution of 0.0007. This is about 1% of the total drag.

With parasitic drag computed for both aircraft, the team used AVL to model the lifting surfaces of the aircraft and estimate induced drag. The estimated span efficiency was 80% for the full configurations. Sub-optimal efficiency was preferred to manufacturing complexity added by sweeping, twisting, or tapering the wings. The full drag polar for both planes are displayed in Figure 4.10 and were calculated by adding the induced drag from AVL and the parasitic drag from above. The drag polar indicated a maximum lift-to-drag ratio around 5.8 for the PA and 4.2 for the MSA. These relatively low values can be attributed to the large fuselage driven by Mission 2 and 3 payload volumes.

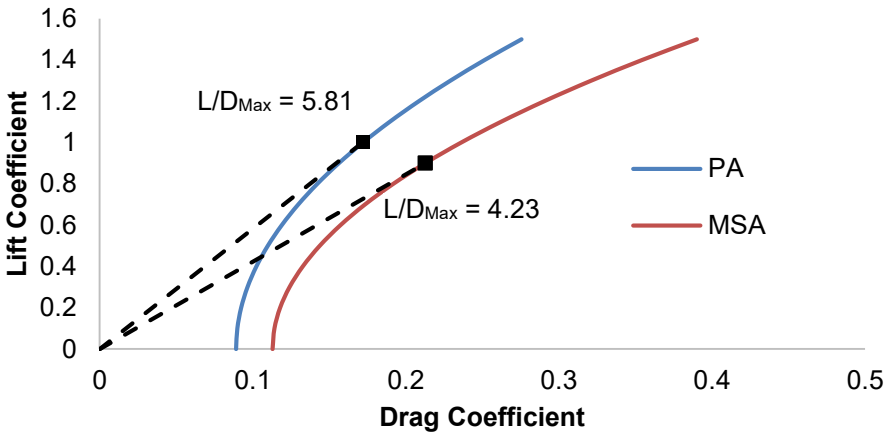

Figure 4.10: Full drag polar for both aircraft.

4.5 Stability and Control

Static and dynamic stability were analyzed to ensure that the aircraft would be able to successfully complete the flight missions. The fastest speeds, slowest speeds, heaviest weights, lightest weights, cruise, climbs, and turns were all considered, with results presented only for the critical flight condition.

4.5.1 Static Stability Analysis

Static stability was evaluated using the vortex lattice method implemented in AVL. The most demanding flight condition for trim was at the highest weight and lowest speed for both aircraft. Stability derivatives are given for these flight condition in Table 4.4. The aircraft are trimmed at this condition with a small elevator deflection and no extreme deflections were required for any of the cases analyzed. All cases indicate the aircraft are longitudinally, statically stable with a static margin of 18.2% for the PA and 12.7% for the MSA. All pitch, roll, and yaw derivatives are stable and within the acceptable range based on previous years' pilot feedback.

Table 4.4: Relevant stability coefficients and derivatives for static stability.

Parameter		Production Aircraft	Manufacturing Support Aircraft
Inputs	W_{total} (lbs.)	3.39	2.10
	V (ft/s)	45.6	25.5
Aerodynamic Parameters	C_L	0.97	1.04
	α (deg.)	11.0	15.0
	β (deg.)	0.0	0.0
Deflections	$\delta_{elevator}$ *(deg)*	-9.28	-8.27
	$\delta_{aileron}$ *(deg)*	0.0	0.0
Stability Derivatives	$C_{l,\beta}$ (rad^{-1})	-0.14	-0.20
	$C_{L,\alpha}$ (rad^{-1})	3.79	3.05
	$C_{m,\alpha}$ (rad^{-1})	-0.69	-0.39
	$C_{n,\beta}$ (rad^{-1})	0.15	0.18
Damping Derivatives	$C_{l,p}$ (rad^{-1})	-0.35	-0.25
	$C_{m,q}$ (rad^{-1})	-6.64	-5.47
	$C_{n,r}$ (rad^{-1})	-0.19	-0.22
Static Margin	% Chord	18.2	12.7

4.5.2 Dynamic Stability Analysis

Knowing the trim conditions from the static stability analysis, the next step was to use the aerodynamic derivatives at the same trim conditions to investigate the dynamic behavior of the aircraft. The stability and control derivatives were obtained using AVL, the mass properties were obtained from the CAD file, and the stability characteristics were calculated using the six degrees of freedom linearized differential equation matrix found in Phillips' *Mechanics of Flight*, Section 9.8. The eigenvalues and eigenvectors of the matrix revealed that both aircraft are stable in the Short Period, Dutch Roll, and Roll modes, unstable in Spiral mode, and neutrally stable in Phugoid mode. The Spiral modes have a doubling time on the order of nine seconds, which is in line with past year's aircraft that flew without issue. The flight conditions used for this calculation were the same ones used in the static stability section, listed in Table 4.4. The dynamic stability characteristics are tabulated in Table 4.5.

Table 4.5: Dynamic stability analysis for least stable case.

		Longitudinal Modes		Lateral Modes		
Production Aircraft	**Mode**	**Short Period**	**Phugoid**	**Dutch Roll**	**Roll**	**Spiral**
	Damping Rate (s^{-1})	4.38	-0.02	0.31	1.81	-0.07
	Time to double/half (s)	0.15	38.30	1.02	0.38	9.57
	Damping Ratio (~)	0.70	-0.04	0.09	-	-
	Damped Natural Frequency (s^{-1})	4.47	0.43	3.29	-	-
	Undamped Natural Frequency (s^{-1})	6.26	0.43	3.3	-	-
Manufacturing Support Aircraft	**Mode**	**Short Period**	**Phugoid**	**Dutch Roll**	**Roll**	**Spiral**
	Damping Rate (s^{-1})	4.87	-0.02	0.57	4.07	-0.08
	Time to double/half (s)	0.14	30.14	1.23	0.17	9.21
	Damping Ratio (~)	0.93	-0.06	0.16	-	-
	Damped Natural Frequency (s^{-1})	1.96	0.39	3.54	-	-
	Undamped Natural Frequency (s^{-1})	5.25	0.39	3.58	-	-

4.6 Mission Performance

Mission 2 is flown with the MSA at MTOW. Mission 3 is flown with the PA at MTOW. Predicting aircraft performance in these missions is key. Lap trajectories for Missions 2 and 3 were estimated using the mission simulation described in Section 4.3, propulsion characteristics from MotoCalc, and aerodynamic characteristics of the airplane. Calculations for both aircraft were performed assuming an 11x8 propeller, a Cobra 2814/12 motor and a 7-cell 1500mAh NiMH battery. The estimated velocity profile for a single lap of Mission 2 is shown on the left of Figure 4.11 and that for a single lap of Mission 3 is shown on the right of Figure 4.11. Both figures include the takeoff run. “Valleys” in the velocity profiles correspond to the required turns over the course of each lap. The maximum velocity estimated for Mission 2 is 35.3 mph (51.8 ft/s), and the maximum velocity for Mission 3 is 43.1 mph (63.2 ft/s). The estimated lap times using optimal propellers for each mission’s first lap are shown in Figure 4.11. The analysis indicates that the PA can achieve the performance target of 3 laps in 5 minutes. The MSA can achieve 3 laps in 5 minutes at Mission 2 loading, indicating that it can easily meet the performace target of Mission 1 at a lighter loading. The estimated ground takeoff roll for Missions 2 and 3 are also included in Table 4.6. Both aircraft can achieve liftoff within the 100ft requirement.

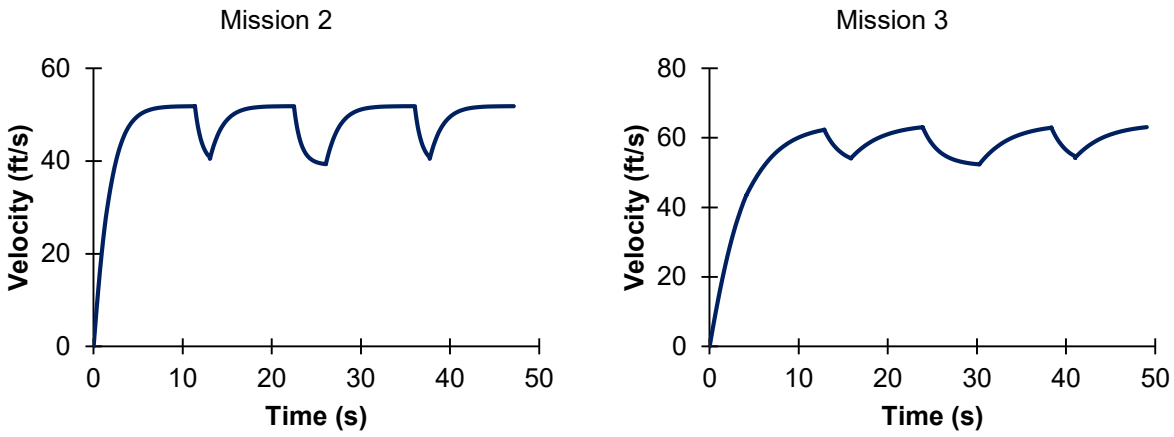

Figure 4.11: Simulation of Mission 2 and 3 lap trajectories.

Table 4.6: Predicted mission performance for each mission-propeller combination.

Mission	Propeller	TO Distance (ft)	Lap Time (s)
M2	11x7	20.7	47.2
M3	11x7	95.2	49.1

5. DETAIL DESIGN

5.1 Final Design

The aircraft dimensions did not vary between the preliminary and detailed design stages because the structural analysis and layout, component selection, and weight-balance calculations did not indicate major changes were needed. With the sizing completed, the final dimensional parameters are listed in Table 5.1. All wing and control surface chords were chosen to allow sufficient thickness for structure, embedded servos, and integration of the system, and then sized to provide stability at the constraint-derived wing area, leaving aspect ratio as a fallout variable. In summary, the final aircraft was designed for flight stability, simplicity, and structural efficiency.

Table 5.1: Final aircraft dimensional parameters.

Overall Dimensions (Production Aircraft)		
Length	33	in.
Wing L.E. X-Location	6	in.
C. G. X-Location	8	In.
Static Margin	18.2%	chord

Overall Dimensions (Manufacturing Support Aircraft)		
Length	41	in.
Wing L.E. X-Location	9.5	in.
C. G. X-Location	12.5	In.
Static Margin	12.7%	chord

Wing (Production Aircraft)		
Span	36	in.
Mean Chord	7.5	in.
Aspect Ratio	4.8	~
Wing Area	270	$in.^2$

Wing (Manufacturing Support Aircraft)		
Span	37.5	in.
Mean Chord	11.5	in.
Aspect Ratio	3.26	~
Wing Area	413	$in.^2$

Vertical Tail (Production Aircraft)		
Span	6	in.
Chord	4	in.
$\delta_{r,\ max}$	45	deg.
Reference Area	24	$in.^2$

Vertical Tail (Manufacturing Support Aircraft)		
Span	7.5	in.
Chord	7.5	in.
$\delta_{r,\ max}$	30	deg.
Reference Area	56	$in.^2$

Horizontal Tail (Production Aircraft)		
Span	8	in.
Chord	4	in.
$\delta_{e,\ max}$	45	deg.
Reference Area	32	$in.^2$

Horizontal Tail (Manufacturing Support Aircraft)		
Span	12	in.
Chord	7.5	in.
$\delta_{e,\ max}$	30	deg.
Reference Area	90	$in.^2$

5.2 Structural Characteristics

5.2.1 Layout and Design

The structural layout was created to ensure that all loads were accounted for and have an adequate load path to the major load-bearing components. The team divided all the loads the aircraft would see into three categories:

Motor Loads: Includes thrust, torque, and sustained vibrations. Components should be made of harder, quasi-isotropic materials such as plywood, and all fasteners must be locked.

Aerodynamic Loads: Includes wing and control-surface lift, drag, and moment, which translate to bending and torsion. Components can be anisotropic for added strength in the load direction.

Ground Loads: Includes aircraft weight and landing impact. Struts should be metal, which sustains impact by bending, not breaking.

The loads on each aircraft need to transfer into the major load bearing components, which includes the wing spar and fuselage attachment point. In flight, the wing may sustain up to a 2.5g load at maximum weight, based on the requirement of the wing tip test, therefore all loads from components not on the wing, such as payload and the empennage, traverse to the spar attachment point via the fuselage, as demonstrated in Figure 5.1. The fuselage is geometrically stiff due to the size required to accommodate the payload, making it an adequate load path. For the ground loads the fuselage has hard-points at the gear attachment locations to ensure impact loads do not damage any components.

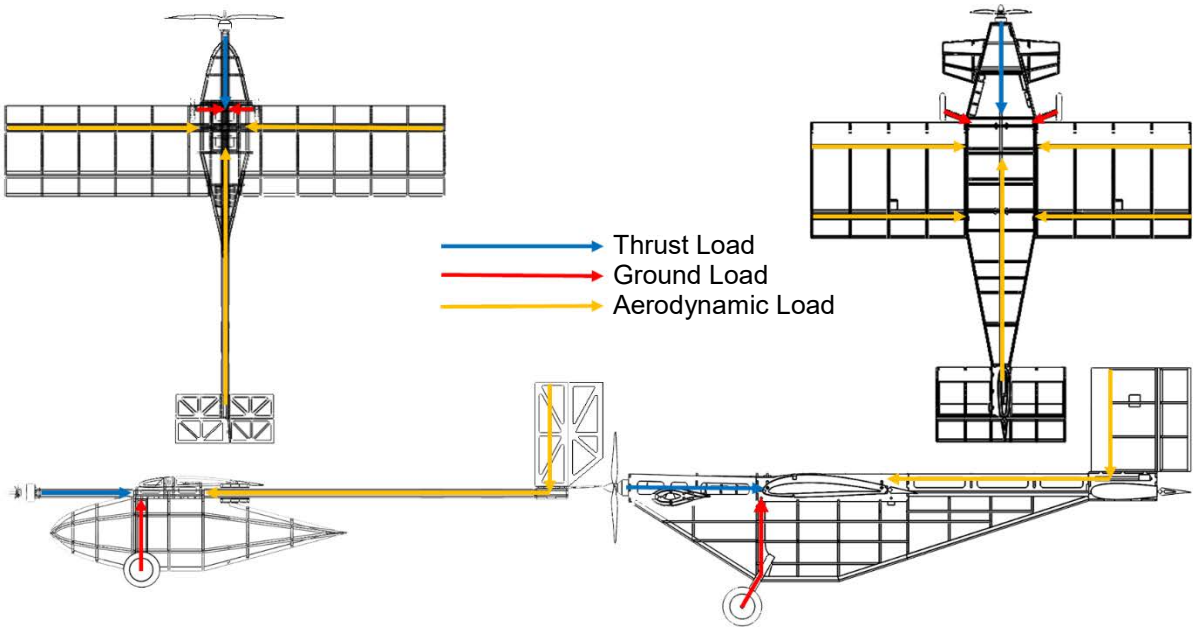

Figure 5.1: Load paths of major forces.

5.2.2 Operating Envelope

With the loads mapped and layouts complete, the structures of the aircraft were designed to withstand the design load of 2.5g at the maximum gross weight of 3.5 lbs for the PA and 2.5g at the maximum gross weight of 2.5 lbs for the MSA. This translates to a 66-degree bank angle for sustained level turns. It was not necessary to analyze the MSA in its unloaded state because the performance is similar while the weight is lower. The ultimate load could not be well quantified because balsawood has significant variation in ultimate strength. The 2.5g design load-limit at small deflections was retained as the maximum positive load envelope. The negative load limit was defined at -1g for both aircraft to prevent the wing attachment area from failing in compressive buckling. The defining structural limits were combined with aerodynamic performance limits at each mission to construct the V-n diagram displayed in Figure 5.2.

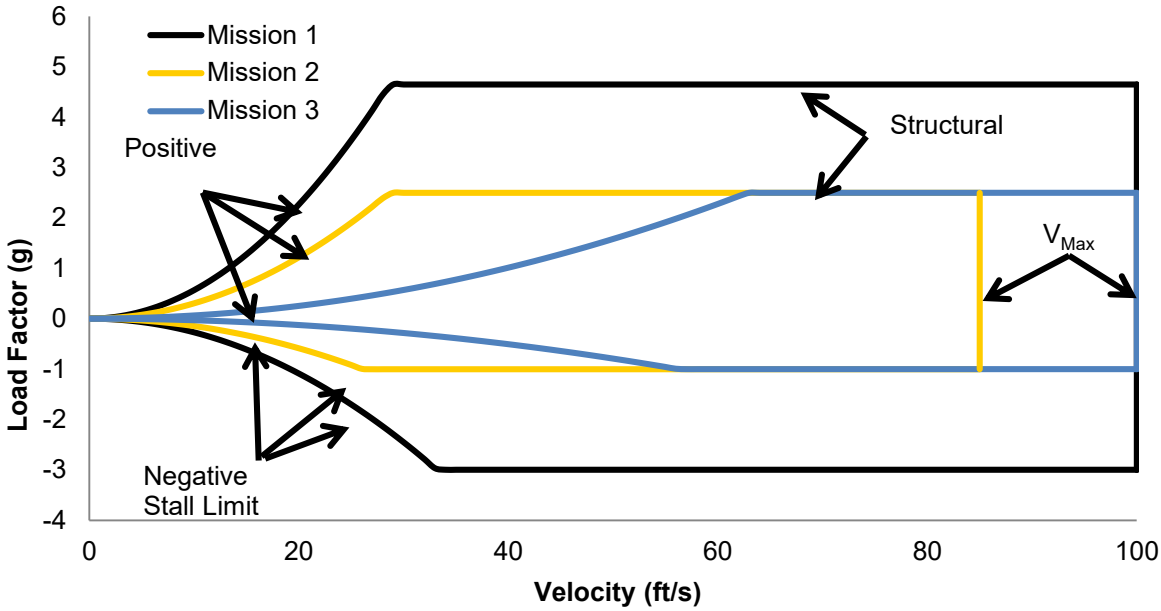

Figure 5.2: V-n Diagram showing loading as a function of velocity for Missions 1, 2, and 3.

5.3 System and Subsystem Design/Component/Selection/Integration

To finalize the aircraft design, the following subsystems were analyzed with greater detail: radio controller, servos, main wing, propulsion system, landing gear, and the structural architecture/assembly for each of these components. Fuselage, wing, motor mount, empennage, payload enclosure, receiver and transmitter, propulsion, and servos.

5.3.1 Fuselage

The PA is a stick and wing design. The fuselage uses balsa for the structural members and a carbon fiber rod as the primary structure. The center body is designed to interface the wing, servo, primary structure, landing gear and payload bay while minimizing weight. The CAD model is developed such that the center body has interlocking slots, allowing parts to fit together like a jigsaw puzzle. This method allows for the grain direction of the balsa to be appropriate for load transfer and more efficient manufacturing. The MSA is a hybrid design. A bulkhead-stringer design is used for the payload compartment, allowing for both minimum weight and adequate load transfer, while the main load-bearing structure follows a stick and wing paradigm. The interlocking method used for the PA is reproduced for the MSA. The CAD models of the Fuselages of the PA and MSA can be found in Figure 5.3.

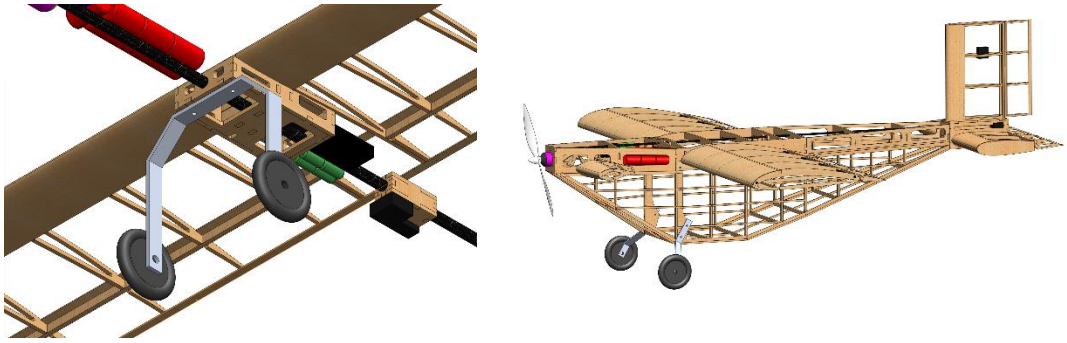

Figure 5.3: PA and MSA fuselage CAD.

5.3.2 Wing

The PA wings follow a conventional rib and spar layout. The main structure is a set of two balsa spars located at the quarter chord reinforced with flat carbon fiber rectangular rods. An aft spar is located at the three-quarter chord for the aileron attachment. Balsa was selected as the material for the spars and ribs due to its unique combination of strength, weight, and machinability. The MSA wings follow a similar design are designed to slide over the PA wings and transfer load through concentric carbon fiber tubes placed at the leading and trailing edge. Both are shown in Figure 5.4 below.

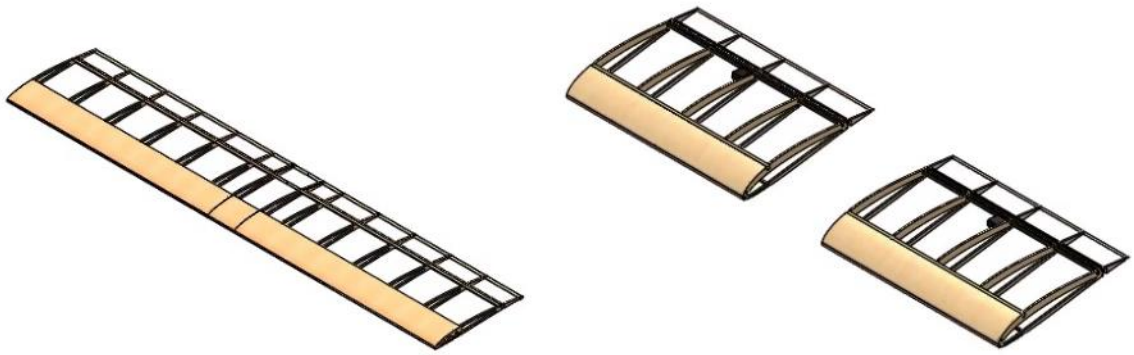

Figure 5.4: Wing design and structural layout.

5.3.3 Motor Mount

The PA motor mount is connected directly to the end of the carbon fiber rod. Four pieces of 1/8th inch thick plywood are glued together as a composite firewall capable of withstanding motor thrust and torque loads. Four bolt holes were cut into the firewall to mount the motor. The MSA motor mount motor attaches directly to 1/8th inch thick plywood plate. This plate is connected directly to the carbon-fiber rod of the main structure with epoxy. This is shown in Figure 5.5 below.

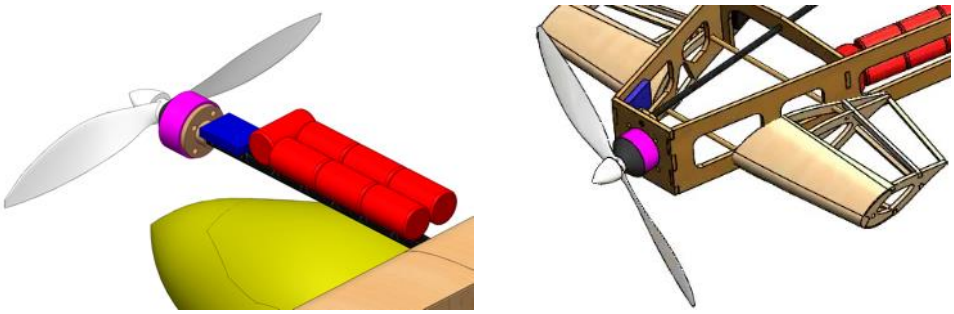

Figure 5.5: Motor mount assembly.

5.3.4 Empennage

The PA empennage was designed in CAD to minimizing size. Flat balsa sheets with lightening holes were used as flat-plate airfoils, with decreased control surface effectiveness mitigated by increasing available deflection. The MSA empennage was designed in CAD to envelope the PA empennage while being lightweight. The construction uses similar materials and construction techniques as the wings, with balsa wood used for the majority of the structure, augmented by plywood members in key locations. The bottom of the empennage hinges to fit the PA empennage. This design is shown in Figure 5.6 below.

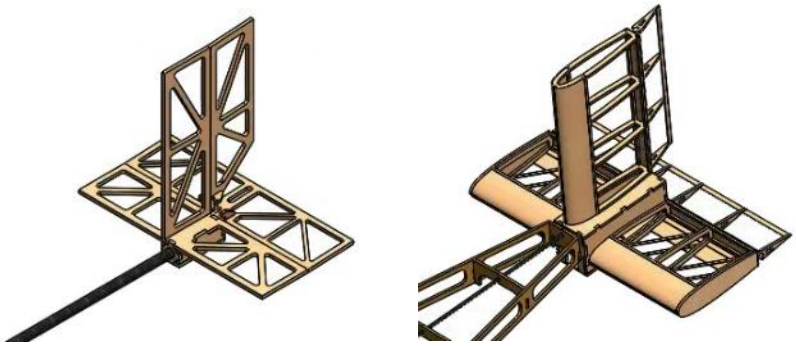

Figure 5.6: Empennage assembly.

5.3.5 Payload Enclosure

The PA payload enclosure was designed to have low drag and low weight without compromising robustness. An aerodynamic shape was made in CAD, then machined out of foam and coated with epoxy to create a mold for thermoformed plastic manufacturing. The enclosure opens along one side to allow access for securing the Mission 3 payload. This is shown in Figure 5.7 below.

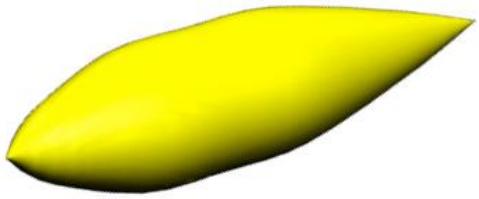

Figure 5.7: Payload Enclosure of the Production Aircraft.

5.3.6 Receiver and Transmitter Selection

The receiver selected is the Futaba R6008HS, as it provides the required failsafe mechanism with minimum weight. *Buzzdryoshka* used a Futaba T8FG 2.4 GHz radio transmitter to communicate with the receiver.

5.3.7 Propulsion System

A 7-Cell Elite 1500 mAH NiMH battery pack was selected to minimize weight while maintaining enough voltage to achieve mission requirements. A variety of motors and propellers were analyzed using the MotoCalc program, as described in Section 4.2.2. Two were selected for further testing, as described in Section 7.2. The Cobra 2814/12 motor was chosen for its weight, size and static thrust. The APC 11x8 propeller was chosen for its desired ratio between thrust required for cruise speed and thrust required for takeoff. The final selected propulsion system consists of a Cobra 2814/12 motor, 7 cell Elite 1500 mAH NiMH battery pack, a Phoenix Edge Lite 50 speed controller with the APC 11x8 propeller.

5.3.8 Servo Selection and Integration

The Futaba S3114 was selected as the servo for the aileron and elevator. These servos were selected by analyzing hinge-moments for each control surface using AVL and then finding servos that had sufficient control power to handle the calculated moments, with the lightest weight possible. The selected components are tabulated in Table 5.2:

Table 5.2: Selected components.

Components	Description
Motor	Cobra 2814/12
Battery	7 cell ELITE 1500
Speed Controller	Phoenix Edge Lite 50
Receiver	Futaba R6008HS
Transmitter	Futaba T8FG
Aileron Servo	Futaba S3114
Elevator and Rudder Servos	Futaba S3114

5.4 Weight and Balance

An important aspect of stability is correct center of gravity (C.G.) location. To estimate the C.G., a simple calculator was created that consisted of a list of all components, their weights, and their locations along the x-axis and z-axis. Component weights were first estimated using the CAD model and then confirmed with the physical vehicle. Table 5.3 contains the results for all mission scenarios for the PA. Table 5.4 contains those for the MSA. The x-axis was measured positive aft of the nose of the aircraft and the z-axis was measured positive above the chord-line of the wing. The predicted C.G. locations from the CAD of the PA and MSA are shown in Figure 5.8.

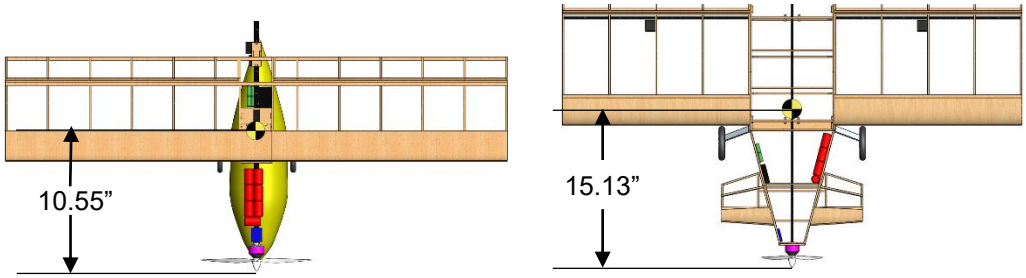

Figure 5.8: PA and MSA C.G. location from CAD model.

Table 5.3: Weight and balance chart – Production Aircraft.

Empty Weight					
Component	**Weight (lbs)**	**C.G. loc.(in, x-axis)**	**Moment (in-lbs, y-axis)**	**C.G. loc. (in, z-axis)**	**Moment (in-lbs, x-axis)**
Fuselage	0.02	12.00	0.24	0.00	0.00
Empennage	0.09	32.00	2.88	0.00	0.00
Speed Controllers	0.04	6.00	0.24	0.00	0.00
Receiver	0.03	11.00	0.33	0.00	0.00
Propeller	0.04	0.25	0.01	0.00	0.00
Wing	0.12	10.75	1.24	0.00	0.00
Carbon Fiber Rod	0.06	17.00	0.94	0.00	0.00
Aileron Servo 1	0.02	12.50	0.21	0.13	0.00
Aileron Servo 2	0.00	0.00	0.00	0.00	0.00
Tail Servo 1	0.02	16.00	0.27	0.13	0.00
Tail Servo 2	0.02	16.00	0.27	0.00	0.00
Main Gear	0.13	8.50	1.06	-4.00	-0.50
Tail Gear	0.01	32.50	0.16	-0.13	0.00
Motor	0.15	1.75	0.25	0.00	0.00
Receiver Battery	0.10	5.00	0.50	0.00	0.00
Aircraft Totals	**0.82**	**10.55**	**8.61**	**-3.88**	**-0.50**
Mission 3					
Battery	0.37	6.25	2.33	0.38	0.14
Payload	2.20	11.40	25.08	-2.75	-6.05
Aircraft Totals	**3.39**	**10.63**	**36.02**	**-1.89**	**-6.41**

Table 5.4 shows that the battery must move significantly in order to balance C.G. for each mission. This is necessary due to the insertion of the PA during Mission 2, where the C.G. is lowered by 1.07. This was not found to be a problem during flight testing, and the team considers the aircraft safe.

Table 5.4: Weight and balance chart – Manufacturing Support Aircraft.

Empty Weight					
Component	**Weight (lbs)**	**C.G. loc.(in, x-axis)**	**Moment (in-lbs, y-axis)**	**C.G. loc. (in, z-axis)**	**Moment (in-lbs, x-axis)**
Fuselage	0.17	19.00	3.23	-3.00	-0.51
Empennage	0.04	39.00	1.56	2.50	0.10
Speed Controllers	0.04	10.00	0.40	0.00	0.00
Receiver	0.03	10.00	0.30	0.00	0.00
Propeller	0.04	0.50	0.02	0.00	0.00
Wing	0.20	18.00	3.60	0.00	0.00
Carbon Fiber Rod	0.06	21.50	1.36	0.75	0.05
Aileron Servo 1	0.02	20.00	0.34	0.00	0.00
Aileron Servo 2	0.02	20.00	0.34	0.00	0.00
Tail Servo 1	0.02	39.25	0.67	0.13	0.00
Tail Servo 2	0.02	39.50	0.67	6.00	0.10
Main Gear	0.11	10.50	1.18	-7.50	-0.84
Tail Gear	0.01	42.00	0.21	-1.50	-0.01
Motor	0.15	1.75	0.25	0.00	0.00
Receiver Battery	0.10	12.00	1.20	0.00	0.00
Aircraft Totals	**1.01**	**15.13**	**15.33**	**-2.63**	**-1.11**
Mission 1					
Battery	0.37	10.00	3.73	0.25	0.09
Payload	0.00	0.00	0.00	0.00	0.00
Aircraft Totals	**1.39**	**13.75**	**19.06**	**-0.73**	**-1.02**
Mission 2					
Battery	0.37	7.15	2.67	0.25	0.09
Payload	0.72	15.25	10.92	-3.88	-2.77
Aircraft Totals	**2.10**	**13.75**	**28.92**	**-1.80**	**-3.79**

5.5 Flight and Mission Performance

5.5.1 Flight Performance

The flight performance of the aircraft may be described by the point performance of the vehicle. Key aspects include the velocity envelope and turn performance, as well as takeoff distance and stall speed. These are given below in Table 5.5.

Table 5.5: System flight performance parameters for each mission.

	Mission 1	Mission 2	Mission 3
Weight (lbs)	1.39	2.10	3.53
W/S (psf)	0.47	0.71	1.81
TOFL (ft)	6.72	20.70	95.20
Vstall (ft/sec)	19.30	23.15	41.50
Vmax (ft/sec)	52.50	51.80	61.00
Load Factor	4.50	2.50	2.50
Turn Radius (ft)	17.10	33.88	50.43
Time for 360 (s)	2.15	4.26	5.19

Weight represents the Mission 1, 2, and 3 gross take-off weights. Both wing loading and stall speed are calculated at 1g assuming steady level flight while using an estimation of C_{Lmax} created with AVL modeling and section lift data. Takeoff field length (TOFL) was computed via numerical integration in MATLAB using the drag polar, friction coefficients, and thrust available from the wind tunnel test data. Load factor for each mission is the maximum allowable based on results from the V-n Diagram. In all cases, the load factor is intended to represent a maximum. Flight-test data indicates that in-flight loads will be lower. The turn radius and time to complete a 360 degree turn were calculated for each mission using the mission's expected maximum velocity and allowable load factor. The maximum velocity of the aircraft occurs at the point when the thrust required is equal to the thrust available. Thrust required is calculated using Equation 5.1 where $C_{D,0}$ and e are calculated in Section 4.4.3.

$$T_R = \frac{1}{2}\rho V^2 S C_{D,0} + \frac{2W}{\rho V^2 S \pi A R e} \tag{5.1}$$

Thrust available as a function of velocity was computed using MotoCalc for both propellers considered and plotted in Figure 5.9, along with the thrust required curves in steady-level flight for the PA and MSA.

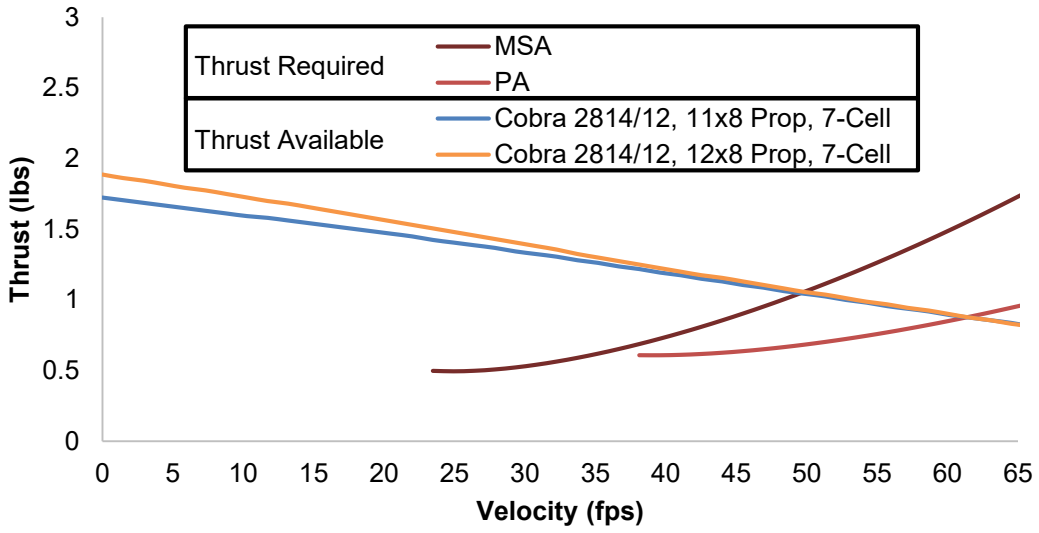

Figure 5.9: Thrust available and thrust required versus velocity.

Figure 5.9 shows that for a constant motor, the 11x8 and 12x8 propellers achieve similar performance at velocity greater than 35 fps. Since the PA stalls at ~38 fps and the propulsion system of the MSA is overpowered, the team preferred the smaller propeller for ease of packaging.

5.5.2 Mission Performance

The mission model described in Section 4.3 was used to estimate the final mission performance of the aircraft. The computed lap times represent an estimate that combines aerodynamics from AVL, power and current characteristics from MotoCalc, and the physics of the mission model as described in Section 4.3. Figure 5.10 displays the projected first lap trajectories for Missions 1, 2 and 3, with an initial ramp-up following takeoff and dips in velocity occurring at the turns. The remaining laps for Missions 1 and 3 are faster because they do not include takeoff. Table 5.6 shows the resulting estimated performance for each of the three missions with the selected propellers. The table also includes scoring estimates based on the updated analysis.

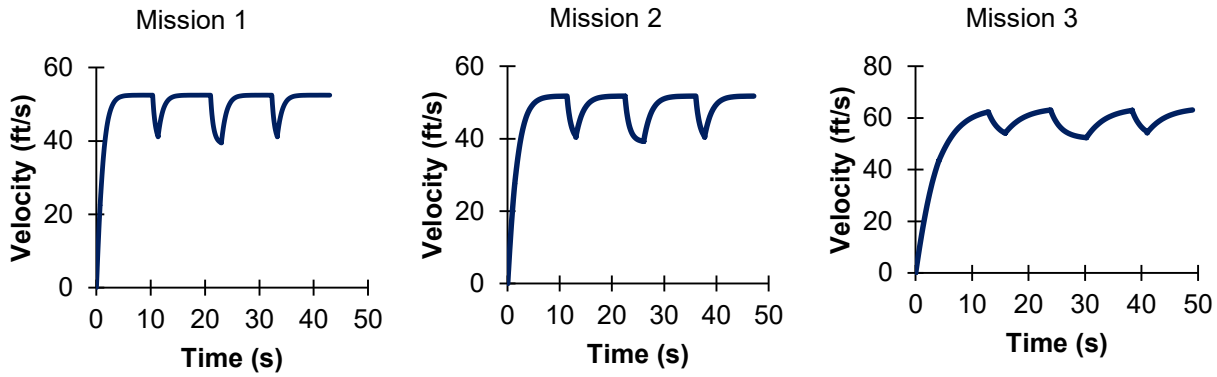

Figure 5.10: Simulation of Mission 1, 2 and 3 lap trajectories.

Table 5.6: Aircraft mission performance parameters.

Mission Parameter	Mission 1	Mission 2	Mission 3
W/S (psf)	0.469	0.709	1.81
Propeller Selection	11x8	11x8	11x8
Max Current (Amp)	19	19	19
Static Thrust (lbs)	1.89	1.89	1.89
1st Lap Time (sec)	43.0	47.2	49.1
Mission Performance	3 laps in 5 minutes	1 lap	3 laps in 5 minutes
Mission Score	2.0	4.0	2.0
RAC	0.961	0.961	0.961

Based on the updated mission performance estimates shown in Table 5.6, the estimated total mission score is 10. After normalization by RAC the score stands at 10.4.

5.6 Drawing Package

The following five pages illustrate the detailed CAD of *Buzzedryoshka* system. The first and second sheets have the three-view diagram with relevant dimensions of the PA and the MSA respectively. The third and fourth sheets show the structural arrangement of all major components and the systems layout and location for the PA and the MSA respectively. The fifth sheet displays the payload arrangements for both aircraft.

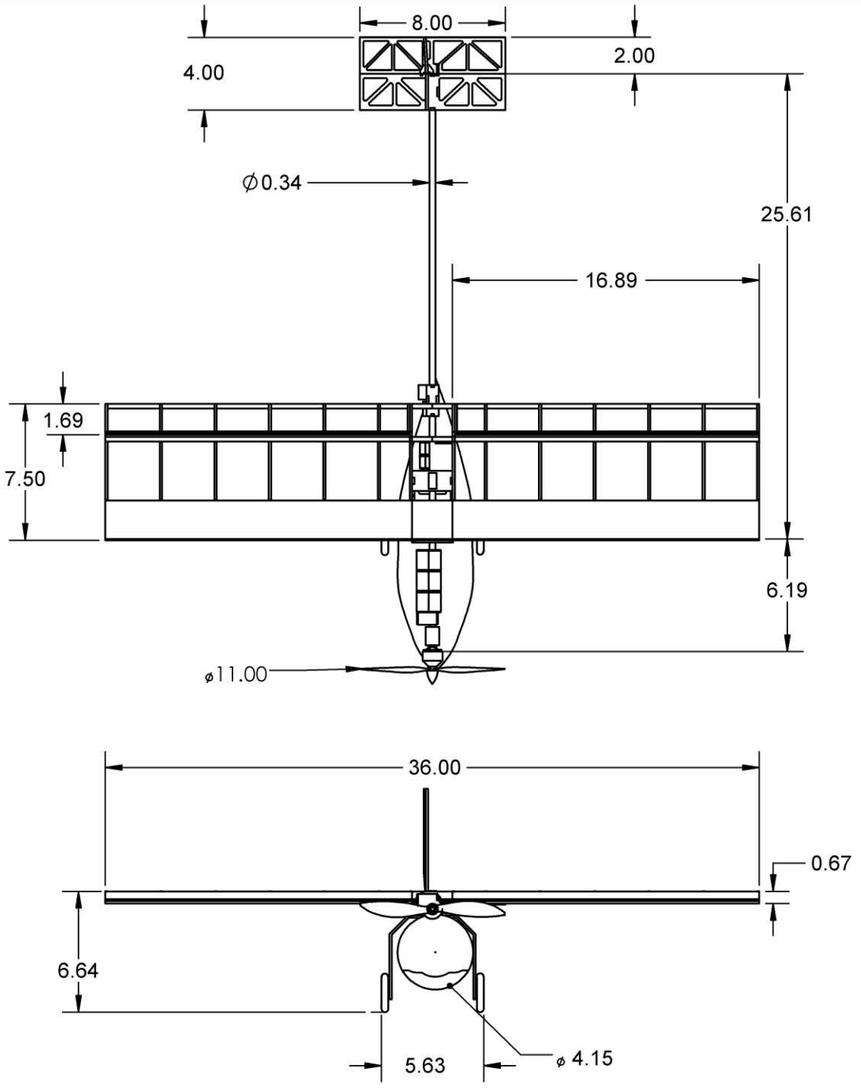

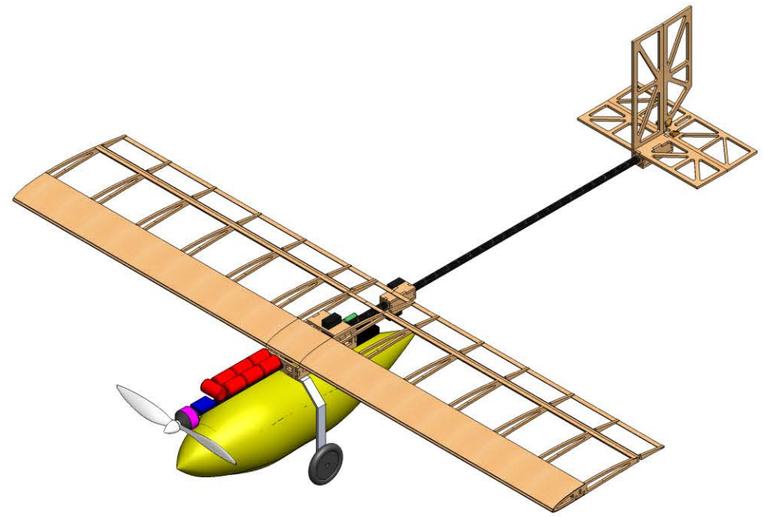

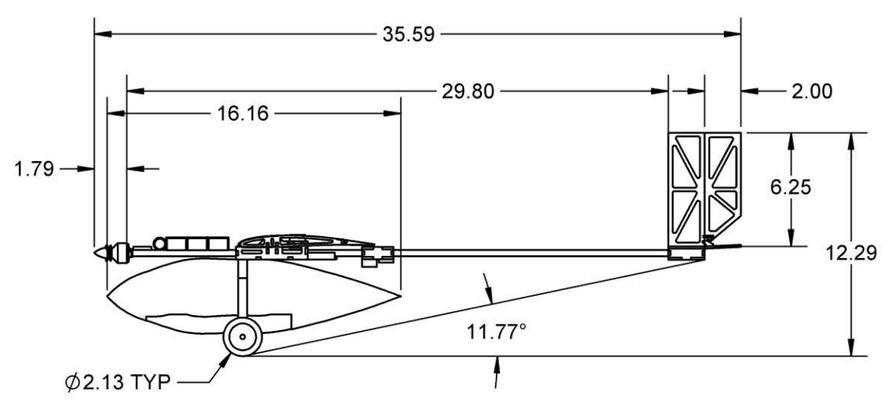

DRAWN Yusuf Ogun Kargin	**Georgia Institute of Technology**
CHECKED George P. Burdell	**Buzzedryoshka**
2/19/2016	SIZE B · DWG PA THREE VIEW DRAWING WITH DIMENSIONS
	SCALE 1:7 · All Dimensions in Inches · SHEET 1 OF 5

SYSTEMS LIST			
Item	Qty.	Item Name	Description
1	1	Propeller	APC 11x8
2	1	Motor	Cobra 2814
3	1	Speed Controller	Phoenix 35A
4	1	Main Battery Pack	7 cell 1500 mAh
5	1	Receiver Battery Pack	4 cell 400 mAh
6	1	Aileron Servo	Futaba S3114
7	1	Rudder Servo	Futaba S3114
8	1	Elevator Servo	Futaba S3114
9	1	Receiver	Futaba H6008S
10	2	Wheel	Rubber Tires
11	1	Payload Fairing	Plastic

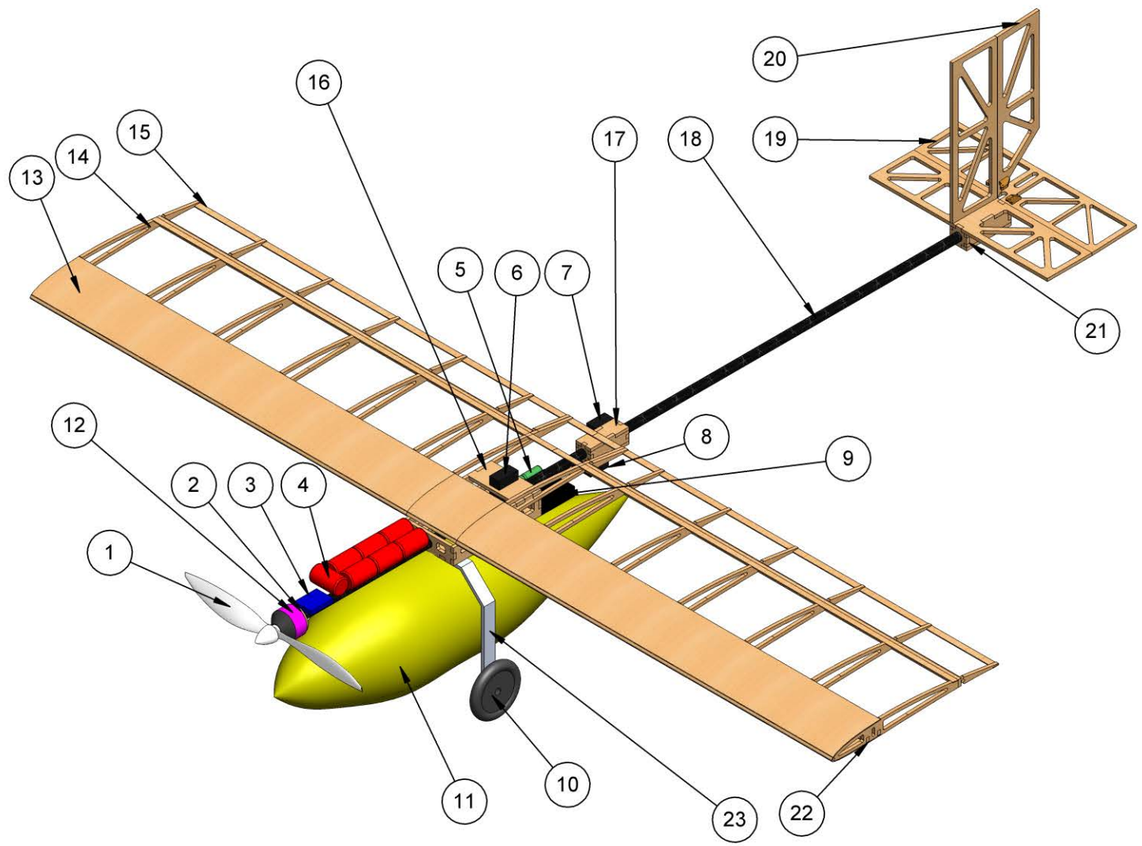

PARTS LIST			
Item	Qty.	Item Name	Description
12	1	Motor Mount	Plywood
13	1	Wing Sheeting	Balsa
14	14	Wing Rib	Balsa
15	2	Aileron	Balsa
16	1	Fuselage Box	Balsa
17	1	Servo Box	Balsa
18	1	Boom	Carbon Fiber
19	1	Elevator	Balsa
20	1	Rudder	Balsa
21	1	Empennage	Balsa
22	2	Spar Capping	Carbon Fiber
23	1	Main Landing Gear Strut	Aluminum

DRAWN
Yusuf Ogun Kargin

CHECKED
George P. Burdell

2/19/2016

Georgia Institute of Technology

Buzzedryoshka

SIZE B | DWG
PA Structural Arrangement and Systems Layout Drawing

SCALE 1:3 | All Dimensions in Inches | SHEET 2 OF 5

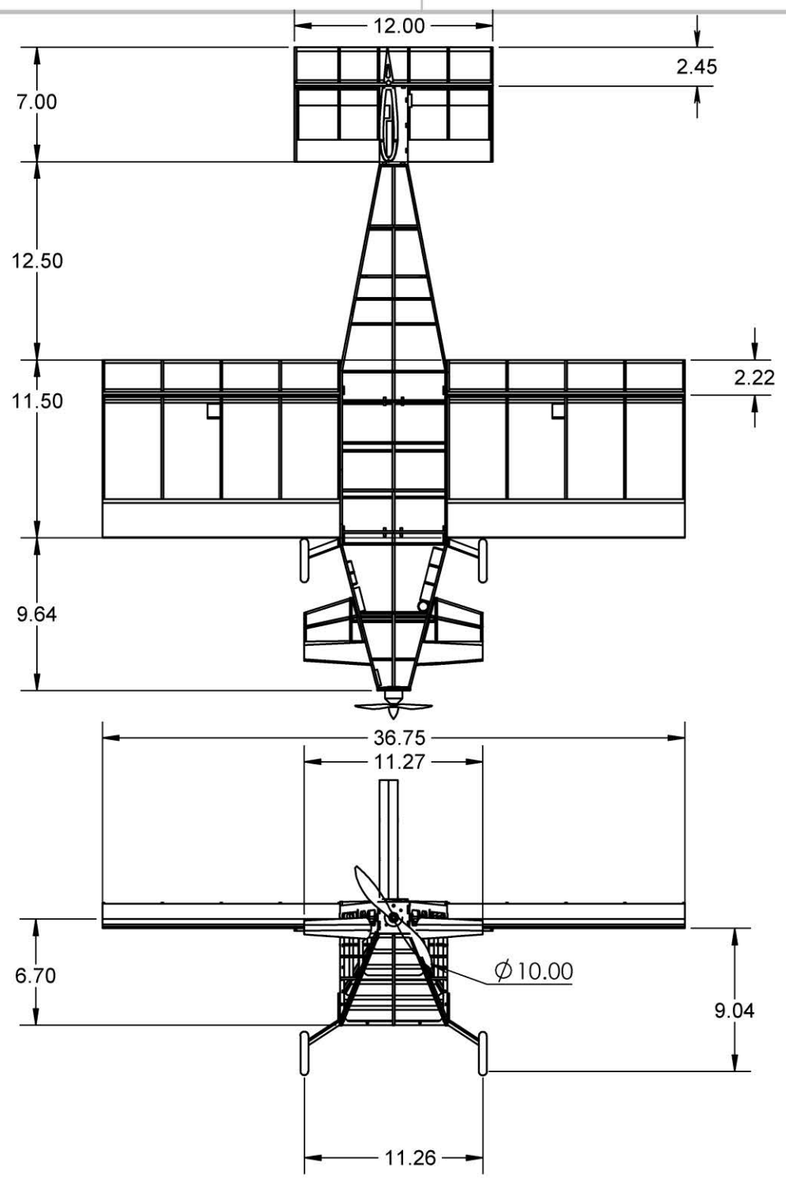

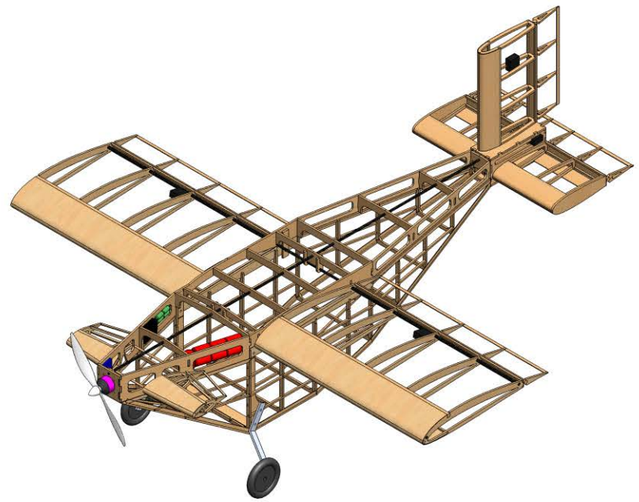

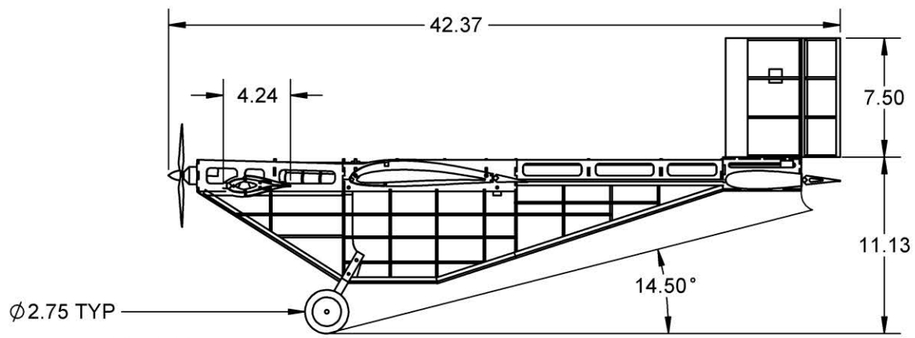

DRAWN Osvaldo Armas	**Georgia Institute of Technology** **Buzzedryoshka**
CHECKED George P. Burdell	SIZE **B** DWG MSA Three View Drawing with Dimensions
2/19/2016	SCALE 1:8 · All Dimensions in Inches · SHEET 3 OF 5

SYSTEMS LIST			
Item	Qty.	Part Name	Description
1	1	Propeller	APC 11x8
2	1	Motor	Cobra 2814
3	1	Speed Controller	Phoenix Edge Lite 50
4	1	Receiver	Futaba R6008HS
5	1	Receiver Battery Pack	4 cell 400 mAh
6	1	Aileron Servo	Futaba S3114
7	1	Rudder Servo	Futaba S3114
8	1	Tail Bottom Lid	Balsa
9	1	Elevator Servo	Futaba S3114
10	1	Detachable Top Fuselage	Balsa
11	2	Detachable Wing	Balsa
12	1	Main Battery Pack	7 cell 1500 mAh
13	2	Wheel	Rubber Tire
14	1	Bottom Fuselage	Balsa
15	2	Detachable Canard	Balsa

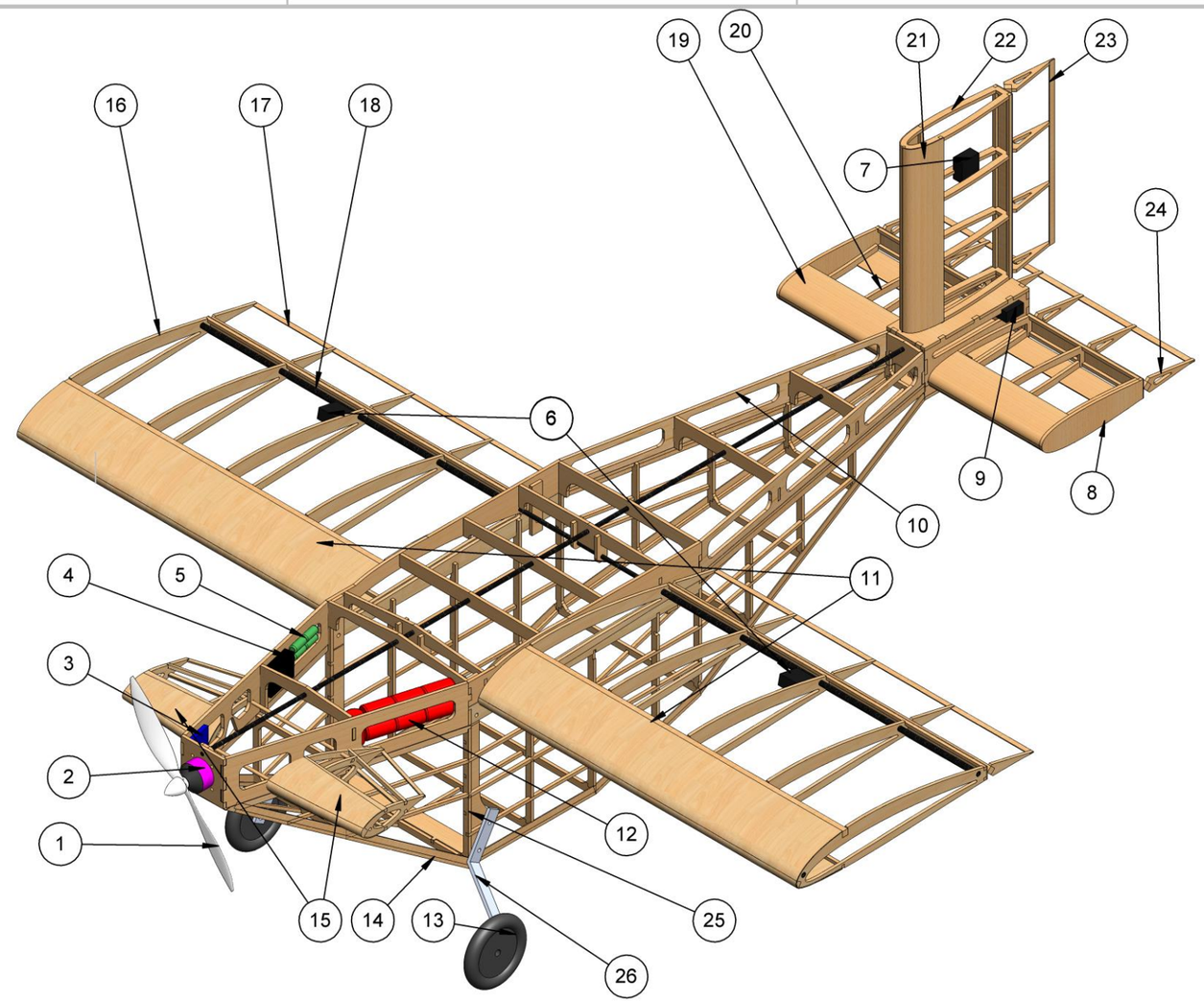

PARTS LIST			
Item	Qty.	Part Name	Description
16	10	Wing Rib	Balsa
17	2	Aileron	Balsa
18	4	Wing/Fuselage Joint	Carbon fiber Rod
19	2	Horizontal Tail Sheeting	Balsa
20	6	Horizontal Tail Rib	Balsa
21	1	Vertical Tail Sheeting	Balsa
22	4	Vertical Tail Rib	Balsa
23	1	Rudder	Balsa
24	1	Elevator	Balsa
25	1	Bulkhead	Plywood
26	2	Landing Gear Strut	Aluminium

DRAWN
Yusuf Ogun Kargin

CHECKED
George P. Burdell

2/19/2016

Georgia Institute of Technology

Buzzedryoshka

SIZE B | DWG

MSA Structural Arrangement and Systems Layout Drawing

SCALE 1:4 | All Dimensions in Inches | SHEET 4 OF 5

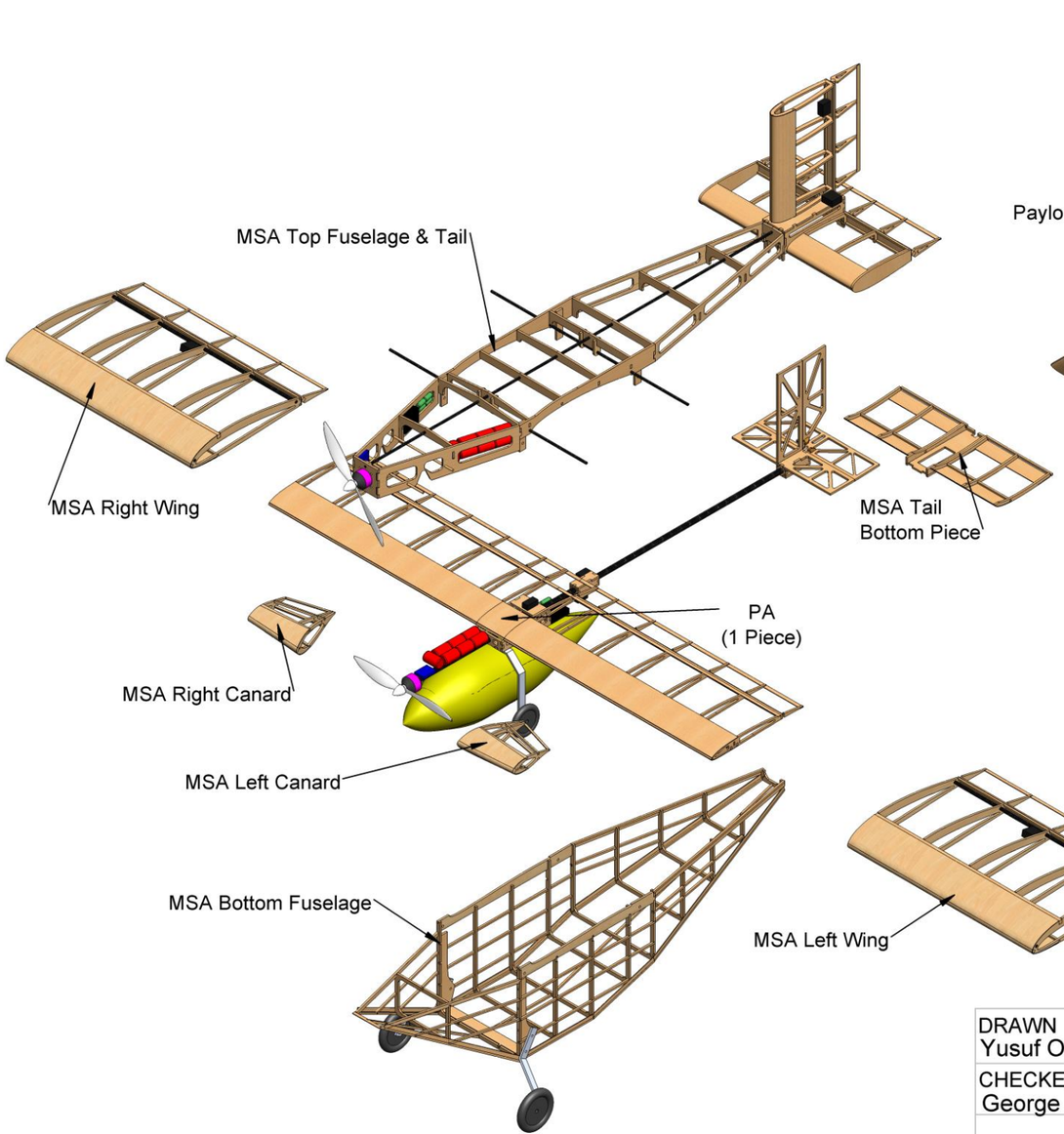

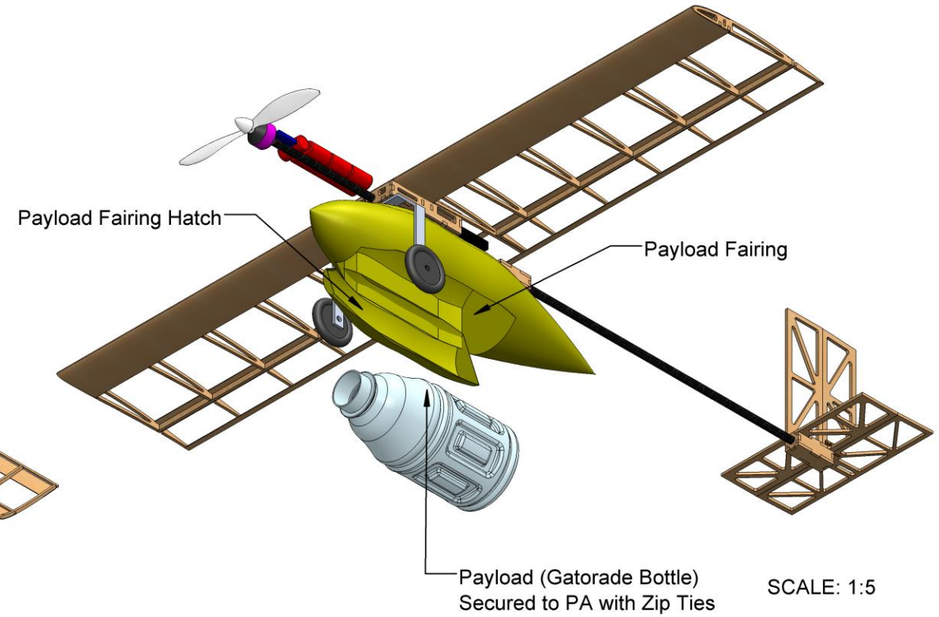

SCALE: 1:5

DRAWN Yusuf Ogun Kargin	**Georgia Institute of Technology** **Buzzedryoshka**
CHECKED George P. Burdell	SIZE B DWG PA & MSA PAYLOAD ACCOMODATION DRAWING
2/19/2016	SCALE 1:7 · All Dimensions in Inches · SHEET 5 OF 5

6. MANUFACTURING PLAN AND PROCESSES

In order to design and build a competitive aircraft, the team considered various manufacturing processes and materials. The manufacturing process selected represented the best combination of weight, reparability, ease of manufacturing, team experience with the process, and cost.

6.1 Manufacturing Processes Investigated

The team had a wealth of experience using the built-up balsa wood manufacturing technique. However, there were other viable manufacturing processes that could be superior. These processes were considered and qualitatively compared to the built up balsa technique using Figures of Merit, detailed below and summarized in Table 6.1.

Weight: similarly to conceptual design, weight is still the most important factor for any design decision, and is assigned a FOM of 5.

Reparability: With ever-present unknown factors, the reparability of the aircraft in case of an accident or a crash has to be accounted for, and was assigned a FOM of 2.

Ease of Manufacture: The ability to produce the aircraft to specification is critical to meet expected performance, and is directly related to Ease of Manufacture. It was therefore assigned a FOM of 3.

Experience: The team's knowledge was given some weighting because it relates to the ability of team members to produce quality results, as well as to refine existing techniques. However, since the team is always willing to learn new techniques, experience was only assigned a FOM of 2.

Cost: Keeping in mind that the team had limited resources, cost was inevitably added as a FOM. However, since the team emphasizes winning above all, cost was assigned a FOM of 1.

Table 6.1: Manufacturing FOM weighting.

Figure of Merit	0	1	2	3	4	5
Weight						5
Ease of Manufacture				3		
Reparability			2			
Experience			2			
Cost		1				

These Figures of Merit were used to investigate the manufacturing processes and materials common to remote control aircraft construction that were investigated detailed below.

Built-up Balsa: Stocks of competition grade balsa wood are laser cut from CAD models and glued together using cyanoacrylate (CA) adhesive to form the skeleton of the aircraft. It is then locally reinforced with more balsa or carbon fiber if necessary, and coated with Ultracote heat shrink film.

Foam Core Composite: Large blocks of foam are cut with a hot-wire or Computer Numerically Controlled (CNC) router to form the basic shape of the aircraft. Structural reinforcements are locally added if needed, and the entire foam-core is coated in fiberglass or carbon fiber, adding strength while providing an aerodynamic skin.

Molded Composite: This process is similar in principle to a foam core; however, the foam parts are only used to mold the composites and are then removed, with the fiberglass or carbon fiber acting as the primary structure.

Thermoformed Plastic: The process starts with a thin sheet of plastic is heated until it becomes moldable. The plastic then made to conform around the mold by application of a strong vacuum and is allowed to cool and assume a new shape. This process is ideal for making fairings and other non-structural components.

The processes were evaluated against each other by assigning each one a FOM score, with a score of five indicating a superior choice, three an average choice, and one equaling an inferior choice. All methods were assumed to result in an aircraft designed for an identical load. The results of the comparison are summarized in Table 6.2.

Table 6.2: Weighting for various manufacturing techniques.

		Manufacturing Process			
FOM	**Value**	**Built-up Balsa**	**Foam Core Composites**	**Molded Composites**	**Thermoformed Plastic**
Weight	**5**	5	3	5	5
Ease of Manufacture	**3**	3	3	1	2
Reparability	**2**	3	1	1	5
Experience	**2**	5	3	3	1
Cost	**1**	5	3	1	5
Total	13	55	35	37	48

Based on the Figures of Merit, built-up balsa was considered the best method for the plane manufacturing. To further confirm this choice, the team laid-up a molded composite wing section, the second-best candidate of the assessment above. The section consisted of 3 oz/yd^2 fiberglass with 1/32" balsa core, and resulted in an area density of 0.12 lbs per square foot of skin. With nearly 10 ft^2 of wetted area, the wing alone would weigh 1.2 lbs, more than the entire balsawood structure of the aircraft as-built. Therefore, the built-up balsa technique was used to construct the aircraft.

6.2 Manufacturing Processes Selected

The team used the above comparison to optimize the built-up balsa technique to achieve the most competitive aircraft by having the lightest structure possible in accordance with competition rules without sacrificing structural integrity. This optimized technique is detailed in Table 6.3 below:

Table 6.3: Built-up balsa manufacturing technique.

Manufacturing Component	Material / Technique
Principal material	Competition Grade balsa wood
Other materials	Local fiber reinforcements
Adhesive	CA, or epoxy if needed
Coating	Ultracote
Part manufacture	CAD-guided laser cutting
Part assembly	Designed-to-fit jigsaw pieces

Of the many different ways to apply built-up balsa, the team chose specific techniques and materials that would minimize the aircraft structure's weight without compromising its strength. These strategies are:

Selective Material Use: Since balsa wood can vary significantly in density and strength, the team sorted its entire stock of balsa by weight. The lightest pieces were selected for construction and were cut using the team's laser cutter, with the lightest of the cut parts reserved for the final competition aircraft.

Local Reinforcements: Due to the very low density of balsa used, the aircraft structure lacked strength in several key locations. Rather than compensate by over-building the entire aircraft, these locations were reinforced with composite or additional balsa, increasing strength with minimal penalty in weight.

Torsion Webbing: The wing for this aircraft provided an uncommon structural challenge for the team due to our method of creating a wing that will fit another wing inside of it. With less central structure to the wing, it is more susceptible to torsion. The team employs cross torsion webbing across the bays to provide additional stiffness. The wing structure can be seen in Figure 6.1.

Figure 6.1: MSA wing in production.

Lightening Holes: The use of a concentrated and localized structure caused most structural members to not experience significant loading. Where possible, the team laser-cut lightening holes into ribs and bulkheads to reduce weight with little losses in the overall stiffness and strength of the aircraft.

Coating: Most balsa aircraft are coated with a heat shrink adhesive infused plastic covering material called Monokote, which is durable and easy to handle. However, the team chose to use a more delicate plastic covering, Ultracote, because it is significantly lighter.

Thermoforming: For the PA payload bay, the team had to choose between a balsa structure or thermoformed plastic. While the plastic shell is heavier, its increased durability and closer fit reduces risk during loading/unloading and decreases drag. These advantages made it the material of choice for the pod. The thermoforming mold is made from foam that is CNC machined and finish-sanded. An epoxy coat is applied to give it rigidity and resistance to temperature. This process is seen in Figure 6.2

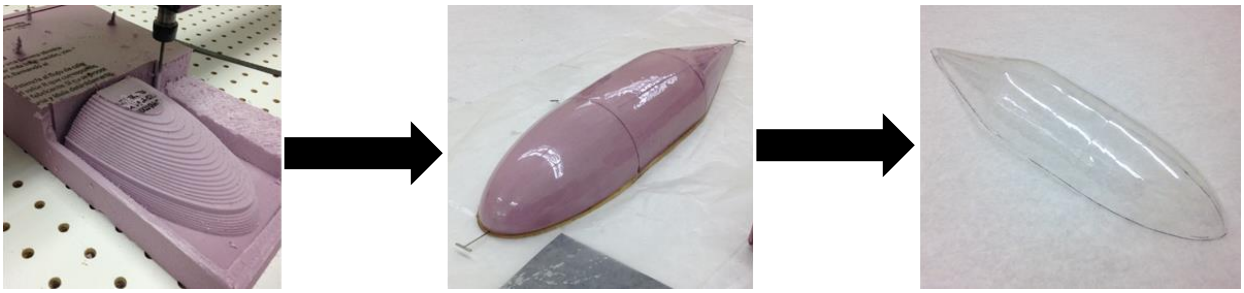

Figure 6.2: Manufacturing process of the thermoformed payload bay.

6.3 Manufacturing Milestones

A milestone chart was established at the beginning of aircraft manufacturing to ensure a logical, consistent order was followed during construction. Progress was recorded and monitored by the team leader to ensure all major milestones were met. The milestone chart is shown below in Figure 6.3, capturing the planned and actual timing of major events.

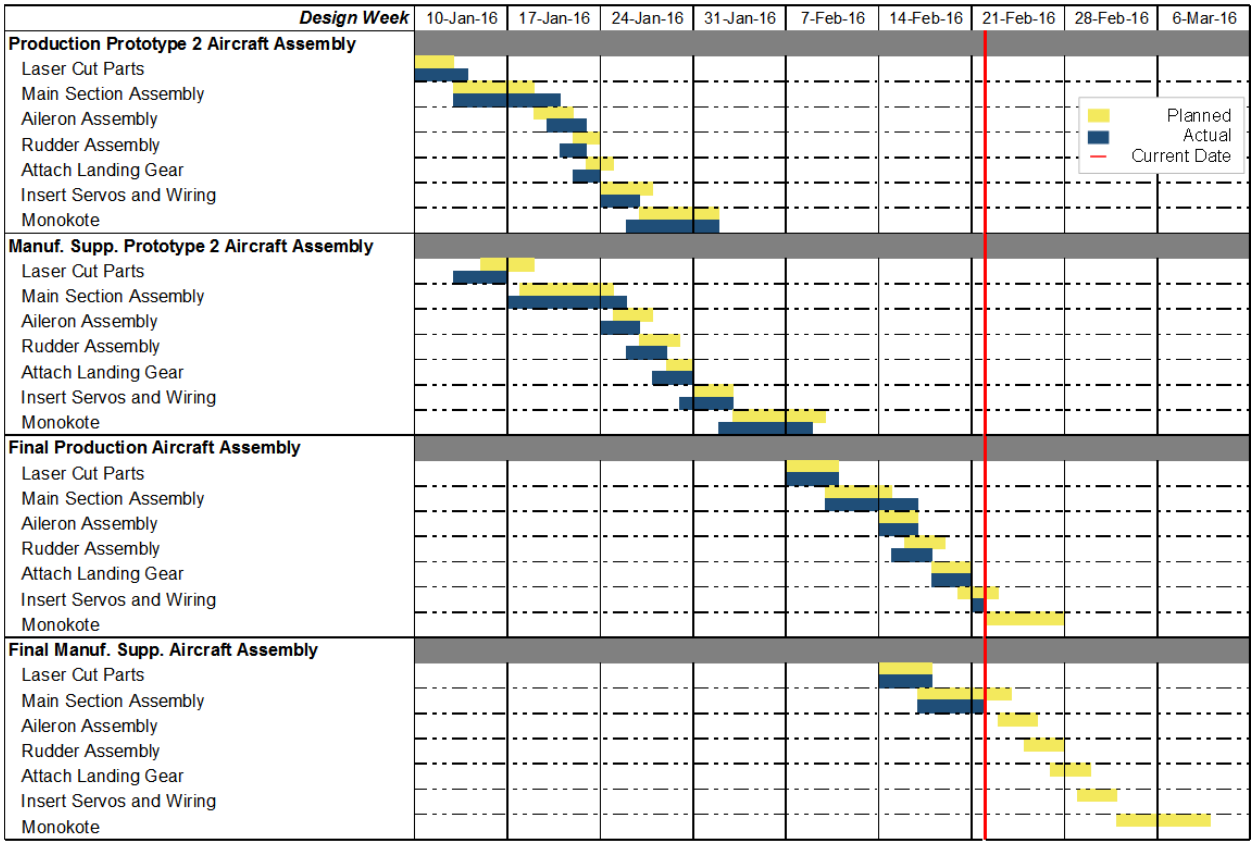

Figure 6.3: Aircraft manufacturing milestone chart showing planned and actual timing of objectives.

7. TESTING PLAN

A plan for an extensive testing campaign to validate the aircraft, and its components, was created to determine what configurations and subsystems would be the most capable. Testing culminates in test flying a full round of competition flights on the final competition airframe.

7.1 Objectives and Schedules

The testing was broken up into three main categories: propulsion, structures, and performance. The propulsion and structures subsystems were tested before flying the whole aircraft to gain knowledge and set realistic and useful objectives at each test flight. A breakdown of the testing schedule is displayed in the following Gantt chart, shown in Figure 7.1 below:

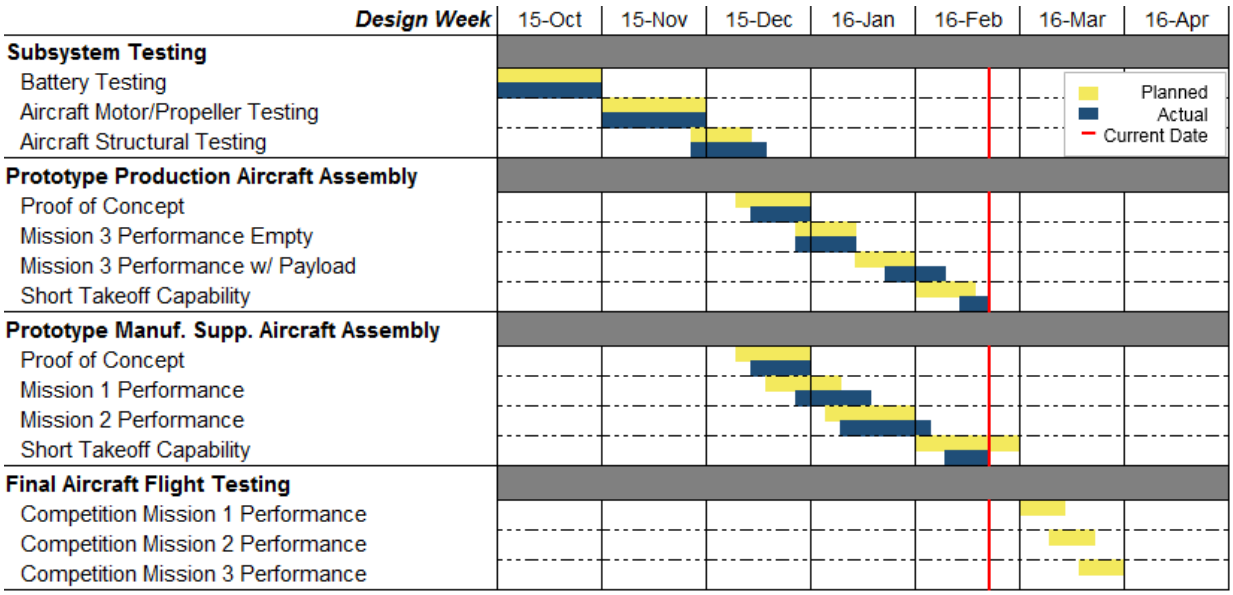

Figure 7.1: Aircraft and subsystem testing milestone chart showing planned and actual timing of objectives.

7.2 Propulsion Testing

The objectives for the propulsion testing were to determine which of the two motors would work best for both aircraft. The motors and propellers tested were based on MotoCalc predictions as expressed in Section 4.2. Thrust versus velocity for vehicle performance and power draw for motor performance for each motor propeller combination were determined using measurements of thrust, torque, RPM, voltage, and current draw. Using data obtained from testing, the team was able to compare the actual performance of the motors to the MotoCalc predictions in order to gather a better estimate of actual performance. This information allowed the team to select the best propulsion system to achieve the best score possible.

A rig that included load cells to calculate thrust and torque as well as an electric motor measurement system was constructed for the wind tunnel testing, and is shown in Figure 7.2. The team used the rig to perform static thrust tests and used the data to compare it with MotoCalc predictions. The electric motor parameters were monitored with an EagleTree system that records the RPM, voltage, and current draw of the motor. Custom written software was used to collect the torque and thrust values as well as to remotely control the motor for 30-second intervals with 10-second full thrust intervals and 10-second acceleration and deceleration intervals.

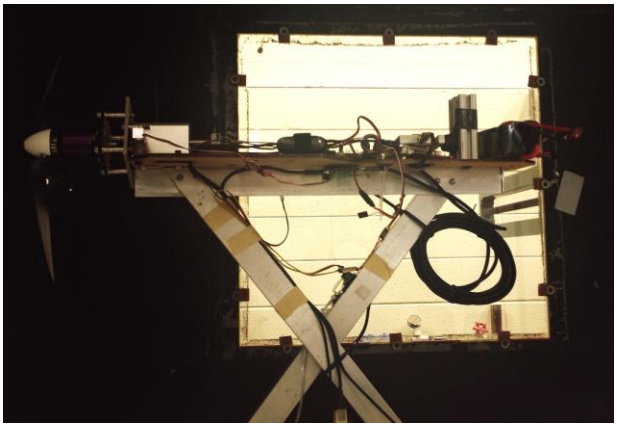

Figure 7.2: Picture of thrust test rig in wind tunnel.

The team will be utilizing the Georgia Tech Low Turbulence Wind Tunnel to conduct its wind tunnel tests. Due to time constraints and scheduling conflicts, the team has not tested within the tunnel as of when this report has been submitted but plans to do so in the near future. The wind tunnel is powered by a fan which forces air through a series of honeycombed grates creating a smooth, even flow of air. The fan creates airflow with a maximum airspeed of about 52 feet per second. The wind tunnel creates an environment closely resembling actual flight conditions and thus providing accurate motor and propeller efficiencies. The results of the static thrust tests are described in Section 8.1.

7.3 Integration of Production Aircraft into Manufacturing Support Aircraft

The system was designed to ensure the PA successfully fits within the MSA which splits into seven separate pieces. Prototypes were constructed to ensure successful operation. Assembly of the MSA around PA was tested in both the lab and flight field. Flight testing ensured the system functioned properly for Mission 2.

7.4 Structural Testing

To validate the design of the wings, the aircrafts were subjected to wing tip tests. A wing tip test simulates the maximum loading the wings would experience in flight by loading the payload bay with the maximum weight and lifting the plane by the wing tip. The tip test simulates a maneuver resulting in a root bending moment of 2.5g. This is shown in Figure 7.3.

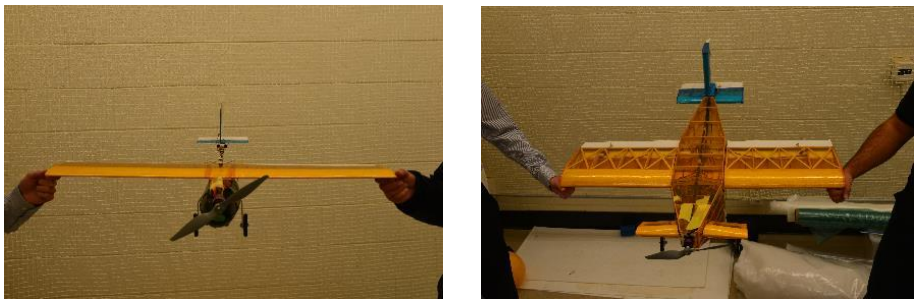

Figure 7.3: Wing tip loading test.

7.5 Flight Testing

Flight testing for both aircraft was conducted across two iterations, with a third planned as the final competition design. Initial iterations were used to determine the flying qualities of the aircraft designs. Verification of structural layouts and load estimates were also conducted. Missions were simulated and the necessary design modifications tabulated.

The second iterations are currently being used as testing platforms. Changes were made to the designs based on pilot and construction group feedback. For the PA, these included modifications to the wing structure and aileron size to make the plane lighter and easier to fit inside of the MSA. For the MSA, modifications included changes to the fuselage design to better mate with the tail and an increase in the main gear height to aid with takeoff and landing.

Currently, the second iteration of the PA is being used to verify the required battery size to complete M3. The second MSA frame is being used to test system M2 viability and determine further refinements to the design. Experience and data gained from all airframes will be used to improve the designs for a third iteration of both airframes that will go to competition. Both of the third iterations will fly simulations of their respective flight missions for proofing. The schedule and flight order is displayed in Table 7.1, seen below.

Table 7.1: Flight test goals and order for both aircraft.

Flight Test	Aircraft	Goal
1	First Iteration	Maiden flight
2	First Iteration	Takeoff distance
3	First Iteration	Mission runs
4	First Iteration	Mission runs
5	Second Iteration	Maiden flight
6	Second Iteration	Takeoff distance
7	Second Iteration	Motor performance testing
8	Second Iteration	Mission runs
9	Final Iteration	Maiden flight
10	Final Iteration	Mission runs

7.6 Checklists

Various tests have specific procedures which must be followed accurately to produce the desired objectives and ensure safety. This section lists the checklists utilized by *Buzzdryoshka* while conducting tests that required a significant amount of steps, such as propulsion and flight testing.

7.6.1 Propulsion Test Checklist

The checklist in Table 7.2 was created to ensure safety while dealing with propellers and electrical equipment, and to make sure the test is not wasted due to some mistake in preparation. This checklist was used in the testing of all motor, battery and propeller combinations.

Table 7.2: Propulsion testing checklist.

Propulsion Test Checklist		
1. Propeller secured? ☐	2. Motor mount secured? ☐	3. All plugs secured? ☐
4. Batteries peaked? ☐	5. Throttle down? ☐	6. Data system on? ☐
7. Custom code running? ☐	8. All clear of testing rig? ☐	9. Wind tunnel closed? ☐

7.6.2 Flight Test Checklist

The checklist in Table 7.3 was created with the important goal of preventing any system from malfunctioning in mid-air, which could lead to the aircraft crashing; its thorough execution is paramount to the team's success, and it will be used at the DBF event as well. ("P:" for PA and "M:" for MSA)

Table 7.3: Pre-flight checklist.

General System Checks								
Structural Integrity	**Center of Gravity Location**						**Time**	**Date**
	X	**P:**	**M:**	**Y**	**P:**	**M:**		
Payload								
Laterally Secure?	**Connections Secure?**		**Battery Pack**		**Receiver Pack**		**Payload Secure?**	
P: **M:**	**P:** **M:**		**P:** **M:**		**P:** **M:**		**P:** **M:**	
Attachment secure?		**Pins locked?**		**Clear of Jams?**				
Control Surfaces								
Ailerons			**Rudder**			**Elevator**		
Deflects?	**Glued?**	**Slop?**	**Deflects?**	**Glued?**	**Slop?**	**Deflects?**	**Glued?**	**Slop?**
P: **M:**	**P:** **M:**	**P:** **M:**	**P:** **M:**	**P:** **M:**	**P:** **M:**	**P:** **M:**	**P:** **M:**	**P:** **M:**
Electronics and Propulsion								
Receiver Battery Charged?	**Primary Battery Charged?**	**Receiver/ Transmitter Go?**	**Wires secure?**	**Battery hot?**	**Prop secure?**	**Prop direction?**		
P: **M:**	**P:** **M:**	**P:** **M:**	**P:** **M:**	**P:** **M:**	**P:** **M:**	**P:** **M:**		
Weather								
V_{wind}		Θ_{wind}		**Temperature**				
Initials for Approval								
Chief Engineer		**Pilot**		**Advisor**				

8. Performance Results

8.1 Component and Subsystem Performance

8.1.1 Propulsion

Batteries: A 10-cell, 1500mAh NiMH battery pack was discharged at 5 amps (3.3 times its capacity) and at 15 amps (10 times its capacity) to characterize the discharge capabilities of the NiMH batteries. The resulting data is shown in Figure 8.1 on a per cell basis. NiMH battery cells have a nominal voltage of 1.2V, and the 5 amp discharge curve is capable of maintaining this voltage. At 15 amps the cell voltage continuously drops, resulting in a small decrease in the available effective power. The higher current draw of the 15 amp discharge is necessary to achieve the power required for the aircraft.

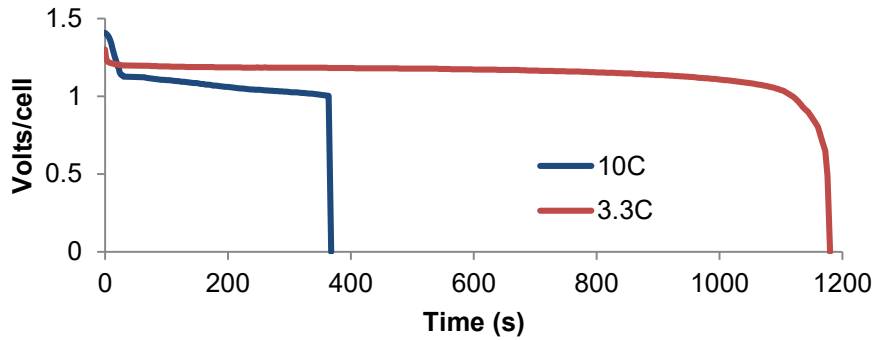

Figure 8.1: Battery discharge rates.

Motors and Propellers: The Cobra 2814/12 motor was tested using the MotoCalc software and the test stand as described in Section 7.2. Figure 8.2 shows the difference between the actual results and the theoretical results posed by the MotoCalc program for the propellers tested.

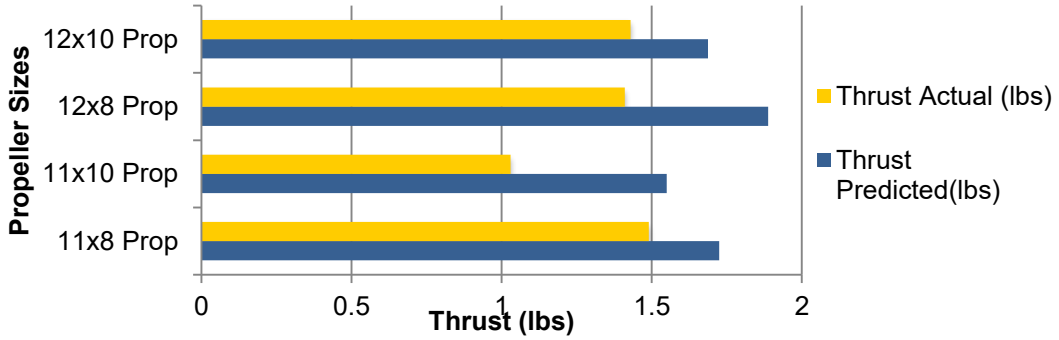

Figure 8.2: Difference between predicted thrust and actual thrust for different propellers.

Figure 8.2 shows that the 11x8 produces the greatest static thrust in the testing environment. This implies superior takeoff performance, leading the team to choose the 11x8 propeller.

8.1.2 Structural Tests

Wing Testing Results: The full size airplane was subjected to the required wing tip testing specified in the rules as part of the technical inspection process. This was done by loading the full internal Mission 2 payload of three blocks into the payload bay, then lifting the airplane by the wing tips. The successful wing tip test is shown in Figure 8.3.

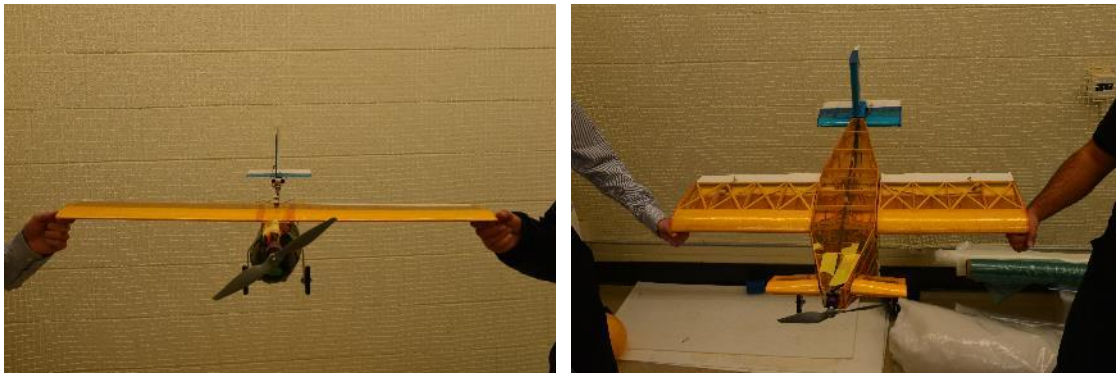

Figure 8.3: Wingtip structural test with full payload of the system.

8.2 System Performance

Testing of the system was conducted in the lab and at the flight field. Test results show that in both cases, assembly is found to be adequately simple and will not present complications during competition. The assembly time of the PA is fifteen seconds, including Gatorade bottle installation. The MSA is not restricted by an assembly time requirement, and fully encloses the PA. This is shown in Figure 8.4 below.

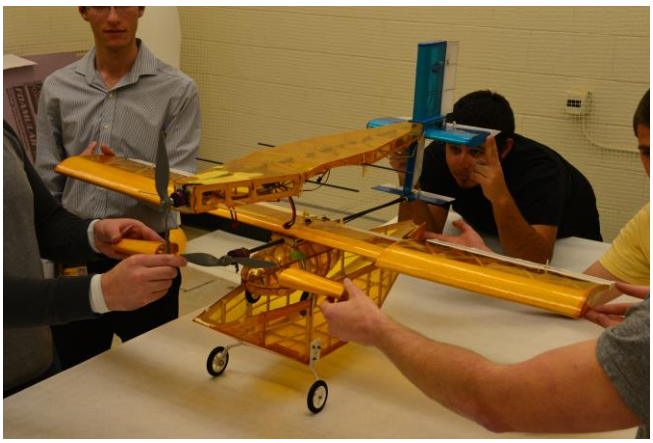

Figure 8.4: Exploded view of final assembled aircraft.

Flight tests of *Buzzedryoshka* were performed to evaluate the performance of the aircrafts and validate the performance predictions. To evaluate system performance during flight testing beyond simple lap timing and takeoff performance, the team equipped the aircraft with a data collection system that could be used to compare to the estimated mission performance in Section 5. The team purpose-built an Arduino-based telemetry system with a live data feed. On a number of test flights, the Arduino was mounted to the aircraft and recorded GPS at 1 Hz to yield trajectory data. An example of a full lap trajectory is displayed in Figure 8.5 superimposed on satellite imagery using Google Earth.

Figure 8.5: Trajectory of aircraft during competition laps from GPS data.

The results of flight testing are shown in Table 8.1. They indicate the performance predictions were optimistic. Further optimization and increasing pilot familiarity with the system should improve system performance to meet or exceed the predicted performance.

Table 8.1: Comparison of Predicted and Actual Performance Averages.

	1st Lap Time (s)		Time for 360		Laps Flown		TOFL		Max. Speed	
	Pred.	**Act.**	**Pred.**	**Act.**	**Pred.**	**Act.**	**Pred.**	**Act.**	**Pred.**	**Act.**
M1	43.0	53.0	2.15	3.5	3	3	6.72	6.5	52.50	52.1
M2	47.2	78.0	4.26	4.0	1	1	20.7	40.0	51.80	51.3
M3	49.1	59.0	5.19	9.0	3	3	95.2	95.0	63.15	61.6

Lap times for M1, M2, and M3 vary significantly between the predicted and actual values. These differences are explained by the uncertainties in the predictions as described in Section 4.3.2. Namely, the mathematical models lack a vertical dimension and any wind model. Furthermore, they assume an ideal flight path, with the aircraft pushed to their performance limits during turns. In reality, the performance target of 3 laps in 5 minutes does not mandate flying the aircraft at the edge of their performance boundaries.

Predicted and actual times for a 360 degree turn are highly variable, again due to pilot behavior. In all cases, time for a 360 degree turn was predicted assuming maximum velocity. However, during testing, the pilot tended to reduce speed significantly when going into a turn, which reduced the turn radius. For M3, the discrepancy was due to the test pilot flying conservatively so as not to slip below stall speed.

Discrepancies between predicted and actual TOFL are low for M1 and M3, but high for M2. While M3 takeoff distance is currently within competition bounds, an increase in power to increase the safety margin is necessary. The M2 discrepancy is a result of differences between pilot actual behavior and assumed behavior. The model used for calculating TOFL assumes that the pilot immediately advances to maximum throttle, but the pilot has been taking off more conservatively to maintain ground steering. The M1 discrepancy is within bounds of error and likely arises due to occasional wind gusts.

The maximum flight speed predictions correlate well to the maximum speeds seen during flight tests. The model predicts this well, because it was written to simulate flight in the horizontal plane.

In summary, as of the time of this report, 21 flights of the PA and 10 flights of the MSA have been performed on two different prototypes of *Buzzedryoshka*. The research, component selection, and testing that fed into the design process resulted in a lightweight MSA capable of completing three laps for Mission 1, ferrying the PA for Mission 2, and flying three laps with the Gatorade bottle loaded in the PA for Mission 3. The concept of a single-engine, high wing, conventional system proved to be successful in completing the loading mission and all flight missions, and was proven through laboratory testing to be lighter than other designs of an equivalent power level. The *Buzzedryoshka* team is eagerly awaiting more testing opportunities to ensure success during all missions at the competition and hone pilot familiarity with the aircraft. The team is confident that the overall configuration for *Buzzedryoshka* as shown in Figure 8.6 will be victorious.

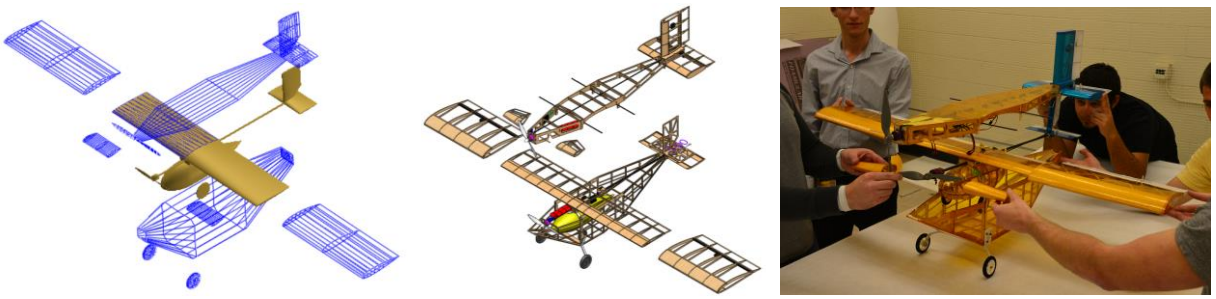

Figure 8.6: Progression from concept to reality of *Buzzedryoshka*.

9. REFERENCES

Anderson. J. D. *Fundamentals of Aerodynamics,* 4th edition, McGraw Hill.

Bauchau, O. A., & Craig, J. I. (January 7, 2009). *Aerospace Structural Analysis.* Springer.

Drela, M., & Youngren, H. (2008, 08 04). *AVL.* Retrieved 01 10, 2009, from [http://web.mit.edu/drela/Public/web/avl/].

Drela, M., & Youngren, H. (2008, 04 07). *XFOIL.* Retrieved 10 01 2008, from Subsonic Airfoil Development System: [http://web.mit.edu/drela/Public/web/xfoil/].

Hoerner, Sighard F. *Fluid Dynamic Drag*. 2nd. Published by author, 1965.

Katz, Joseph and Maskew, Brian. "Unsteady low-speed aerodynamic model for complete aircraft configurations," *Journal of Aircraft.* Vol. 25, pp. 302-310. Apr. 1988.

McDaniel, Katie et al. (2008). *Georgia Institute of Technology Team Buzzed*. Editor: Johnson, Carl.

Phillips, Warren F. *Mechanics of Flight*. 1st. Hoboken, NJ: Wiley, 2004.

Roskam, Jan. *Airplane Design Part VI*. Darcorp, 2000.

Roskam, Jan. *Airplane Flight Dynamics and Automatic Flight Controls Part I*. Darcorp, 2007.

Selig, M. (2008, 02 19). *UIUC Airfoil Data Site*. Retrieved 10 01, 2008, from [www.ae.uiuc.edu/m-selig/ads.html].

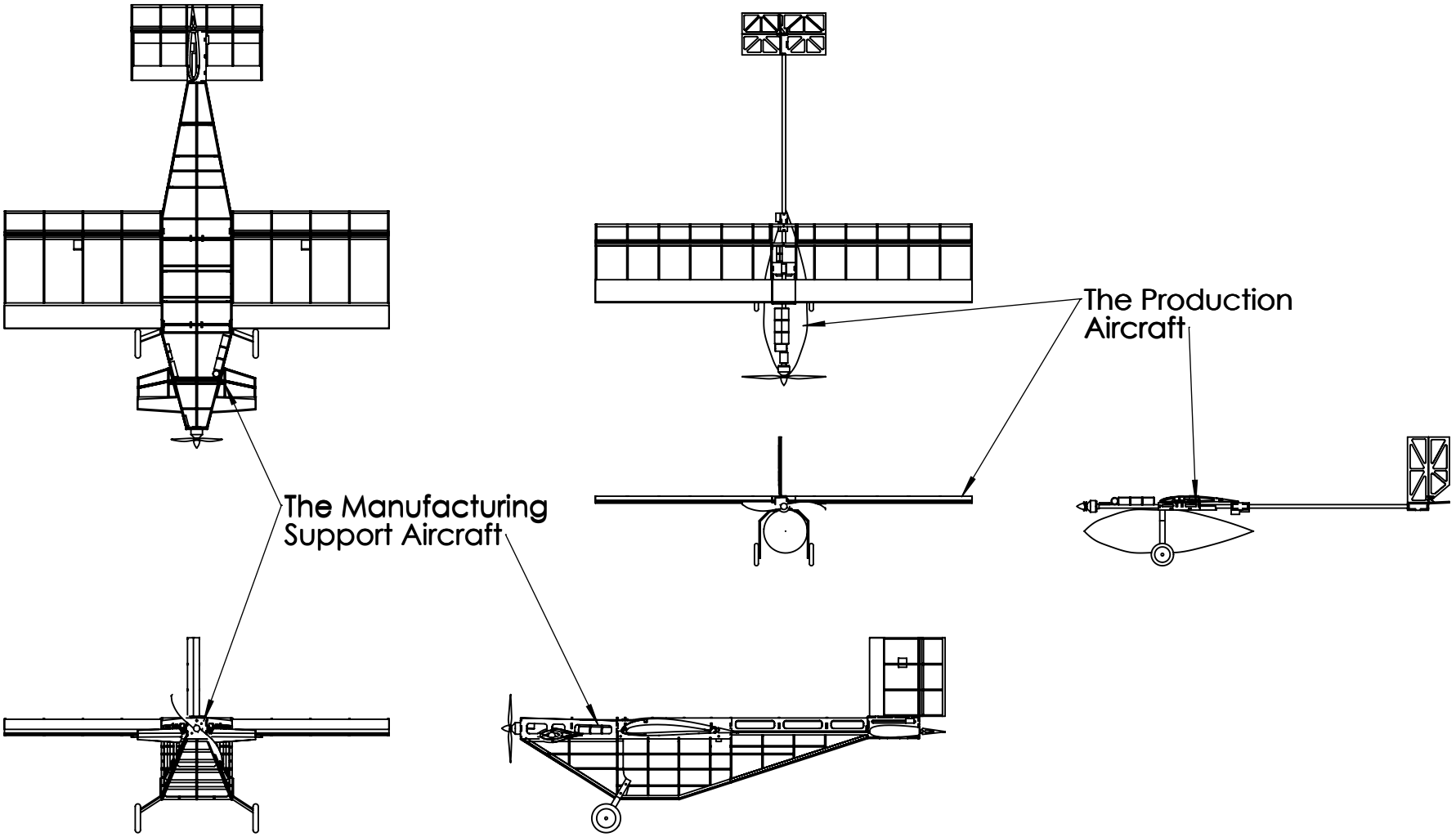

DRAWN Yusuf Ogun Kargin	Georgia Institute of Technology	
CHECKED George P. Burdell	Buzzedryoshka	
2/19/2016	SIZE A	DWG PA and MSA 3 View Drawings
SCALE 1:15	All Dimensions in Inches	SHEET 1 OF 1

2015-2016 AIAA/Cessna/Raytheon Design Build Fly Competition

University of California Irvine

Electrolyne

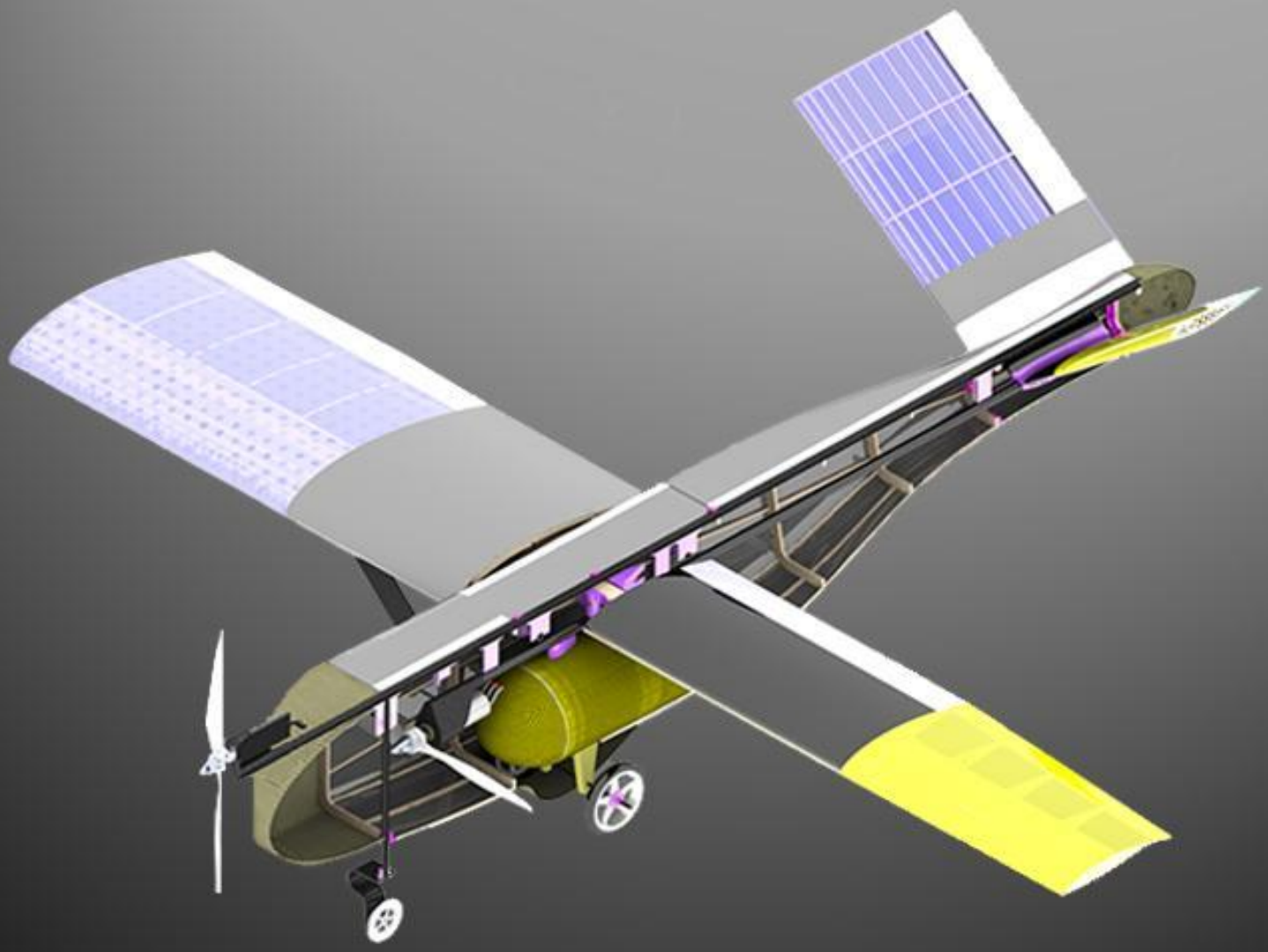

Contents

Nomenclature List & Acronyms Used:

MA - Manufacturing Support Aircraft

PA - Production Aircraft

M1 - Mission One

M2 - Mission Two

M3 - Mission Three

MF1 - Score for completing Mission 1

MF2 - Score for completing Mission 2

PF - Score for completing Mission 3

Bonus - Score for completing Bonus Mission

N - Number of Sub - Assemblies

EW1 - Empty Weight of Production Aircraft

BW1 - Battery Weight of Production Aircraft

EW2 - Empty Weight of Manufacturing Support Aircraft

BW2 - Battery Weight of Manufacturing Support Aircraft

RAC - Rated Aircraft Cost

WRS - Written Report Score

TMS - Total Mission Score

AR - Aspect Ratio

FOM - Figures of Merit

GTOW - Gross Takeoff Weight

RAC - Rated Aircraft Cost

AVL - Athena Vortex Lattice

CG - Center of Gravity

L - Lift

D - Drag

D_i - Induced Drag

D_p - Parasitic Drag

T - Thrust

q - Dynamic Pressure

C_L - Lift Coefficient

C_D - Drag Coefficient

C_{Di} - Induced Drag Coefficient

C_{Dp} - Parasitic Drag Coefficient

b - Span

c - Chord Length

m.a.c - Mean Aerodynamic Chord

AR - Aspect Ratio

t/c - thickness to chord ratio

S - Reference Area

S_{wet} - Wetted Area

e - Oswald Efficiency

V - Voltage

A - Amps

W - Watts

kV - Revolutions per Volt

1. Executive Summary

This report details the design, analysis, manufacturing, and testing performed by the University of California, Irvine team entry for the AIAA Design/Build/Fly 2015-2016 competition. The objective of the competition is to produce two electric radio controlled aircraft that best meet the mission requirements and maximizes the Total Mission Score (TMS). The theme of the first mission is the arrival of the empty Manufacturing Support Aircraft (MA). The second mission models the MA delivery flight, in which the MA aircraft will transport the Production Aircraft (PA) sub-assemblies required to complete the third mission. The third mission is designed to fly the PA with the internally carried payload, a 32 oz. Gatorade bottle.

The highest total score is comprised of a combination of the Written Report Score, Total Flight Score (TFS), and Rated Aircraft Cost (RAC). In order to achieve this, key mission requirements were identified; through score analysis, the team determined that the winning aircraft would be one built with the lightest possible empty weight and with the lowest number of sub-assemblies allowed. Focusing only on weight or one mission alone does not yield a winning aircraft. Successful completion of each flight mission under the allowed time would grant full mission scores. The configuration of each aircraft was dependent on the other, and factoring in the key design parameters used in the score analysis allowed for the first conceptual design of both aircraft to be made.

The need for effective ground handling adds another level of complexity to the design. To address the challenges posed by each mission, the team designed an aircraft that could balance the mission requirements: flight endurance for Mission 1 (M1), minimum number of sub-assemblies for Mission 2 (M2) flight including ground maneuverability for taxi, endurance for Mission 3 (M3) flight, and the Bonus Mission. After considering several aircraft configurations, a conventional aircraft design consisting of a high wing with a V-tail, a taildragger landing gear, and a single tractor motor was selected for the PA. The design of the MA was a derivative of the PA, considering one sub-assembly, a conventional aircraft design comprised of a high wing with V-tail, a tricycle landing gear, and a single tractor motor was selected.

Aircraft optimization revealed that one sub-assembly should be carried during Mission 2 in order to maximize score. In order for the aircraft to fly at the speed for best range, the aircraft needs to be built with the lightest combination of structure and propulsion weight. Battery packs were sized to provide enough energy for all missions while minimizing weight. For both aircraft, the team chose a high kV motor and opted to decrease the voltage. For the MA, the propeller diameter was increased, while the PA's propeller diameter was decreased. Propulsion design choices were made in order to gain enough thrust for takeoff during the payload missions while adhering to the 100-ft. takeoff requirement. The MA's wing was sized specifically for carrying the minimum number of sub-assemblies during Mission 2 takeoff. The fuselage length adequately accommodates the required payload, and the landing gear attached to the wing spar allows loads to transfer from the landing gear to the central wing carbon rods that are attached to the main boom. To minimize structural weight, the fuselage section is constructed mainly of balsa stringers with Microlite™ covering as skin. Constraints on how to position the Mission 2 payload drove the fuselage design to minimize the cross-section of the fuselage to fit the payload longitudinally.

The third flight mission objective is to fly the PA with a 32 oz. Gatorade bottle payload. The wing is designed with a high aspect ratio (AR), and the propulsion system is designed to emphasize minimizing the power required to complete the mission.

Both aircraft are being tested to their performance limits while the design of the aircraft and its components are continually being improved and optimized. Test flights to date demonstrate that the MA completes Mission 1 and Mission 2 within the time allocated; the PA also completes Mission 3 within the time limit.

2. Management Summary

The UCI *Electrolyne* team implements an organizational structure and design timeline that focuses on maximizing efficiency and team collaboration. With over 30 dedicated members, the team benefits from a wide range of interests and capabilities.

2.1 Team Organization

The UCI *Electrolyne* team follows a hierarchical structure similar to those in industry, placing responsibility on members to perform their required tasks shown in Figure 2.1.

The Project Manager is responsible for facilitating productivity in all areas of the project by acquiring material, scheduling, and leading team meetings. The Chief Engineer steers the design effort and facilitates communication between design groups. The Operations Engineer aids the Project Manager and Chief Engineer in the finance and business aspect of the project by managing logistics and keeping a budget portfolio. All three individuals lead the project, supported by the following teams:

- **Aerodynamics** computes flight characteristics and predicts the aircraft's flight performance from numerical models and ensures that the aircraft meets control and stability standards.
- **Balsa Structures** experiments with new manufacturing methods for the wings and fuselage in order to decrease overall weight while maintaining structural integrity.
- **Control surfaces** manufactures ailerons, elevators, rudders, and composite fuselage frames.
- **Battery and Propulsion** analyzes and tests the propulsion system to find the optimal motor, propeller, and battery combination.
- **CAD** creates detailed drawings of the components of the aircraft system and aids in the rapid visualization of possible aircraft solutions.
- **Fuselage** designs and builds the fuselage, fairings, and payload restraint mechanisms.
- **Motor Mount** focuses on fabricating motor mounts that attach to the fuselage boom.
- **Landing Gear** designs and fabricates landing gears and its integration with the fuselage.
- **Testing** fabricates apparatuses and conducts load simulation for manufactured parts to collect documentation for designs.
- **Pilot** organizes and conducts test flights, performs preflight/post-flight inspection and collects flight data.
- **Integration** assembles the aircraft components and is responsible for component compatibility.
- **Advisors** guide and offer insightful suggestions. Graduate Advisors look over aerodynamic

aspects of the design. Professional Advisors offer manufacturing tips from previous and current industry experience.

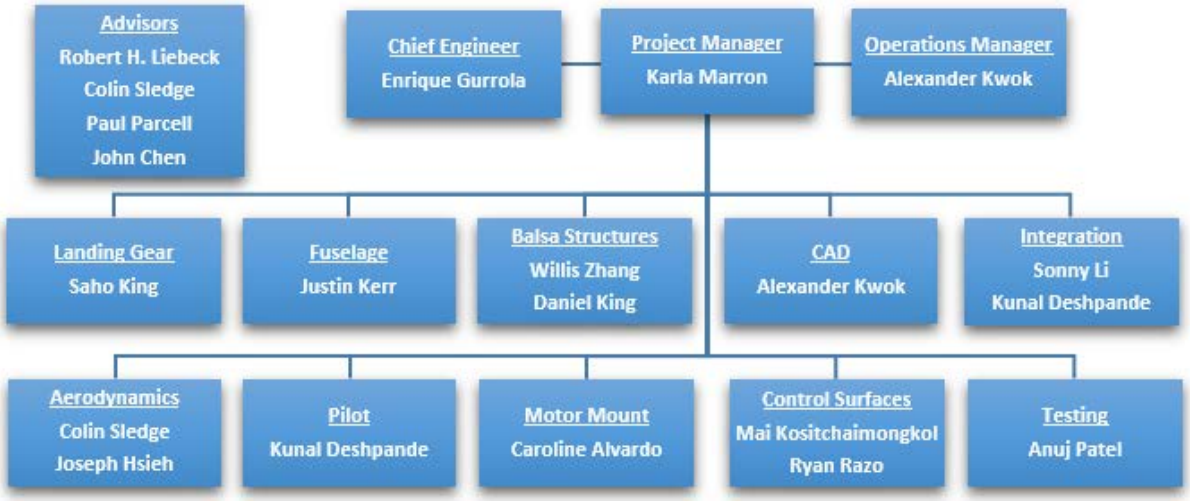

Figure 2: 1 UCI DBF Electrolyne Team Organization Chart

2.2 Milestone/Gantt Chart

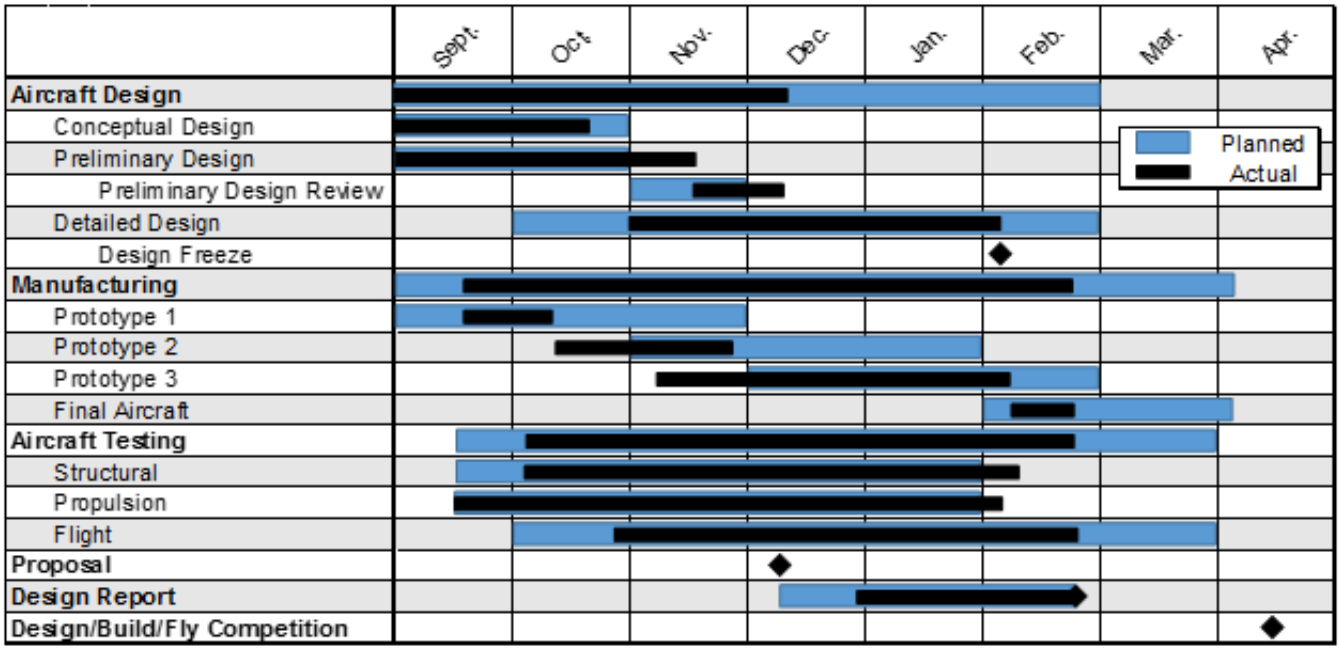

Figure 2: 2 Project Milestone/Gantt Chart

3. Conceptual Design

The objective of the conceptual design process is to obtain possible solutions that will satisfy the given design request. Possible solutions are compared and analyzed using figures of merit (FOM) extracted from the analysis of the mission goals, requirements, and the design constraints provided in the contest rules. The result of this process is a combination of designs that maximize the overall flight score.

3.1 Mission Sequence

The mission sequence consists of three flight missions and a bonus ground mission. A new mission cannot be attempted until a successful score is obtained for the preceding mission. Aircraft must be designed to be capable of performing all required missions. Aircraft must pass the wing tip load test with the largest payload loading intended to fly. The maximum load demonstrated will be recorded and cannot be altered after completing tech inspection. The aircraft is limited to a 100 ft. takeoff field length for all flight missions. The initial upwind turn on the first lap of each mission will occur after passing the turn judge. All turns will only be made after passing the markers which are 500 ft. away from the start line. Aircraft must be "straight and level" when passing the turn marker before initiating a turn. The pilot will have unaided visual control of the aircraft at all times. Finally, to receive a score on any mission, the aircraft must successfully land without dropping any component during flight, completed subsequently.

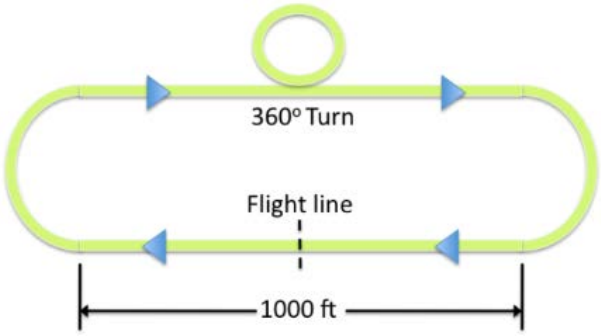

Figure 3: 1 Flight Course Outline for all Missions

3.1.1 Mission 1 - Manufacturing Support Aircraft Arrival Flight

Within a five-minute window, the Manufacturing Support Aircraft must complete three laps of flight with no payload. Time starts when the throttle is advanced for take-off. A lap is complete when the aircraft passes over the start/finish line in the air. Mission 1 scoring is indicated below:

- MF1 = 2.0 – Aircraft completes the mission
- MF1 = 0.1 – Aircraft does not attempt or complete a successful flight

3.1.2 Mission 2 - Manufacturing Support Aircraft Delivery Flight

The Manufacturing Support Aircraft must internally transport the Production Aircraft sub-assemblies, excluding its battery and 32 oz. Gatorade payload, within a ten-minute window. For each sub-assembly, the Manufacturing Support Aircraft must fly one lap, land, and deliver the part to the designated payload change area. In the designated area, the ground crew will exchange sub-assemblies into the MA. The payload may be a group of PA components, that do not require gluing or bonding to reassemble, reducing the number of laps required for transport. The mission will begin with the first payload installed. Time ends when the aircraft passes the start line in the air at the end of the final flight. Successful landings are required for each lap to receive a score. Mission 2 scoring is indicated below:

- MF2 = 4.0 – Aircraft completes all sub-assembly group transport flights successfully within the time window
- MF2 = 1.0 - Aircraft completes less than all the sub-assembly flights within the designated time allowance but at least 1 group is successfully transported
- MF2 = 0.1 – Aircraft does not attempt or complete a successful flight

3.1.3 Mission 3 - Production Aircraft Flight

The Production Aircraft must fly three laps with a 32 oz. Gatorade payload within a five-minute window. Time starts when the throttle is advanced for take-off. A lap is complete when the aircraft passes over the start/finish line in the air. PF scoring is indicated below:

- PF = 2.0 – Aircraft completes the required flight within the time period carrying the full payload
- PF = 1.0 - Aircraft completes less than the required laps or exceeds the time period
- PF = 0.1 – Aircraft does not attempt or complete a successful flight

3.1.4 Bonus Mission (Ground Only) - Production Aircraft Assembly

The Production Aircraft sub-assemblies and the Gatorade payload must be assembled within two minutes by the ground crew immediately after the final flight in the designated area. Upon completion, the reassembled aircraft must pass a wing tip lift test and a control systems check. The bonus score is determined by the following criteria:

- Bonus = 2.0 – Aircraft assembled in specified time and passes wing tip lift test
- Bonus = 0.0 – Any other result

3.2 Scoring Formula

The 2016 AIAA Design/Build/Fly competition consists of three flight missions, one bonus (ground) mission, and a written report. The total score is contingent on the Total Mission Score, the Rated Aircraft Cost, and the Written Report Score. The formula to determine a team's score is shown below:

$$SCORE = Written\ Report\ Score * Total\ Mission\ Score/RAC$$

$$Total\ Mission\ Score = (MF1 * MF2 * PF) + BONUS$$

$$RAC = (EW1 * Wt_{Battery1} * N_{Components}) + (EW2 * Wt_{Battery2})$$

The TMS is the product of the individual mission scores plus the Bonus Mission. The RAC is a function of the empty weight (EW), battery weight (BW), and number of sub-assemblies for transport (N).

3.3 Design Constraints

The team analyzed the contest rules in order to determine design constraints and decided on the following as the main requirements:

- All payloads must be carried internally and be properly secured.

- Any component from the PA that detaches, folds, or moves from flight position will count as a sub-assembly.
- PA cannot have a folding propeller.
- There is a time limit for the three flight missions, they are 5, 10, 5 minutes respectively.
- The ground rolling takeoff length must take place within 100 ft. runway distance.
- There is no limit to the battery pack weight.

3.4 Sensitivity Analysis

The score equations were analyzed to see the impact of each parameter on the total score. The first stage of the analysis considered extreme cases to determine unusual behavior in the scoring conditions. Following this stage was an analysis using MATLAB to determine the score sensitivity of the parameters for different PA components. To perform this analysis, the scores were estimated using past years' competition data. The estimated parameters for PA were 2.0 lbs empty weight and 0.5 lbs battery weight. The estimated parameters for MA were 2.5 lbs empty weight and 0.6 lbs battery weight. Maximum mission scoring was assumed.

3.4.1 Extreme Cases

Reasonable extreme aircraft are analyzed to see if certain variables have an extreme effect on the overall score. Each case makes use of estimates for performance and total weight. The scores for each mission along with the RAC and TMS/RAC are shown in Figure 3.2.

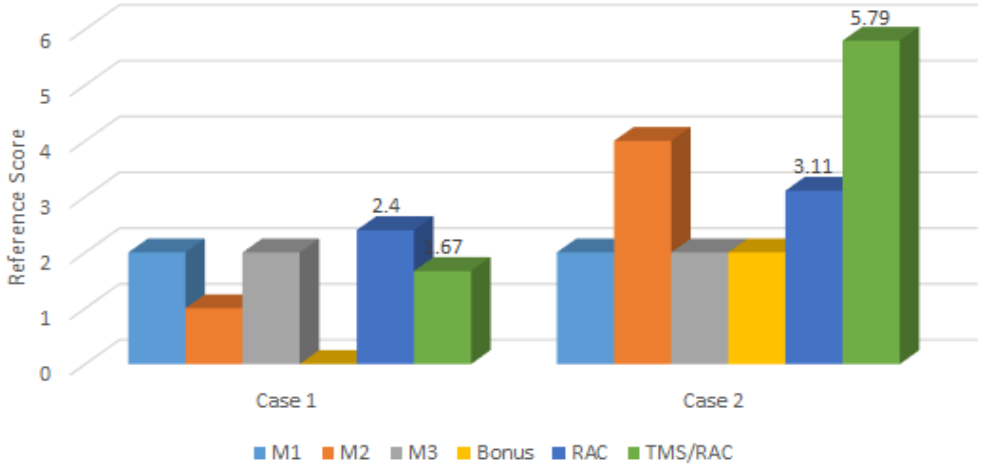

.

Figure 3: 2 Projected scores of three different cases are shown above.

The graph indicates a comparison of an extreme Case 1 and a reference Case 2:

- Case 1 (extreme case): If the MA is designed to carry only the lightest and smallest PA sub component (for example a propeller) for M2, the size and battery weight of the MA can be minimized for takeoff. This means only partial points for M2 is awarded, and zero point is received

for Bonus mission. Assuming the PA is designed to fully complete M3 with the total number of sub-assemblies of two. The TMS is 4, and the RAC is estimated to 2.4. The TMS/RAC is 1.67.

- Case 2 (reference case): Assume the PA is designed to fully complete M3 with the total number of sub-assemblies of one. The MA and PA are designed to receive full points for all missions, the MA size has to be as small as possible to cover the entire PA. The TMS is 18, and the RAC is estimated to 3.11. The TMS/RAC is 5.79.

Not attempting, or having an unsuccessful flight in any mission will have a detrimental impact on the Total Mission Score. Comparing the two cases indicates that partially completing Mission 2 should result in a lower RAC than case 3, but the ratio of the TMS to the RAC of the extreme Case 1 largely suffers due to very low TMS. Therefore, the second case is the chosen aircraft design.

3.4.2 Sensitivity Analysis

A score sensitivity analysis was performed to understand how the design and mission parameters affect the score. MATLAB was used to evaluate percent changes of the score parameters from an estimated baseline based on past competition data. Since N is measured in integer increments, the sensitivity analysis was performed to consider N = 1 and N = 2 shown in the following figure. Each analysis varied one parameter while holding the others constant. Results show that the battery weights for each aircraft and PA components have the largest influence on the total score compared to other parameters.

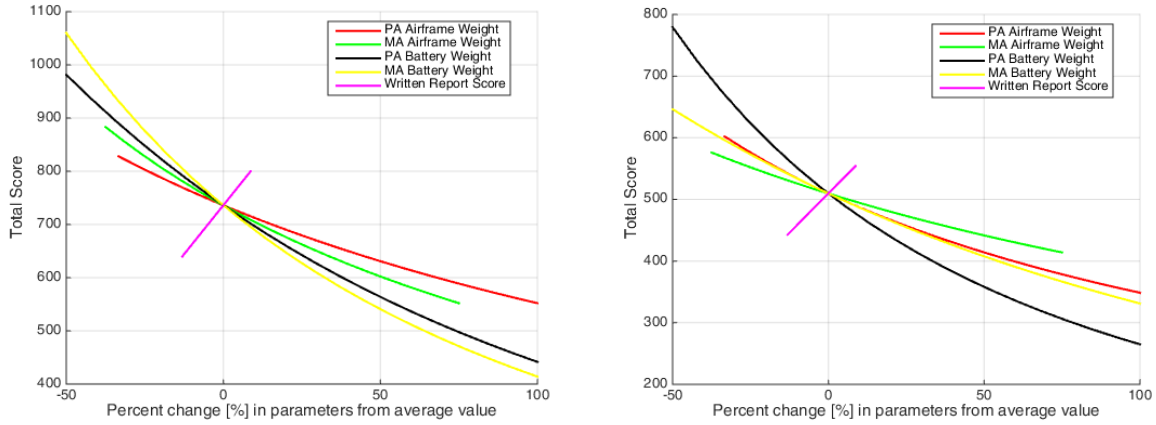

Figure 3: 3 (A) N = 1 Sensitivity Score Analysis, (B) N = 2 Sensitivity Score Analysis

The aircraft empty weight was separated into airframe (fixed) weight plus battery weight to observe their differences in the sensitivity analysis. The battery weight is accounted for twice in the RAC and therefore has a larger influence on the score. The TMS was assumed to be the maximum value during this analysis. In conclusion, to increase the total score the RAC must be decreased.

3.5 Design Requirements

The sensitivity analysis concluded the following, in descending order of importance:

PA Components: The number of sub-assemblies greatly affects the overall score since it comes in integer increments as opposed to other parameters. This parameter affects the wetted area of the MA because of loading accommodations that need to be considered to secure the payload(s). The less sub-assemblies there are, the more complex the MA design will be to minimize wetted area and fully enclose the PA sub-assembly payload.

Battery Weight: For given aircraft specifications, the power requirements will vary with speed and mission segments. Battery weight is separated from aircraft weight since the battery weight is a significant percentage of the total system weight. Battery weight is a unique parameter since batteries have discrete incremental weight, capacitance, and cells.

Aircraft Weight: Any aircraft must be manufactured to minimize system weight without compromising structure in order to reduce RAC.

3.6 Configuration Selection

A few basic aircraft configurations were evaluated as possible options for this year's design. They were evaluated according to the mission requirements resulting from the sensitivity analysis. The conventional configuration acts as the baseline comparison. Configurations considered are:

- **Conventional:** The stability and control characteristics of this configuration are more reliable than the flying wing or a biplane. Additionally, the conventional wing is the most convenient to manufacture and design rapidly. However, a single component conventional aircraft causes the optimization of the PA and MA to be difficult to design.
- **Flying Wing:** This configuration offers a greater L/D and less drag than the conventional design. However, control authority and ground handling suffers.
- **Biplane:** The biplane configuration offers greater wing area per span. However, it requires additional structure, thus contributing more to weight and drag.

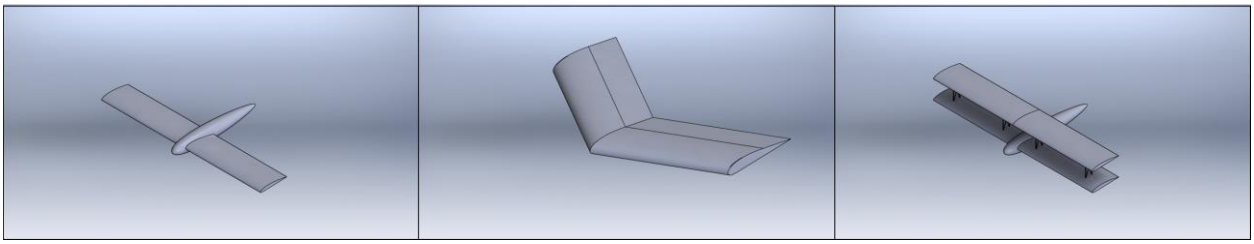

Figure 3: 4 Aircraft Configuration

Table 3: 1 Aircraft Configuration Figures of Merit

	PA					MA			
FOM	Weight	Conventional	Flying Wing	Biplane	FOM	Weight	Conventional	Flying Wing	Biplane
Weight	35	0	0	-1	PA Components	45	1	-1	0
Handling	30	0	-1	0	Weight	25	0	0	-1
L/D	20	0	1	0	L/D	20	0	1	0
Manufacturability	15	0	0	-1	Manufacturability	10	0	0	-1
Total	100	0	-10	-50	Total	100	45	-25	-35

The conventional configuration was selected for both aircraft because it offers the best combination possible for efficiency and mission requirements. By utilizing the unused interior of the MA main wing to house the PA main wing, the wetted area of the MA can be reduced.

3.7 Subsystems Selection

After a conventional aircraft configuration was selected, the major sub-systems were analyzed using figures of merit (FOM) analysis to determine the best options. The main sub-systems considered were motor, empennage, and landing gear.

3.7.1 Motor Configuration

The team investigated the placement and number of motors, which affects the aircraft's efficiency and ability to carry payloads. A FOM was used to compare the different propulsion systems, using the single tractor configuration as the baseline for comparison.

- **Single Tractor:** The single tractor is lightweight and provides the best ground clearance for takeoff and landing. It also has high efficiency because of the clean air acting through the propeller. However, this causes prop wash for the rest of the aircraft.
- **Double Tractor:** Double tractor uses two motors/propellers of reduced size to obtain similar thrust for single tractor configuration. Cells packs can be split to power each motor, but there is additional weight in the setup along with an extra ESC requirement.
- **Single Pusher:** This configuration reduces scrub drag as the aircraft operates in clean air. However, a motor mounted aft of the aircraft will operate in the wing/fuselage wake, which causes a decrease in propulsion efficiency.

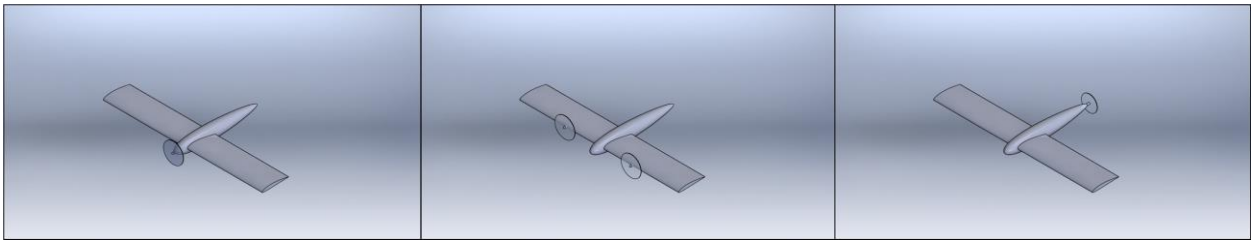

Figure 3: 5 Motor Configuration

Table 3: 2 Motor Configuration Figures of Merit

PA					MA				
FOM	Weight	Single Tractor	Double Tractor	Single Pusher	FOM	Weight	Single Tractor	Double Tractor	Single Pusher
Efficiency	35	1	1	0	System Weight	40	0	-1	0
Packaging	30	-1	0	-1	Structural Weight	30	0	-1	-1
Structural Weight	20	1	-1	-1	System Efficiency	15	1	1	-1
Ground Clearance	15	0	0	-1	Aircraft Efficiency	15	0	0	1
Total	100	25	15	-65	Total	100	15	-55	-30

The single tractor configuration was selected for both aircraft because it results in a lighter aircraft and simplified balancing of the aircraft center of gravity (CG).

3.7.2 Empennage

Three empennage configurations are considered with conventional design as the baseline. Packaging (40%) was most important for PA because it designs the MA empennage and affects the RAC by the number of sub-assemblies. Stability/Control (25%) and Weight (25%) are measured equally because the aircraft will be flying above stall speed to minimize power requirements and the weight is reflected in the RAC. Manufacturing (10%) was least important in terms of empennage design.

- **Conventional Tail:** Simplest to install and provides sufficient stability/control. For single component, it is more difficult to package.
- **T-Tail:** Horizontal stabilizer gets clean air by joining with the vertical stabilizer on top, but adds structural weight. The T-Tail also has greater packaging difficulty.
- **V-Tail:** Two surfaces form a "V" with the tail boom and provide both elevator and rudder control. Control authority is compromised for reduced weight. V-Tail has the best packaging capability.

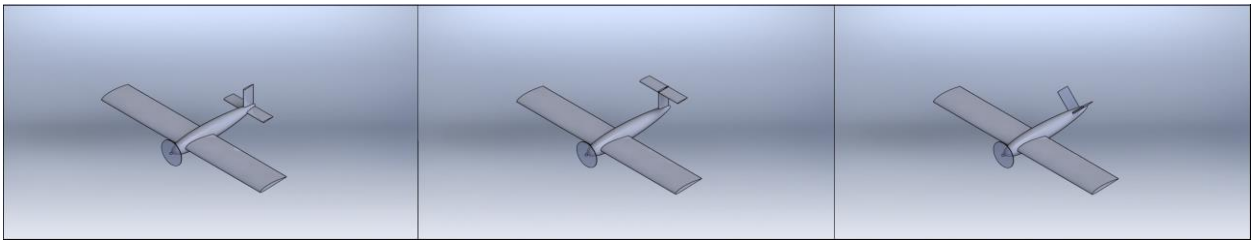

Figure 3: 6 Empennage Configuration

Since the MA empennage is designed around the PA empennage for a single component, a FOM was only performed for the PA.

Table 3: 3 Empennage Configuration Figures of Merit

PA and MA				
FOM	Weight	Conventional	T-Tail	V-Tail
Packaging	40	0	0	1
Stability and Control	25	0	0	-1
System Weight	25	0	-1	0
Manufacturing	10	0	0	0
Total	100	0	-25	15

Test flights have demonstrated that a V-tail configuration has similar stability characteristics compared to a conventional tail at low speeds. The V-tail empennage was selected for both airplanes for packaging reasons. The V-tail design allows the MA empennage to slide over the PA empennage in two sections, reducing joint drag when compared to sliding three sections for a conventional tail. Though this design compromises on handling/stability, the loading of the PA into the MA fuselage is simplified.

3.7.3 Landing Gear

Takeoff and landing are critical to the successful completion of the missions. Ground handling is particularly important for the taxi segment of M2. Therefore, the challenge at takeoff is to maintain sufficient control during the ground roll until the aircraft attains takeoff. In addition to vertical and

horizontal loads, the landing gear must also withstand bending moments. Three landing gear configurations were considered: Tricycle, Bicycle, and Tail Dragger. Handling (30%) and Durability (35%) were most important for the PA and MA respectively. Weight is always crucial to the score, being second and third most important for PA and MA respectively.

- **Tricycle:** The tricycle configuration has two main wheels under the wing and directly aft of the aircraft CG, and a centerline nose wheel for steering. The nose wheel is exposed to the propeller wake, causing a significant drag penalty. However, it provides excellent ground handling on flat terrain.
- **Bicycle:** The bicycle has two centerline main wheels and two wing tip wheels. The landing gear structure can be reduced as the main loads are transferred through the center wheel, but the additional wheels and struts add drag.
- **Tail Dragger:** The tail dragger has two main wheels under the wing and one smaller wheel under the tail of the aircraft. This configuration does not have excellent ground handling in crosswind, but it does have less drag than the tricycle configuration. It also allows a larger rotational clearance.

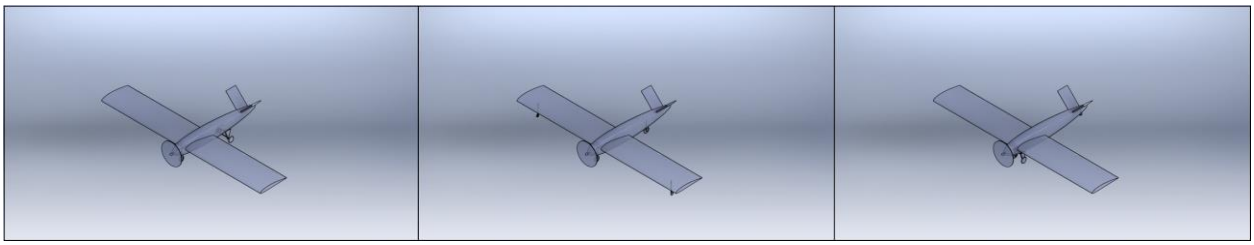

Figure 3: 7 Landing Gear Configuration

Table 3: 4 Landing Gear Configuration Figures of Merit

PA					MA				
FOM	Weight	Tricycle	Bicycle	Tail Dragger	FOM	Weight	Tricycle	Bicycle	Tail Dragger
Handling	30	1	-1	1	Durability	35	0	-1	0
Weight	25	0	1	0	Handling	30	1	-1	0
Durability	25	0	-1	0	Weight	25	0	1	0
Drag	20	-1	-1	1	Drag	10	-1	-1	1
Total	100	10	-50	50	Total	100	20	-50	10

The tail dragger was selected for the PA because of good handling and reduced drag. The tricycle configuration was chosen for the MA because of excellent ground handling that will be necessary for M2.

3.8 Final Conceptual Design Summary

The PA aircraft's conceptual design was created with an emphasis on a compact form factor with minimal weight. This is because the PA aircraft is the main limiting factor when sizing the MA aircraft. The MA is designed to wrap around the PA aircraft as tight as possible since the PA is intended to be only one

component. These final concepts reflect the designs the team deemed important in order to obtain a high score at the competition.

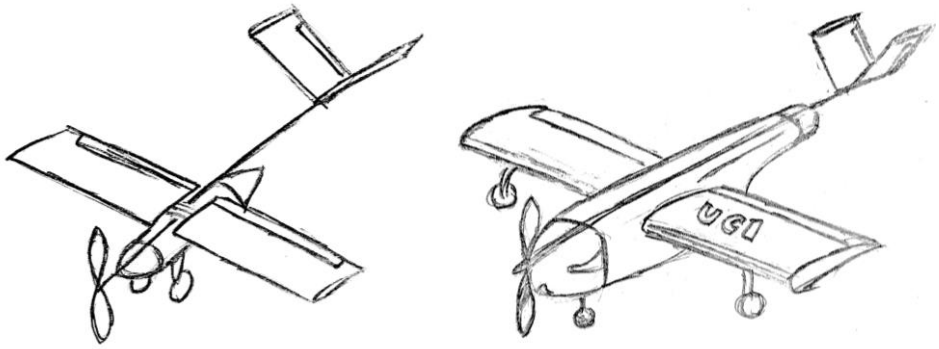

Figure 4: 1 (A) Conceptual Sketch of PA, (B) Conceptual Sketch of MA

4. Preliminary Design

Preliminary design took the configuration proposed during the conceptual design phase and applied it to a mission model that would output several aircraft. This section shows how the sizing and optimization of each subsystem was completed to converge on an aircraft that would score the highest at the competition.

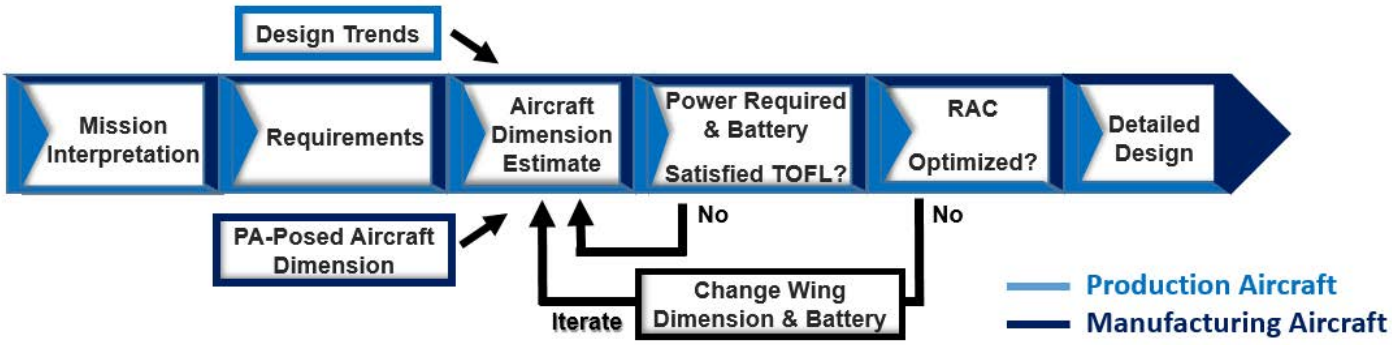

Figure 4: 2 Optimization Program Flow Chart

4.1 Design Methodology

The fuselage is intended to contour to the bottle surface with an additional cap at the aft of the bottle to reduce pressure drag. The wings were designed to use a larger span to lower the induced drag. By lowering the induced drag, the required power to fly decreases; thus effectively reducing the battery weight and overall weight of the PA.

The design constraints set on the aircraft by the competition rules and the location of the competition allowed a conceptual design to be established shown in the FOM in Section 3.6. The competition rules state that the PA aircraft has to carry a 32 oz. Gatorade bottle, meet a takeoff length of 100 ft., and fly the course within a given amount of time. Since there is a fixed time to complete all three

laps, individual lap times are also constrained. Considering the environment of the competition, wind will significantly affect ground speed and influence lap times.

In addition to the constraints established in the competition rules, design constraints based on design trends were set. The trends were chosen based on previous DBF experience and experience working with similar scale electric aircraft. The trends are: wing loading range, power loading range, and payload mass fraction. From the design trends, wing loading typically ranges between 1-2 lb/ft^2 and power loading ranges between 50-100 W/lb. Lastly, the relation between the payload and gross takeoff weight (GTOW) is estimated to be about 60%.

From the combination of design requirements and design trends, a reasonable estimate of the size of the aircraft was created. This prediction was then evaluated using two tools. The first tool was a MATLAB code that evaluated whether the aircraft with the given power and wing area could meet the takeoff requirement. The second tool used was an aircraft performance estimator that gave power requirements that the battery must provide in order for the aircraft to successfully complete the mission. From the initial power requirement and wing area estimates, an estimated RAC was calculated. This RAC was used as a benchmark for further iterations. Figure 4.2 indicates that the battery weight averages 15% of the gross aircraft weight.

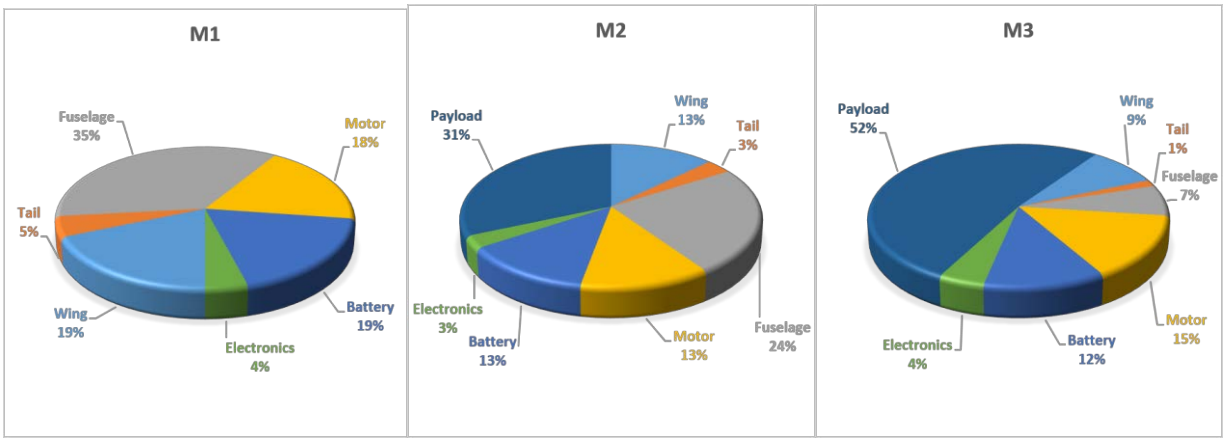

Figure 4: 3 Weight Build-ups per Mission

Once the PA was sized, the MA was designed around the PA; thus, constraining the minimum dimensions of the MA. The process of designing the MA uses the same methodology as the PA. A reasonable estimation is made and then iterated using the aforementioned tools: the RAC is calculated for the MA design and the design is iterated to minimize RAC, while staying within the dimensional constraints set for the MA.

The MA's empennage location is preset due to the empennage location of the PA; however, issues arise when the MA empennage favors a different location than the present position. The process returns to sizing the PA to obtain a moment arm of the MA empennage. Finally, the MA follows the same process as the PA to determine its final dimensions.

4.1.1 Mission Model

The mission model was used to estimate the power and energy requirements for each aircraft by simulating the basic flight segments as shown in Figure 4.3. The goal of the mission model was to find the edges of the flight envelope for the aircraft. To find the power and energy required, three sections of the flight regime were analyzed: the takeoff, climb out, and cruise. For most of the flight envelope, the takeoff and climb out power requirements size the battery required to complete the mission. The cruise portion of the mission was modeled both with and without wind. The only time the cruise segment sized the power requirement for the mission was when there was a significant amount of wind. A MATLAB code was used to evaluate these flight conditions and provided the power and energy required for the aircraft.

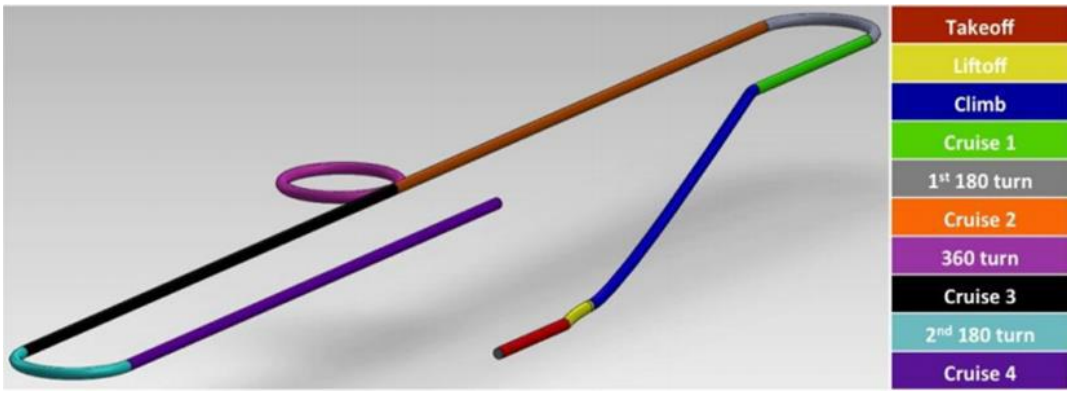

Figure 4: 4 Mission Model Segments

Table 4: 1 Mission Model Constraints and Segment Descriptions

Flight Segment	Constraints	Description
Takeoff	Constant angle of attack Rotation when V=1.2•V_stall	Aircraft accelerates on the ground until rotation
Liftoff	Constant altitude	Aircraft accelerates to ideal climb speed
Climb	Constant load factor	Aircraft climbs to cruise altitude of 80-ft
Cruise	Constant altitude	Aircraft maintains altitude
Turn	Constant load factor	Aircraft turns without overloading wings

4.2 Trade Studies

In Figure 4.4 A, applicable only for configurations of N > 1, the span for PA and MA is varied at a fixed wing chord of 7 in. for both aircraft. Higher scores were achieved for chords smaller than 7 in., but the chord was limited for practical considerations of structure and airfoil performance due to low Reynolds numbers for speeds above stall. The lower wing span limit was set by the minimum wing area necessary to make the takeoff field length for a given propulsion system. The discontinuities in the figure depict the increase in battery weight while holding the cell count constant.

For a single component PA configuration, Figure 4.4 B, the MA wing is driven by the PA aircraft. The MA span and chord must always be larger than the PA aircraft to house internally. In addition, the modularity of the MA increases its weight; thus, the MA aircraft becomes less optimal. However, the single component PA offers a more favorable PA/MA combination than an optimized two component PA.

Even with conservative estimates, the single component combination has a decrease in RAC by approximately 10%. Therefore, it is evident to pursue the modular MA, single component PA.

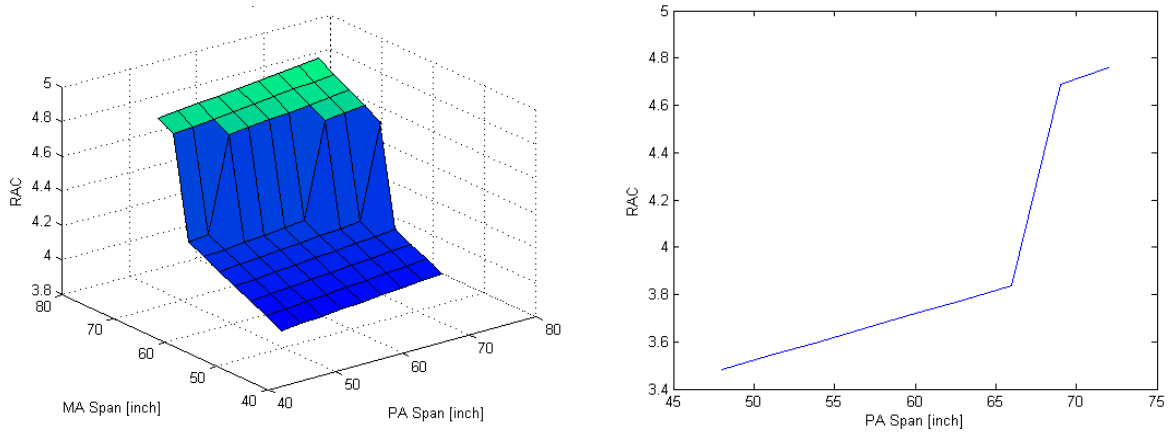

Figure 4: 5 (Left) Span vs. RAC. (Right) PA Span vs. RAC for One Component

4.3 Design and Sizing Trades

4.3.1 Aerodynamic Trade-Offs Selection

Chord

To minimize induced drag (D_i) and thereby reduce power requirements, wingspan should be maximized according to the induced drag equation, where b is the wingspan, q is dynamic pressure, and e is aerodynamic efficiency:

$$D_i = (L/b)^2/(\pi*q*e)$$

In theory, for a given lift and wing area, the chord should be minimized. However, wing chord is limited by both Reynolds number and structural constraints. Aerodynamic performance degrades for most airfoils at low Reynolds numbers. Therefore, the PA chord was fixed at 7 in. to maintain a Reynolds number of 150,000 for a cruise speed of 45 ft/s. Since the MA wing is used to internally house the PA wing, the MA chord is dependent on airfoil geometry.

Wing Airfoil

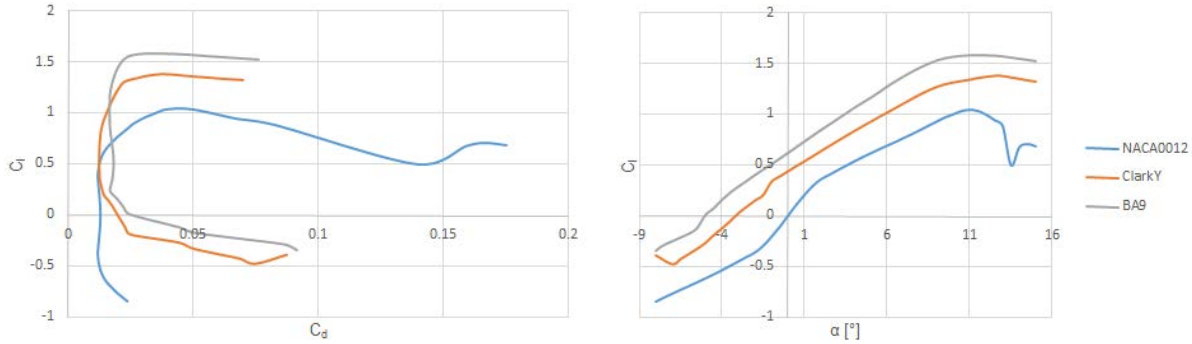

Figure 4: 6 (Left) Cl vs Cd for Various Airfoils (Right) Cl vs Angle of Attack for Various Airfoils

To reduce climb and cruise power, flying at low speeds for both the Production and Manufacturing Support Aircraft is desired. This design point focuses the search on airfoils having high desirable characteristics at low Reynolds numbers. The desired characteristics include high maximum lift coefficient for takeoff and given wing design, and max average thickness for wing structure. The airfoils are shown in Figure 4.6, using NACA 0012 as a baseline, and their polars are shown in Figure 4.5.

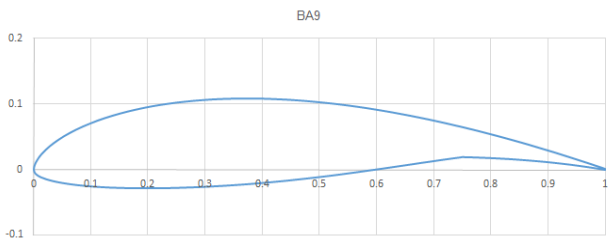

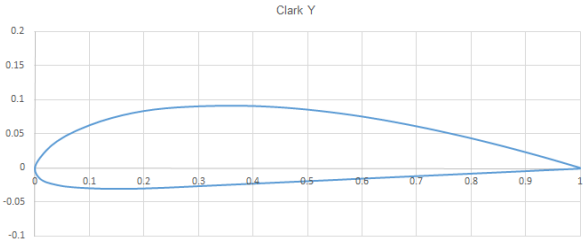

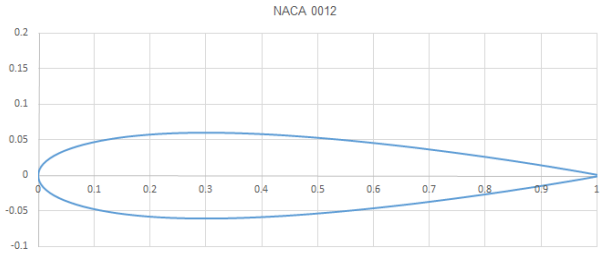

	BA9	Clark Y	NACA 0012
max Cl	1.35	1.17	0.89
Max t/c	13.3	11.7	12
Cd @ Cl = 0.69	0.0171	0.0127	0.0167

Figure 4: 7 Airfoil Profiles and Characteristics

Shorter chords benefit from higher lift coefficients and thickness. Therefore, the BA9 was chosen because of the 0.18-0.46 max lift coefficient increase when compared to the Clark Y and NACA0012 airfoils and the 1-2% thickness of the BA9 allows for a higher strength-to-weight ratio, allowing the wing to handle higher loads.

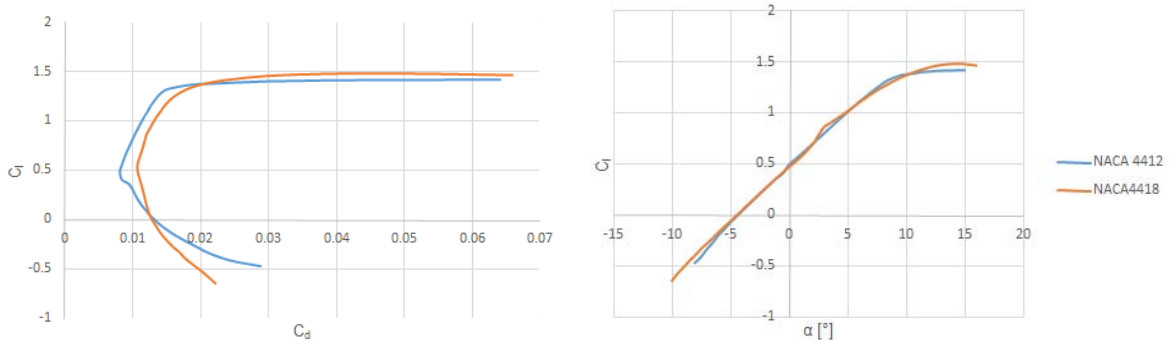

Figure 4: 8 Airfoil Polars

After deciding on the PA airfoil, the MA airfoil was selected based on similar characteristics at low Reynolds numbers along with the geometry to house the PA wing and clearance for aileron control horns. Two NACA 44xx series were chosen because of the high max lift coefficients indicated by Xfoil data shown in Figure 4.7 and high camber to accommodate a BA9 section as illustrated in Figure 4.8. The NACA 4418 has a higher sectional drag coefficient than the NACA 4412, but the geometry is more favorable for loading the PA wing within the MA wing. Therefore, the NACA 4418 was chosen, although

the sectional drag coefficient is slightly greater as shown in the polar, the induced drag is less than the NACA 4412, due to the added thickness to accommodate the PA wing in a shorter chord.

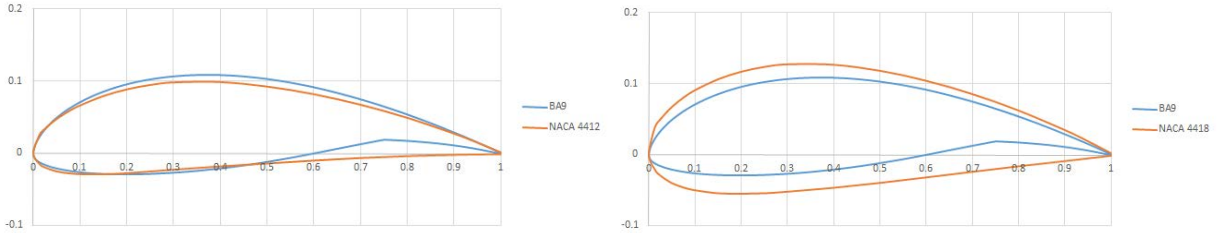

Figure 4: 9 Airfoil Profiles

Tail Airfoil

For the empennage of the PA, two commonly used airfoils were considered: SD8020 and NACA0012. The NACA0012 was chosen because the thinner SD8020 has a maximum thickness of 10.1%. Therefore, it could structurally impact the tail. The MA uses NACA0015, the same airfoil with a larger thickness to permit tolerance between the tails.

4.3.2 Propulsion System Trade-Offs

Motor

Table 4: 2 Motor Selection

Motor	kV (RPM/V)	Weight with Gearbox	Maximum Voltage (V)	Maximum Power (W)	Specific Maximum Power (W/oz)
Neu 1110-3Y	1512	6.6	36	1000	172
Neu 1105-2.5Y	3800	5	15	400	81
Neu 1107-6D	1900	5.6	28.5	600	107
Neu 1107-3Y	2050	6.7	27	600	120
Turnigy G10 810	810	5.4	15	375	69
Turnigy G10 1100	1100	5.4	11	355	66

Several motor and gearbox combinations were compared to find the optimal propulsion system. Initially, low kV motors were considered to operate efficiently with larger diameter propellers at low speeds. However, since foldable propellers are not allowed for the PA, a smaller propeller for that aircraft is favored during loading in Mission 2. Although, a compromise must be made since as propeller diameter decreases, the power required to produce the same thrust increases. In addition, the RPM required to produce the same thrust increases for the same battery weight system. Therefore, a higher kV motor must be used. From Table 4.2, the Neu 1107-3Y, 1107-6D, and 1110-3Y cannot be used for any combination of gearbox. Therefore, the Neu 1105-2.5Y with a 4.4:1 gearbox is chosen for the PA over the Turnigy motors because it has a greater specific power. The MA has a larger ground clearance than the PA, so it is able to operate with larger diameters to generate the necessary dynamic thrust. Therefore, the Neu 1105-2.5Y with a 6.7:1 gearbox is chosen because the excess specific power in the Neu 1110 and 1107 is not needed for flight conditions. The Turnigy G10's has a weight disadvantage.

Battery Selection

Table 4: 3 Battery Selection

Battery	Capacity (mAh)	Resistance (ohms)	Weight (oz.)	Energy Density (kJ/oz.)
Elite 1500	1500	0.009	0.81	1852
Elite 2000	2000	0.009	1.06	1724
KAN 650	650	0.014	0.49	1327
KAN 500	500	0.019	0.6	833

A selection of battery cells outlined in Table 4.3 were analyzed for M2 and M3 to determine which could provide the power necessary for climb and endurance for cruise. M1 will use the same battery system as M2; therefore, M1 is not considered for the battery selection. Initially, a number of cells is chosen for an estimated flight time to calculate the current and energy for the propulsion system. The amount of energy dictates the necessary capacitance of the cell. The process is repeated to find the minimized battery weight. As a result, the Elite 1500 were used because the required KAN battery system would outweigh the Elite battery system. The capacitance of the Elite 2000 was excessive, so it was not chosen. During the motor selection, the battery cell count was taken into consideration to evaluate the motor necessary for propeller performance.

4.3.3 Final Optimized Aircraft

Manufacturing Aircraft				
Wing Airfoil	*Tail Airfoil*	*Motor & Gearbox*	*Battery*	*Number of Payloads*
NACA 4418	NACA 0015	Neu 1105 6.7:1	12 Cell Elite 1500	1

Table 4: 4 Optimized Aircraft Selections

Production Aircraft			
Wing Airfoil	*Tail Airfoil*	*Motor & Gearbox*	*Battery*
BA-9	NACA 0012	Neu 1105 4.4:1	8 Cells Elite 1500

The final aircraft configurations are shown in Table 4.4. They represent the combination of features which maximize the total score: high lift, thick airfoils, and a propulsion system.

4.4 Lift, Drag, and Stability Characteristics

The L/D and drag polar for the aircraft are shown with in-flight C_L for each mission in Figure 4.9 and 4.10. Mission 2 flies with a payload, so it has a higher C_L and C_D than Mission 1.

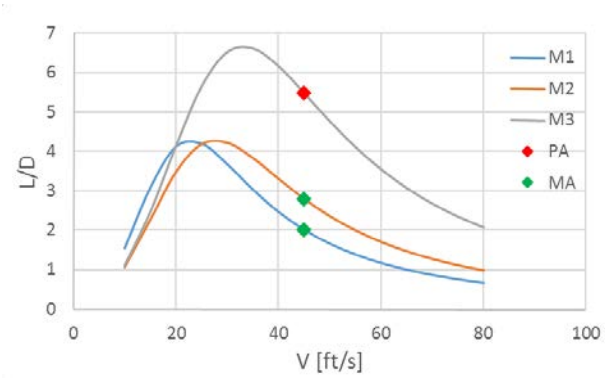

Figure 4: 10 Airplane Drag Polar

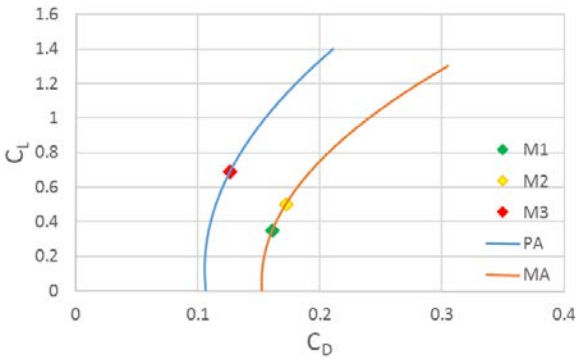

Figure 4: 11 Airplane L/D vs Velocity

The drag buildup for each mission is shown in Figure 4.11. Fuselage drag has the highest contribution for Mission 1 and 2 with wing and induced drag being the second highest respectively. Mission 3 has induced, landing gear, and wing drag as the largest contributors.

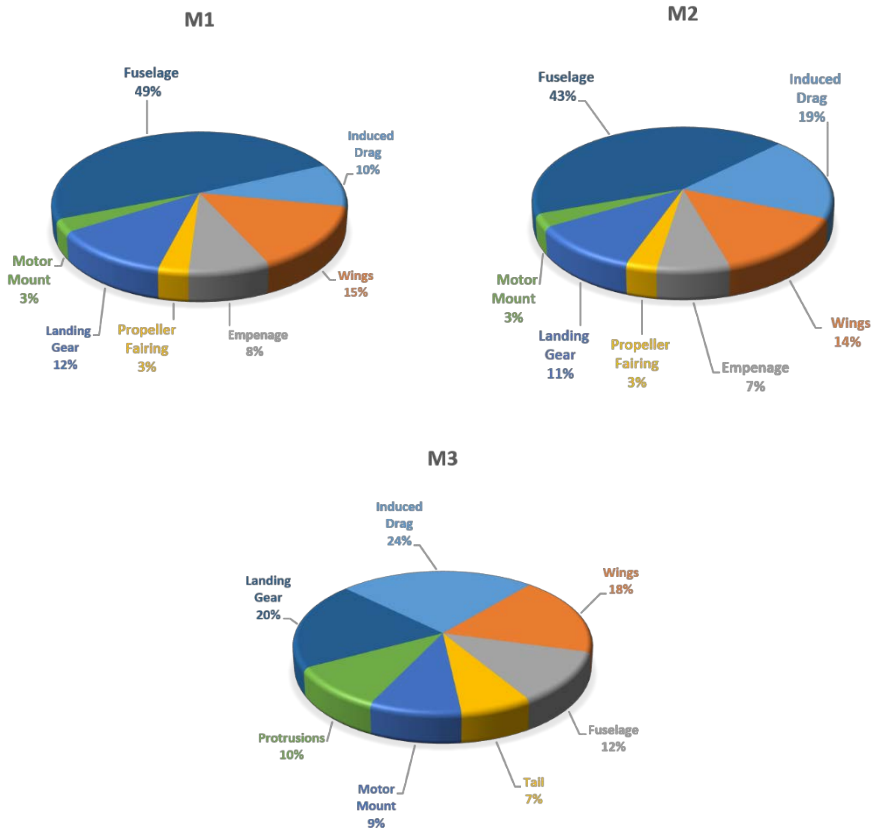

Figure 4: 12 Drag Buildup for missions 1,2,3

4.4.1 Stability and Control

Athena Vortex Lattice (AVL) is used as preliminary analysis tool to evaluate the span loads for preliminary structural sizing, neutral point for CG location, preliminary estimations for stability and control

of the aircraft, as well as assistance V-tail size and angle optimization. In one scenario, AVL was used to evaluate the possible lack of control in a heavy cross-wind landing. The aircraft was put in a large sideslip, then trimmed using the rudder while forcing the plane to CL_{max} at approach speed. This was a possible scenario that may be encountered due to the windy conditions at the Cessna Field. Both aircraft were deemed to have necessary control authority to trim for the sideslip and flare for landing.

A Trefftz plot, shown in Figure (4.13), was created with the geometry input in Figure (4.14). This plot verified the peak CL occurred within 50% of the semi-span and that any section, specifically the wingtips, CL's did not exceed CL max.

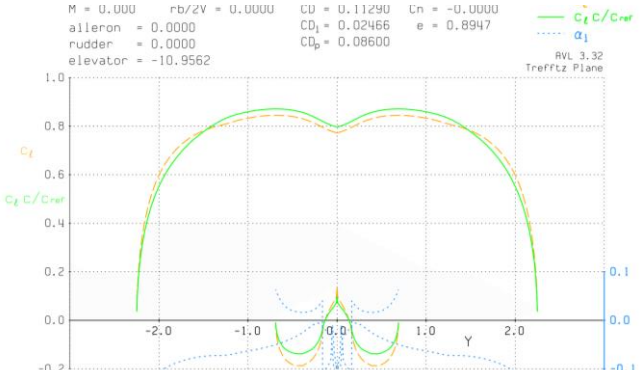

Figure 4: 13 PA Trefettz Plot

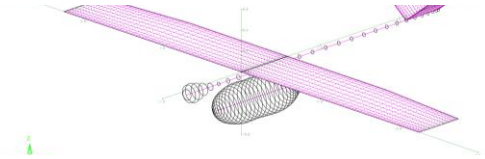

Figure 4: 14 PA AVL Geometry Input

Using preliminary weights and drag build-up, the simulation was conducted, providing an estimate for C_{Dp} the mass properties, and inertia of the aircraft.

AVL takes the input geometry and uses an extended vortex lattice method to calculate the aerodynamic performance as well as the stability and control derivatives for the MA. Figure (4.15) shows the resulting pole-zero map of the eigenvalues calculated by the program.

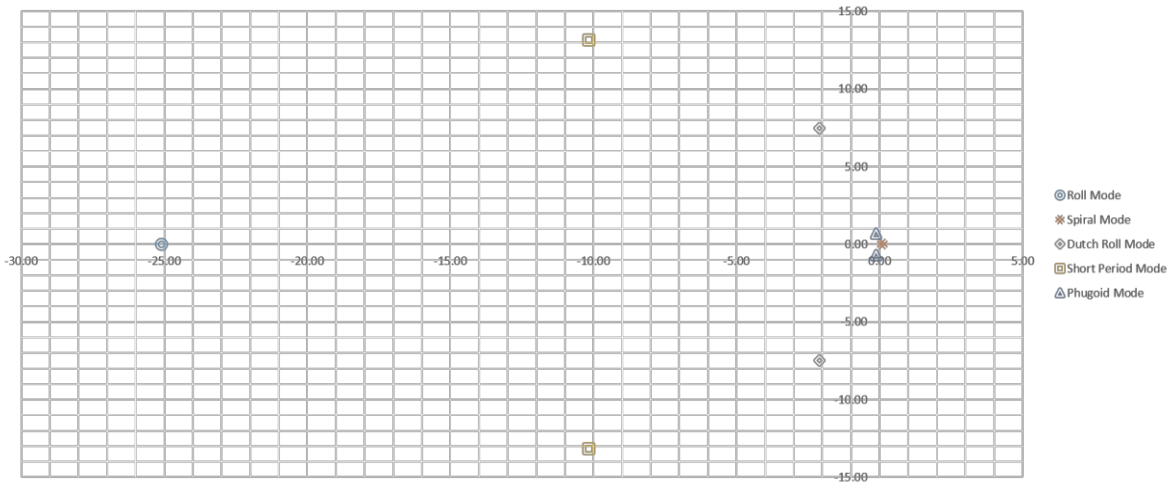

Figure 4: 15 PA Pole-Zero Diagram

All modes achieve level one criteria for a class I plane per MIL-F-8785C [1] with two exceptions. The spiral mode was unstable with a slight divergence; however, it satisfies level two handling qualities with a time-to-double of 8 seconds. In addition, the Control Anticipation Parameter satisfies the level two handling qualities criteria, having an η/α of 4.27 G's/rad with a short period natural frequency of 13.16 rad/sec. As discussed by Cook [2], level two handling qualities are stated as, 'Flying qualities adequate to accomplish the mission flight phase, but with an increase in pilot workload,' thus not requiring augmentation for mission performance. Upon conducting further research, it was found that the recommendations in MIL-SPEC 8785C are applicable to small-scale Unmanned Aerial Vehicles (UAVs) [3].

A Trefftz plane, shown in Figure (4.16), was created with the geometry input in Figure (4.17). This plot verified that the peak C_L occurred within 50% of the semi-span and that at any section, specifically the wingtips, C_L's did not exceed $C_{L\ max}$.

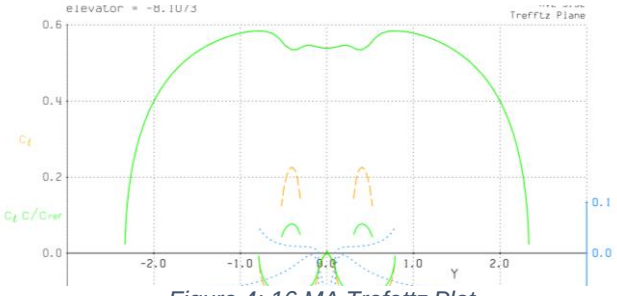

Figure 4: 16 MA Trefettz Plot

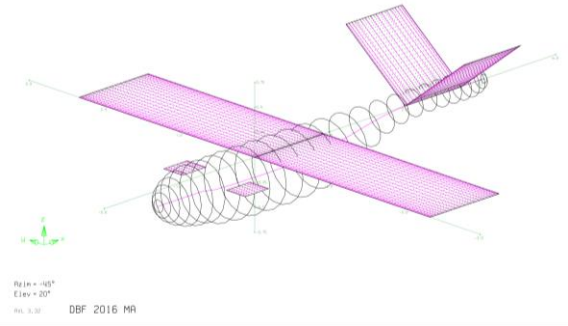

Figure 4: 17 MA AVL Geometry Input

Using preliminary weights and drag build-up, the simulation was conducted, providing an estimate for C_{Dp} the mass properties, and inertia of the aircraft.

AVL takes the input geometry and uses an extended vortex lattice method to calculate the aerodynamic performance as well as the stability and control derivatives for the MA. Figure (4.18) shows the resulting pole-zero map of the eigenvalues calculated by the program.

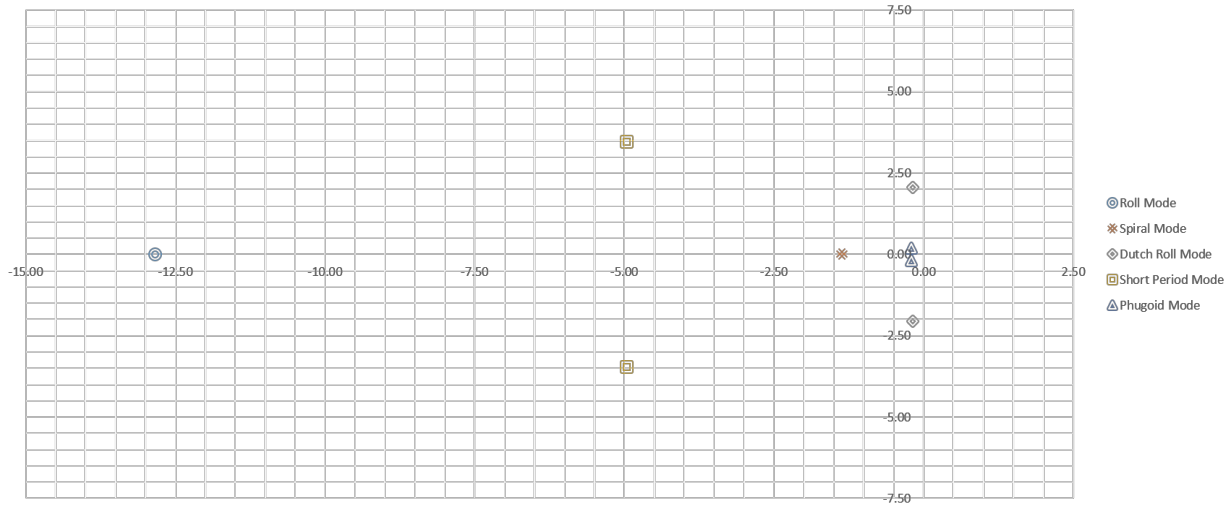

Figure 4: 18 MA, Pole-Zero Diagram

All modes achieve level one criteria for a class I plane per MIL-F-8785C [1] with two exceptions. The Dutch roll damping and Dutch roll frequency multiplied by damping were both level two with values of 0.0912 and 0.187 rad/sec, respectively. The possible deficiency in Dutch roll damping was predicted before the initial flight of the MA. During flight, there was oscillation on the roll axis, confirming the the predictions from AVL. However, the Dutch roll mode did not increase pilot workload to a hazardous level; thus, it was deemed unnecessary to improve the Dutch roll damping.

4.5 Predicted Mission Performance

Table 4: 5 Mission 1 Predictions

Mission 1			
Flight Conditions			
Cruise Airspeed (ft/s)	45		
Wind Speed (ft/s)	22		
Climb Rate (ft/min)	300		
Turn Load Factor (g)	2		
Flight Segment	*Time (s)*	*Power (W)*	*Energy (J)*
Take Off	4.5	248	1116
Climb	10	241	2410
180° Turn	2.5	277	693
500' Down Wind	7.5	218	1635
360° Turn	5.1	277	1413
500' Down Wind	7.5	218	1635
180° Turn	2.5	277	693
1000' Up Wind	43.5	218	9483
2 More Laps	137.2	N/A	31101
Total/Max/Total	220.3	277	50178
Max Available	300	325	77760
Margin	27%	15%	35%

Table 4: 6 Mission 2 Predictions

Mission 2			
Flight Conditions			
Cruise Airspeed (ft/s)	45		
Wind Speed (ft/s)	22		
Climb Rate (ft/min)	300		
Turn Load Factor (g)	1.5		
Flight Segment	*Time (s)*	*Power (W)*	*Energy (J)*
Take Off	5.8	302	1752
Climb	10	272	2720
180° Turn	3.9	292	1139
500' Down Wind	7.5	239	1793
360° Turn	7.9	292	2307
500' Down Wind	7.5	239	1793
180° Turn	3.9	292	1139
1000' Up Wind	43.5	239	10397
Landing	36.5	206	7519
Taxi	120	75	9000
Total/Max/Total	246.5	302	39557
Max Available	600	325	77760
Margin	59%	7%	49%

Table 4: 7 Mission 3 Predictions

Mission 3			
Flight Conditions			
Cruise Airspeed (ft/s)	45		
Wind Speed (ft/s)	22		
Climb Rate (ft/min)	300		
Turn Load Factor (g)	1.5		
Flight Segment	*Time (s)*	*Power (W)*	*Energy (J)*
Take Off	6.1	244	1488
Climb	10	238	2380
180° Turn	2.5	209	523
500' Down Wind	7.5	112	840
360° Turn	5.1	209	1066
500' Down Wind	7.5	112	840
180° Turn	2.5	209	523
1000' Up Wind	43.5	112	4872
2 More Laps	137.2	N/A	17326
Total/Max/Total	221.9	244	29857
Max Available	300	271	64800
Margin	26%	10%	54%

5.0 Detail Design

Once aircraft dimensions were finalized, the PA was manufactured to confirm the mission profile predictions. Since the MA dimensions are driven by the PA dimensions, confirmation for the MA mission predictions followed closely after the PA.

5.1 Design Parameters

Table 5: 1 Dimensional Parameters

5.1: Design Parameters					
Wing			***Motor***		
	PA	*MA*		*PA*	*MA*
Span (in)	54	56	Brand / Model	Neu 1105	Neu 1105
Chord (MAC)	6.9	11	Gear Box	Maxon (4.4:1)	P29 (6.7:1)
Aspect Ratio	7.9	5.1	Effective Kv	864 RPM/V	567 RPM/V
Wing Area (sq in)	366	616	Max RPM	13,600 RPM	8950 RPM
Airfoil	BA9	NACA 4418	No Load Current (A)	0.7	0.7
Static Margin	12%	15%	Winding Resistance (mΩ)	28	28
Aileron			Peak Power Output (W)	400	400
	PA	*MA*	Propeller(s)	APC 12x6E	APC 13x8E, 14x7E
Span (in)	14	30	***Propulsion Batteries***		
Chord (% of wing)	25%	16%		*PA*	*MA*
Deflection	±30°	±30°	Cell Type	Elite 1500 NiMH	Elite 1500 NiMH
Fuselage			Cell Capacity	1500 mAh	1500 mAh
	PA	*MA*	Number of Cells	8	12
Length (in)	12	52	Nominal Voltage (V)	12	14.4
Width (in)	4	7.5	Max Current (A)	30	30
Height (in)	4	8.5	Pack Energy (kJ)	64.8	77.7
V-Tail			Internal Resistance (mΩ)	144	160
	PA	*MA*	Max Power (W)	271	325
Airfoil	NACA 0012	NACA 0015	***Flight Control System***		
Chord (in)	5	9		*PA*	*MA*
Span (in)	10	12	Speed Controller	DYS 30Amp Mini Opto	DYS 30Amp Mini Opto
Area (sq in)	50	108	Radio Reciever	Futaba R6008HS	Futaba R6008HS
V-Tail Control Surfaces			Number of Servos	4	5
	PA	*MA*	Servo Type(s)	Dymond D47	HS-65 MG, Dymond D47
Span (in)	10	10.5			
Deflection	±30°	±30°			
Chord	25%	20%			

5.2 Structural Characteristics and Capabilities

The PA is designed so the impact energy from landing is quickly transferred through the landing gear and absorbed by the foam fuselage interior. The landing gear's position minimizes the moment applied upon the root of the landing gear. The entire weight of the PA plane is supported by the boom.

The MA plane is characterized by its large size and high wing inertia compared to a conventional RC aircraft of similar size. The shell of the MA is structurally weak, so the design utilizes the boom as the main load bearing component. The wings of the PA fit inside the wings of the MA, providing structural strength as well as packaging. The landing gear of the MA plane transfers the impact energy directly to the boom.

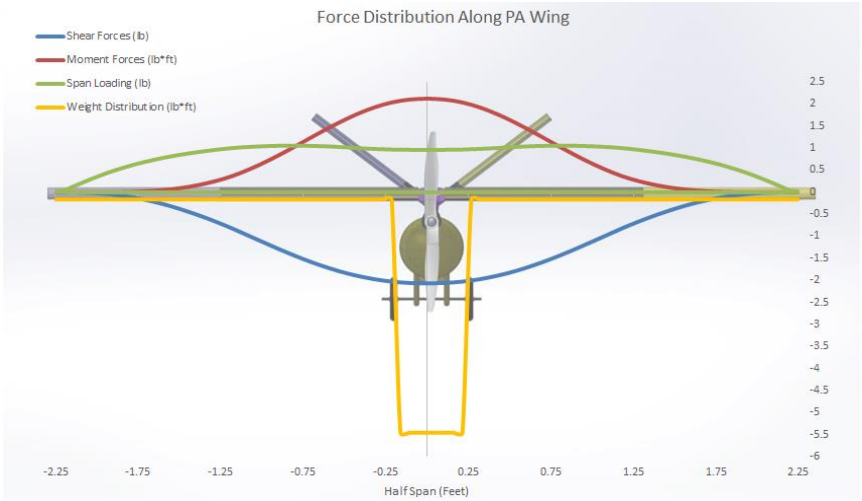

Figure 5: 1 Shear Moment Diagram for PA

In Figure 5.1, the diagram exhibits the force distribution along the PA wing while cruising. This diagram is indicative of the elliptical load distribution found on the wings; therefore, the structure of the wing changes significantly. The concentration of forces is primarily located within the central 30 inches of the PA, requiring more structurally rigid supports. As such, the central 30 inches of the wing spar includes carbon fiber tape to handle the increased amount of force. The last 7 inches of each wingtip encounters minimal amounts of force, allowing some material in the structure to be taken out. This led to the decision to use hollow webs in the tips to reduce weight, while keeping solid webs in the center, where the structure requires more strength.

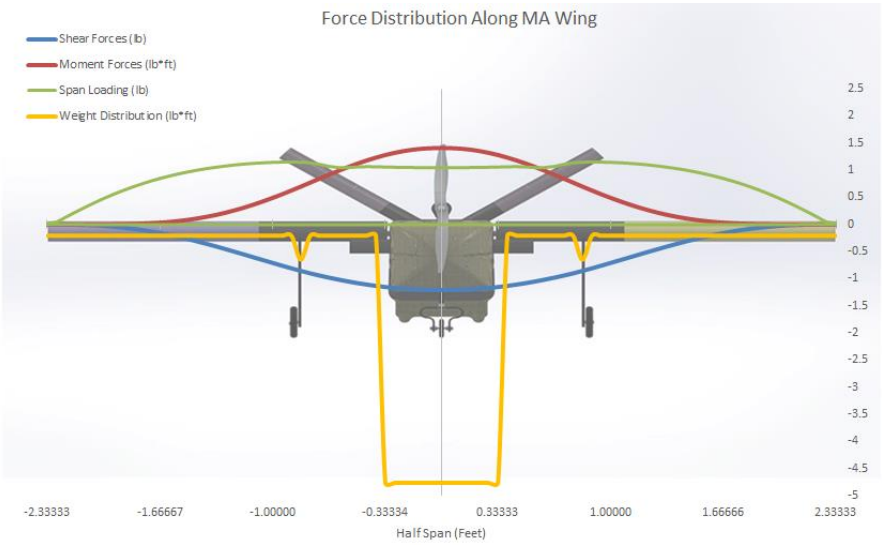

Figure 5: 2 Shear Moment Diagram for Manufacturing Aircraft

In Figure 5.2, the diagram exhibits the force distribution the MA wing experiences while cruising. The MA has a similar elliptical load distribution found on the PA. However, due to the fuselage design, the MA utilizes carbon fiber rod slots to hold the detachable wings. The carbon fiber rods run 1.5 feet out of the fuselage and absorb the majority of the landing gear impact. Similar to the PA, solid webs are used in the spar box structure in the center to handle the increased torsional loads, and hollow webs on the outer

section of the wings. Additionally, because the MA wings are required to be hollow, the wing spar could not be set at quarter chord. As a result, the MA wing uses two wing spars instead of one, providing the equivalent rigidity of a single spar.

5.3 System Design and Component Selection/Integration

The following subsystem components were analyzed with more detail to finalize the aircraft design.

5.3.1 Wings

- Balsa Structured Wings

The balsa built-up wing consists of balsa ribs, spar(s), sheeting, and skin. The ribs take bending and compression loads from the wing and some of the torsional load from the skin, while the shear webs in the spar take the shear load. The balsa spar caps are thicker on the top to withstand compressive loads experienced in flight. Composite materials are integrated into the spars to increase the bending and torsional rigidity. The wing is sheeted with balsa on the top and bottom to cover the pressure recovery region which is about 35% chord length from the leading edge. Balsa sheeting provides torsional strength and maintains the airfoil shape. Microlite™ is used to cover the wings and tails to provide additional rigidity and reduce surface roughness.

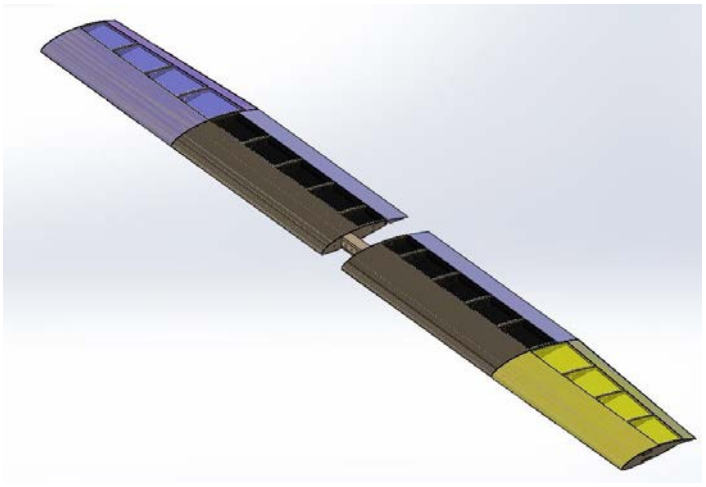

Figure 5: 3 Tapered Wing

- Production Aircraft Wings

The tapered PA wing is designed to decrease the wing area while maximizing span, thus increasing the aspect ratio and decreasing the weight. The maximum takeoff weight of the PA is 4.25 lb (1G) and the wings are designed to withstand a load factor of 2.5G in bending and a minimum safety factor of 1.25G. The ribs include lightening holes to lighten the wings while preserving structural integrity.

- Manufacturing Support Aircraft Wings

The maximum takeoff weight of the MA is 4.875 lb (1G), for Mission 2. The wings are designed to withstand a load factor of 3.5G in bending and a minimum safety factor of 1.25G. The purpose of the MA wings is to house the PA wings for Mission 2. Therefore, the balsa ribs are hollowed out slightly larger

than the PA wings so that the MA wings can slide over the PA wings. The carbon fiber tubes connect the wings to the fuselage by sliding over slightly smaller tubes and are secured to the boom. Balsa sheeting covers the pressure recovery region throughout the wings, however, towards the root the balsa sheet covers the airfoil completely to increase torsional rigidity.

5.3.2 Empennage

The V-tail empennage was selected for both aircraft for packaging reasons. The balsa structured empennage consists of balsa ribs, stringers, carbon rod spars, and Microlite™. Balsa stringers are embedded around the balsa ribs to maintain the airfoil shape and take bending and torsional loads. Additionally, the front and rear carbon rod spars are used to strengthen the tails in bending and torsion.

The PA tails are designed as V-tails to be covered by the MA V-tails for Mission 2. The PA V-tails are attached to the carbon fiber boom using carbon fiber rods that slide to a desired angle of 38 degrees. This angle is calculated using guidelines in Mechanics of Flight [4]. The balsa ribs have truss structure cutouts to reduce weight while preserving structural integrity. The MA tails are designed to slide over the PA tails and attach to the MA fuselage. The balsa ribs are hollowed slightly larger than the PA tails to house them.

5.3.3 Control Surfaces

The control surfaces are designed to be approximately 25% chord length for stable maneuvering. To maintain the airfoil shape and the aerodynamic properties of the airfoil, they must be manufactured as close to the airfoil shape as possible. A foam-fiberglass composite is chosen over a balsa structure because it is similar in weight, provides more torsional stiffness, and can be consistently manufactured.

5.3.4 Motor Mount

The motor mount is designed to endure the torque and thrust emitted from the motor. The carbon fibers are oriented so that their resistance to torque is maximized. The mount is designed to dampen vibrations by encompassing the motor. The motor mount is secured to the fuselage boom in front of the aircraft, and the motor attaches to the faceplate. This design is used on both the PA and MA.

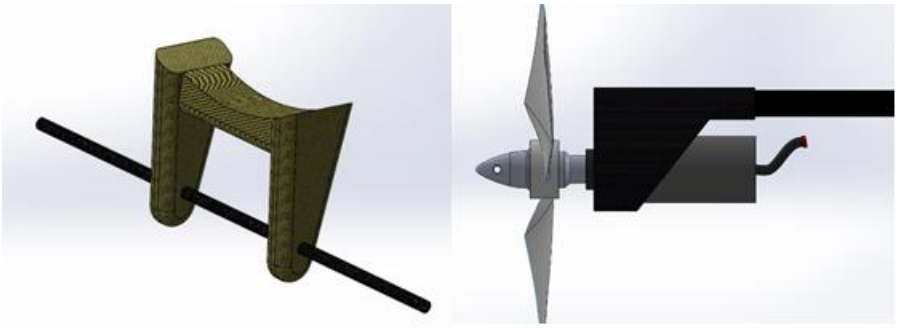

Figure 5: 4 (Left) Landing Gear, (Right) Motor Mount

5.3.5 Landing Gear

- Production Aircraft Landing Gear

  A landing gear integrated with the fuselage was chosen for the PA so that the fuselage can elastically deform to absorb some of the forces of landing. The structure was made as lightweight and compact as possible while maintaining rigidity for landing impact. A continuous axle was used for extra support and rigidity in case of possible crosswind landing impacts.

- Manufacturing Support Aircraft Landing Gear

  A tricycle landing gear setup was chosen for the MA to ensure good handling in taxiing maneuvers. Two options were considered for the main gear: two V-shaped rigid struts anchored to the wing spars and an inverted U-shape designed to hug the fuselage. While the inverted U-shape is shock-absorbing and allows for some flexibility, the placement with respect to CG on the aircraft was not ideal. A V-shape configuration anchored onto the wing spars was selected since the wing spars are reinforced loading members.

5.3.6 Fuselage/Payload

- Production Aircraft Fuselage:

  The PA fuselage was designed to have a quick loading and unloading of the payload while securing the payload tightly. The design constraints led to the creation of a tube in which the payload sits between foam inserts to securely fasten in-place. Fairings are used to close out the fuselage and make the payload fully internal.

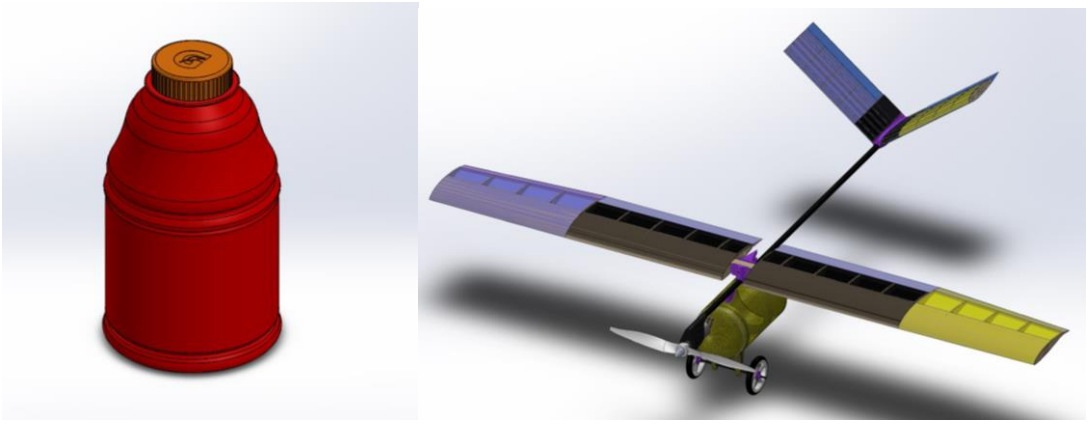

Figure 5: 5 (Left) Gatorade Payload (Right) MA Mission 2 Payload

- Manufacturing Support Fuselage:

  The MA fuselage is a semi-monocoque design that minimizes material and the wetted area required to hold the PA. Additionally, prop fairings and landing gear fairings were added to contain the PA. The front and back of the fuselage are also closed out with fairings. The bottom portion of the MA fuselage is designed to be removable to facilitate loading the Mission 2 payload.

5.3.7 Structural Spine

The central carbon fiber boom on the PA and MA is the main structural member connecting the entire aircraft. The motor, battery, wings, fuselage, and empennages are all connected to this boom.

5.3.8 Receiver Selection

A Futaba R6008HS 8-channel was selected for both aircrafts because they are lightweight and offered the fail-safe feature required for the competition.

5.3.9 Servo Selection

There were two criteria when choosing a servo: the servo must have the torque required for control surface deflection and be light enough to not significantly increase the RAC. Three servos were found that could be potential candidates for application:

Table 5: 2 List of Servo Considered

Servo Selection			
Servo	**Stall Torque 4.8v (in-oz)**	**Speed 4.8v (sec/60°)**	**Weight (oz)**
Requirement	> 8.8	< 0.15	lowest
HS - 55	15	0.17	0.28
Dymond D47	20	0.14	0.17
HS - 65 MG	25	0.14	0.44

By analyzing the hinge moments from each surface using AVL, the Dymond D47, HS - 65MG servos were selected for both aircrafts because of its weight and its ability to meet the torque requirements.

5.3.10 Speed Controller Selection

Table 5: 3 List of Speed Controllers Considered

Speed Controller Selection			
ESC	**Max Current (A)**	**Max Voltage (V)**	**Weight (oz)**
Requirement	> 27	> 18	lowest
Flycolor Raptor Mini 30A	30	16.8	0.3
DYS 30Amp Mini Opto	30	22.2	0.51
Phoenix HV 30	30	50	1.13

The competition regulations do not limit the motor current. For the given continuous 15V limit of the 1105 motor, amps in the range of 15-20A must be drawn from the battery pack. ESCs rated above 20A must be used. The Phoenix HV 30 is used for both aircraft because of its 30A rating and low resistance.

5.4 Weight and Balance

Manufacturing Support Aircraft weight was estimated to be 3.35 lb with maximum empty weight of 4.8lb. The Production Aircraft weight was estimated to be 2 lb with a maximum empty weight of 4.25lb. All measurements were taken from the front of the propeller. Components were placed so the CG would fall

between 25-28% of the aircraft length to ensure stability. Table 5.4 to 5.7 tabulates the aircraft weight at each mission.

Table 5: 4 Mission 1 Weight and Balance

Empty							
		Manufacturing Aircraft			Production Aircraft		
	Component	Arm (in)	Weight (oz)	Moment (oz-in)	Arm (in)	Weight (oz)	Moment (oz-in)
Structure	Boom	27	2.06	55.62	20	1.54	30.8
	Motor Mount	2	0.22	0.44	3	0.22	0.66
	V-Tail Stabilizer	47	2	94	35.2	1	35.2
	Fuselage	20	6	120	11.5	1.6	18.4
	Wing	20	9.6	192	10	5.5	55
Propulsion	Speed Controller	4	2	8	5	2	10
	Battery	8	10	80	7.5	8	60
	Motor/Gearbox/Metal Propeller Spinner	3	6.64	19.92	3	6.64	19.92
	Propeller	1	1.22	1.22	1	1.22	1.22
Avionics	Reciever Battery	9.5	1.2	11.4	15	1.2	18
	Reciever	25	1	25	15	1	15
	Reciever Switch	25	0.1	2.5	15.5	0.1	1.55
	V- Tail Servo	46	0.5	23	36	0.5	18
	Ailerons Servo	21	0.4	8.4	12	0.5	6
	Nose Gear Servo	15	0.3	4.5	–	–	–
Landing Gear	Main Gear	20	3	60	10	0.4	4
	Wheels	20	0.5	10	10	0.5	5
Miscellaneous	3D printed Payload Mounts	15	1.9	28.5	–	–	–
	Battery Holders	7	2	14	–	–	–
	Empenage Mounts	45	0.2	9	–	–	–
	Propeller Fairings	10	0.8	8	–	–	–
	Wing Mounts	20	2	40	–	–	–
Total	Aircraft	–	53.64	815.5	–	31.92	298.75
	Center of Gravity (in)	15.20			9.36		
	Center of Gravity (% chord)	27.65			27.45		

Table 5: 5 Mission 1 Weight and Balance

Mission 1				
	Component	Arm (in)	Weight (oz)	Moment (oz-in)
Aircraft	Aircraft Without Battery	--	43.64	735.5
	Battery	8	10	80
Payload	Empty	0	0	0
	Payload Restraints	0	0	0
Total	Aircraft	--	53.64	815.5
	Center of Gravity (in)	15.20		
	Center of Gravity (% chord)	27.65		

Table 5: 6 Mission 2 Weight and Balance

Mission 2				
	Component	**Arm (in)**	**Weight (oz)**	**Moment (oz-in)**
Aircraft	Aircraft Without Battery	--	43.64	735.5
	Battery	7	10	70
Payload	PA Subassemblies	15	24	360
	Payload Restraints	15	0.2	3
Total	Aircraft	--	77.84	1168.5
	Center of Gravity (in)	15.01		
	Center of Gravity (% chord)	26.72		

Table 5: 7 Mission 3 Weight and Balance

Mission 3				
	Component	**Arm (in)**	**Weight (oz)**	**Moment (oz-in)**
Aircraft	Aircraft Without Battery	--	23.92	238.75
	Battery	7.5	8	60
Payload	32 oz. Gatorade Bottle	9	35.2	316.8
	Payload Restraints	0	0	0
Total	Aircraft	--	67.12	615.55
	Center of Gravity (in)	9.17		
	Center of Gravity (% chord)	25.96		

5.5 Flight Performance Parameters

Table 5.8 details the flight performance parameters for the three flight missions that were predicted by the mission model. These predictions were later compared to actual parameters obtained through test flights.

	CL max	**e**	**L/D max**	**Available Energy (kJ)**	**Empty Weight (lbs)**
Production Aircraft	1.3	0.75	6.3	77.7	2.03
Manufacturing Aircraft	1.15	0.7	4.1	64.8	3.37

	M1	M2	M3
Cruise CL	0.32	0.46	0.77
CDp	0.126	0.126	0.085
Cruise L/D	2.5	3.2	5.9
Wing Loading (lbs/sq-ft)	0.79	1.14	1.65
Power Loading (W/lbs)	96	67	64
Cruise Speed (ft/s)	45	45	45
Stall Speed (ft/s)	24	29	33
Max Level Speed (ft/s)	53	52	68
Max Climb Rate (ft/min)	560	312	660
Takeoff Distance (ft)	26	57	69
Turn Load Factor (g)	2	1.5	2
Turn Rate (deg/s)	71	46	71
Mission Time (s)	220	247	222
Energy Required (kJ)	50.2	39.6	29.9
TOGW (lbs)	3.38	4.88	4.25
Cruise Current (amps)	18.2	19.9	11.2

Assumptions	
Density (2000ft msl) (slugs/cu-ft)	0.002241
Wind (ft/s)	22

Table 5: 8 Flight Performance Parameters

5.6 Predicted Mission Performance

Aircraft parameters and mission outcomes from the mission model were used to predict the estimated final competition score.

Table 5: 9 Predicted Mission Performance

Mission 1		Mission 2		Mission 3		Bonus Ground Mission	
Laps Flown	3	Laps Flown	1	Laps Flown	3	Loading Time (s)	120
Estimated Time (s)	220	Estimated Time (s)	247	Estimated Time (s)	222		
Empty Weight (lb)	2.72	Empty Weight (lb)	2.72	Empty Weight (lb)	1.5		
Battery Weight (lb)	0.6375	Number of Components	1	Battery Weight (lb)	0.525		
		Battery Weight (lb)	0.6375				
		RAC	**2.52**	**Total Flight Score**	**18**		

- *Flight Mission 1: Manufacturing Support Aircraft Arrival Flight*

The MA completes Mission 1 empty, focusing on flying three laps within five minutes with a take-off runway of 100 feet. The maximum score is based on completion of the mission. Therefore, the entire mission requires a battery that is sized for take-off and climb. The MA must also fly to close stall speed during cruise, and still be able to complete the mission.

- *Flight Mission 2: Manufacturing Support Aircraft Delivery Flight*

The objective of Mission 2 is to individually fly each sub-assembly of the PA inside the MA and then taxi to the designated payload change area. For maximum score, this must all be completed within a ten-minute window. In this design, there is only one sub-assembly that needs to be flown and taxied back to

the designated payload area. The battery is sized to take off with one sub-assembly payload, but is small enough to be able to cruise near stall speed. This is done to achieve a higher RAC and take advantage of the ten-minute window.

- *Flight Mission 3: Production Aircraft Flight*

The objective of Mission 3 is to fly the PA with the 32 oz. Gatorade bottle within a five-minute window. The battery must be sized large enough to take off within 100 feet, but not so large that it will surpass the minimum power required to fly for three laps during the five-minute allotted time.

- *Bonus Mission: Ground Mission*

The Bonus Mission allows only two minutes for the Production Aircraft to be assembled and for the Gatorade bottle to be re-installed by a single ground crew member. The one component aircraft allows the assembly to be simplified greatly and for the ground crew member to focus on securing the Gatorade bottle. The estimated time determined through field based tests averages 28 seconds.

5.7 Drawing Package

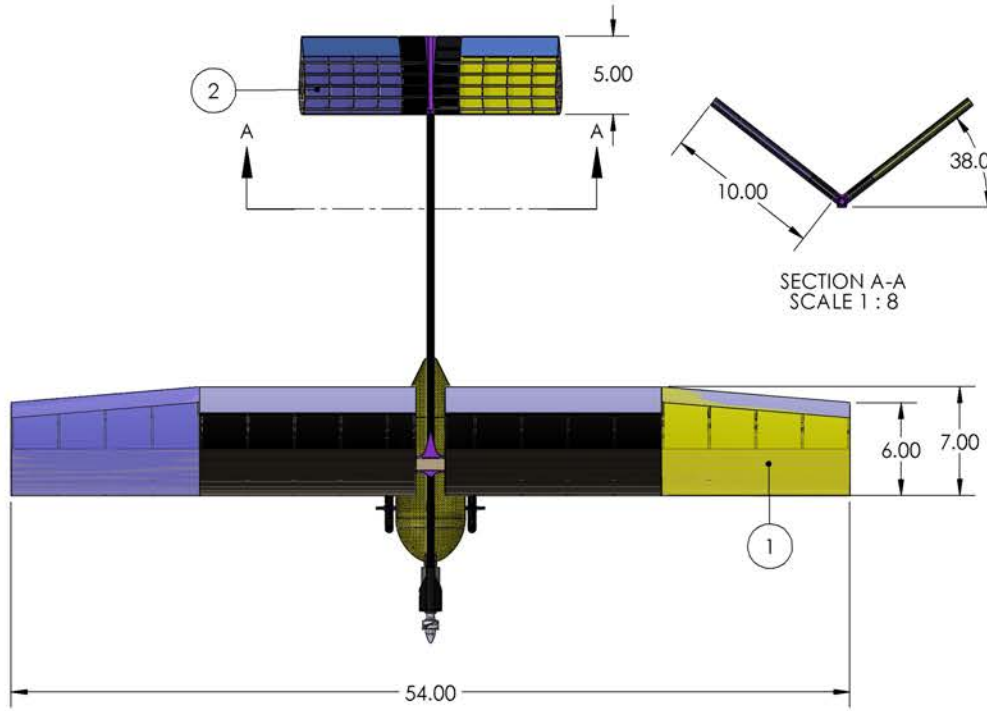

SECTION A-A
SCALE 1 : 8

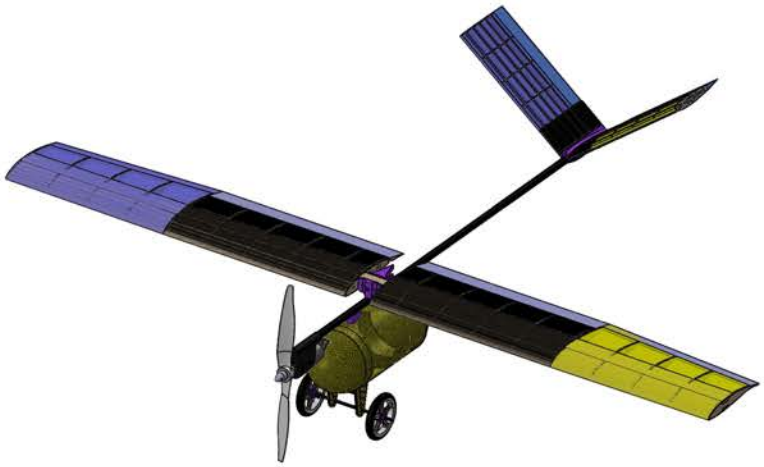

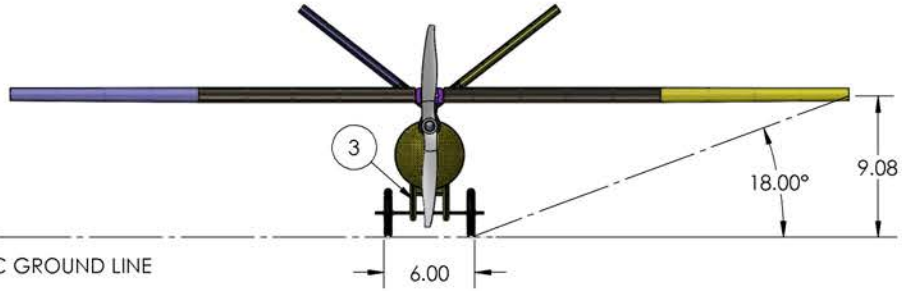

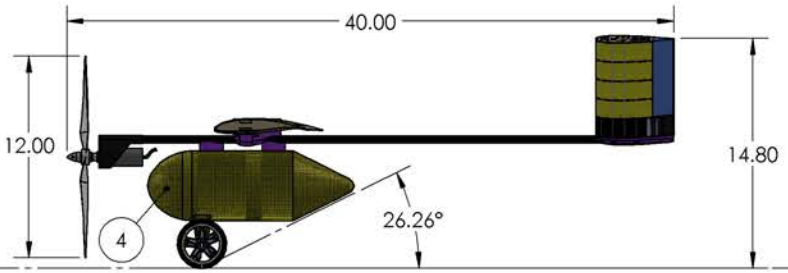

STATIC GROUND LINE

STATIC GROUND LINE

ITEM NUMBER	NAME
1	WING ASSEMBLY
2	V-TAIL ASSEMBLY
3	LANDING GEAR
4	FUSELAGE

UNLESS OTHERWISE SPECIFIED:
DIMENSIONS ARE IN INCHES
TOLERANCES:
ANGULAR: BEND ± .5°
ONE PLACE DECIMAL ±.100
TWO PLACE DECIMAL ±.030
THREE PLACE DECIMAL ±.005

SAMUELI

	NAME	DATE
DRAWN BY:	M. ESTRADA	2/21/2016
CHECKED BY:	C. SLEDGE	2/21/2016
CHIEF ENGINEER:	E. GURROLA	2/21/2016

UNIVERSITY OF CALIFORNIA IRVINE

CESSNA-RAYTHEON-DESIGN/BUILD/FLY 2015-2016

DOCUMENT TITLE:
3-VIEW, PRODUCTION AIRCRAFT

SIZE	APPROVAL DATE:	REPORT TITLE:	REV
B	2016-02-21	DRAWING PACKAGE	A
	SCALE: 1:8	PAGE 1 OF 8	

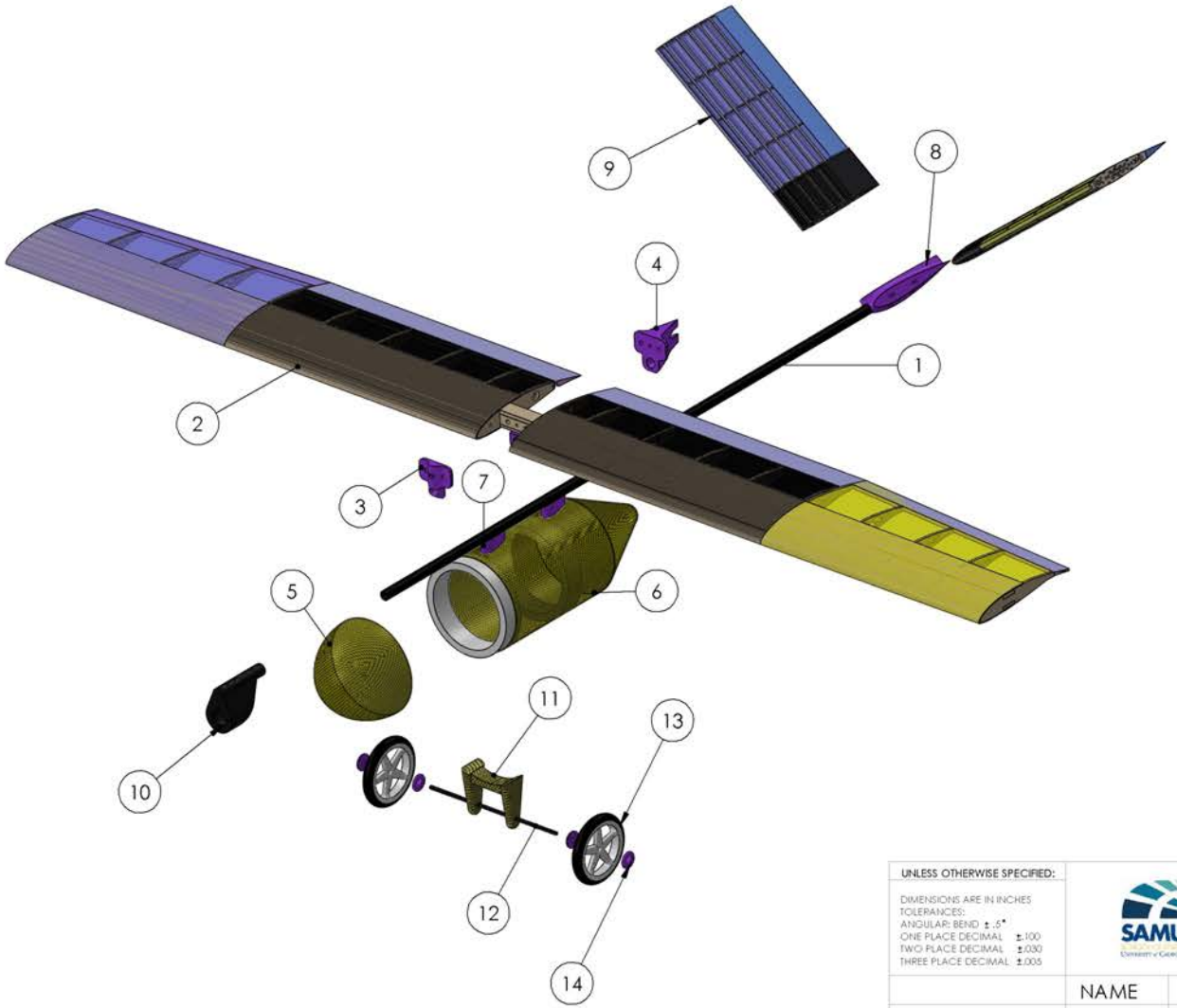

ITEM NO.	NAME	MATERIAL	QTY
1	BOOM	CARBON FIBER	1
2	MAIN WING ASSEMBLY	BALSA-FOAM-MICROLITE	1
3	FORE WING MOUNT	ABS PLASTIC	1
4	REAR WING MOUNT	ABS PLASTIC	1
5	FRONT FAIRING	KEVLAR	1
6	FUSELAGE	KEVLAR - WHITEFOAM	1
7	FUSELAGE STANDOFF	ABS PLASTIC	2
8	V-TAIL MOUNT	ABS PLASTIC	1
9	V-TAIL ASSEMBLY	BALSA- FOAM-MICROLITE	1
10	MOTOR MOUNT	CARBON FIBER	1
11	LANDING GEAR ASSEMBLY	BALSA - KEVLAR	1
12	LANDING GEAR AXLE	CARBON	1
13	LANDING GEAR WHEEL	PLASTIC - FOAM	2
14	LANDING GEAR WHEEL WASHER	ABS PLASTIC	4

UNLESS OTHERWISE SPECIFIED:
DIMENSIONS ARE IN INCHES
TOLERANCES:
ANGULAR: BEND ±.5°
ONE PLACE DECIMAL ±.100
TWO PLACE DECIMAL ±.030
THREE PLACE DECIMAL ±.005

SAMUELI

UNIVERSITY OF CALIFORNIA IRVINE

CESSNA-RAYTHEON-DESIGN/BUILD/FLY 2015-2016

DOCUMENT TITLE:
STRUCTURAL ARRANGEMENT, PRODUCTION AIRCRAFT

	NAME	DATE
DRAWN BY:	A.KWOK	2/21/2016
CHECKED BY:	J. CHEN	2/21/2016
CHIEF ENGINEER:	E. GURROLA	2/21/2016

SIZE B | APPROVAL DATE: 2016-02-21 | REPORT TITLE: DRAWING PACKAGE | REV NC

SCALE: 1:5

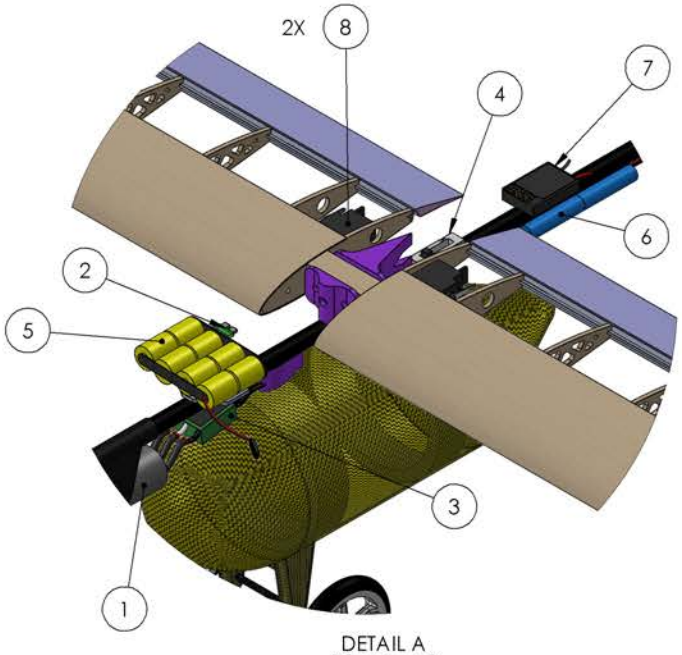

DETAIL A
SCALE 1 : 3

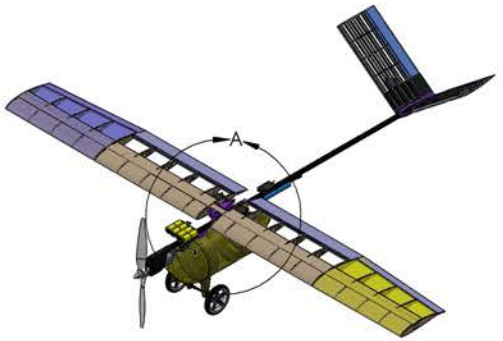

NOTE: CENTER WING AND TAIL SKINS OMITTED FOR CLARITY.

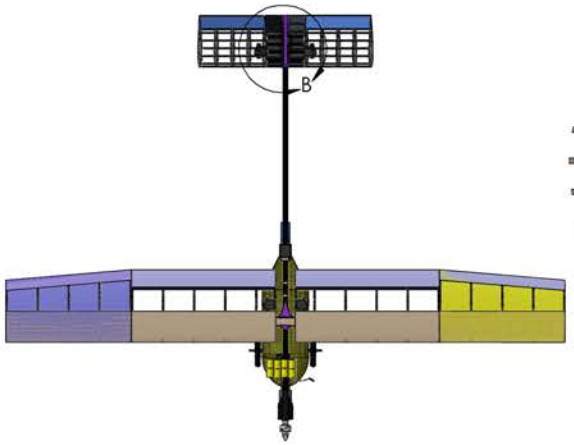

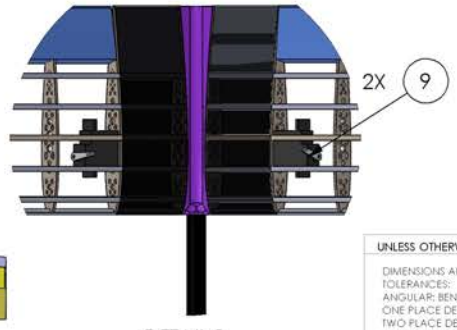

DETAIL B
SCALE 1 : 3

ITEM	NAME	MANUFACTURER	MODEL
1	MOTOR	NEU MOTORS	1105-2.5Y
2	FUSE	ALTRONIX	BF15
3	SPEED CONTROLLER	CASTLE CREATIONS	EDGE LITE HV-40
4	SWITCH	AIRTRONICS	96334
5	BATTERY	ELITE POWER PRODUCTS	ELITE 1500
6	RECEIVER BATTERY	FUTABA	NR4J
7	RECEIVER	FUTABA	R617FS
8	AILERON SERVO	HITEC	HB65
9	EMPENNAGE SERVO	HITEC	HS55

UNLESS OTHERWISE SPECIFIED:
DIMENSIONS ARE IN INCHES
TOLERANCES:
ANGULAR: BEND ± .5°
ONE PLACE DECIMAL ±.100
TWO PLACE DECIMAL ±.030
THREE PLACE DECIMAL ±.005

SAMUELI

UNIVERSITY OF CALIFORNIA IRVINE

CESSNA-RAYTHEON-DESIGN/BUILD/FLY 2015-2016

DOCUMENT TITLE:
SYSTEMS LAYOUT, PRODUCTION AIRCRAFT

	NAME	DATE
DRAWN BY:	A. HE	2/22/2016
CHECKED BY:	A. KWOK	2/22/2016
CHIEF ENGINEER:	E. GURROLA	2/22/2016

SIZE B | APPROVAL DATE: 2016-02-22 | REPORT TITLE: DRAWING PACKAGE | REV NC

SCALE: 1:12 | PAGE 3 OF 8

NOTE: FUSELAGE SKIN OMITTED
FOR CLARITY

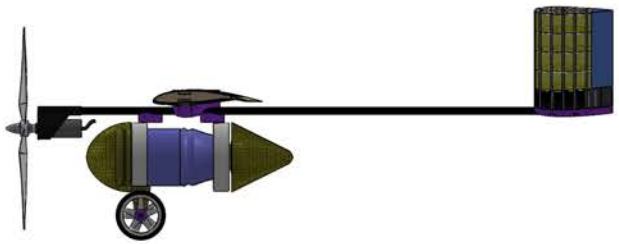

SCALE: 1:8

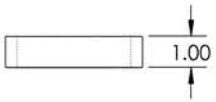

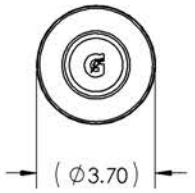

NOTE: FRONT AND REAR FAIRING
AND LANDING GEAR OMITTED
FOR CLARITY

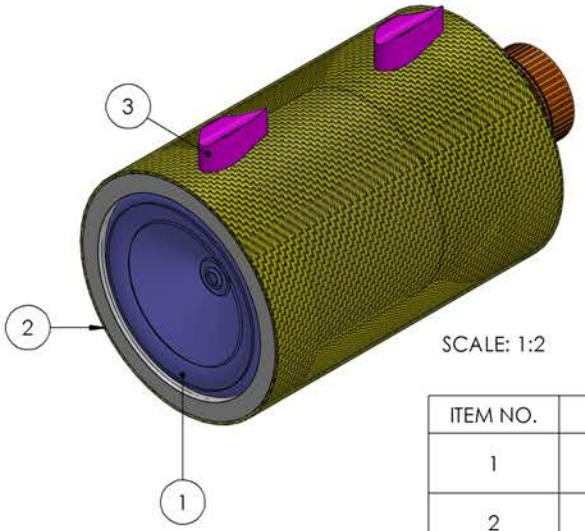

SCALE: 1:2

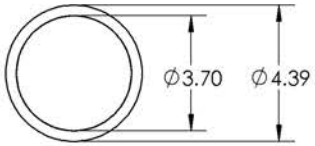

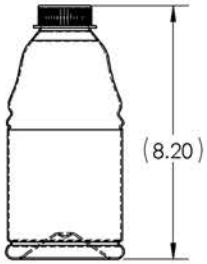

ITEM NO.	NAME	QTY.
1	INTERNAL PAYLOAD	1
2	PAYLOAD RESTRAINT	2
3	FUSELAGE BOOM STANDOFF	2

UNLESS OTHERWISE SPECIFIED:
DIMENSIONS ARE IN INCHES
TOLERANCES:
ANGULAR: BEND ±.5°
ONE PLACE DECIMAL ±.100
TWO PLACE DECIMAL ±.030
THREE PLACE DECIMAL ±.005

SAMUELI

	NAME	DATE
DRAWN BY:	A.KWOK	2/21/2016
CHECKED BY:	C.SLEDGE	2/21/2016
CHIEF ENGINEER:	E.GURROLA	2/21/2016

UNIVERSITY OF CALIFORNIA IRVINE

CESSNA-RAYTHEON-DESIGN/BUILD/FLY 2015-2016

DOCUMENT TITLE:
MISSION 3 PAYLOAD ACCOMODATION

SIZE	APPROVAL DATE:	REPORT TITLE:	REV
B	2016-02-21	DRAWING PACKAGE	NC
	SCALE:1:4	PAGE 4 OF 8	

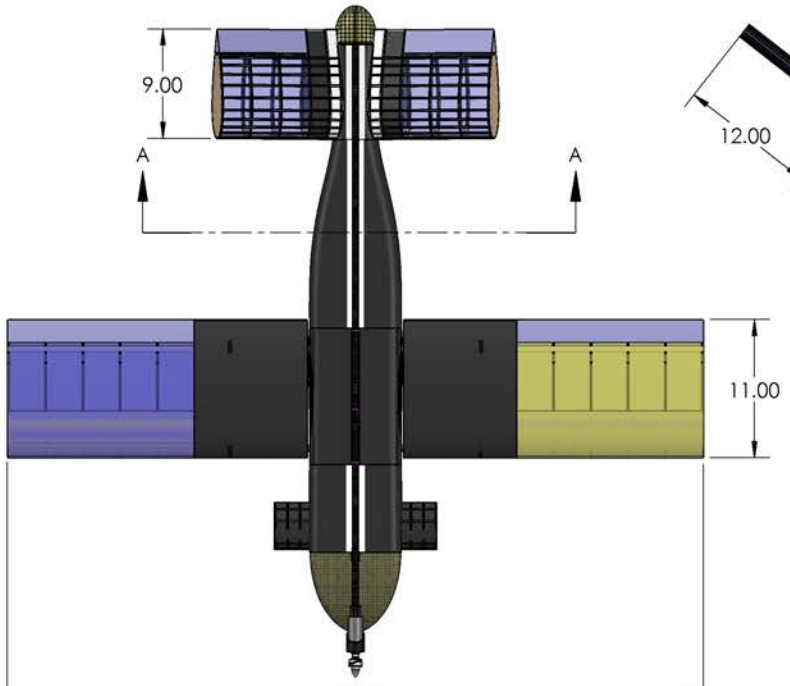

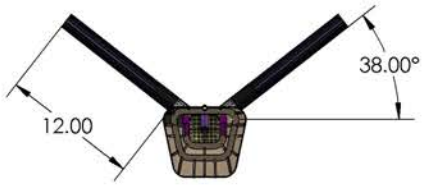

SECTION A-A
SCALE 1 : 10

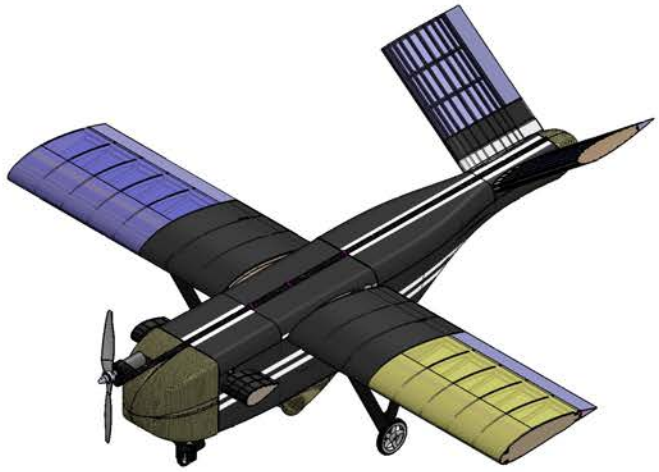

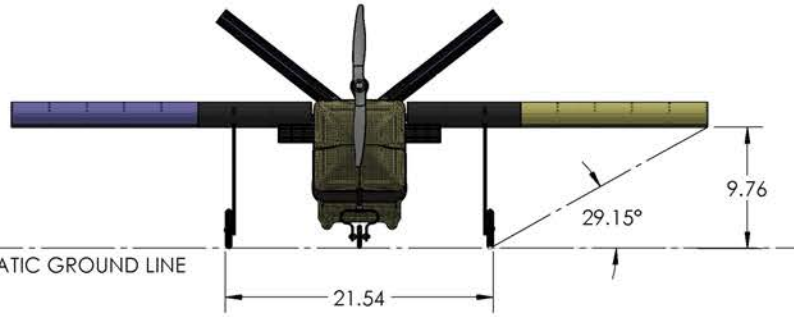

STATIC GROUND LINE

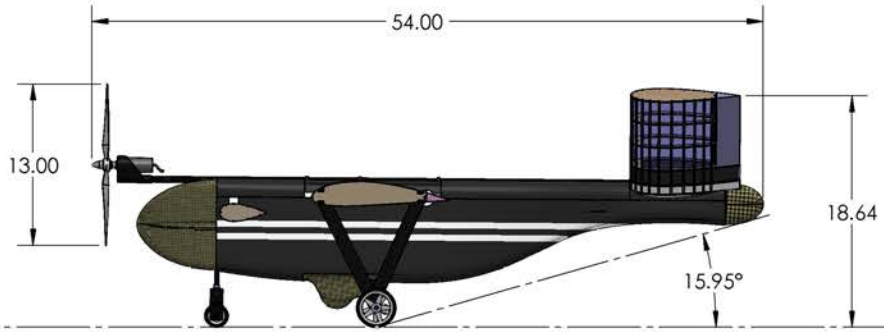

STATIC GROUND LINE

UNLESS OTHERWISE SPECIFIED:
DIMENSIONS ARE IN INCHES
TOLERANCES:
ANGULAR: BEND ±.5°
ONE PLACE DECIMAL ±.100
TWO PLACE DECIMAL ±.030
THREE PLACE DECIMAL ±.005

SAMUELI

UNIVERSITY OF CALIFORNIA IRVINE

CESSNA-RAYTHEON-DESIGN/BUILD/FLY 2015-2016

DOCUMENT TITLE: 3-VIEW, MANUFACTUING AIRCRAFT

	NAME	DATE
DRAWN BY:	A.KWOK	2/21/2016
CHECKED BY:	C. SLEDGE	2/21/2016
CHIEF ENGINEER:	E.GURROLA	2/21/2016

SIZE B | APPROVAL DATE: 2016-02-21 | REPORT TITLE: DRAWING PACKAGE | REV NC

SCALE: 1:10 | PAGE 5 OF 8

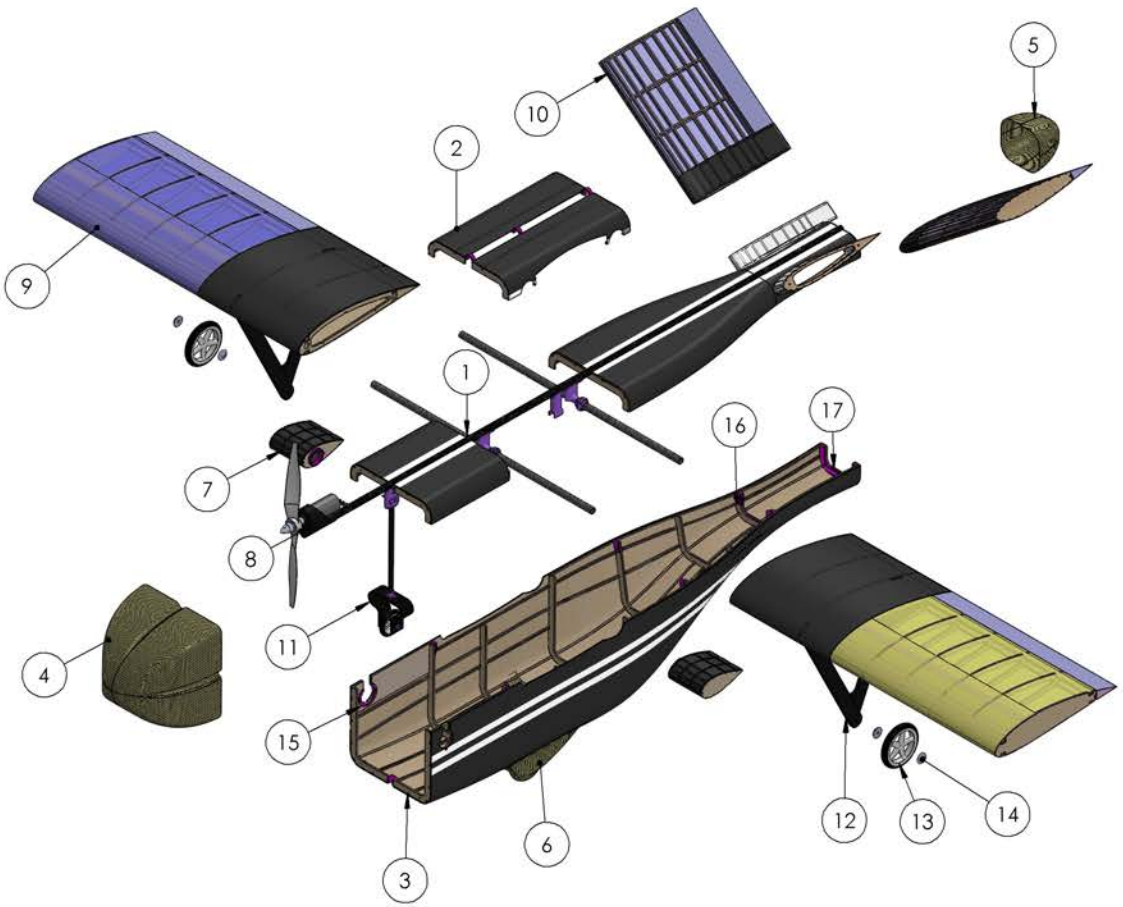

ITEM	NAME	MATERIAL	QTY
1	TOP FUSELAGE ASSEMBLY	BALSA-CARBON FIBER-FIBERGLASS-ABS PLASTIC - MICROLITE -	1
2	TOP FUSELAGE HATCH	BALSA-ABS PLASTIC - MICROLITE -	1
3	BOTTOM FUSELAGE ASSEMBLY	BALSA-FIBERGLASS-ABS PLASTIC - MICROLITE -	1
4	FRONT FAIRING	KEVLAR	1
5	REAR FAIRING	KEVLAR	1
6	LANDING GEAR FAIRING	KEVLAR	1
7	PROPELLER FAIRING	BALSA-MICROLITE	2
8	MOTOR MOUNT	CARBON FIBER	1
9	MAIN WING ASSEMBLY	BALSA-CARBON FIBER-MICROLITE	1
10	V-TAIL ASSEMBLY	BALSA-CARBON FIBER-MICROLITE	1
11	NOSE GEAR ASSEMBLY	CARBON FIBER-ABS PLASTIC	1
12	LANDING GEAR STRUT	BALSA-CARBON FIBER	2
13	LANDING GEAR WHEEL	PLASTIC-RUBBER	2
14	LANDING GEAR WHEEL WASHER	ABS PLASTIC	4
15	PROPELLER FAIRING MOUNT	ABS PLASTIC	2
16	FUSELAGE BODY CLIPS	ABS PLASTIC	6
17	REAR FAIRING MOUNT	ABS PLASTIC	2

UNLESS OTHERWISE SPECIFIED:

DIMENSIONS ARE IN INCHES
TOLERANCES:
ANGULAR: BEND ±.5°
ONE PLACE DECIMAL ±.100
TWO PLACE DECIMAL ±.030
THREE PLACE DECIMAL ±.005

SAMUELI

	NAME	DATE
DRAWN BY:	A.KWOK	2/21/2016
CHECKED BY:	C.SLEDGE	2/21/2016
CHIEF ENGINEER:	E.GURROLA	2/21/2016

UNIVERSITY OF CALIFORNIA IRVINE

CESSNA-RAYTHEON-DESIGN/BUILD/FLY 2015-2016

DOCUMENT TITLE: STRUCTURAL ARRANGEMENT, MANUFACTURING AIRCRAFT

SIZE	APPROVAL DATE:	REPORT TITLE:	REV
B	2016-02-21	DRAWING PACKAGE	NC
	SCALE: 1:10	PAGE 6 OF 8	

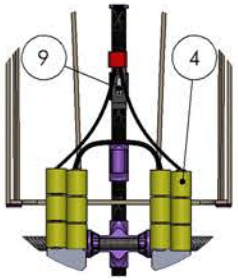

DETAIL A
SCALE 1 : 4

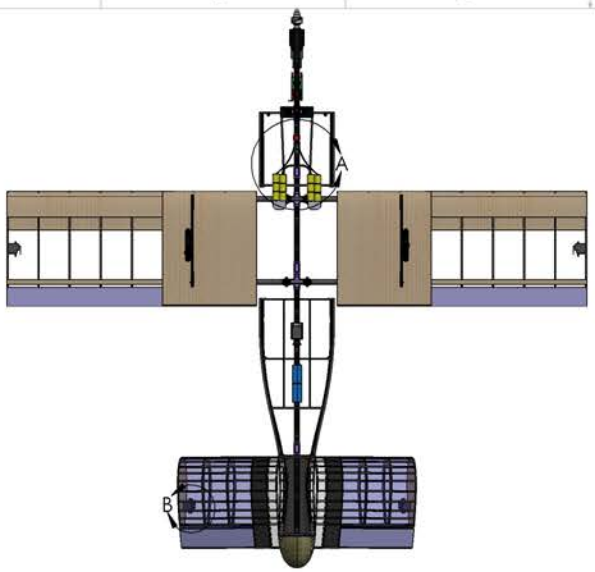

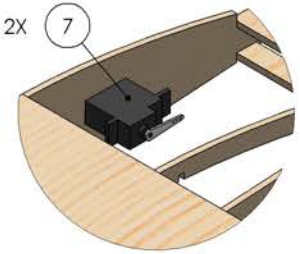

DETAIL E
SCALE 1 : 2

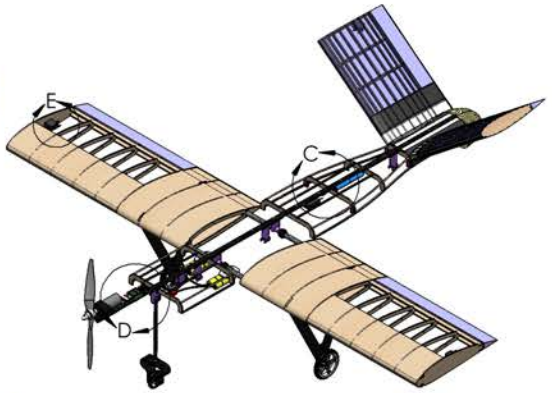

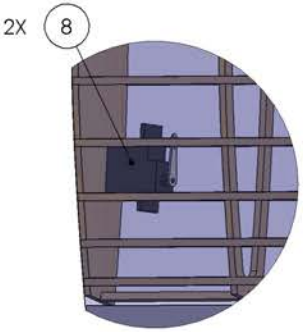

DETAIL B
SCALE 1 : 2

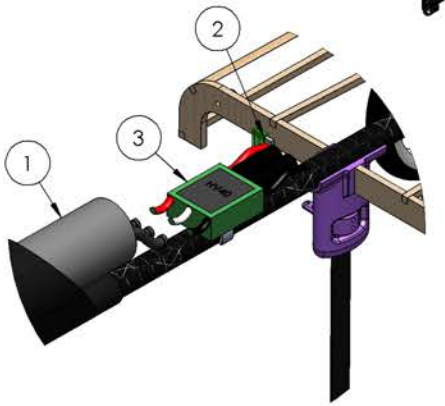

DETAIL D
SCALE 1 : 2

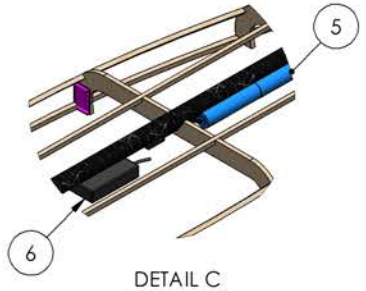

DETAIL C
SCALE 1 : 3

ITEM	NAME	MANUFACTURER	MODEL
1	MOTOR	NEU MOTORS	1105-2.5Y
2	FUSE	ALTRONIX	BF15
3	SPEED CONTROLLER	CASTLE CREATIONS	EDGE LITE HV-40
4	BATTERY	ELITE POWER PRODUCTS	ELITE 1500
5	RECEIVER BATTERY	FUTABA	NR4J
6	RECEIVER	FUTABA	R617FS
7	AILERON SERVO	HITEC	HB65
8	EMPENNAGE SERVO	HITEC	HS55
9	NOSE GEAR SERVO	HITEC	HB65

NOTE: CENTER WING AND TAIL SKINS OMITTED FOR CLARITY.

UNLESS OTHERWISE SPECIFIED:
DIMENSIONS ARE IN INCHES
TOLERANCES:
ANGULAR: BEND ±.5°
ONE PLACE DECIMAL ±.100
TWO PLACE DECIMAL ±.030
THREE PLACE DECIMAL ±.005

SAMUELI

UNIVERSITY OF CALIFORNIA IRVINE

CESSNA-RAYTHEON-DESIGN/BUILD/FLY 2015-2016

DOCUMENT TITLE: SYSTEMS LAYOUT, MANUFACTURING AIRCRAFT

	NAME	DATE
DRAWN BY:	D.KING	2/22/2016
CHECKED BY:	A. KWOK	2/22/2016
CHIEF ENGINEER:	E. GURROLA	2/22/2016

SIZE B | APPROVAL DATE: 2016-02-22 | REPORT TITLE: DRAWING PACKAGE | REV NC

SCALE: 1:16 | PAGE 7 OF 8

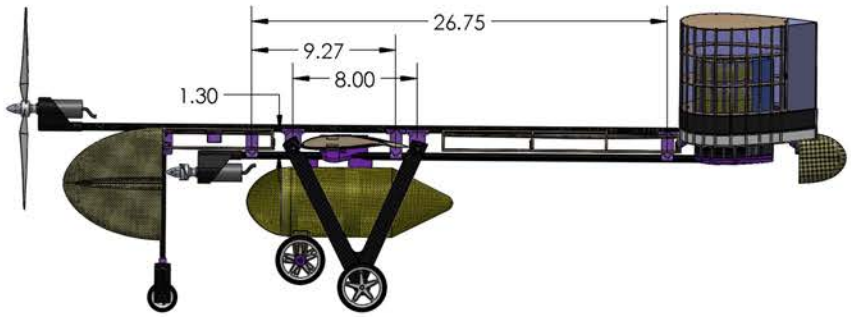

NOTE: MANUFACTURING AIRCRAFT LOWER FUSELAGE ASSEMBLY AND MAIN WING OMITTED FOR CLARITY

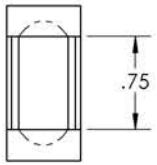

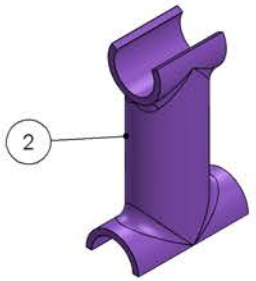

SCALE 1:1

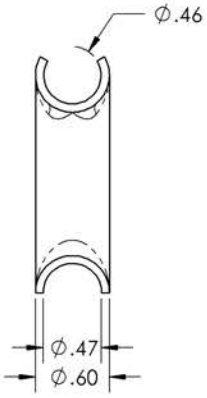

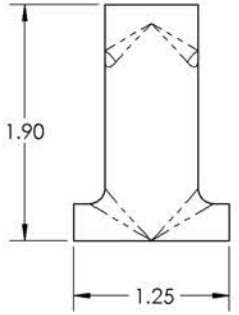

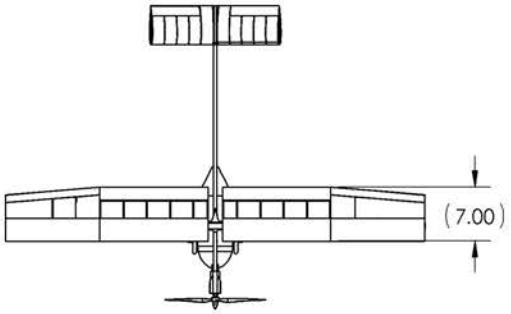

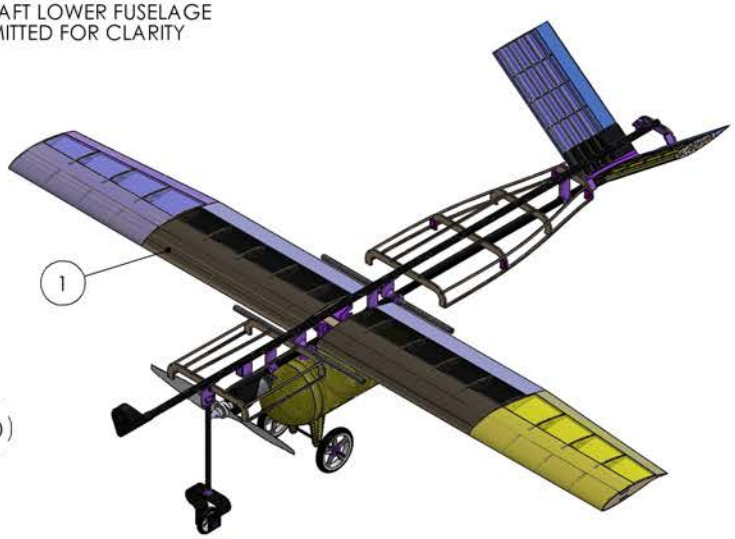

NOTE: PRODUCTION AIRCRAFT AND UPPER FUSELAGE ASSEMBLY ISOLATED FOR CLARITY

ITEM NO.	NAME	QTY
1	INTERNAL PAYLOAD	1
2	PRODUCTION AIRCRAFT STANDOFF	3

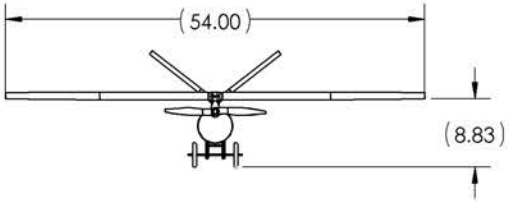

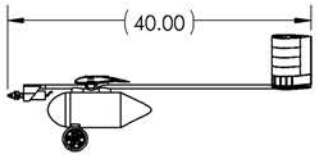

UNLESS OTHERWISE SPECIFIED:
DIMENSIONS ARE IN INCHES
TOLERANCES:
ANGULAR: BEND ±.5°
ONE PLACE DECIMAL ±.100
TWO PLACE DECIMAL ±.030
THREE PLACE DECIMAL ±.005

SAMUELI

UNIVERSITY OF CALIFORNIA IRVINE

CESSNA-RAYTHEON-DESIGN/BUILD/FLY 2015-2016

DOCUMENT TITLE:
MISSION 2 PAYLOAD ACCOMODATION

	NAME	DATE
DRAWN BY:	A.KWOK	2/22/2016
CHECKED BY:	C.SLEDGE	2/22/2016
CHIEF ENGINEER:	E.GURROLA	2/22/2016

SIZE B | APPROVAL DATE: 2016-02-21 | REPORT TITLE: DRAWING PACKAGE | REV NC

SCALE: 1:8 | PAGE 8 OF 8

6.0 Manufacturing Plan

The manufacturing plan focused on the major components of the aircraft: fuselage, fairings, landing gear, motor mount, wings, and tails. The manufacturing processes selected were based on the application, feasibility to manufacture, and ability to produce high quality components.

6.1 Manufacturing Processes Investigated

Balsa Structures

Balsa wood is the material of choice due to its impressive strength-to-weight and stiffness-to-weight ratios. Tools are used to help align the balsa ribs or bulkheads to allow rapid manufacturing and precise balsa structures, such as the wings, tails, and the MA fuselage.

Composites

Composite materials such as fiberglass, Kevlar, and carbon fiber have anisotropic properties that make it possible to achieve desirable strength and stiffness while minimizing weight. The majority of the composite materials are used in conjunction with molding techniques to manufacture components.

Foam

Polystyrene foam is used for the airplane components that are not required to have strong internal structures. A two axis CNC foam cutting machine can reproduce these parts quickly and accurately.

3D Printing

3D Printing using ABS plastic is one of the fastest ways to create rigid rapid prototypes of parts.

6.2 Manufacturing Processes Selection

6.2.1 Fairings

The following methods were considered for the manufacturing of the fairings.

- Male molding- A male mold is designed and with 3D printing until the mold is slightly undersized to account for the material thickness of the desired parts. The use of 3D printing with this technique allows for rapid mold production, allowing new improvements to be incorporated into the mold. Male molding is recommended for a smooth inner surface and fast mold production.
- Female Molding - A female mold is created as the negative of the male mold after a smooth surface male plug is made. It is recommended for a smooth outer surface.

Figure 6: 1 (Left) Fairings and Fuselage for PA (Right) Rear Fairing for MA

Both methods are implemented on each aircraft. The front and rear fairing for both aircraft are made using the female molding method due to the complex geometry and parasitic drag reduction.

6.2.2 Wings and Tails

- Foam Wings – Foam wings are cut by a CNC hot-wire machine. The foam is then stiffened with composite material, sanded, and waxed for a smooth surface.
- Balsa Wing - Ribs are laser cut from airfoil CAD drawings. Once laser cut, ribs are placed into a tool to ensure precise alignment and spacing. The spar structure provides additional torsional strength in flight. The wing is then covered with thin, flexible balsa sheets from the leading edge to the spar caps to preserve the contour of the airfoil at the leading edge. The wing is then covered with Microlite™ to maintain the airfoil shapes and provide torsional stiffness.

Figure 6: 2 Balsa Built Up Assembly

Balsa wood was implemented in the majority of the wings and tails since it is lightweight compared to foam wings. The main critical structure was made from balsa ribs, spars, and sheeting. Foam with composites are used on the trailing edges and ailerons.

6.2.3 Landing Gear

- Landing Gear Struts – For this structure, the general shape of the struts is cut from balsa. The triangular balsa pieces are then sanded to shape and reinforced by wrapping Kevlar. These struts are then attached to a balsa block and the PA fuselage. This manufacturing method incorporates the frame structure of the aircraft to minimize the weight of the aircraft and its drag.
- V-shaped Landing Gear - This main gear for the MA was designed to anchor directly to the wing carbon rod spars. The balsa structure is reinforced with layers of bidirectional and tapered unidirectional carbon fiber to maximize strength while minimizing weight.

- Nose Gear - A carbon rod is used as the strut and a carbon fiber mushroom axle mount is attached at the bottom. Layers of composite are wrapped around the mold for additional strength.

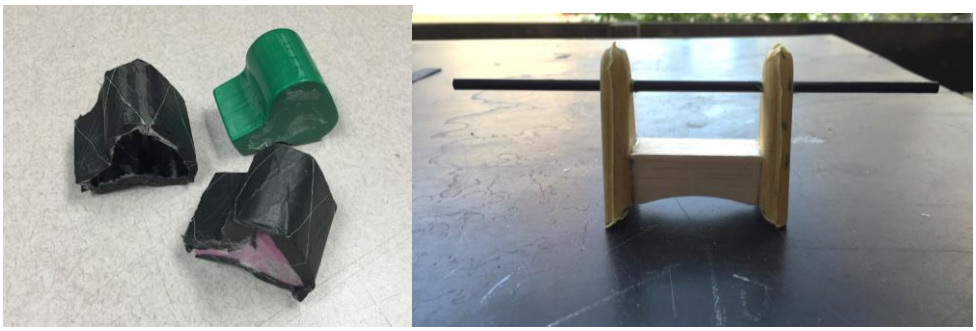

Figure 6: 3 Manufacturing Landing Gear Nose (Left), Production Landing Gear (Right)

6.2.4 Motor Mount

The motor mount is designed to take the thrust loads of the motor. Two methods of manufacturing a lightweight and resilient motor mount were considered.

- 3D Printing: A motor mount is designed on SolidWorks and 3D printed using ABS plastic.
- 3D Printing Female mold: Layers of composite, cut out with specific fiber orientation, were inserted into the mold. Everything is then vacuum bagged and allowed to cure.

The 3D printed female mold method was selected for both the MA and PA. Using multiple layers of unidirectional and bidirectional carbon, this method allows orientation to be controlled throughout the mount. This helps with torsion and lets the carbon fiber sleeve transfer the motor's forward momentum to the rest of the aircraft.

6.2.5 Payload

Mission 2 Payload Restraint

The payload for Mission 2 are the PA sub-assemblies. To carry the payload internally, 3D printed clips are used to secure the payload and the fuselage is manufactured from balsa bulkheads and stringers. Prop fairings were manufactured to cover the PA propeller.

Mission 3 Payload Restraint

The payload for Mission 3 is a sealed 32 oz. Gatorade bottle, which is housed in a Kevlar sleeve with a foam ring that secures it in place. The Kevlar sleeve is then attached to the boom through 3D printed standoffs.

6.3 Manufacturing Milestone Chart

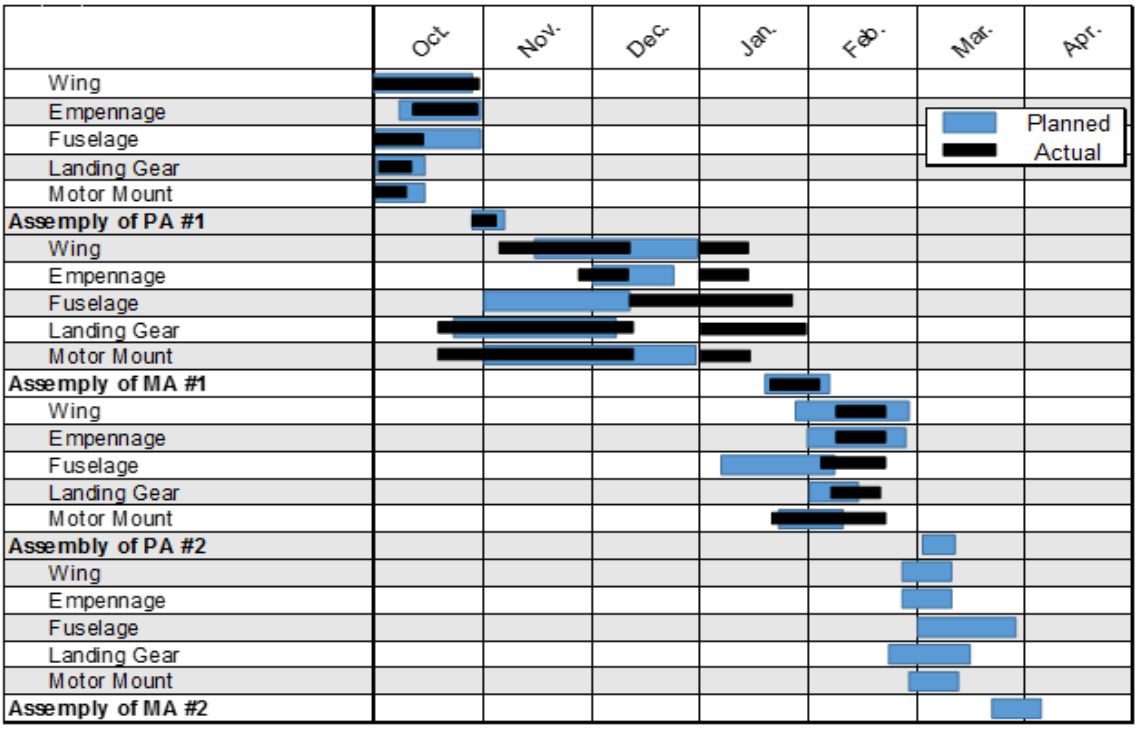

Figure 6: 4 Manufacturing Milestone Chart

7. Testing Plan

Testing was conducted to validate design choices and examine performance. Individual components, as well as, the entire aircraft were tested throughout the design process. Results from testing helped provide areas of improvement and direction for the final design.

7.1 Objectives and Schedule

In order to provide data and proper feedback for designs, testing must adhere to a schedule. The schedule is broken down into structural, propulsion, and flight testing, as shown in Figure 7.1. The objective of testing is to analyze key parameters of design elements and reflect upon the effectiveness of the design. The end objective is to produce a reliable and lightweight aircraft that successfully completes all missions.

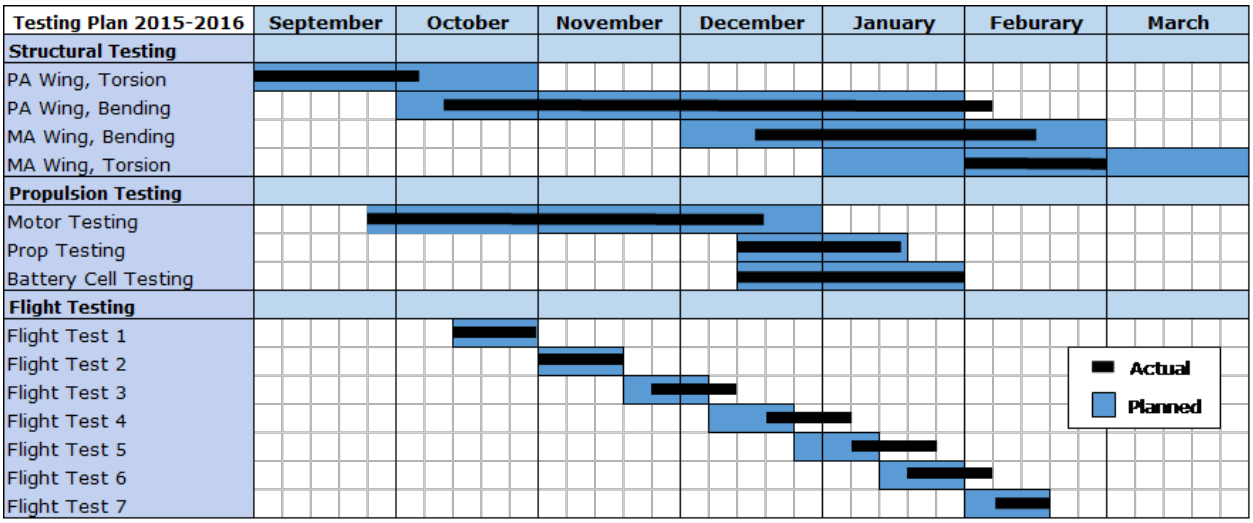

Figure 7: 1 Testing Plan

7.2 Structural Testing

Structural wing testing is emphasized due to its relevance in flight performance and packaging. Wing testing consists of torsion and bending tests. Both are probable causes for wing failure during flight.

To test wing torsion, a painter's stick was glued on at the wing tip as a moment arm. A pivot point was created using a wooden stand with a metal tube placed right under the spar. A bag is attached to the end of the painter's stick with weights to induce torque. An inclinometer was then placed adjacent to the spar to measure the twist angle as weights were added incrementally. The wing is loaded and unloaded multiple times to simulate fatigue. Each loading set adds additional weight until torsional failure. Multiple trials are plotted against each other to check for permanent twisting.

Figure 7: 2 Wing Torsion Testing and Wing Bending Testing

To test wing bending, the wing is loaded with weight along its span. Sandbags are weighted according to the lift distribution generated per wing by using AVL. The sandbags are placed at the quarter-chord position of the airfoil at three inch stations along the span from the wing root to the wing tip. The weight placed onto the wing emulates 1G, 2G, and consecutive G's of loading on the wing. The loading is done in trials to simulate fatigue testing. The amount of G's at failure and the location of the failure are recorded. When the sandbags are placed for a corresponding G loading, the deflection of the

leading edge at the tip is measured for each trial. The deflection results are plotted to analyze the deflection curve per trial. Any change in the deflection curves per trial indicates structural degradation, which may result in future wing failure. Once a wing design has been tested and reviewed, further proof testing is conducted by loading the wing up to 3G's. This ensures that the wing is able to withstand the required flight loads and is approved to be placed onto an aircraft.

7.3 Propulsion Testing

Propulsion testing is done to analyze the motor, battery, and propeller combination performance. Static tests are done with a thrust stand by varying one component and holding all others constant. Data is recorded through the electronic speed controller attached to the motor. Testing is done by examining the watts and amps being drawn for a given static thrust requirement. The objective is to determine the relationship between different propulsion configurations. Then the configuration that produces the necessary static thrust and minimizes the battery weight required can be determined.

7.4 Pre-Flight Test List

Table 7: 1 Pre-Flight Checklist

Pre-flight Check List			
Flight Date:	Plane (MA or PA):	Location:	Additional Info:
Flight Time:	Prototype #:	Wind Speed:	
Takeoff Weight:	CG Location:	Battery Used:	
Flight Check	Instructions: Check off each box with Initials		
Structural Integrity - Visual inpection for damaged components			
Control Surfaces/Linkages		V - Tail Stabilizer	
Payload Mounts		Propeller	
Boom/All Fairings		Landing Gear	
Wing		Motor Mount	
Avionics - Ensure all wires and electrical components are connected and performing properly			
Servo Wiring		Power-Up Test	
Motor Wiring		Range Test	
Reciever Properly Connected		Receiver Battery Peaked	
Failsafe Engaged		Main Battery Peaked	
Propulsion - System should perform as desired			
Motor Test		Reciever Battery Connected	
Servo Test		Main Battery Connected	
Landing Gear Servo Test		Telemetry Connected	
Final Inspection - Must be done right before takeoff			
Control Surface Movement		Mission / Objective Restated	
Ground Crew Clear		Pilot and Spotter Ready	

The purpose of this pre-flight checklist, as shown in Table 7.1, is to ensure that the aircraft is flight ready. A pre-flight checklist helps facilitate flight testing and eliminate possible issues during flight.

7.5 Flight Test Plan

Flight tests are performed for both the PA and MA aircrafts. Each prototype requires test flights to understand the flight capabilities of the aircraft as well as mission performance. Table 7.2 is used to provide goals for each test flight session. A well-defined test plan as shown in Table 7.3 outlines the conditions and objectives that the aircraft is expected to meet during a flight test. Flight test performance data is recorded using Eagle Tree data logging telemetry system. Data recorded from telemetry is used to calculate performance metrics for the aircraft. The performance metrics are then compared to the predicted values for that prototype and are used to gauge and improve the aircraft design.

Table 7: 2 Master Test Schedule

Flight Test	Aircraft	Goal
1	PA	Maiden Flight, Determine flying qualities, takeoff distance
2	PA	Mission 3 simulation
3	MA	Maiden Flight, Determine flying qualities, takeoff distance
4	MA	Mission 2 simulation: maximum payload test with taxi
5	MA	Mission 1 performance
6	MA	Mission 2 performance
7	PA	Mission 3 performance

Table 7: 3 Flight Test Plan

Flight Test Plan 2/14/2016 - Prototype 1			
Acquire telemetry for mission 1 and 2			
Live tracking of battery capacity, speed, current, and altitude			
Ramp throttle to 100% before each flight on the ground			
First Flight: Trim flight Battery		First Flight: Mission 1 Simulation Battery: 12 cells (1500 mAh) Propeller: 13x8	
Trim aircraft		Takeoff weight: ~3.38 lbs.	
Understand behavior in straight away and turns		Cruise Speed: 50 ft/s	
		Stall Speed: 22.6 ft/s	
		Flight duration: 4 minutes	
		Fly course with spotters	
First Flight: Mission 2 Simulation Battery: 12 cells (1500 mAh) Propeller: 14x7		First Flight: Mission 3 Simulation Battery: 8 cells (1500 mAh) Propeller: 12x6	
Takeoff weight: ~4.88 lbs.		Takeoff weight: ~4.25 lbs.	
Cruise Speed: 55 ft/s		Cruise Speed: 45 ft/s	
Stall Speed: 27.16 ft/s		Stall Speed: 31.70 ft/s	
Flight duration: 3 minutes		Flight duration: 4 minutes	
Fly course with spotters		Fly course with spotters	

8.0 Performance Results

8.1 Performance of Key Subsystems

8.1.1 Structural Performance

Wing Testing was performed on prototype wings for the PA and MA aircraft. Initial bending tests for PA wings revealed weak spots located near the center spar, where the bending moment is highest. Early PA balsa wings broke at a failure load of 3G (12.75 lbs of force distributed over the wing). Later prototypes reinforced the areas around the center spar and outward tapering towards the tip with carbon tape and carbon rods. These PA wings failed at a load of 4G (17 lbs). Bending fatigue testing for these wings was conducted and the deflection at the leading edge was recorded. Figure 8.1 shows the data recorded for fatigue and deflection test for a PA wing with a span of 54in and an M.A.C. of 6.79 in.

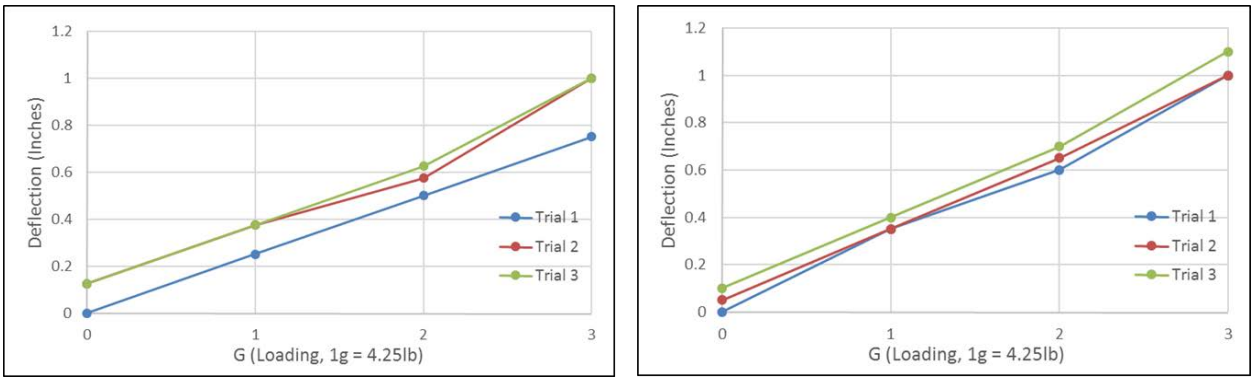

Figure 8: 1 Left (A) and Right (B) Wing Loading Deflection Curve for PA, b=54in, M.A.C.=6.79in.

Deflection curves help predict how the performance of the wing changes with each flight. It is necessary to make sure that the performance of the wing does not change over time, otherwise plastic deformation or fracture on wing components can cause failure during flight.

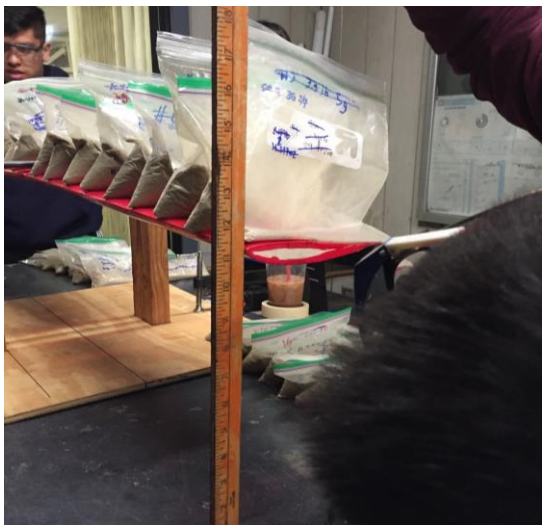

Figure 8: 2 Measuring leading edge deflection during wing bending testing.

Torsion testing was performed to understand the effects of torque and twist on wings. Torsion testing was also conducted to see if aileron reversal could occur on the wing, which is a problem for flight stability and control. Test data included the twist angle, the torque applied, and calculated G and J for the wing. The goal was to establish a linear pattern between twist angle and torque applied and for GJ to be constant for each loading. Figure 8.3 shows the torsion plots for a MA wing. Fatigue testing was performed by conducting several trials. At loads close to failure, the relationship between twist angle and torque becomes non-linear, indicating deformation. G and J trends show that the wing structure changes and becomes non-constant when both twist angle increases and number of trials increases.

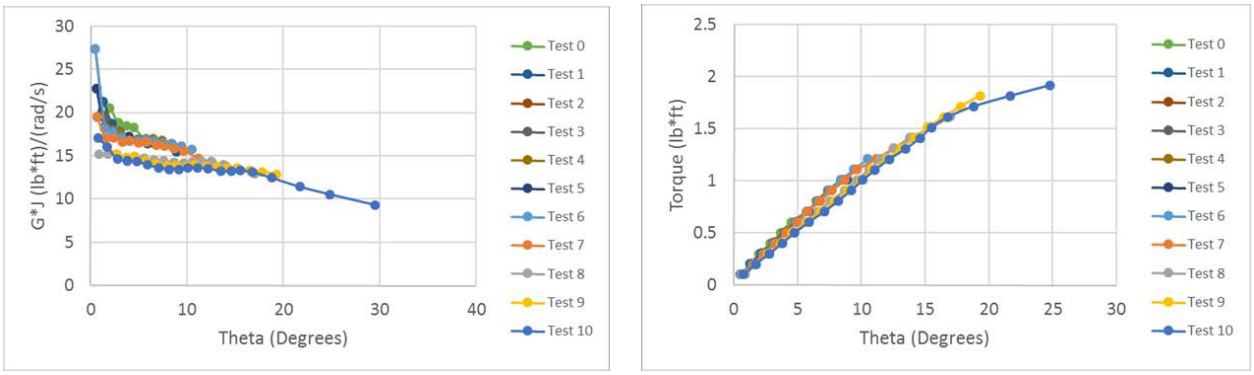

*Figure 8: 3 G*J vs Theta(A) and Torque vs Theta (B) Torsion Test for MA, b=66in, M.A.C. = 11 in*

Wing testing provides failure limits and experimental data that can predict performance of wing components. The data collected from testing was used to set values for load and safety factor. The wings were then designed to withstand a load factor of 2.5G for the PA and 3.5G for the MA, and have a safety factor of 1.5G. Using the data gathered from testing, future iterations of wings can be built stronger and more lightweight.

8.1.2 Propulsion Performance

Table 8.1 (B) shows empirical values from tests performed on the static thrust stand using a Neu 1105 with a 4.4:1 gearbox and 8 cell 1500mAh NiMH battery. Propeller sizes shown were found by analyzing APC propeller performance data for estimating thrust and power. Actual values recorded have a small error as noted in Table 8.2 B. Similarly, empirical values for a Neu 1105 with a 6.7:1 gearbox and 12 cell 1500mAh NiMH battery are shown in Table 8.1 (A) and the associated errors in Table 8.2 A.

Table 8: 1 (A) Actual and Expected Propeller Data, MA

MA Climb Power ~ 280 - 320 W				
Propeller	*Actual Thrust (lbs)*	*Actual Power (W)*	*Expected Thrust (lbs)*	*Expected Power (W)*
12x8	2.73	210	2.93	178
13x8	3.81	300	4.09	313
14x7	4.2	310	4.8	335

Table 8: 2 (B) - Actual and Expected Propeller Data, PA

PA Climb Power ~ 200 W				
Propeller	*Actual Thrust (lbs)*	*Actual Power (W)*	*Expected Thrust (lbs)*	*Expected Power (W)*
10x5	2.31	160	2.48	149
11x7	2.39	170	2.5	155
12x6	2.73	200	2.93	160

Table 8: 3 (A) Percent Error, MA (B) Percent Error, PA

MA Static Error		
Propeller	*Thrust %*	*Watt %*
12x8	6.83	17.98
13x8	6.78	4.15
14x7	12.5	7.46

PA Static Error		
Propeller	*Thrust %*	*Watt %*
10x5	6.85	7.38
11x7	4.4	9.68
12x6	6.83	25

The percent errors can be attributed to vibrations through the thrust stand, which was evident. Figure 8.4 represents mission simulations of the propulsion systems for each mission. They are modeled at 100% throttle for approximately 30 seconds to consider takeoff and climb followed by 70% throttle for remainder of time for cruise. Each was considered for a simulation of a 5-minute window to ensure sufficient energy for completion using the Elite 1500mAh cells.

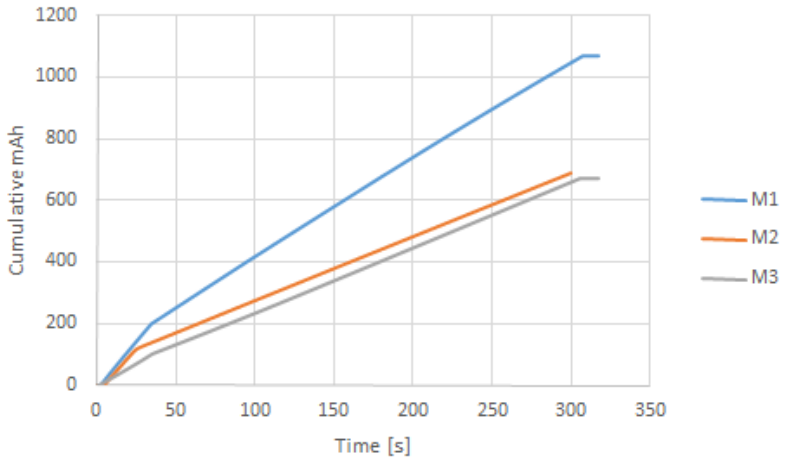

Figure 8 1 Battery Mission Simulation

8.2 Test Flight Performance

Eagle Tree Telemetry as well as Castle Creations Castle Link was used to record and monitor flight performance in real time. Test flight data was used to optimize the aircraft for later iterations. Table 8.3 below shows predicted propulsion data and field flight data obtained from telemetry.

Table 8: 4 Measured Flight Data and Predicted Performance

Mission	Predicted Thrust (lbs)	Actual Thrust (lbs)	Predicted Cruise Power (W)	Actual Cruise Power (W)	Predicted Current (A)	Actual Current (A)
M1	1.4	1.25	261	225	18.1	16
M2	1.5	1.4	280	240	19.4	18
M3	0.7	0.65	95	90	9.9	7.7

Table 8: 5 Flight Calculation Percent Errors

Flight Error			
Mission	*Thrust %*	*Current %*	*Watt %*
M1	10.71	11.6	13.79
M2	6.67	7.22	14.29
M3	7.14	22.22	5.26

Predicted propulsion data was initially conservative to oversize the systems and provide safety margins. The errors in the flight performance for each mission is depicted in Table 8.4.

Mission 1

Flying at the lowest allowable power setting is the primary focus of Mission 1, where three laps are to be flown in a five-minute window to receive a full flight score. Flights resulted in an average lap time of 75 seconds and achieved takeoff within 60 ft. The mission must be flown maintaining constant altitude following climb out, while executing shallow bank angles at the 180 degree and 360 degree turns in order to conserve cruising power. Important parameters that need to be recorded and monitored are the power drawn during takeoff and cruise. Power drawn is calculated by measuring the voltage and current drawn by the motor via the ESC. It is important to consider the power drawn by the motor because it helps to size the appropriate battery pack required by the propulsion system.

Mission 2

Mission 2 does not require the aircraft to fly at the lowest allowable power setting because only one lap needs be completed to deliver the one and only component. Since the RAC will be unaffected by a battery change, the same number of cells are used for the propulsion battery pack as Mission 1. This eliminates any concern regarding power conservation.

Mission 3

The primary focus of Mission 3 is to fly at the lowest allowable power setting while completing three laps in a five-minute window in order to receive a full flight score. This flight averaged a lap time of 85 seconds and achieved takeoff within 80 feet with no headwind. Just like Mission 1, this mission must be flown at a constant altitude while executing shallow bank angles in the 180 degree and 360 degree turns.

Summary

At the time of this report, nine test flights have been performed on five different prototypes: four different PA prototypes and one MA prototype. Flight testing has shown that the PA and MA aircraft will be competitive, both are capable of meeting takeoff and flight requirements. The concept of a single-engine, high wing, V-tail, one component PA aircraft has proven to be a capable design that minimizes

Figure 8: 4 Production Aircraft Prototype Flight

Figure 8: 5 Manufacturing Aircraft Prototype Flight

RAC and will give the *Electrolyne* team a scoring edge against two component designs and other one component designs. The team is confident in the *Electrolyne* design and anticipates the configuration chosen will allow the team to place well in Wichita.

9. References

[1] MIL-F-8785C. Military Specification: Flying Qualities of Piloted Airplanes, November 1980
[2] M.V. Cook, Flight Dynamics Principles Second Ed, Reprinted 2008
[3] T. M. Foster, Dynamic Stability and Handling Qualities of Small Unmanned-Aerial-Vehicles, Brigham Young University, April 2005.
[4] W. F. Phillips, Mechanics of Flight 2nd Ed, India: John Wiley & Sons, 2009

10. Works Cited

1. AIAA Design/Build/Fly Competition 2015/2016 Rules, 31 Oct. 2015, <http://www.aiaadbf.org/>
2. D. P. Raymer, Aircraft Design: A Conceptual Approach 5th Ed., Reston: American Institute of Aeronautics and Astronautics, 2012
3. J. D. Anderson Jr., Aircraft Performance and Design, Columbus: McGraw-Hill, 1999
4. J. Hodgkinson, Aircraft Handling Qualities, Osney Mead: Blackwell Science Ltd., 1999
5. J. R. Wright & J. E. Cooper, Introduction to Aircraft Aeroelasticity and Loads, Reston: American Institute of Aeronautics and Astronautics, 2007
6. M. A. Page, Notes on small-scale aircraft design, September 2002
7. M. Simmons, Model Aircraft Aerodynamics 4th ed, Poole: Special Interest Model Books Ltd., 2000
8. M. S. Selig, et. al., Summary of Low-Speed Airfoil Data, Virginia Beach: SoarTech Publications, 1995
9. R. D. Schaufele, The Elements of Aircraft Preliminary Design, Santa Ana: Aries Publications, 2000
10. R. S. Shevell, Fundamentals of Flight 2nd Ed., Upper Saddle River: Prentice Hall, 1983

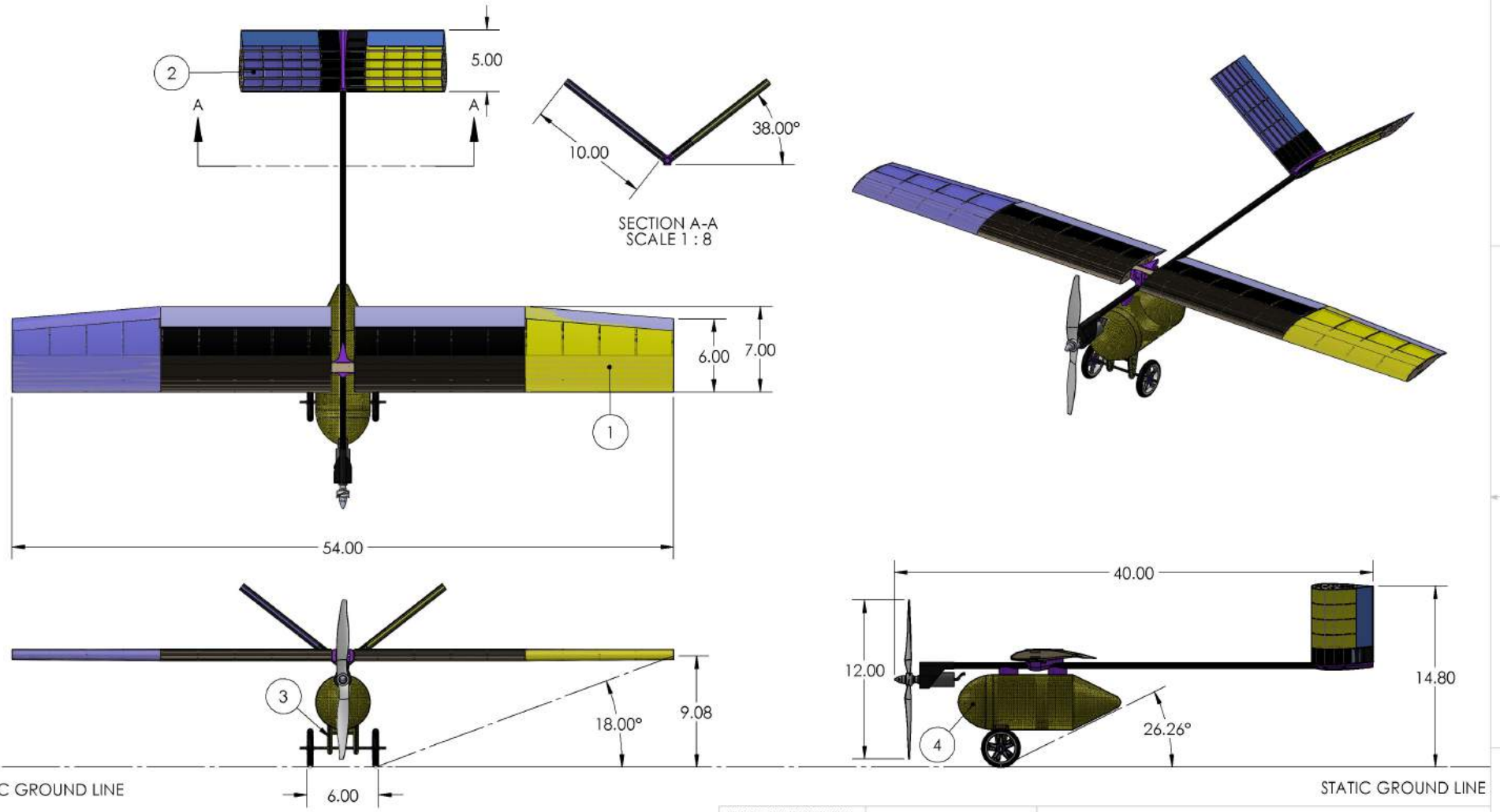

ITEM NUMBER	NAME
1	WING ASSEMBLY
2	V-TAIL ASSEMBLY
3	LANDING GEAR
4	FUSELAGE

UNLESS OTHERWISE SPECIFIED:
DIMENSIONS ARE IN INCHES
TOLERANCES:
ANGULAR: BEND ± .5°
ONE PLACE DECIMAL ±.100
TWO PLACE DECIMAL ±.030
THREE PLACE DECIMAL ±.005

	NAME	DATE
DRAWN BY:	M. ESTRADA	2/21/2016
CHECKED BY:	C. SLEDGE	2/21/2016
CHIEF ENGINEER:	E. GURROLA	2/21/2016

SAMUELI

UNIVERSITY OF CALIFORNIA IRVINE

CESSNA-RAYTHEON-DESIGN/BUILD/FLY 2015-2016

DOCUMENT TITLE: 3-VIEW, PRODUCTION AIRCRAFT

SIZE	APPROVAL DATE:	REPORT TITLE:	REV
B	2016-02-21	DRAWING PACKAGE	A
	SCALE: 1:8	PAGE 1 OF 8	

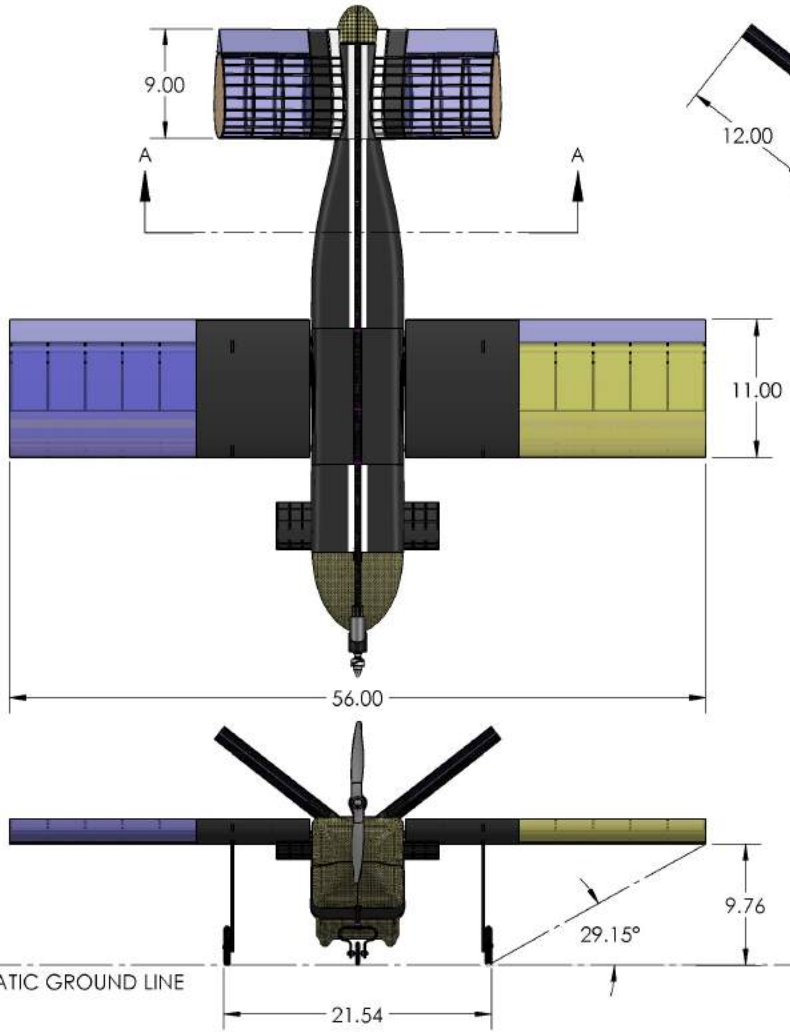

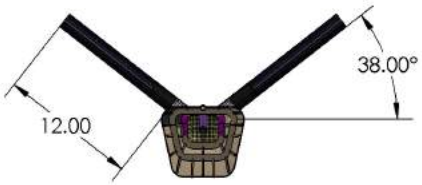

SECTION A-A
SCALE 1 : 10

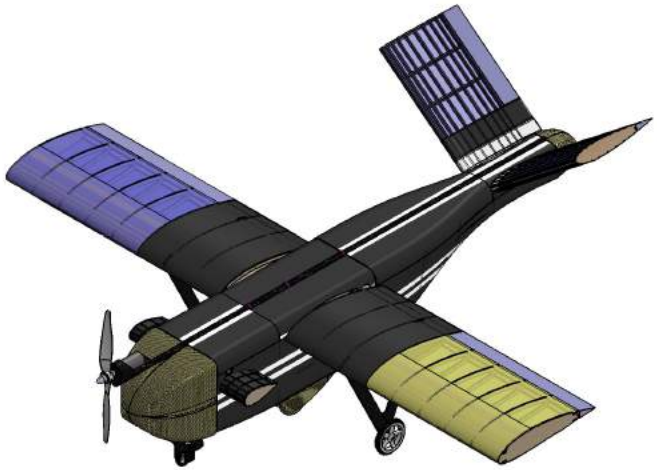

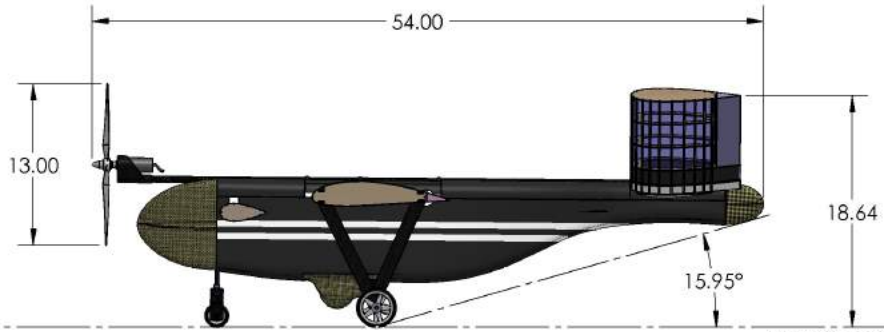

STATIC GROUND LINE

STATIC GROUND LINE

UNLESS OTHERWISE SPECIFIED:			UNIVERSITY OF CALIFORNIA IRVINE			
DIMENSIONS ARE IN INCHES TOLERANCES: ANGULAR: BEND ± .5° ONE PLACE DECIMAL ±.100 TWO PLACE DECIMAL ±.030 THREE PLACE DECIMAL ±.005	SAMUELI		CESSNA-RAYTHEON-DESIGN/BUILD/FLY 2015-2016			
			DOCUMENT TITLE: 3-VIEW, MANUFACTUING AIRCRAFT			
	NAME	DATE				
DRAWN BY:	A.KWOK	2/21/2016	SIZE B	APPROVAL DATE: 2016-02-21	REPORT TITLE: DRAWING PACKAGE	REV NC
CHECKED BY:	C. SLEDGE	2/21/2016				
CHIEF ENGINEER:	E.GURROLA	2/21/2016		SCALE: 1:10	PAGE 5 OF 8	